HM Consultoria e Projetos de Engenharia Ltda

ESTUDO AMBIENTAL

DRAGAGEM DO ACESSO AO CANAL DO TOMBA

CARAVELAS/BA

Relatório Técnico HM RT-007-08

VOLUME 10/10

Caravelas, abril de 2008

HM Consultoria e Projetos de Engenharia Ltda
Alameda das Grevíleas, 420 – Vinhedo – SP – CEP 13280-000
Tel: (19) 3826-1204 – Cel.: (19) 9743-7134 – E-mail: hm@hmengenharia.com

ANEXO S – 2ª Parte

- Second Opinion on the Caravelas Channel Dredging Maintenance Assessment – Cepemar/CPE - 2004
- Channel Maintenance Programme: Numerical Modelling of Sedimentation Processes – DHI - 2006
- Taxas de Sedimentação e Alternativas de Dragagem para o Canal de Acesso a Barra do Tomba, Caravelas-BA – Cepemar/CPE - 2006

COASTAL PLANNING & ENGINEERING, INC.

ENGINEERING REPORT

SECOND Opinion on the Caravelas Channel Dredging Maintenance Assessment

Submitted
December 2004

Prepared for
Aracruz Celulose

ARACRUZ

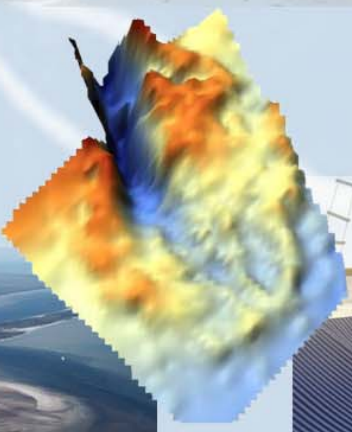

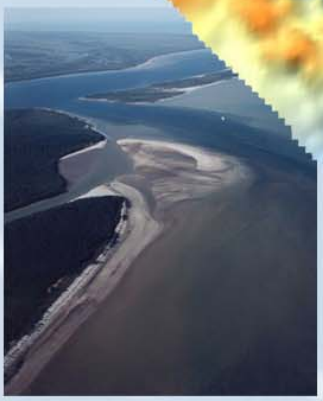

Planning

Engineering

Geotechnical Services

Environmental Services

GIS and Mapping Services

Survey Operations

CEPEMAR

CPE®
WWW.COASTALPLANNING.NET
COASTAL PLANNING & ENGINEERING, INC.

2481 N.W. Boca Raton Blvd. | Boca Raton, FL 33431 | phone 561.391.8102 | fax 561.391.9116 | mail@coastalplanning.net

SECOND OPINION ON THE CARAVELAS CHANNEL DREDGING MAINTENANCE ASSESSMENT

Prepared for

Aracruz Cellulose Inc.

Prepared By

Coastal Planning & Engineering Inc.
Thomas Campbell, P.E.
Lindino Benedet
Gordon Thompson, P.E.
Christopher Day, P.E.

CEMEPAR Environmental Services
Nelson Saldanha
Jim Miller

December, 19th, 2004

EXECUTIVE SUMMARY

CEPEMAR and CPE (Coastal Planning & Environmental *Inc.*) were contracted by Aracruz Cellulose SA in October 2004 to perform coastal engineering services. This project is a second opinion to evaluate dredging maintenance requirements for the Barra do Tomba channel, located at the mouth of Rio Caravelas, in the southern part of the State of Bahia.

The study described in this report used guidance and predictive capabilities of numerical models, supplemented by measured performance data, geomorphic historic-evolution trends, and the expertise of a multi-disciplinary team to provide the second opinion recommendations. The main results include:

- Historically a large ebb-shoal developed offshore Boca do Tomba. This shoal accumulated about 14 million m^3 of sediments since the inlet breached in the early 1960s. Sources that contributed to the ebb shoal growth include channel development (widening and scouring) alongshore sediment transport, river bank erosion and river sediment load. Historically about 226,000 m^3/yr were supplied into the channel/ebb shoal system offshore Boca do Tomba from sources other than channel development.

- Based on multiple lines of evidence we recommend that, to maintain the Tomba channel navigable for the following years, dredging maintenance volumes in the order of 200,000 m^3/yr (+/- 50,000) are required between channel stations 2000 m and 5000 m offshore. Intensification of dredging is required in problematic areas such as the 1 km stretch between channel stations 3000 m and 4000 m, where sedimentation is higher and navigation is currently problematic. Maintenance dredging is not required in the channel throat section (landward of station 2000 m) and very low requirements exist offshore of station 5000 m.

- High channel sedimentation rates occur mainly due to:

(a) Diffusion (backfilling) of sediments from the ebb-shoal into the channel.

(b) Wave-induced gross alongshore sediment transport.

(c) Channel migration.

- The Boca to Tomba channel is '*stable'* (self-scouring) in its throat section (landward of channel station 2000 m) but it is not self-scouring in the nearshore zone (between stations 2000 m and 5000 m) where the channel flows reduce and sandy sediments deposit. Material shoaling in the channel zone where sedimentation is higher (between stations 3000 and 4000 m) is predominantly sand.

INTRODUCTION

CEPEMAR and CPE (Coastal Planning & Environmental *Inc.*) were contracted by Aracruz Cellulose SA in October 2004 to perform coastal engineering services. This project is a second opinion to evaluate dredging maintenance requirements for the Barra do Tomba channel, located at the mouth of Rio Caravelas, between Ponta da Baleia and Ponta do Catoeiro, in the southern part of the State of Bahia (Figure 1).

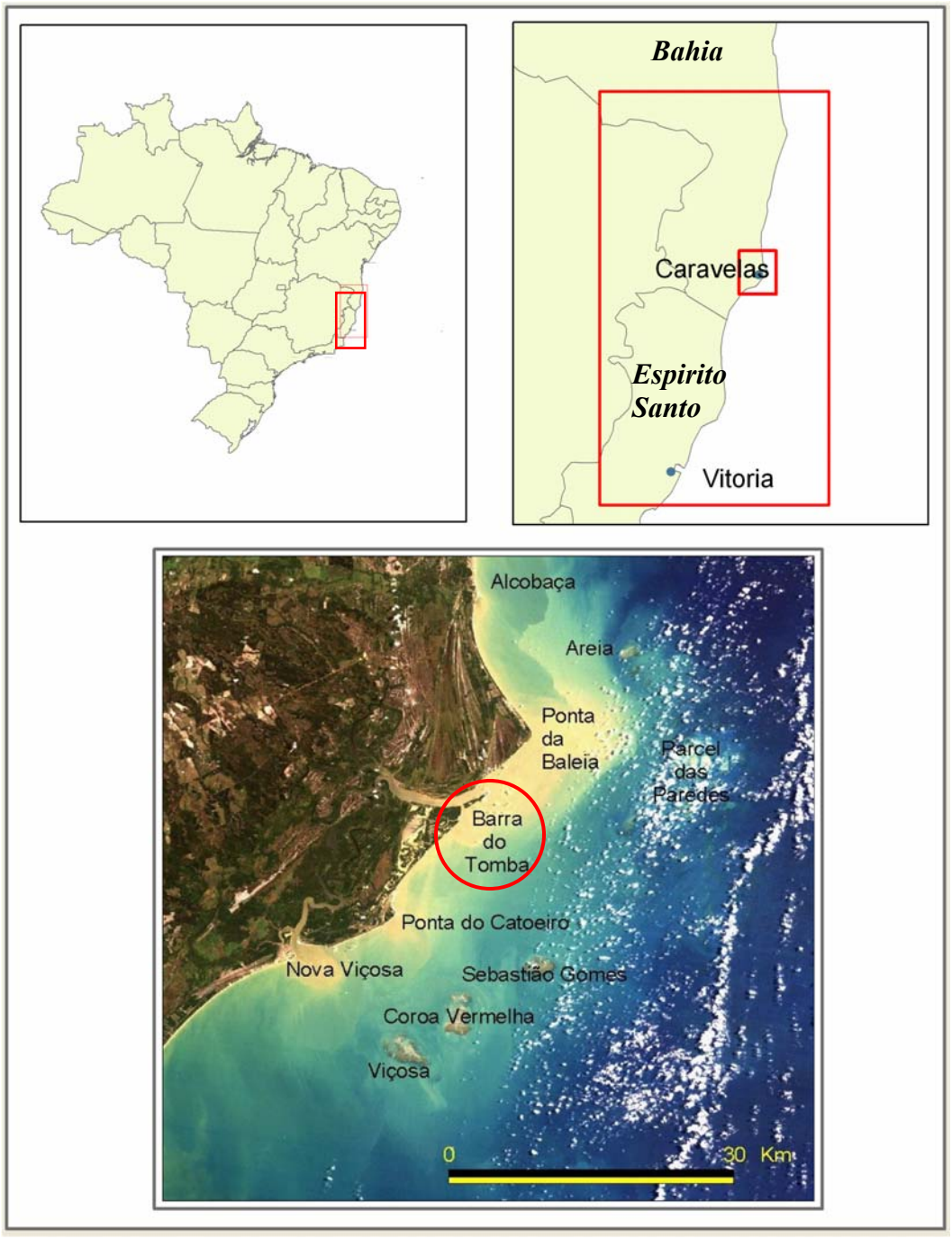

Figure 1. Location of the study area (red box) in relation to major coastal features.

Specific tasks performed in this work include:

(1) Geomorphic evaluation of the study area.
(2) Analysis of the historical evolution of the inlet, ebb-shoal and adjacent shorelines.
(3) Analysis of equilibrium and stability dimensions of the inlet and ebb-shoal.
(4) Volumetric analysis of channel and ebb-shoal bathymetric surveys, and beach profiles monitoring surveys.
(5) Analysis and modeling of measured waves for the period of January 2002 to September 2004 using the STWAVE (STeady State spectral WAVE) model.
(6) Modeling of alongshore sediment transport using GENESIS (GENEralized Model for SImulating Shoreline Change) and sediment transport estimates using analytical equations.
(7) Elaboration of a regional sediment budget and sediment budget modeling using the RESERVOIR model.
(8) Design channel analysis.
(9) Identification of potential alternatives to reduce future dredging costs

IDENTIFICATION OF THE PROBLEM

The Barra do Tomba channel was dredged from February 2002 to August 2004 to provide navigable waters for the Aracurz Cellulose Marine Terminal at Caravelas. The excavation of the channel was took longer that it was expected and required removal of almost twice the volume of material that was estimated. Sedimentation (shoaling) in the channel during construction was higher that had been predicted by hydrodynamics and sediment transport studies conducted by DHI (1998, 2000).

The purpose of this study is to provide a second opinion of future maintenance dredging needs for the Boca do Tomba channel. This second opinion work, conducted by CPE-CEPEMAR is based on the comparison of design predictions with monitoring data, geomorphic and historic evaluation of the study site, additional numerical modeling, and elaboration of an updated sediment budget for the project area. It is the intent of this study to update the previous DHI studies using current measured performance (monitoring) data to project future dredging requirements for Boca do Tomba in order to secure a safe navigable channel.

STUDY AREA

Geology/Geomorphology

The geology of the southern Bahia coast is dominated by Tertiary deposits (Barreiras Formation) and Quaternary sediments (coastal sand, mud, swamps, mangroves, *etc.*). In Caravelas, the coastal plain is wider than to the north and south, reaching widths of about 15 km. Quaternary sediments formed in response to climatic-sea-level fluctuations cover the Caravelas region (Martin *et al.*, 1980), including Pleistocene and Holocene marine sediments, lagoonal sediments, swamps and mangroves (Figure 2).

Figure 2. Geologic map of the study area showing the distribution of major sedimentary deposits and features (modified from Andrade, 2000).

Marine Pleistocene terraces occur generally inland at elevations of 6 to 11 m above NR (*nivel de referência* or 0 DHN). These terraces are composed of coarse sand, white to brown in color

and well sorted, similar to the sediments found in the northern bank of the Boca do Tomba. Holocene marine sediments occur at elevations of a few centimeters up to 6 m above NR (0 DHN). They are composed of fine sands, well sorted, yellow colored and similar to the sands updrift of the Boca do Tomba channel (Ilha da Caçumba). Along the coast, Holocene deposits have limited thickness (about 3 m) and overlie gray colored plastic muds of marine origin. These gray muds occur in the nearshore zone as relict sediments, ranging in age from 7500 to 3900 YBP (years before present) (Andrade, 2000). Lagoonal sediments occur about 1 m above NR and are composed of gray to brown mud with inclusions of organic debris such as oyster shells and other types of shellfish remains.

Tidal swamps and mangrove stands dominate the coast up- and downdrift of Boca do Tomba (Figure 2). These mangrove stands and swamps occur landward of the beaches. Sediments of the swamp-mangrove platforms are mainly plastic muds (silty-clay sediments), rich in organic matter (trees and shellfish fragments). Exposures of mangrove trees and sediments occur along the beach updrift of the Boca do Tomba channel (Ilha da Caçumba) (Figure 3). These exposures are geo-indicators of accelerated erosion of the shoreline along Ilha da Caçumba. Holocene sandy sediments of limited thickness occur along the beaches, as evidenced by shallow exposure of mangrove muds. Sand thickness, however, increases towards the Boca do Tomba channel.

Figure 3. Southward view of the beach at Ilha da Caçumba, 1 km south of the Boca do Tomba channel, showing dead mangrove trees and exposure of plastic muds on the mangrove platform lying below the regressing beach.

Prominent geomorphic features in the study area include the Ponta do Catoeiro south of Boca do Tomba and Ponta da Baleia to the north. These cuspate forelands are built up by sandy beach ridges accumulations. These types of cuspate forelands commonly form where there are offshore bathymetric highs that protect the coast from direct wave attack (shelter zones). Beach ridge

accumulation and advancement seaward commonly occurs in response to sea-level fluctuations combined with pulses of sediment supply. Previous studies (CEPEMAR, 2001; DHI, 2000) describe the predominant littoral drift direction as north-to-south north of Ponta da Baleia and from south-to-north south of Ponta da Baleia, indicating that Ponta da Baleia is a littoral drift divider that separates two distinct littorall cells. This littoral drift pattern emerges due to changes in shoreline orientation (from NW-SE north of Ponta da Baleia and SW-NE from Ponta do Catoeiro to Boca do Tomba) and from wave sheltering effects from offshore reefs.

Between Ponta do Catoeiro and Boca do Tomba, geomorphic indicators such as headland advancement to the north (Ponta do Catoeiro) and spit growth to the north (Barra do Sul) confirms the direction of predominant littoral drift (south to north) in this segment.

2. Inlet History and Geomorphology

The Boca do Tomba Inlet was breached in the early 1960s due to natural shoreline recession, combined with human-induced changes. Prior to that in the late 1950's the Boca do Tomba channel was a interior tidal creek (Figure 4) separated from the Atlantic Ocean by a thin strip of beach.

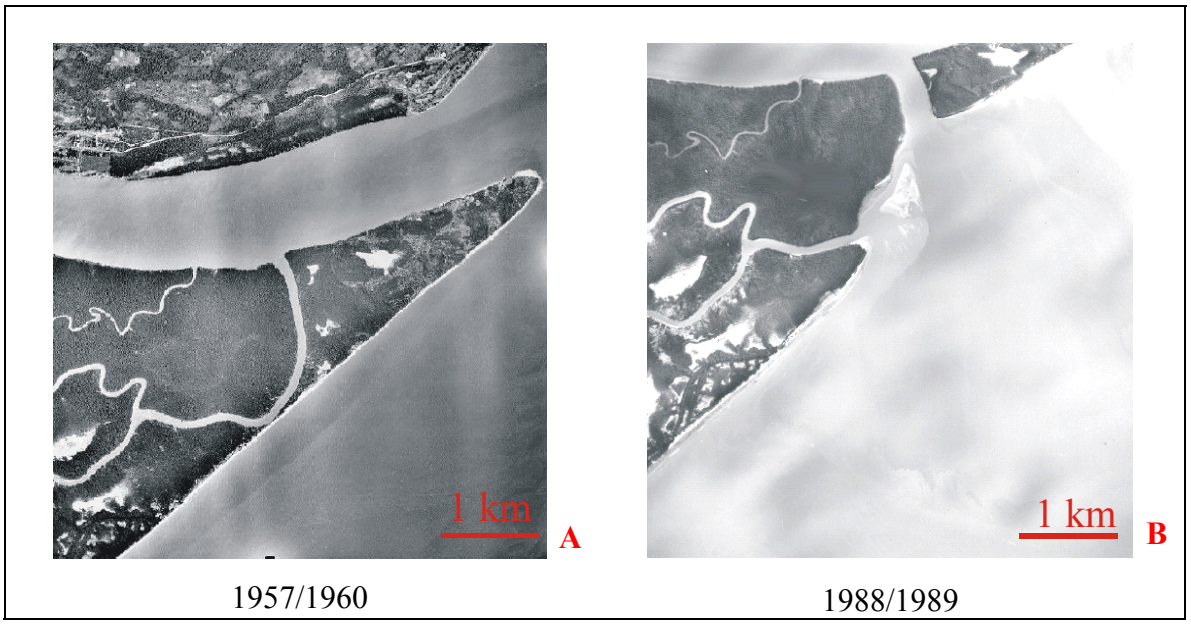

Figure 4. Vertical aerial photos of the Boca do Tomba area before and after inlet development. Photo A was obtained from 1957 to 1960 and displays a straight shoreline backed by tidal creeks. At the Boca do Tomba inlet, a very narrow beach (arrow) separates the Atlantic Ocean and the tidal channel. After inlet opening (Photo B), the shoreline downdrift of the inlet receded about 500 m and a large section of the updrift shoreline disappeared.

According to local fishermen, the inlet was breached artificially. A small channel was manually shoveled across the narrow beach to open a short cut to the Atlantic Ocean for small fishing boats from the communities of Ponta da Areia and Caravelas. After artificial opening, the inlet captured part of the tidal prism (flow volume), and became wider and deeper while a large ebb-tidal shoal (offshore sand bar) formed offshore. Recent analyses by CEPEMAR (2001) and DHI (2002) indicate that Boca do Tomba is now the dominant inlet for Rio Caravelas, capturing most of the tidal prism of the area.

The historical erosional trends in the area (*e.g.* Anderson, 1994) and aerial photographs shown in Figure 4 indicate that the Boca do Tomba inlet probably would have opened despite help from the local community, but the process was thus accelerated. When an inlet breaches an otherwise straight coast, major coastal realignment and erosion adjacent to the new inlet is commonly observed as the inlet re-adjusts in response to physical forcing (*e.g*. tides and waves). Morphological components typical of most inlets around the world are shown diagrammatically in Figure 5 viz. ebb- and flood-tidal shoals, channel margin linear bars, swash bars, bypassing bars, *etc.* The ebb-tidal shoal accumulates sandy sediments seaward of the inlet throat. This sandy feature is formed primarily by ebb-tidal currents depositing sediment in the ocean. The ebb current has higher velocities in the inlet throat, but the current slows as it enters the larger water body (loss of hydraulic gradient) depositing the sediments. Waves and longshore currents then modify the shape of the shoal to semi-circular bar features.

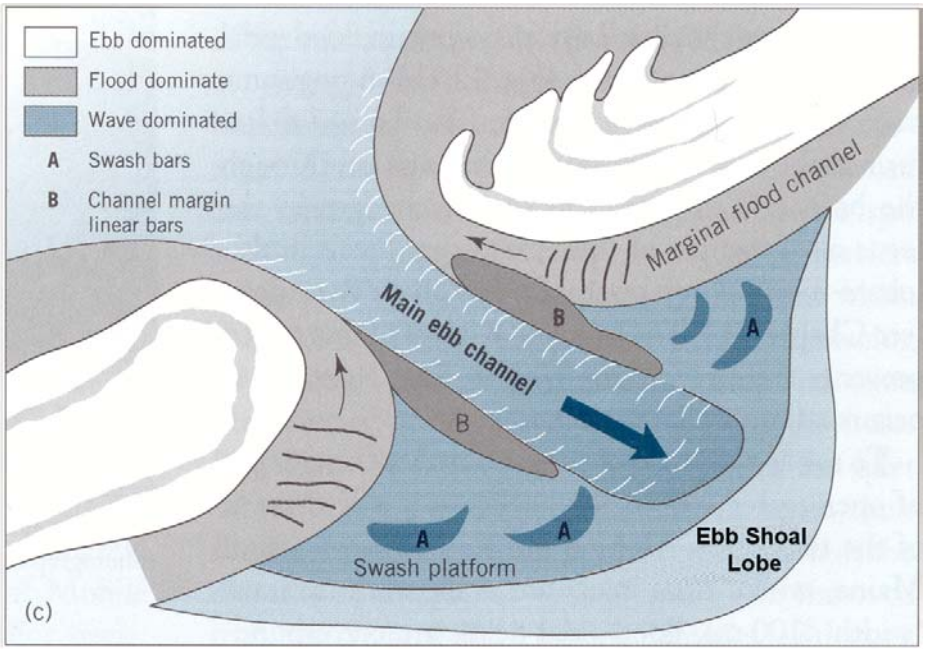

Figure 5. Morphological components of a typical tidal inlet (after Davis and Fitzgerald, 2004).

Various morphologic models and classification schemes have been proposed for tidal inlets (*e.g.* Walton and Adams, 1976; Hayes 1980; Fitzgerald, 1996; Hicks and Hume, 1996). These models are mainly a function of tidal and wave forcing in a given location (Figure 6) and can provide an indication of equilibrium sizes and locations of the inlet's morphological features. The notion of tide- and wave-dominance has been applied, for example, to the morphology of tidal inlets in the Georgia Bight by Hubbard (1977) and in the German Bight by Nummedal and Fischer (1978). Flood shoals are well developed along wave dominated coasts, but absent or under developed in tide-dominated environments such as Boca do Tomba. Ebb-shoals occur close to the inlet mouth (*i.e.* 200 to 800 m) when the effects of littoral drift exceed the effects of tidal currents (wave dominated inlets), but they occur further offshore (*e.g.* up to 5 km) when the effects of ebb-tidal currents exceed the effects of waves (tide-dominated inlets, Figure 6). Tide-dominated inlets typically have a deep central channel (ebb dominated) flanked by extensive channel-margin bars and ebb-shoals, similar to the morphology observed at Boca do Tomba.

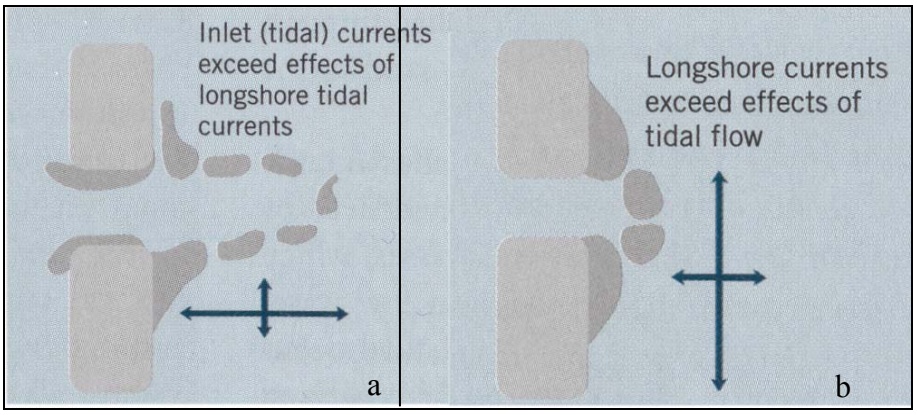

Figure 6. Schematic diagram showing differences in ebb-shoal morphology for inlets that are tide dominated (a) and wave dominated (b). The Boca do Tomba inlet has a morphology that approximates tide-dominated inlets. Navigation problems at these inlets tend to occur further offshore in contrast to wave dominated inlets that have ebb-shoals interrupting the channel closer to the shore.

The ebb-shoal at Boca do Tomba delta extends about 3.5 km offshore and exhibits an overall fan-shape with long channel margin bars, a semi-circular outer bar (outer lobe), and channel migration scars (Figure 7).

In tide-dominated inlets, navigation problems due to shoaling occur where the ebb-shoal bypasses the channel and transfers sediments in the form of bypassing bars. Sediments that formed the Boca do Tomba ebb-shoals originated mostly from adjacent shorelines. After inlet opening, the downdrift island (Barra do Sul) eroded more than 500 m landward. The updrift island eroded at rate of about 5.45 m/yr (Anderson, 1994). Erosion of sediments from adjacent shorelines plus inlet scouring and episodic input from riverine sources contributed to the formation of a major ebb-tidal shoal off Boca do Tomba (Figure 7). The ebb-shoal shown in Figure 7 currently stores about 14 million m^3 of sandy sediments.

3. Waves, Tides, Winds and Currents

Wind measurements obtained from the National Institute of Meteorology Station in Caravelas, Bahia, indicate that NE winds are predominant from August to April with peak mean velocities of 4 m/s (during November) and from the S-SE from May to July with peak mean velocities of 2.8 m/s in July. Mean monthly precipitation fluctuates from 63 mm (24 inches) from September to February to 203 mm (79 inches) in November. Rainy seasons occur from March to May and from October to December, the latter being more intensive.

Directional wave characteristics were compiled from nearshore wave measurements obtained from 2002 to 2004 by CEPEMAR. Offshore waves propagate most frequently from the south-southeast to south (about 60% of the waves). Average wave heights are 0.37 m with a respective peak period and direction of 6.9 s and 153 degrees. Due to the large percentage of waves propagating from these direction bands, the net longshore sediment transport is from southwest to northeast. Winter cold fronts generate nearshore waves up to 2 m height from the southeast. Winter waves propagate from the south-southeast (162 degrees), exhibiting an average wave height of 0.39 m and a peak period of 7.6 s. Wave climate and wave propagation nearshore is further discussed in the wave modeling section of this report.

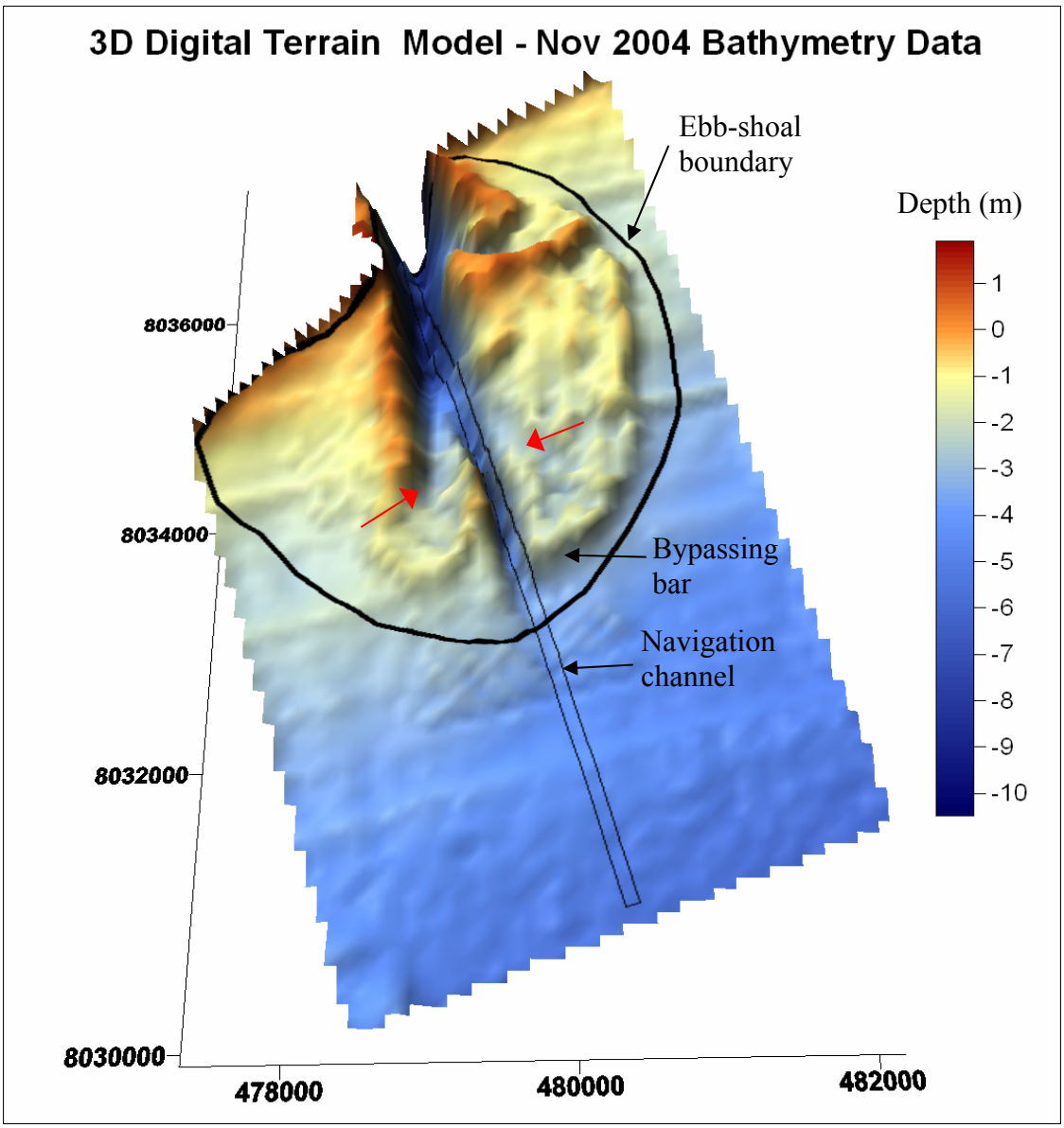

Figure 7. Digital terrain model of the Boca do Tomba inlet and ebb-shoal complex showing ebb-tidal delta morphology in relation to dredged channel. Note that the navigation channel has minimum width near the distal margin of the ebb-shoal where sediments historically bypassed the channel as a semi-circular bar. The red arrows point to scour holes that are remnants of seasonal channel migration.

Based on the balance between incident waves and tides in the area, the Caravelas coast can be classified as a "mixed-energy coast" in the Davis and Hayes Scale (Davis and Hayes, 1983). On mesotidal coasts with moderate waves (mixed-energy coasts) such as Boca do Tomba, ebb-tidal deltas are considerably larger than flood-tidal deltas.

CEPEMAR (2001) conducted current measurements in the new Boca do Tomba channel and the old channel. During May-June 2000, maximum spring current speeds were 1 m/s whereas maximum neap current velocity was 0.5 m/s Boca do Tomba channel. During April 2001, maximum spring current velocities of 1.4 m/s were measured at Boca do Tomba while current

velocities of 0.8 m/s were measured in the old channel; somewhat stronger currents were measured during ebb flow.

Tides in the study area are semi-diurnal with an average spring tidal range around 2.6 m (mesotidal) and a neap range of 1.2 m. Tides in the Caravelas region have larger amplitude than to the south (*e.g.* Mucuri) or to the north (*e.g.* Ilheus). Tidal Datums in the area are shown in table 1. The previous consultant (DHI, 2000) used as a reference the datum CD (chart datum) of Nova Viçosa which according to DHI (2000) is roughly equivalent to MLWS.

Table 1. Tidal datums in the study area.

Datum	Elevation above 0 m DHN (in meters)
MLWS (Mean Low Water Springs)	0.3
MHWS (Mean High Water Springs)	2.9
MLWN (Mean Low Water Neap)	1.0
MHWN (Mean High Water Neap)	2.2
MSL (Mean Sea Level)	1.6 m.

SEDIMENTATION PROBLEMS (SHOALING) IN NAVIGATION CHANNELS

Analytical and empirical relationships have been developed in the past to predict channel shoaling (*e.g.* Vincent and Uva, 1984). Channel shoaling is the result of a balance between riverine/tidal processes, sediment supply and littoral processes (*i.e.*, waves and coastal currents). For each zone of the inlet, the interactions of the different sediment transport processes conspire to produce shoaling trends that are similar in most inlets around the world. Channel and ebb-shoal migration, natural sand bypassing, sand shoaling across the ends of the entrance structures, side slope failure, river sedimentation *etc*. are common inlet shoaling problems. Dredging of coastal inlet navigation channels is typically greatest in the vicinity of the "entrance channel" or the outer ebb-shoal bar (*e.g.* Rosati, 2003; Pope, 2000).

Rosati (2003) indicates that deepening and/or widening of inlet channels generally increases the dredging rate of a given area. She indicated that annual maintenance rates of dredged navigation channels have a direct correlation with the deficit of sediment in the channel (defined as the difference between the natural channel and dredged channel volumes). In other words, Rosati (2003) demonstrated that annual maintenance rates are directly proportional to capital dredging volumes. For example, if two channel layouts are evaluated, Layout 1 that requires 300,000 m^3 of dredging and Layout 2, which requires 600,000 m^3 of dredging, the annual maintenance volumes of Layout 2 would be twice that of Layout 1 even though physical forcings (waves and currents) remained generally the same.

Some of channel maintenance rates presented by Rosati (2003) are as much as three times higher than the local littoral drift rates of a given area. For example, Pensacola Pass, Florida, experienced an annual maintenance dredging rate of 424,00 m^3/yr after deepening, about 2.5 times higher than the pre-deepening dredging rate; and about 4 times higher than the local net littoral drift rates of the coastal area. The author attributed the excess channel infilling volume to diffusion (backfilling) of sediments from the ebb-shoal to the channel. The principle behind this effect is that a deepened, widened, and lengthened channel is out of equilibrium when compared to its natural state. After a channel is dredged, it tends to return to its natural dimensions that are in quasi-equilibrium with inlet processes resulting in excess shoaling of the dredged area.

Pope (2000) discussed and classified the most commonly observed shoaling problems in inlets. Channel shoaling mechanisms include channel migration, morphodynamic pathways of ebb-shoals and bars, loss of hydraulic gradient, channel abandonment, bed form regimes, regional siltation and geotechnical failure (*e.g.* Figure 8).

Channel migration is the lateral movement of a channel due to the natural flow regimes or development of shoals in the deltas or spits in the mouth. Channel migration is evidenced by shoaling on one side of the thalweg as the other side of the channel erodes. A seasonal channel migration is observed at Boca do Tomba and further discussed in this report.

Ebb-shoals and bars develop and migrate as sand bypass navigation channels to feed adjacent shorelines. As sand moves along the coast, the material will cascade into the dredged channel depression at high rates, causing a localized and distinctive feature that frequently reappears after removal. This type of shoaling is localized near the outer lobe of the ebb-shoal, which occurs between the -2m and the -3m contour offshore Boca do Tomba.

Loss of hydraulic gradient also contributes to shoaling near the end of the ebb-shoal. In this zone, the currents that transport the sediment decrease velocity and the sediment is deposited. This frequently occurs where the channel or confining banks widen or when the current field meets some energy-dissipating force (*e.g.* waves). The result is usually a localized area of rapid deposition where a recognizable shoaling feature evolves. This is the primary mechanism behind the growth of ebb-shoals and river deltas.

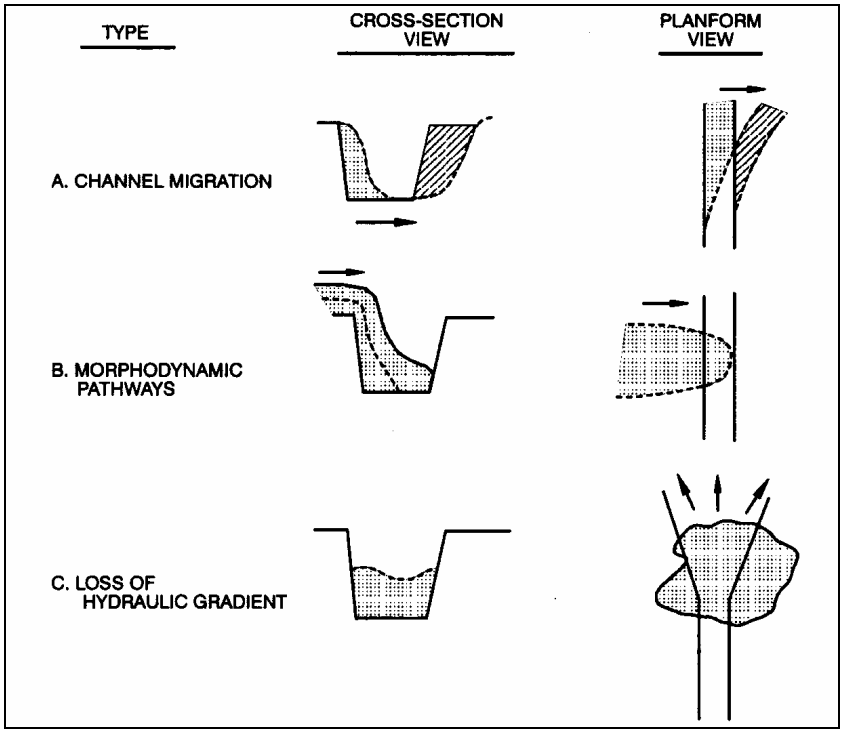

Figure 8. Common shoaling problems observed at Boca do Tomba.

Typical inlets have four major regions: an offshore, nearshore, inlet mouth, and inland water body. These regions are defined for Boca do Tomba in Figure 9. Navigation problems can occur ain any of these regions; however, at Boca do Tomba, they concentrated in the nearshore.

Tidal currents in the inlet mouth and interior water body (landward of channel station 2000 m) are strong enough to continually scour the channel (the channel is predominantly self-scouring from 0 to 2000 m). Episodically, geotechnical failure occurs at the channel mouth of Boca do Tomba, but strong ebb-currents remove sediments from this zone. Additionally, littoral currents driven by waves and local winds transport channel into the channel mouth.

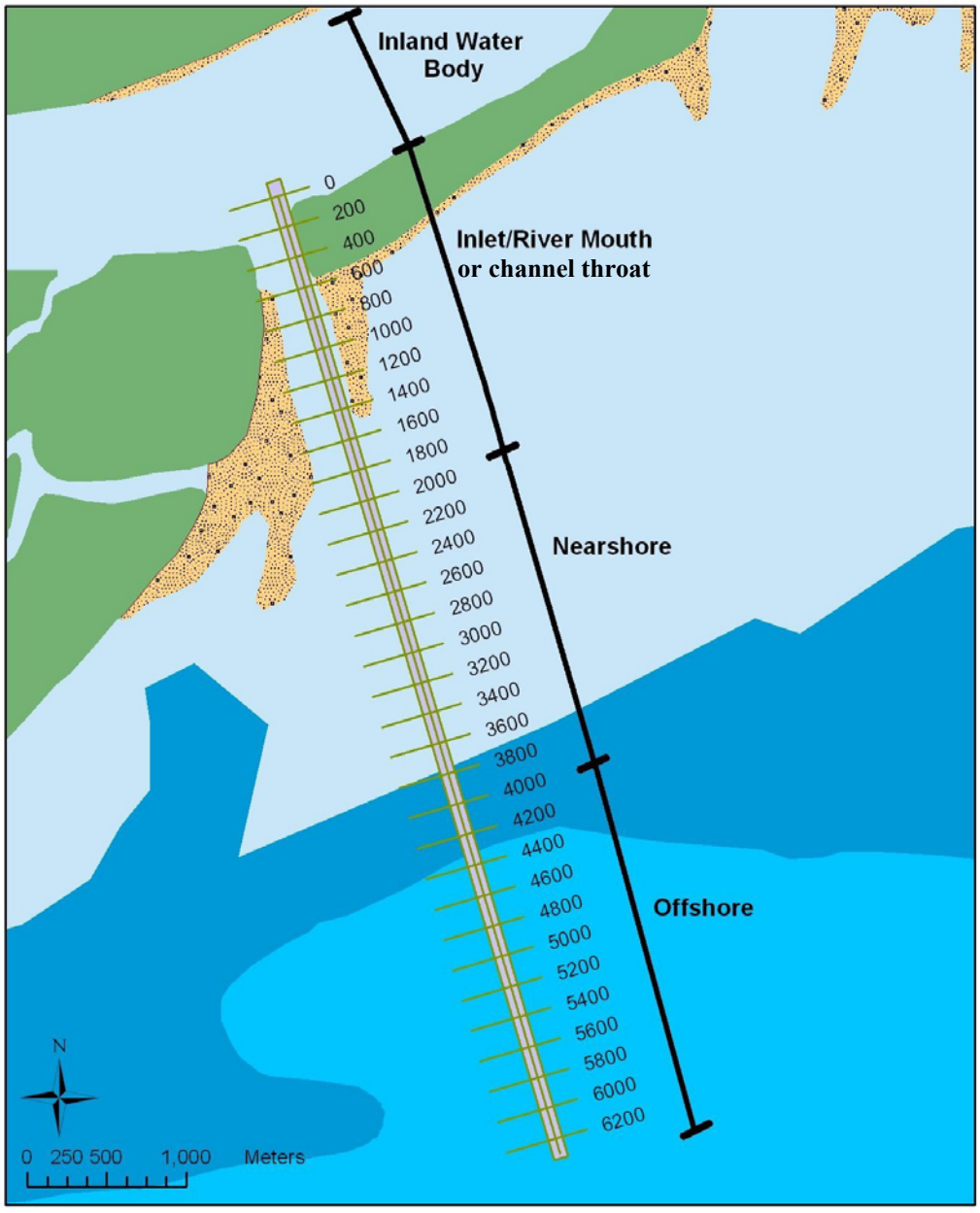

Figure 9. Typical zones of the Boca do Tomba channel. Numbers indicate channel stations measured in meters from the inland water body to offshore.

In the nearshore (between stations 2000 m to 4000 m) and offshore zones (seaward of Station 4000 m), shoaling problems are mainly related to channel migration and movement of shoals (sediment transport along the shoals), loss of hydraulic gradient, and regional siltation. Shoaling

is more pronounced in the nearshore zone and is discussed in other sections of this report. As described by Pope (2000), shoaling associated with a loss of hydraulic head tends occur in channel areas where a constricted flow discharges into a wider water body, for example, at the nearshore where the channel margin linear bars spread into a wider area and do not confine the channel as they do in the channel mouth section. Channel migration, morphodynamic pathways (migration of shoals), and channel abandonment are characteristic of areas that experience a changing balance in tidal/riverine processes and coastal transport processes such as occur in the nearshore zone. Regional siltation occurs mostly in the offshore zone.

Quantification of the magnitudes, rates, and patterns of geomorphic changes is central to sediment budget calculations, estimation of dredging requirements, and assessments of whether inlet changes have a significant effect on adjacent beaches. Before new construction or modification of existing inlet channels, historic evolution and trends should be understood. Historic evolution of the inlet and ebb-shoal at Boca do Tomba is discussed in what follows.

FIELD INSPECTION

A field inspection was conducted by Thomas Campbell, Lindino Benede of CPE and Henrique Frasson of CEPEMAR on 18 October 2004. Observations from the field trip include:

Beach Conditions: Beaches up- and downdrift of the channel are severely eroded (see Field Photos 1 and 2). Erosion geo-indicators include clay/peat outcrops on the beachface, and erosion of mangroves by ocean waves. Beaches are generally rolling over on-top of mangroves. In the inner surf-zone (during low tide), sand transitions offshore to plastic mud sediments. At approximately 2 km south of the inlet, the beach is composed of a very thin veneer of sand covering plastic muds. Adjacent to the inlet, sand thickness increases and extends further offshore in the form of channel linear bars. Beaches are generally composed of medium and fine sand with coarser material found on the north side of the channel.

Inlet Conditions: It was verified that the channel is relatively shallow in some segments and that navigation problems are currently experienced around 3 km offshore. Shoals extend long distances perpendicular to the channel (up to 2 km) in the form of channel margin linear bars (see Field Photos 3 and 4). These channel linear bars are striking geomorphic features to the field observer. Breaking wave patters indicated further extension of ebb-shoals and bars up to 3.5 km offshore. The channel margin bars situated on the north side of the channel were composed of coarse sand. Strong currents were observed moving over the north bar to the south (wind and tide induced currents) indicating a potential sediment transport pathway to the channel. Side slopes on both sides of the channel were extremely step (about 1V/3H). Sediment sampling conducted in the field indicated that the deep sections of the channel (*e.g.* 5 m below NR or more) were generally composed of muddy sediments while shallower segments (less than 3 m) were generally composed of sand. Sediment sampling also indicated that sand was shoaling in the area near buoy 6. Additional samples obtained in the ebb-shoal bar (south of the channel) indicated the presence of fine sand on the seabed. No loose muddy sediments were found in shallow segments of the navigation channel indicating that most of the sedimentation problems can be attributed to sand. Interpretation of the geomorphology indicates that the channel section with higher shoaling rates coincides with the general offshore area where ebb-shoal sand bypasses the channel.

Field Photo 1. Test pit 2 km downdrift of the inlet on the beachface showing a thin veneer of sand covering plastic mud

Field Photo 2. Peat exposure and dead mangrove trees, indicating accelerated beach erosion

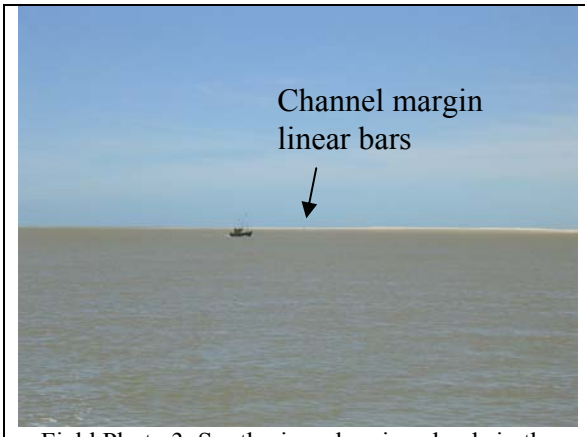

Field Photo 3. South view showing shoals in the form of channel margin linear bars bordering the south margin of the channel.

Field Photo 4. Offshore breaking waves indicating the presence of extensive ebb-shoals

2. Sediment Grain Size of Beach and Inlet System

Historical sediment samples compiled by CEPEMAR (2004) and sediment samples collected during the October 2004 field trip were imported into a GIS database for analysis of seabed sedimentological composition; results are shown in Figure 10.

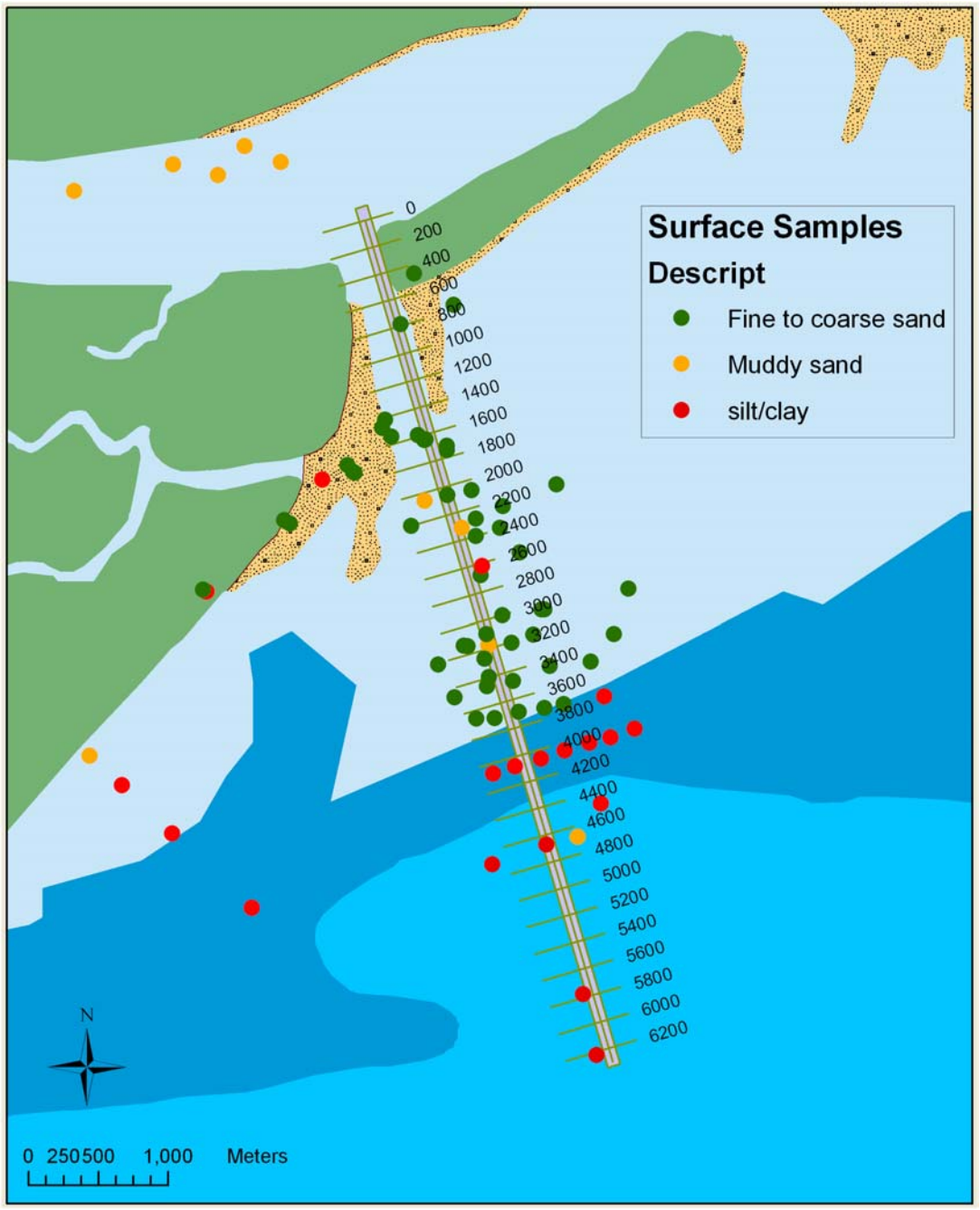

Figure 10. Surface sediment samples at Boca do Tomba.

Figure 10 indicates that the seabed areas adjacent to the inlet throat and the inlet nearshore zone are mostly covered by sandy sediments while the offshore zone is covered predominantly by mud. The inland water body is composed by mixtures of sand/silt and clay here termed *muddy sand*. Sand predominates nearshore (where an ebb-shoal is verified) and where most navigation problems are encountered. There is a sharp transition between the nearshore sand and the offshore mud near channel station 4000 m.

It has been hypothesized by DHI (2004) that excess shoaling in the channel area may be due to the sedimentation of muddy sediments within the channel. To further investigate this

hypothesis, bathymetric surveys with a dual-frequency fathometer (24 kHz and 200 kHz) were conducted in the Boca do Tomba Channel in October 2003. High frequency sensors (*e.g.* 200 kHz) have a distinguishable sound signal return in consolidated and unconsolidated surface (hard bottom, compacted sediments, or loose mud) while low frequency sensors (*e.g.* 24 kHz) will tend to penetrate into loose, unconsolidated, muddy sediments and only return the signal when it meets a consolidated subsurface layer. If mud sedimentation predominated in the channel, a significant difference in elevation between the data obtained with each frequency would be expected (shallower elevations would have been obtained with the higher frequency sensor and deeper elevations would have been obtained with the lower frequency sensor). To evaluate this, the 2000 kHz data and the 24 kHz data were grid separately and then subtracted (200 kHz – 24 kHz) (Figure 11).

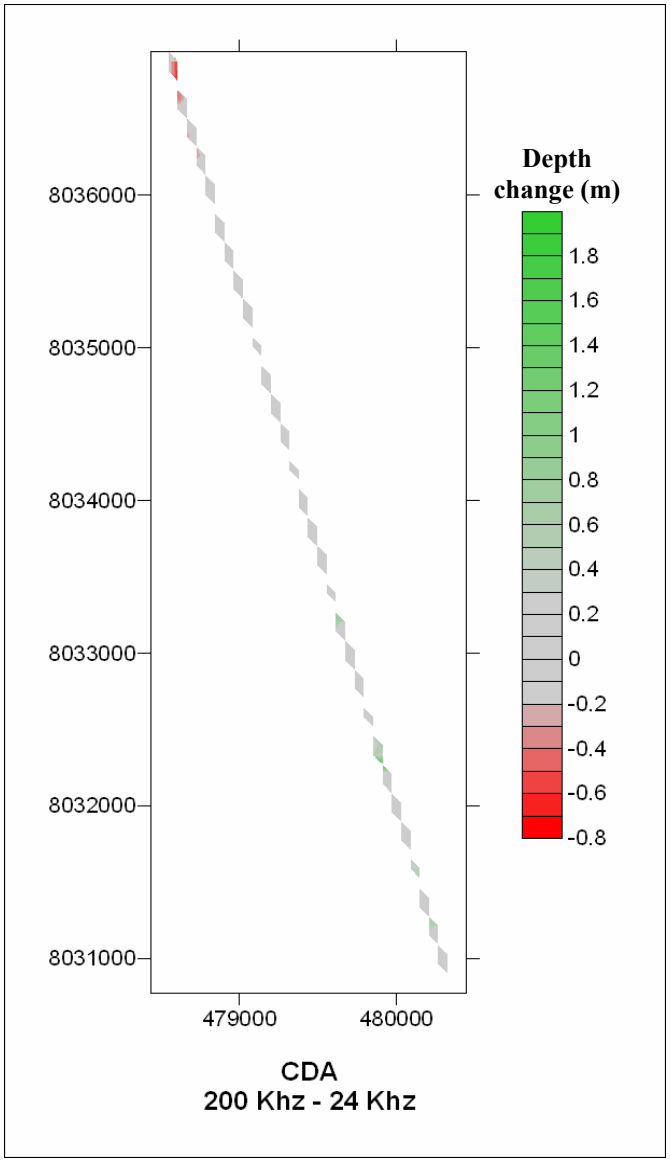

Figure 11. CDA (Change Detection Analysis) between the 200 kHz and the 24 kHz datasets showing no significant change.

Figure 11 indicates that there is no significant change in depth between the two datasets, and that most of the channel area presented a depth change less than 0.2 m as indicated by the gray colors shown in the figure. If mud sedimentation predominated in the channel, most of Figure 11 would appear in shades of green (positive depth change). The areas that indicated the presence of muddy sediments were located in the offshore zone (seaward of channel station 4000 m), as evidenced by localized shades of green. Combined evidence from field inspection, sediment sampling (Figure 10), and dual-frequency bathymetric survey (Figure 11) indicate that sedimentation of muddy sediments is not the problem at the Boca do Tomba channel. Muddy sediments occur exclusively in deep scoured sections of the channel or in the offshore zone where sedimentation problems are minor. The area where most navigation problems are encountered is the nearshore, specifically between channel stations 2000 m and 4000 m. Sediments that predominate in this region are sands that originate mainly from three sources: (1) (1) adjacent beaches, (2) ebb-shoal and local lag-deposits, and (3) episodic riverine input and erosion of river-margin banks.

EQUILIBRIUM RELATIONSHIPS (Cross-Section, Ebb-Shoal, Inlet Stability)

Any given inlet on an open coast is controlled by the balance between forces by flow, waves and sediment transport. An inlet can be said to in constant "dynamic equilibrium". Stability and sediment trapping capacity of tidal inlets have been discussed by many authors (*e.g*. Bruun *et al.* 1978; Walton and Adams, 1976; Hicks and Hume, 1996; O'Brien, 1969; Jarret, 1976).

Stability of tidal inlet can be given in respect to geographical location or throat cross-sectional area. Geographic stability pertains to the lateral migration of channels in response to coastal currents. Geographical migration can be detected by analysis of historical data and channel surveys. Generally, a migrating channel exhibits sedimentation on one side and scouring on the opposite side. Channels can migrate as a whole or in segments. At Boca do Tomba there appears to be seasonal channel migration to the north and to the south (according to seasonal wave climate changes) as shown in Figure 7. Channel migration does not prohibit navigation in the inlet mouth section where ebb currents are strong enough to maintain the required navigation depth. Channel migration is problematic in the nearshore zone, however, where flushing is not sufficient to remove sandy sediments that migrate into the channel.

Previous authors (DHI, 2000; CEPEMAR, 2001) investigated the stability of the Boca do Tomba channel using the throat cross-sectional area stability and tidal prism relationships of O'Brien (1969) and Jarret (1976) (Table 2). These empirical relationships relate the inlet throat (mouth) cross-sectional area to the tidal prism (the volume of water entering or leaving the inlet on ebb and flood tide). The relationships are given by:

$$A_c = (6.6 \times 10^{-5})\, P \qquad \text{(O'Brien, 1969)} \qquad \text{(Eq. 1)}$$

$$A_c = (3.78 \times 10^{-5}) P^{1.03} \qquad \text{(Jarret, 1976)} \qquad \text{(Eq. 2)}$$

where A_c is the equilibrium cross-sectional area (m^2) and P is the tidal prism (m^3). Results presented in Table 2 indicate that the cross-sectional area of Boca do Tomba is close to its equilibrium dimension, while the cross-sectional area at the old channel is significantly larger than its equilibrium dimension. Generally, if the equilibrium area is larger than the existing area, the inlet tends to open. On the other hand, if the equilibrium area is smaller the inlet tends to close. At Boca do Tomba, the equilibrium area is slightly larger than the existing area indicating

that the inlet will remain open and widen. Therefore, the throat section of the channel (the mouth) can be classified as *stable*. At the old river, the equilibrium area is smaller than the existing area, indicating that the inlet throat is unstable and is expected to narrow and shoal.

Table 2. Equilibrium cross-sectional area values from CEPEMAR (2001) and DHI (2002).

	Tomba	**Old Channel**
O'Brien (Cepemar, 2001)	3459 m^2	3822 m^2
Jarret (Cepemar, 2001)	3724 m^2	4128 m^2
Existing (Cepemar, 2001)	3345 m^2	5328 m^2
Stability Ratio	1.1	0.7
O'Brien (DHI, 2002)*	4585 m^2	1825 m^2
Jarret (DHI, 2002)*	4514 m^2	1748 m^2
Existing (DHI, 2002)*	3770 m^2	4317 m^2
Stability Ratio	1.2	0.4

*ebb tide tidal prism and cross-sectional area values were used

A stable cross-sectional area indicates that the flushing capacity of the inlet, at the mouth, is enough to remove sediments transported into the throat section of the channel. It does not indicate however that the same will occur further offshore. Therefore a channel can have its throat section expanding but at the same time experience active shoaling in the nearshore zone where current velocities are not strong enough to remove sandy sediments from the channel.

Many studies have also shown that tidal inlets are effective sediment traps or sinks, this is particularly true of sand storage on ebb-tidal deltas, as shown by Walton and Adams (1976) and Hicks and Hume (1996). Similar to the empirical relationship between inlet cross-sectional area and tidal prism, these researchers were able to establish an empirical relationship between the tidal prism, wave action and the equilibrium size of the ebb-shoal. Ebb-shoal equilibrium size equations are given by:

$$V=6.08\times10^{-3} P^{1.23} \qquad \text{Walton and Adams (1976)} \qquad \text{(Eq. 3)}$$

$$V=1.37\ 10^{-3} P^{1.32}(\sin\alpha)^{1.33} \qquad \text{Hicks and Hume (1996)} \qquad \text{(Eq. 4)}$$

where V is the ebb-shoal volume, P is the tidal prism and α is the angle between the inlet channel and the adjacent shoreline. A spring ebb-tidal prism of 53.9×10^{-6} m^3 was given by CEPEMAR (2001). This indicates an ebb-shoal equilibrium volume of 19,660,000 (Eq. 3) and 18,170,100 m^3 (Eq. 4). Measured ebb-shoal volumes offshore Boca do Tomba are in the range of 14,100,000 m^3 to 16,000,000 m^3 as discussed subsequently. This indicates that more sediment will be trapped in the inlet/shoal system until it reaches its equilibrium volume.

VOLUME LOSSES ASSOCIATED WITH HISTORICAL SHORELINE CHANGES

Accreting sand headlands, river channels and shoals are notable "littoral barriers" for littoral drift sediments. In these zones where shoals and/or protuberances occur, changes in the offshore bathymetry and shoreline orientation generate local drift reversals that affect erosion and sedimentation patterns. Inlet-river channels, on the other hand, are notable sediment traps due to shore-perpendicular (cross-shore) flows and the presence of a depression hole. In the study area

there are many geomorphic features that changed significantly after inlet opening, and that may have significantly contributed to ebb-shoal growth offshore Boca do Tomba. A history of inlet and ebb-shoal development was provided earlier. In this section, volumetric calculations of sediment gains and losses in the inlet, ebb-shoal, and adjacent beaches are described.

Historical mapping conducted by Andrade (1994) demonstrated that Ponta do Catoeiro, formed as a shoreline response to the offshore reef systems (Coroa vermelha, Viçosa and Sebastião Gomes). This feature is accreting at accelerated rates (24.9 m/yr from 1955 to 1988) and therefore acts as a sediment trap for littoral drift sediments. The beach between Ponta do Catoeiro and Boca do Tomba is eroding. Erosion and deposition trends in the study area are shown in Figure 12.

Shorelines changes south of Boca do Tomba inlet were converted into volumes according to the methodology proposed by Rosati and Kraus (1999). The change in shoreline position *y* averaged over a given longshore distance *x* was converted to a volume change by assuming that the beach profile translates parallel to itself over an active depth D_A, given by:

$$D_A = B + D_C \qquad \text{(Eq. 5)}$$

in which B is the elevation of the seaward most active berm relative to a datum, and D_c is seaward boundary of sand transport. The volume change rate (ΔV) is then given by:

$$\Delta V = \Delta y \, \Delta x D_A / \Delta t \qquad \text{(Eq. 6)}$$

where Δy is the measured shoreline change and Δx is the alongshore distance. The active height used for the calculations was 2.5 m for the beaches updrift (south) of Boca do Tomba and 3.5 m for the beaches downdrift (north) of Boca do Tomba. A reduced D_A was used south of Boca do Tomba because the beach is composed by a thin veneer of sand perched on marine mud at very shallow depths. Volumetric results for the Ponta do Catoeiro and the beaches between the Boca do Tomba and the Ponta do Catoeiro are summarized in Table 3.

Table 3. Historical volumetric changes for the shorelines south of Boca do Tomba for the period 1955 to 1988.

	Shoreline Change (m/yr)	Distance (m)	Volume Change (m^3/yr)
Boca do Tomba to Ponta do Catoeiro	-5.45	11,250	-150,000
Ponta do Catoeiro	24.9	2,000	124,500

Table 3 indicates that, historically, Ponta do Catoeiro built up at an approximate rate of 124,500 m^3/yr, while the beach between Ponta do Catoeiro and Boca do Tomba Eroded at a rate of 150,000 m^3/yr.

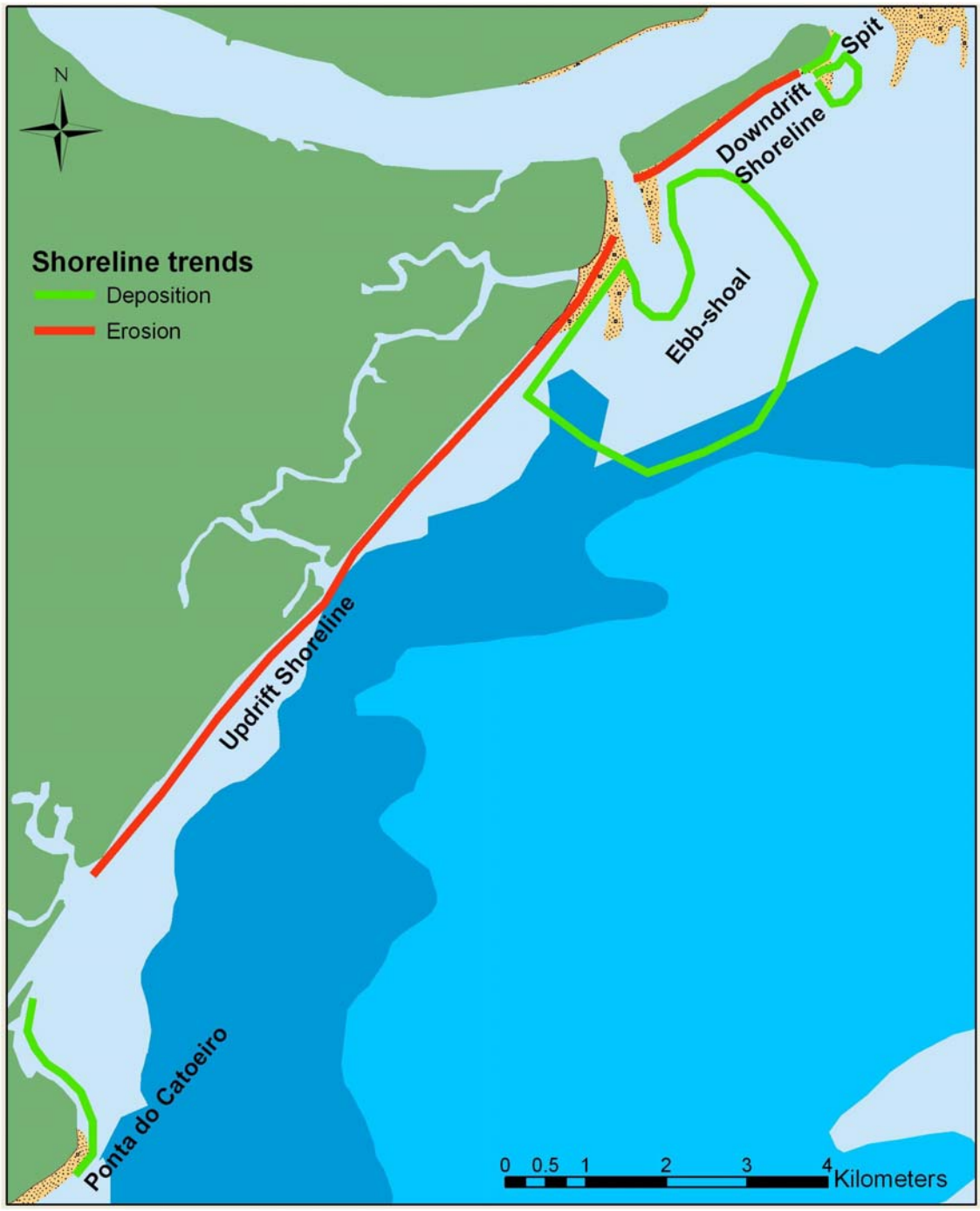

Figure 12. Trends in erosion and deposition adjacent to Boca do Tomba.

The predominant direction of transport between Ponta do Catoeiro and Boca do Tomba is from south to north. Prior to inlet opening, the sediments eroded from these beaches built up the spit where Barra Sul is now located, and on the shoals offshore of the old channel. After opening the inlet, the volume eroded from the beaches to the south (about 153,200 m^3/yr) was deposited in the ebb-shoal offshore Boca do Tomba. Considering that the inlet opened in the early 1960s (DHN nautical charts of 1966 already show the presence of an inlet in the area) it is estimated

that the updrift beaches contributed about 5,800,000 m^3 of sandy sediments to ebb-shoal development. The magnitude of sand trapping at Ponta do Catoeiro is similar to the magnitude of erosion at the beaches between Ponta do Catoeiro and Boca do Tomba, indicating the potential for historical littoral transport rate around 125,000 to 150,000 m^3/yr.

The volume of sediments eroded from the downdrift island (Barra do Sul) was calculated based on digitization of shorelines from DHN nautical charts dated 1966 and 1992. Since 1966, a very large area of the downdrift island adjacent to the Boca do Tomba Channel was eroded, while at the same time period, a sand spit formed in the northern end of the island as shown in Figure 13.

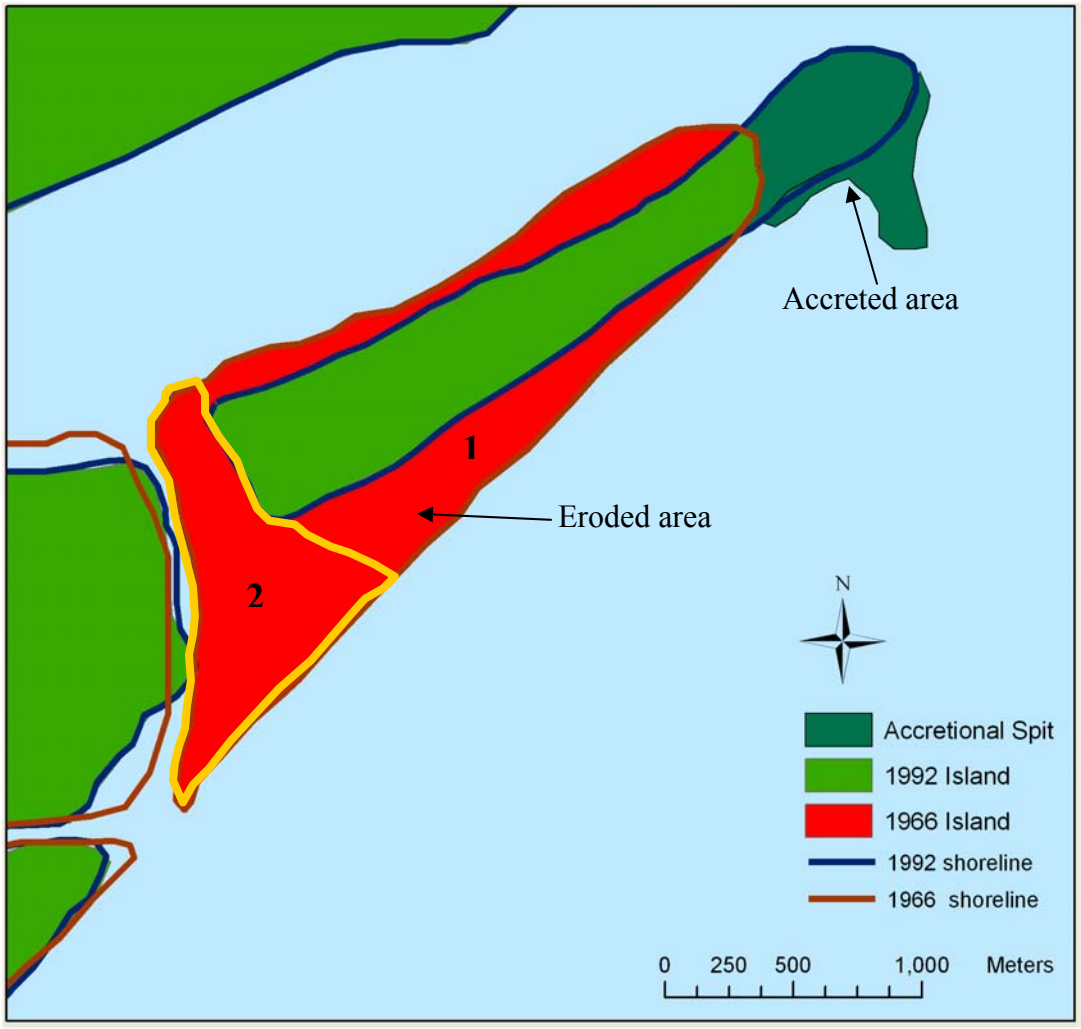

Figure 13. Area change from 1992 to 1966 of the downdrift barrier island (Barra do Sul) situated north of the Boca do Tomba channel.

A large area was lost from the downdrift island (as shown by red colors in Figure 13), adjacent to the inlet. This area lost can be dividided into two components (numbered in Figure 13): (1) sediment starvation as the new opened channel blocked alongshore transport to the north side of the inlet and (2) Inlet formation and scouring (the inlet expanded to achieve equilibrium cross-section and scoured through the existing island). In this section component (1) is

quantified, while component (2) is quantified in the ebb-shoal growth section of this report. It is noticeable from Figure 13 that the island area loss from 1992 to 1966 (red shaded area) exceeds the accretion of the northern spit (dark green area). Sediments that eroded from the downdrift barrier island that did not accrete in the northern spit were transported to the ebb-shoal offshore Boca do Tomba. Therefore, historically, the island north of Boca do Tomba contributed with sediments for the development of ebb-shoal and channel linear bar deposits.

By converting area change rates (erosion of area 1) to volume change rates (see Table 4) it can be observed that, historically, the downdrift island may have contributed about 47,000 m^3/yr of sandy sediments into the Boca do Tomba inlet/ebb-shoal system (Table 4).

Table 4. Area and volume change rates for the island situated north of the Boca do Tomba channel.

	Area (m^2)	Volume (m^3)	Annualized Volume (m^3/yr)
1992 (without spit)	885,600	2,656,900	N/A
1992 acretional spit	387,100	1,161,200	N/A
1966	1,680,842	5,042,526	N/A
Erosion*	-795,242	-2,385,726	-91,759
Deposition*	387,100	1,161,300	44,600
Net change	-408,142	-1,224,426	-47,000

*Erosion was calculated as the difference between the volume of the 1992 island without spit and the volume of the 1966 island. Deposition is equal to the volume stored in the northern spit. An active profile height of 3 m was used for the conversion of areas to volumes.

EBB-SHOAL GROWTH

Volumes stored in the ebb-shoal off Boca do Tomba were calculated using two independent methods: (1) comparing historic bathymetry (digitized from the 1966 nautical charts) with the November 2004 bathymetry and (2) multiplying delta area as mapped from interpretation of seabed geomorphology by the average thickness of sand in the ebb-shoal deposit (sand thickness was obtained from jet probes presented by CEPEMAR (2004).

The comparison of historical bathymetry (1966) with recent bathymetry (Nov. 2004) is shown in Figure 15. It can be seen from Figure 15 that the area in the ebb-shoal experienced overall deposition, with some locations accreting as much as 5 m during this time period while the channel throat (inlet mouth) showed overall scouring. The area that was occupied by the barrier island in 1966 experienced scouring up to 12 m deep, as shown by red shades in the landward portion of Figure 15. The volume changes that occurred between this time period is shown in Table 5.

Table 5. Volumetric changes in the ebb-shoal from 1966 to 2004.

	Volume (m^3)	Annualized volume (m^3/yr)
Shoaling	14,169,000	363,000
Scouring	5,567,000	147,000
Net Change	8,602,000	226,000

Table 5 indicates that, since 1966, about 14,169,000 m^3 of sand accumulated in the ebb-shoal offshore of Boca do Tomba; this corresponds to an annual accumulation rate of sediments in the order of 363,000 m^3/yr. Channel scouring, however, contributed with about 5,567,000m^3 of sediments from the inlet throat and sediment contributed to ebb-shoal growth as well. By subtracting the amount of scouring the amount of ebb-shoal growth, a net volumetric change of 8,602,000 m^3 results, or 226,000 m^3/yr. This historical volume input into the system (226,000 m^3/yr) was supplied to the ebb-shoal by a few potential sources that include (1) erosion of updrift and downdrift barrier islands by littoral currents, (2) erosion of river bank, (3) episodic riverine sediment load, and (4) transport form adjacent shoals (*e.g.* shoal offshore the Old Inlet).

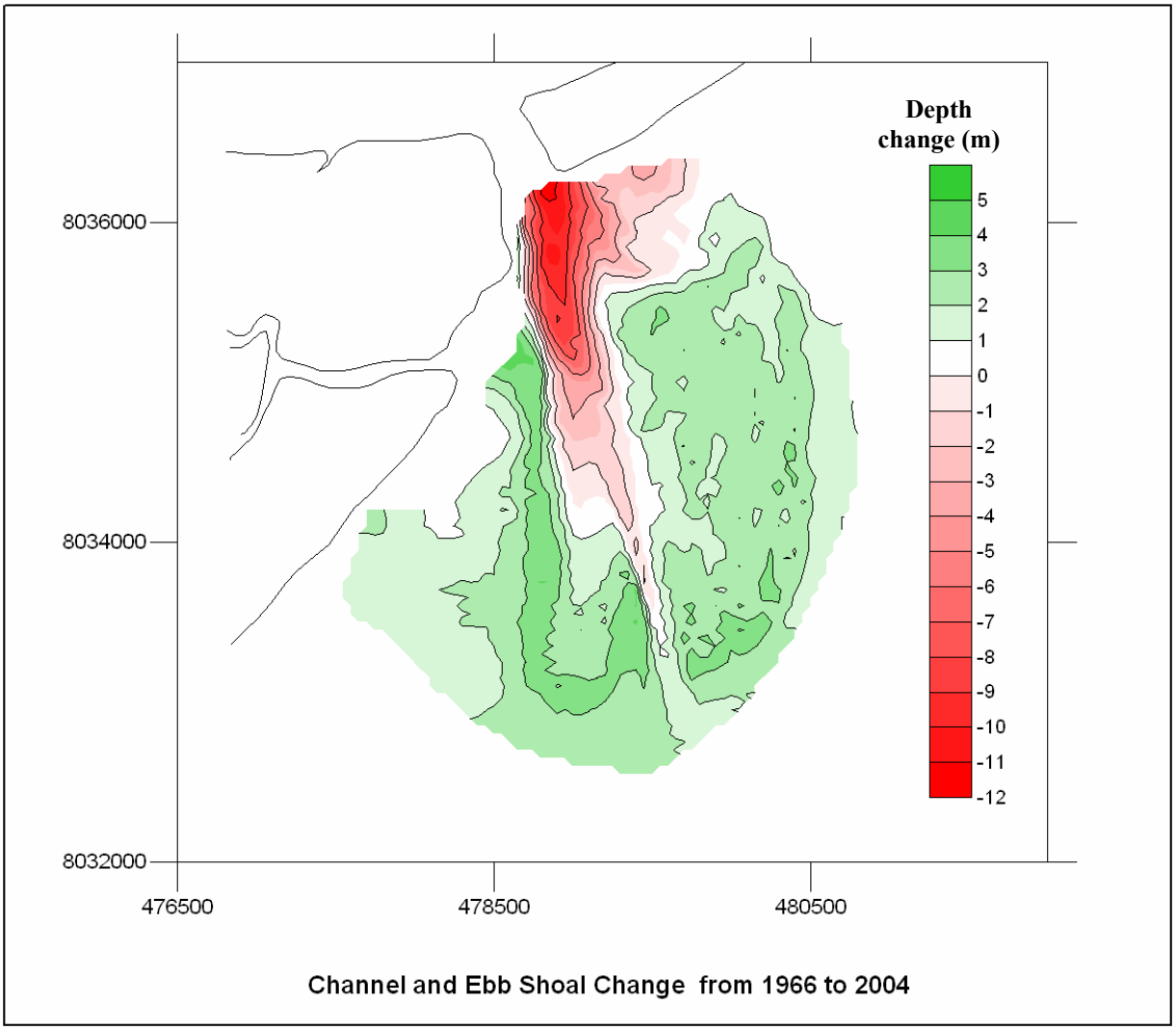

Figure 15. Contour map showing channel and ebb-shoal elevation changes between 1966 and 2004.

The second method used to calculate ebb-shoal volume was multiplying ebb-shoal area, as interpreted from 2004 bathymetric data, by sand thickness in the shoal. Interpreted ebb-shoal boundaries are shown in Figure 16. It was assumed that any surface sand accumulated offshore of Boca do Tomba was due to ebb-shoal growth (prior to inlet opening the offshore was dominated by plastic mud).

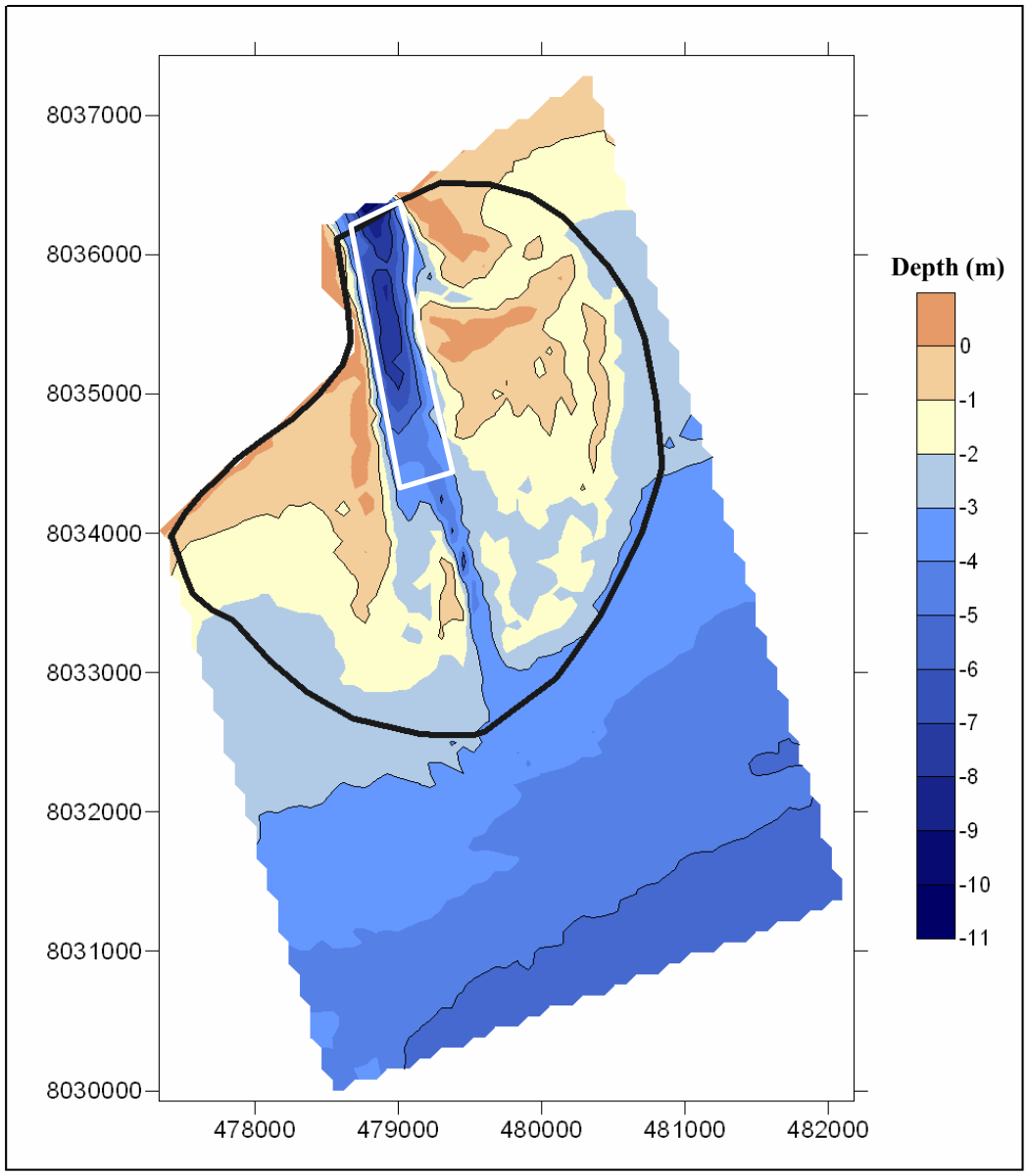

Figure 16. Contour map of November 2004 bathymetric data showing interpreted ebb-shoal boundary (thick black polygon) and channel throat area (thick white polygon).

Thirty-five jet probes were obtained in the channel and ebb-shoal area off Boca do Tomba; these are reported by CEPEMAR (2004). Geologic interpretation of the jet probe data by CEPEMAR (2004) permitted the differentiation of several sediment layers and indicated that a distinguishable surface sand layer occurred on-top of marine mud. This surface sand layer had an average thickness of 1.8 m. A volume of 16,050,000 m^3 of sand was obtained by multiplying the ebb-shoal area (shown in Figure 16) by the sand thickness of 1.8 m. If the channel throat area (shown by the white polygon in Figure 16) is subtracted from the total ebb-shoal area the ebb-shoal volume resultant is 14,650,000 m^3. Ebb-shoal volumes obtained by both methods are therefore in the same range and confirm the magnitude of historical ebb-shoal growth.

DESIGN CHANNEL CONSIDERATIONS

Layout 3 of DHI (2000) channel was about 5 m depth below CD (Chart Datum of Nova Viçosa), in which they indicated that is roughly equivalent to MLWS or 0.3 m above 0 DHN for Caravelas. This corresponds to a channel depth of 4.7 m bellow the Caravelas chart datum. Figure 17 shows the channel conditions for November 2004. All the areas that are not in shades of blue in figure 17 are not up to its design specifications. The green areas are slightly bellow design specifications (0.2 m to 1.2 m shallower) while the areas where shades of orange penetrate into the channel are between 1.2 m to 2.2 m shallower than design expectations. The channel segment between stations 2600 to 4600 is not up to design specifications. Figure 17 illustrated that from 2600 m to 4200 m the adjacent ebb-shoals are migrating into the channel and backfilling it from both sides. Figure 17 shows also that, while the middle section of the channel is in problematic conditions with respect to navigation, landward of station 2000 the channel is wider and deeper than the navigation needs. Offshore of channel station 5000 m there is a zone where channel depths are slightly shallower than 4.5 m bellow 0 DHN, but because the channel bed in this zone is composed predominantly of muddy sediments ebb currents are enough to maintain a constant, navigable elevation.

The most problematic zone, from a sedimentation point of view, is located between stations 3000 m and 4000 m offshore. Channel width with water depths greater than 3.5 m between stations 3600 to 4000, for example, is not wider than 50 m and water depths between stations 3000 m and 3600 m are less than 3.5 m across the channel in some segments. Channel cross-sections were extracted from the November 2004 bathymetries and compared with theoretical design cross-sections with water depths of 4 to 5.5 m bellow 0 DHN. In order to obtain a channel of 90 m wide and 4 m depth NR, a total of 103,330 m^3 of capital dredging is necessary (as per the November 2004 survey). In order to obtain a channel that is 90 m wide and 5 m deep about 418, 300 m^3 of capital dredging would be required. Most of this volume is situated between channel stations 3500 and 4500 m. Channel design cross-sections compared with the November 2004 channel survey conditions are available in Appendix A.

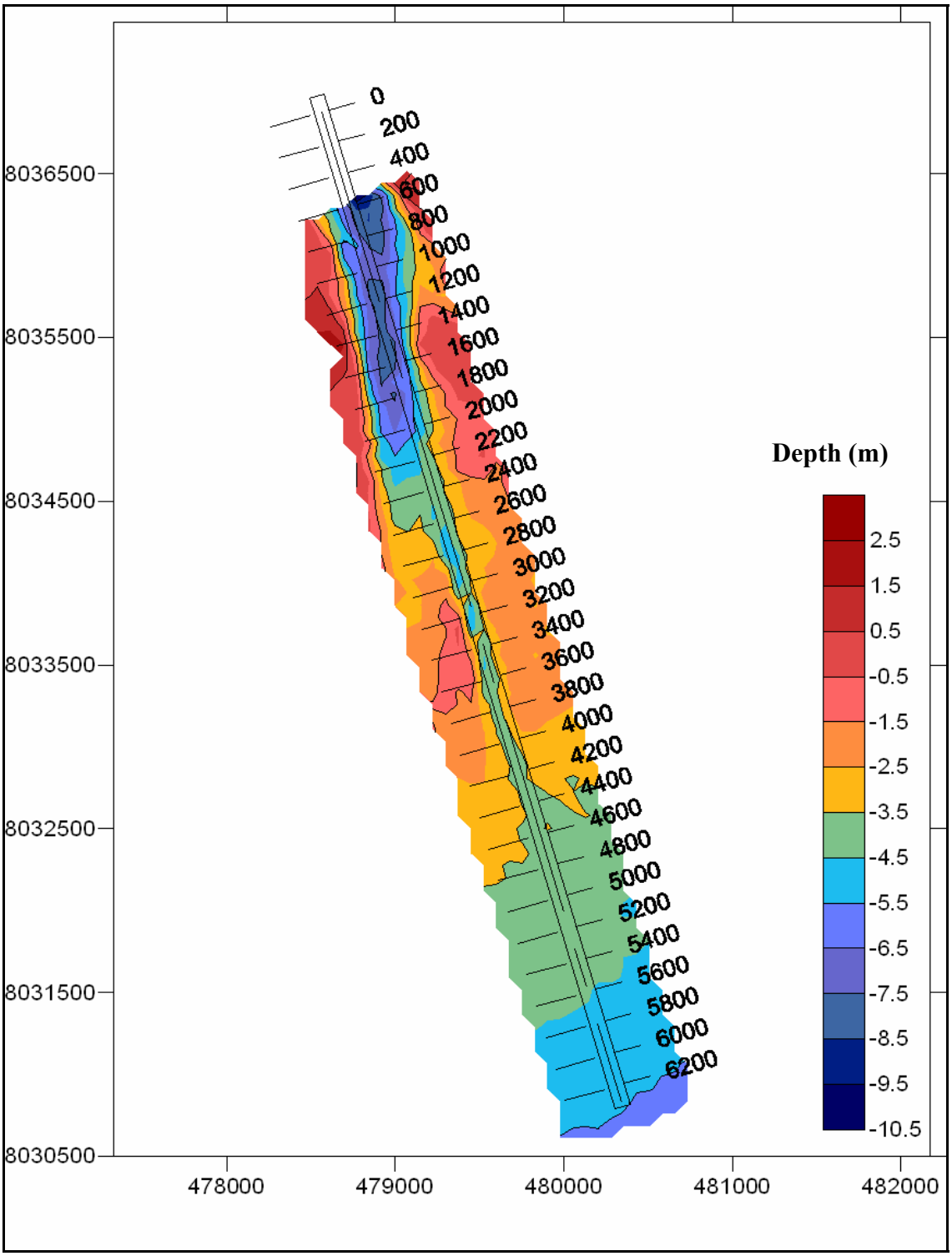

Figure 17. November 2004 bathymetry offshore Boca do Tomba (in m) overlaid by the channel design location. The figure shows that navigation problems concentrate in the nearshore zone and that channel design width and depth is currently violated in some segments. Channel segments that are represented in other colors rather than blue are shallower than the design depths of 4.7 m bellow NR (local reference level, or 0 DHN).

ANALYSIS OF CHANNEL SURVEYS

Volume changes in the channel were obtained by comparing the channel survey bathymetries supplied to CPE by ARACRUZ and historical bathymetries digitized from nautical charts. Historically the channel at Boca does Tomba eroded at the throat (river mouth) and shoaled offshore due to ebb-shoal growth. Figure 18 shows that historically, the sedimentation within the channel concentrated between channel stations 2600 to 5200 m, which is the zone that is currently experiencing navigation problems.

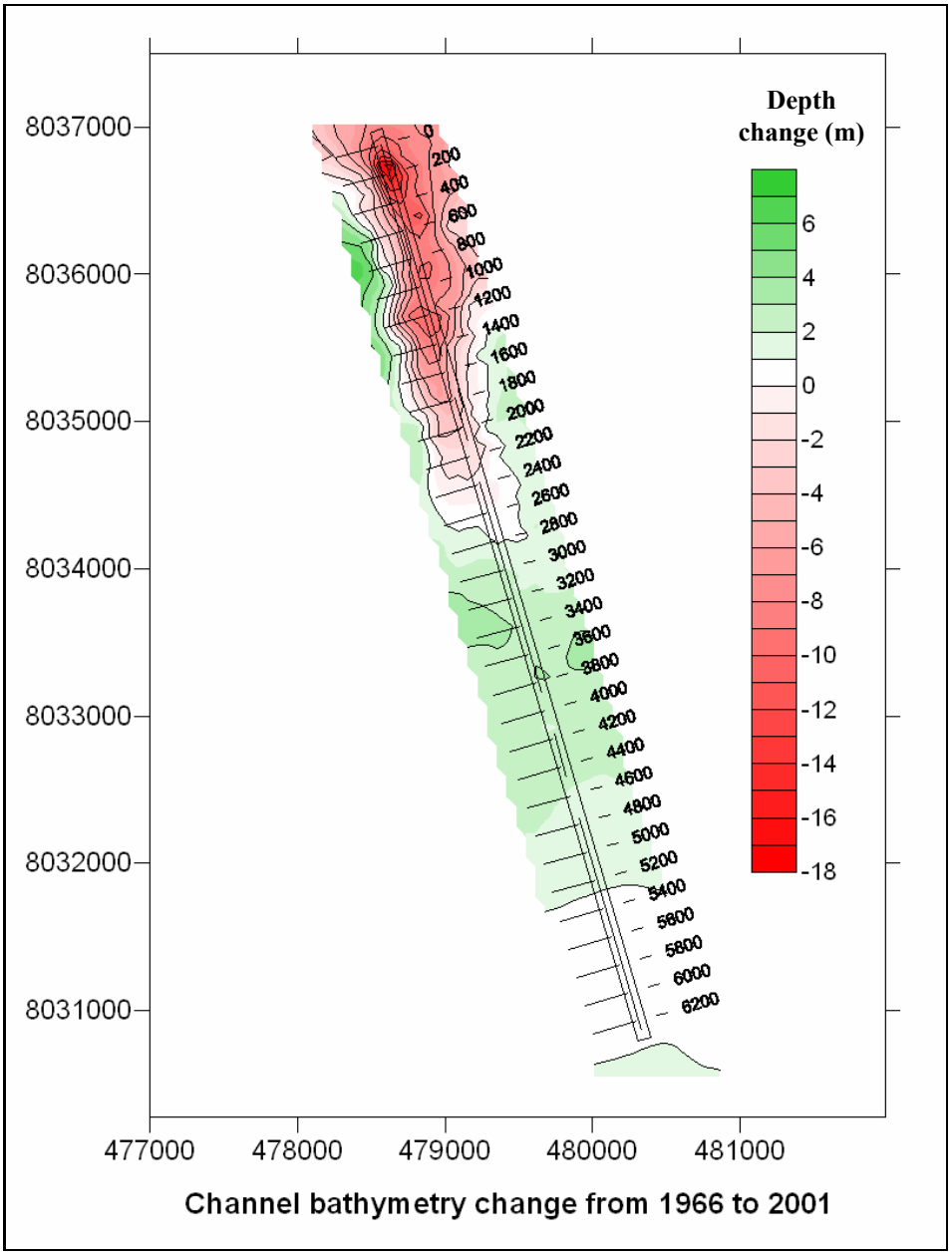

Figure 18. Bathymetric change in the 90 m design channel between March 1966 and 2001 showing historical trends that include overall scouring (erosion) in the channel throat (river mouth) and shoaling (sedimentation) offshore from station 2600 m.

Surveyed bathymetric changes from March 2001 (prior to dredging) to November 2004 (as shown in Figure 19) indicate a net change of -502,000 m^3 (-135,700 m^3/yr) within the 90 meter design channel. Considering that during this time period about 1,613,000 m^3 (435,900 m^3/yr) were removed by dredging during this time , an annual sedimentation in the channel of about 300,300 m^3/yr can be inferred (see Table 6 and Figure 19).

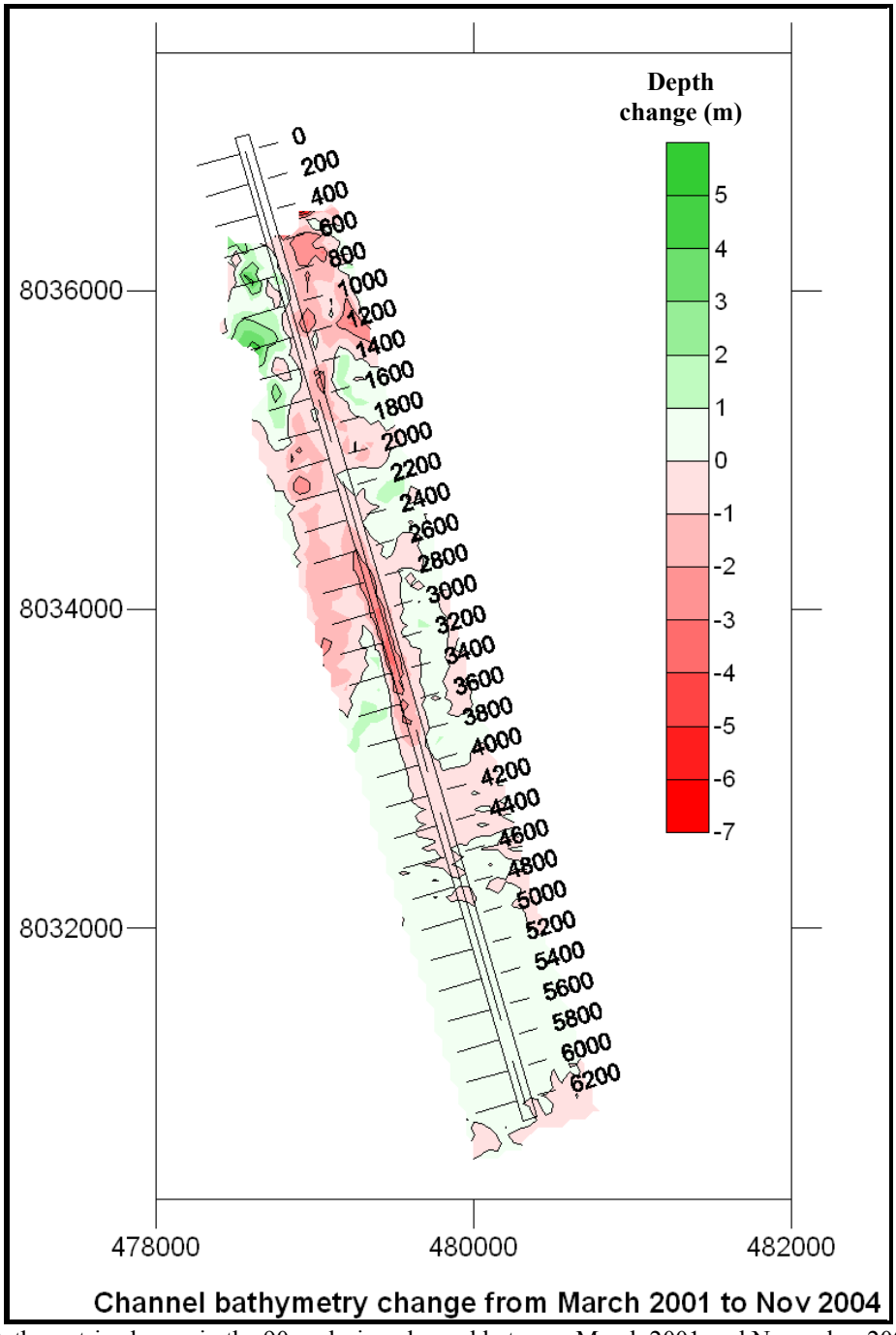

Figure 19. Bathymetric change in the 90 m design channel between March 2001 and November 2004 showing concentrated sedimentation between channel stations 2600 and 3600.

Figure 19 shows that between March 2001 and November 2004 most of the dredging occurred between channel stations 2600 m to 3600 m offshore (as indicate by darker shades of red), the offshore zone experienced mild positive change while the channel mouth section experienced shoaling (positive change) in the south side and scouring in the north side. It is interesting to note that the channel segment that experienced the most dredging (nearshore zone) is also the zone where navigation problems are currently verified (see design channel considerations) indicating large sedimentation rates in this segment.

Table 6. Observed changes within the 90 m design channel from March 2001 to Nov 2004

	Total Volume (m^3)	Annualized (m^3/yr)
Shoaling	125,600	33,900
Scouring	-627,600	-169,600
Net Change	-502,000	-135,700
Dredging*	1,613,000	435,900
Corrected Shoaling	1,111,000	300,300

Dredging volumes were obtained by dividing bid volumes by the 2.06 ratio.

It is necessary to consider that a level of uncertainty may be involved in this calculation due to the 2.06 ratio applied to the dredge bid volumes. In other words, if the ratio applied is smaller (more volume was actually dredged) annual sedimentation rate increases, and if the ratio applied is greater (less volume was actually dredged) annual sedimentation rate decreases. In order to observe seasonal and inter-annual variability, a series of sedimentation rates for different time periods were calculated by CPE, results are summarized in Table 7.

Table 7. Sedimentation rates for the Boca do Tomba channel during different time periods.

Time Period	Channel Stations	Volume Change (m3)	Dredging Volume (m3/yr)	Corrected Volume Change (m3)	Sedimentation Rate (m3/yr)
March 2001 to Nov 2004	Entire Channel	-502,000	1,613,000	1,111,000	300,300
Dec 2001 to Dec 2002	Entire channel	-93,796	524,800	431,000	431,000
May to Nov 2004*	2000 to 5000	134,401	41,000	175,400	271,000
Aug to Dec 2003 (DHI)	2400 to 3800	55,000	0	55,000	130,000
May to July 2004	2000 to 5000	45,600	0	45,600	182,400

*dredging may have occurred out of the stations and sedimentation rate may be inferior

Results from March 2001 to Nov 2004 cover the entire dredging period and represent a long term average of sedimentation rates within the channel. From December 2001 to December 2002 a large sedimentation rate of 431,005 m^3/yr was observed (Table 7). However, as shown by Figure 20, considerable sedimentation near the inlet mouth was observed during this time period. Because sedimentation in the inlet mouth is not a problem for navigation at Boca do Tomba this high sedimentation rate does not directly indicate dredging requirements. The most problematic zone, from a sedimentation point of view at Boca do Tomba, is the nearshore zone (between

channel stations 2000 m and 5000 m offshore). However for periods when dredging occurred the sedimentation in the nearshore zone cannot be isolated because the channel location where dredging occurred is not known (sedimentation during dredging events is the sum of dredging volume and net channel bathymetric changes). Additionally the constant 2.06 ratio applied to dredging volumes introduces a degree of uncertainty in the sedimentation rates.

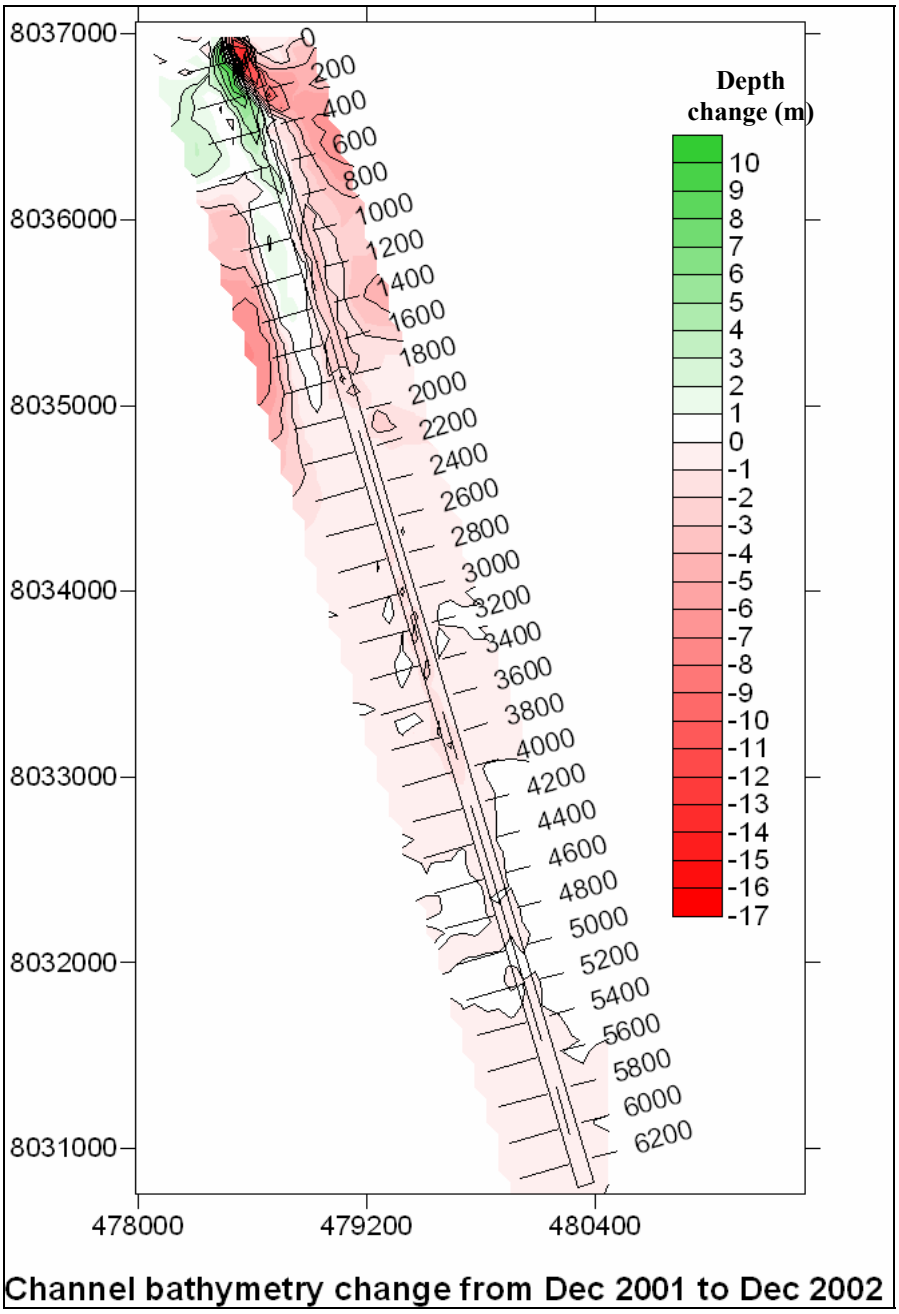

Figure 20. Bathymetric change in the 90 m design channel between December 2001 and December 2002 showing overall negative change due to dredging but localized sedimentation in the channel mouth due to channel migration to the north.

In order to exclude uncertainties related to dredging volumes, and exclude sedimentation in the channel mouth, sedimentation rates during non-dredging periods were evaluated. The analysis of non-dredging periods concentrated on the area of the channel area navigation problems is currently experienced.

DHI (2004) analyzed sedimentation rates during a period of 5 months (August to December 2003) where no dredging occurred and found a sedimentation rate of 130,000 m^3/yr in the middle section of the channel (approximately between CPE channel stations 2400 m to 3800 m). DHI suspected that this higher tan expected sedimentation was possibly mud deposition, which. However this was not confirmed by later field inspection and sediment samples (see Figure 10). It is interesting to note, however, that most of the sedimentation shown by the DHI (2004) analysis occurs in the same channel region as shown by Figure 18 of this report (the nearshore zone), where the sand ebb-shoal is located.

Another non-dredging period occurred between May 3rd and July 2004. Analysis of bathymetric data obtained in the months of May and July 2004, between channel stations 2000 m and 5000 m, indicates a total sedimentation of 45,600 m^3 during the 3-month time period, corresponding to an approximate annual sedimentation in the middle section of the channel on the order of 182,400 m^3.

Both CPE and DHI sedimentation rates measured during the non-dredging intervals involve annualizing sedimentation rates based on measured sedimentation during short periods of time (5 months and 3 months respectively) seasonal variability may add some level of uncertainty to these results. Sedimentation rate from May 2004 to November 2004 was also calculated to increase the sampling time period (7 months) and at the same time reduce dredging uncertainties because only one dredging event occurred during these seven months. Results from this analysis, illustrated in Figure 20, indicate a sedimentation rate of 271,000 m^3/yr between channel stations 2000 m and 5000 m offshore. Figure 21 shows that between May and November 2004 the channel shoaled mostly form the north, with sedimentation concentrated between stations 2000 m to 4400 m. Negative change (scouring) occurred from stations 2000 to 3000 m, on the south side of the channel, and is probably due to the one dredging event that took place during this time interval.

All the estimated sedimentation rates calculated here significantly exceed the 65,000 m^3/yr predicted by DHI (2000). Volumes shown here indicate that the sedimentation rate can vary from 300,300 m^3/yr to 430,000 m^3/yr for the entire channel, and from 130,000 m^3/yr to 271,000 m^3/yr for the middle section of the channel, where navigation problems are currently experienced (offshore of channel station 2000 m).

Analysis of channel surveys have also shown that it is not necessary to perform annual maintenance dredging in areas near the inlet throat (mouth landward of channel station 2000 m) or offshore from station 5000 m. These channel segments contain enough buffer (channel is deep and wide enough) to support navigation for longer periods of time. Significant shoaling that will require maintenance dredging is currently experienced in a 3 km zone from channel stations 2000 m to 5000 m, being more pronounced in a 1 km long segment from channel station 3000 m to 4000 m. Dredging volume requirements and dredging strategies for this channel segment are further discussed at the end of this report.

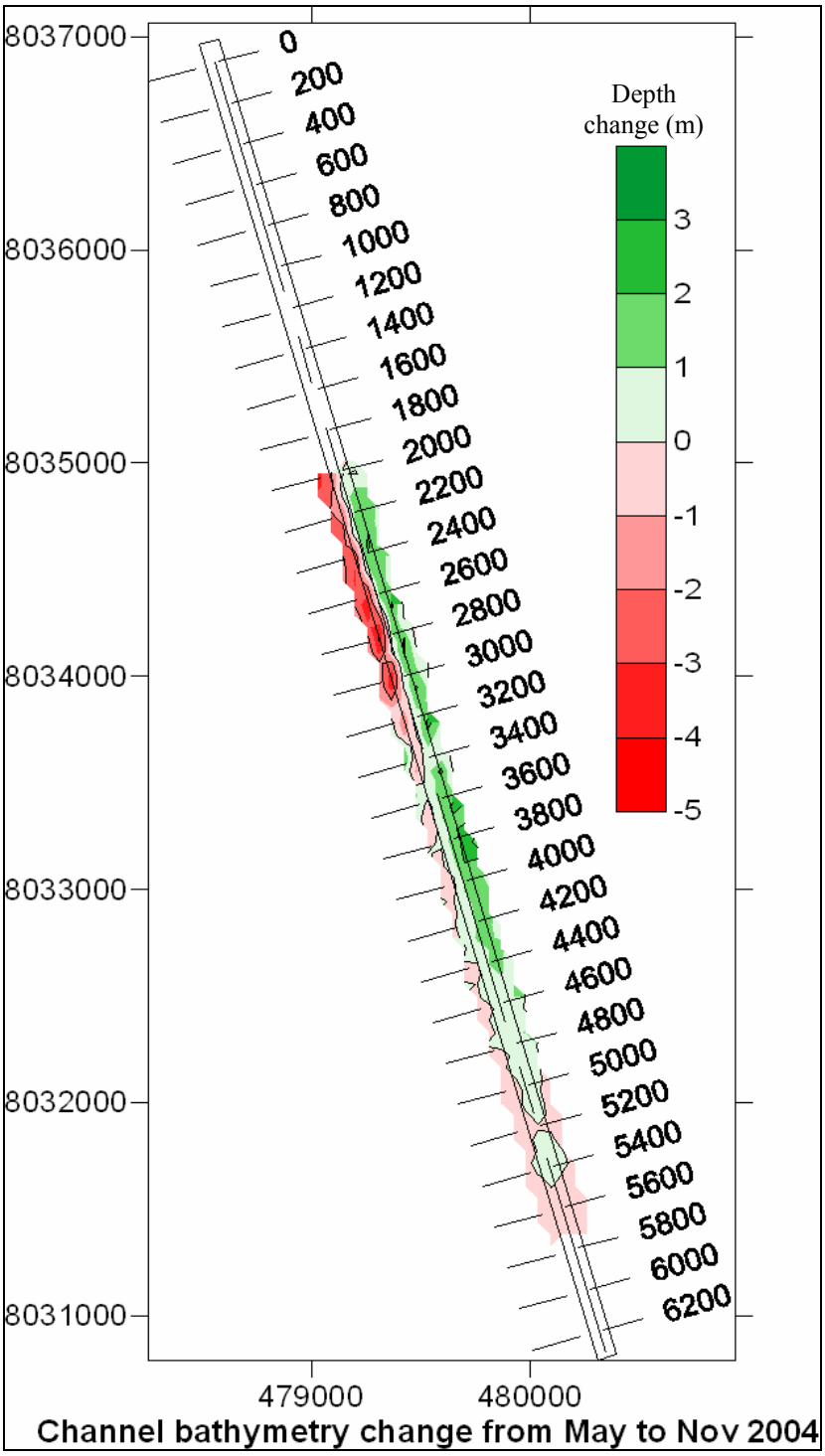

Figure 21. Bathymetric change in the 90 m design channel between May and November 2004 showing sedimentation concentrated between channel stations 2000 m and 4400 m offshore.

WAVE ANALYSIS AND MODELLING

The objectives of this section of the report are to: (1) to summarize the nearshore wave climate and (2) to model nearshore wave propagation and to estimate littoral drift (sediment moving along the coast) by waves.

The wave data used in this study was measured at CEPEMAR Wave Gage 106 between January 2002 and August 2004. The location of the wave gage appears in Figure 22. The mean depth at Wave Gage 106 is approximately 6 m.

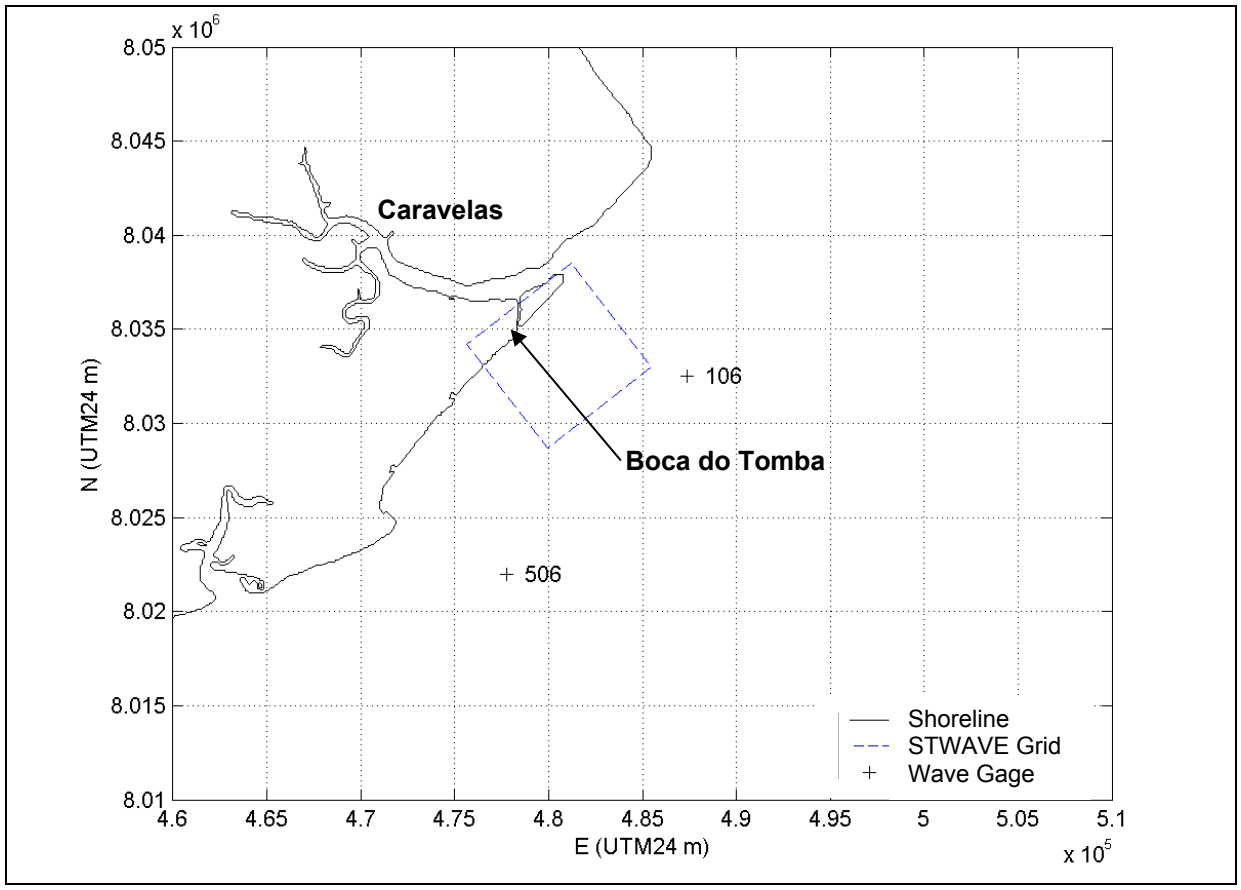

Figure 22. Wave gauge location, Caravelas, Brazil.

Directional wave characteristics from 2002 to 2004 appear in Figure 23. Figure 23 shows that the offshore waves propagate most frequently from the south-southeast to south. These direction bands accounts for 60 percent of the waves observed offshore, and include the average wave, which exhibits a height of 0.37 m, with a corresponding peak period and direction of 7 seconds and 153 degrees. Due to the large percentage of waves propagating from these direction bands, the net alongshore sediment transport (littoral drift due to waves) is from southwest to northeast.

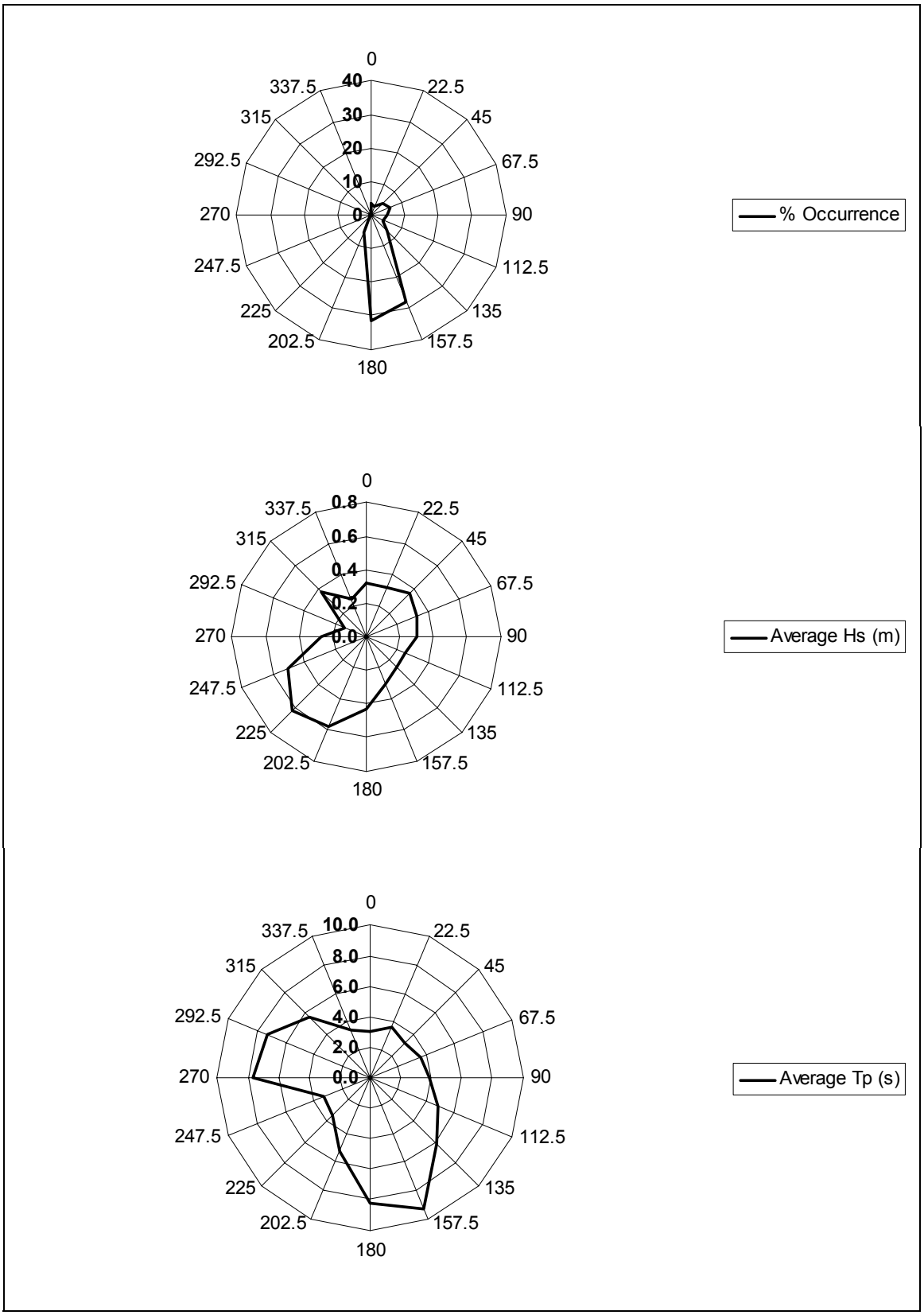

Figure 23. Directional wave statistics, Wave Gage 106, Caravelas, Brazil.

Seasonal wave statistics from 2002 to 2004 appear in Figure 24. During the winter months (March – September), the average wave propagates from the south-southeast (162 degrees), exhibiting a wave height of 0.4 m and a peak period of 7.6 s. Much of the sediment transport towards the northeast occurs between March and September, which generally experiences the highest wave activity. Individual winter storms during this time period can generate nearshore waves up to 2 m high.

During the summer months (September – March), the average wave propagates from the east-southeast (119 degrees), with a height of 0.35 m and a peak period of 5.8 s. As some of the summer waves propagate from the east, sediment transport reversals observed during this period. Nevertheless, since wave activity is generally lower, wave induced sediment transport towards the southwest at most locations is generally small when compared to the transport to the northeast.

Wave Transformation

Wave transformation estimates near the Boca do Tomba utilize the STWAVE model (Smith, 2001). STWAVE is a spectral wave model that evaluates the refracted wave height and wave angle based on a spectrum of waves given steady-state waves, winds, currents, and water levels. The model utilizes linear wave theory and assumes negligible bottom friction. Inputs to the STWAVE model include the bathymetry, the wave spectra, and the water levels. For this investigation, the water level was assumed to be equal to mean tide level, +1.6 m above NR (zero DHN).

Bathymetric Data

Bathymetric data for the wave model was compiled from bathymetric surveys taken in March 2001, September 2000, and nautical charts from 1992, and 1966 (Figure 25). The March 2001 survey served as the primary data source, with the earlier surveys providing supplementary data. The 7 x 7 km bathymetric grid created using this data appears in Figure 26.

The primary feature of the nearshore bathymetry is the Boca do Tomba channel and its ebb-shoal. The maximum depth of -14 m NR occurs inside the throat of the inlet near its northeast bank. The inlet's natural channel (prior to dredging) exhibits an "S" shape, meandering from a NNW-SSE orientation near the shoreline, to a N-S orientation 1 to 2 km offshore, to a NNW-SSE orientation further offshore. Landward of the -4 m NR contour, the bathymetry is defined by the Boca do Tomba's ebb-shoal and the old inlet's remnant ebb-shoal at the north corner of the grid. The Boca do Tomba's ebb-shoal exhibits an elliptical shape, approximately 4 km long by 2.5 km wide, oriented NNW-SSE. Seaward of -4 m NR contour, the bathymetric contours are roughly parallel, running southwest to northeast.

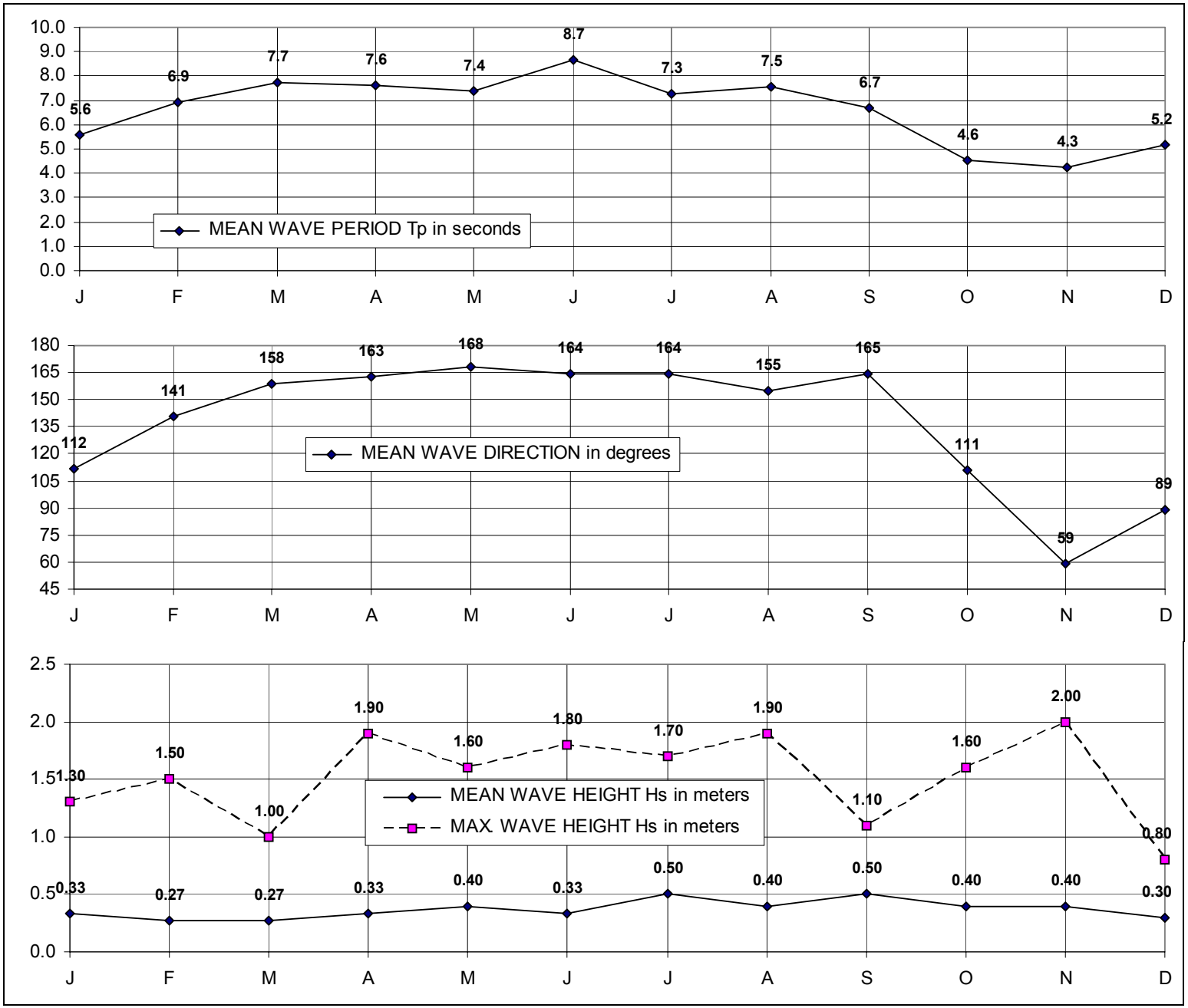

Figure 24. Seasonal wave statistics, Wave Gage 106, Caravelas, Brazil.

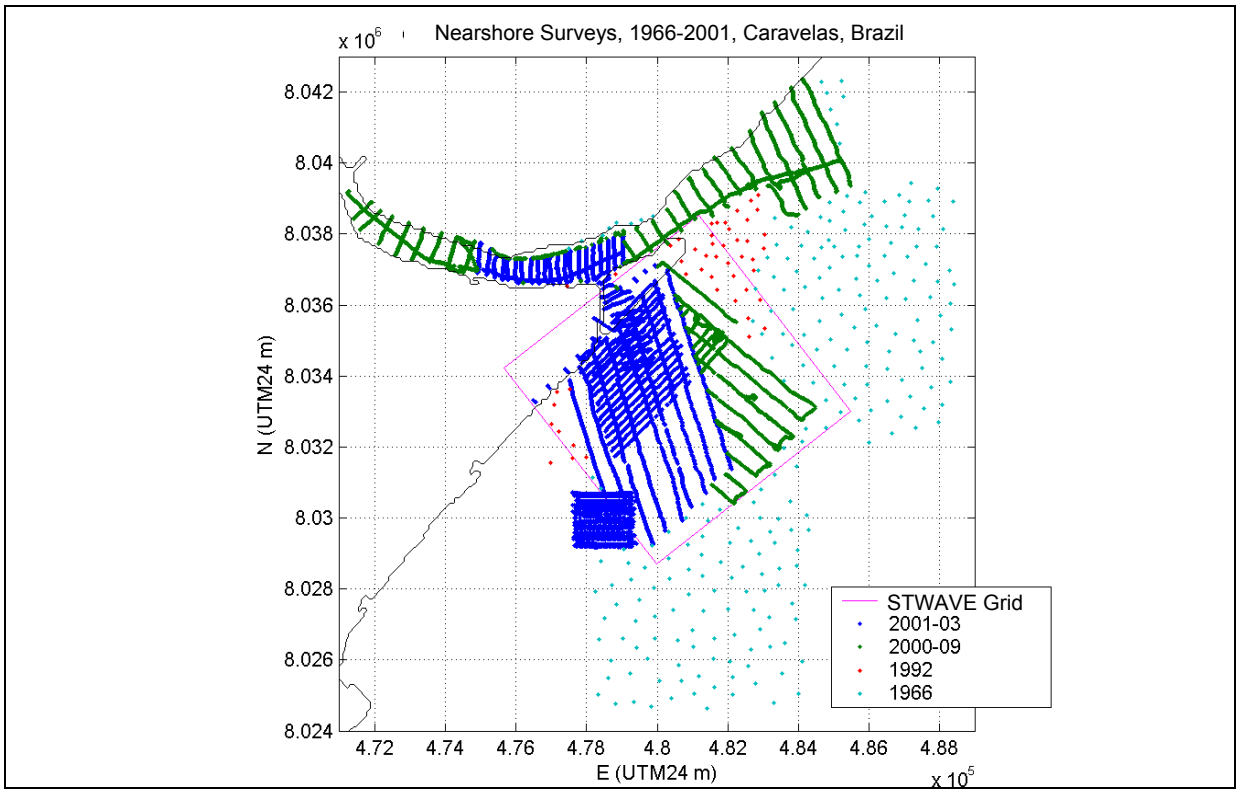

Figure 25. Bathymetric data, Caravelas, Brazil.

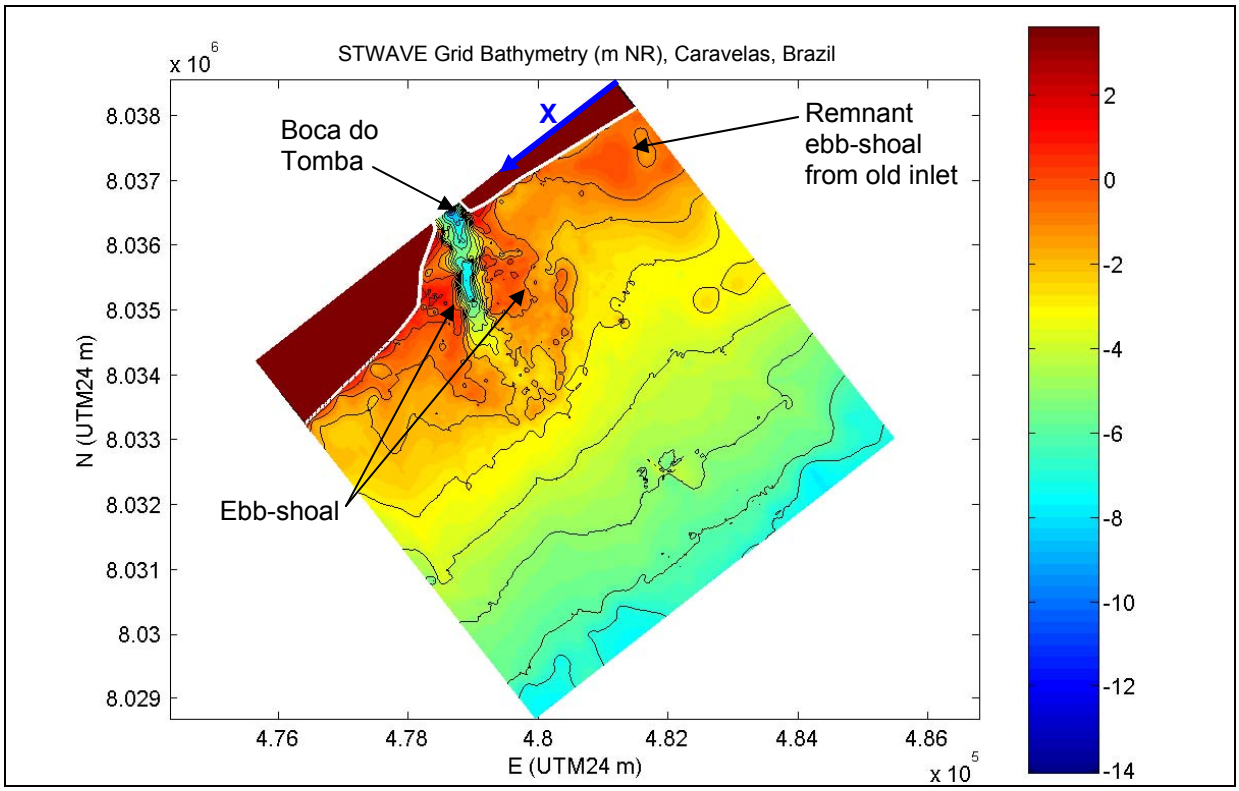

Figure 26. STWAVE bathymetric grid, Caravelas, Brazil.

Selected Wave Cases

To examine wave propagation during typical conditions, six wave cases were selected (Table 8). Input wave spectra for the STWAVE model were developed based on the six cases presented in table 8. Wave refraction results appear in Appendix B.

Table 8. Representative wave cases, wave gage 106, Caravelas, Brazil.

	Hs (m)	Tp (s)	Dir. (deg.)
AVERAGE WAVE	0.37	6.9	153
PRINCIPAL DIRECTION	0.43	8.3	180
PRINCIPAL DIRECTION	0.31	9.3	157.5
AVERAGE SUMMER WAVE	0.35	5.8	119
AVERAGE WINTER WAVE	0.39	7.6	162
HIGHEST WAVE	1.96	5.9	203

Model Results

Average Wave

During average wave conditions, the wave height and wave angle generally remain uniform until reaching the -4 m NR contour. Landward of this depth, the Boca do Tomba's channel and ebb-shoal cause the wave height and wave angle to vary. Southwest of the inlet, the highest waves (~0.6 m) occur over the ebb-shoal at approximately 1 km offshore. Wave focusing southwest of the inlet occurs near the ebb-shoal, the southwest bank of the inlet, and the shoreline 1 km from the inlet's mouth. On the southwest bank of the inlet, the incoming waves assume an east-southeasterly wave direction. Northeast of the inlet, the highest waves (0.6 – 0.7 m) occur over the ebb-shoal at two locations 300 m and 1 km offshore. A third area of high wave energy (H_s ~ 0.5 m) occurs near the old inlet's remnant ebb-shoal. Wave focusing northeast of the inlet occurs over Boca do Tomba's ebb-shoal and the old inlet's remnant ebb-shoal.

Southerly (180 degrees) Wave

Waves propagating from the south (180 degrees) generally exhibit a wave height variation similar to the average wave case. The exceptions are areas of high wave energy (H_s ~ 0.5 m) that occur in two locations (1) the shoreline adjoining the southwest bank of the inlet, and (2) a 2 km long band along the outer ebb-shoal northeast of the inlet's channel.

As the waves approach the shoreline, they assume a more south-southeasterly direction. Along the southwestern bank of the inlet, the waves assume an east-southeast to southeasterly direction. A divergence in the wave angle occurs at the shoreline

approximately 500 m northwest of the inlet, suggesting a nodal point in the associated longshore sediment transport.

South-Southeast (157.5 degrees) Waves

Waves propagating from the south-southeast generally remain uniform in height and direction until reaching the -3 m NR contour. Because the incoming waves from this direction are lower than the Average Wave case, wave heights do not exceed 0.4 m until reaching this location. Southwest of the inlet, the highest waves (~ 0.5 m) occur over the ebb-shoal approximately 1 km offshore. On the southwest bank of the inlet, the incoming waves assume an east-southeasterly wave direction. Northeast of the inlet, the highest waves (0.6 – 0.7 m) occur over the ebb-shoal at two locations 400 m and 1 km offshore. A third area of high wave energy (H_s ~ 0.5 m) occurs near the old inlet's remnant ebb-shoal. Wave focusing occurs in the same locations as it does during the Average Wave condition. However, a divergence in the wave angle occurs at the shoreline approximately 500 m northwest of the inlet. Similar to other wave cases, this suggests a nodal point in the associated longshore sediment transport.

Average Summer Wave

The average summer propagates from east-southeast, resulting in sediment transport reversals. During the summer period, waves generally remain uniform until reaching the -2 m WGS contour. Southwest of the inlet, the wave height remains below 0.45 m except over the ebb-shoal 1-2 km offshore and along the 2 km of shoreline adjoining the southwest bank of the inlet. On the southwest bank of the inlet, the incoming waves assume an east to east-southeasterly wave direction. The highest waves occur northwest of the inlet's channel, over the ebb-shoal 500 m and 1-2 km offshore. A third area of high wave energy (H_s ~ 0.45 m) occurs near the old inlet's remnant ebb-shoal.

Average Winter Wave

The variation in wave height during average winter conditions is similar to the 180 degrees wave case. Wave focusing tends to occur over the Boca do Tomba's ebb-shoal 1-2 km offshore and near the old inlet's remnant ebb-shoal. Along the southwestern bank of the inlet, the waves assume an east-southeast to southeasterly direction. Approximately 1 km northwest of the inlet, a divergence in the wave angle occurs at the shoreline, suggesting a nodal point in the associated longshore sediment transport.

Highest Wave

The highest wave in the 2002-2004 wave record occurred on November 3, 2003. This wave exhibited an offshore height and period of 2.0 m and 6 seconds, propagating from the south-southwest (203 degrees). Although this event took place during the summer, the conditions associated with this event are common during the winter (see Figure 24). Between March and September, the highest monthly waves generally propagate from the south-southwest (195 degrees) and range from 1.0 to 1.9 m in height.

Accordingly, the Highest Wave case can occur during winter cold fronts, in addition to the eventual, less frequent, southeastern storms occurring in non-summer conditions, such as the conditions that occurred on November 3, 2003.

During periods of high wave activity, the estimated wave height quickly drops from 2.0 to 1.6 m as it approaches the -6 m NR contour. Further reductions in wave height associated with the Boca do Tomba's ebb-shoal commence approximately 4 km offshore near the -4 m NR contour. A localized area of higher wave energy ($H_s \sim 1.7$ m) occurs over the ebb-shoal northeast of the channel at approximately 3 km offshore. A second such area occurs 1 - 1.5 km offshore approximately 2.5 km southwest of the inlet's channel. Zones sheltered from wave energy occur in the offset area bounded by the southwest bank of the inlet and the northeastern ebb-shoal, along with the 2 km of adjoining shoreline. Moderate wave energy ($H_s \sim 1$) occurs along the shoreline northeast of the inlet. As the waves approach the shoreline, they assume a south-southeast to southerly wave direction. The exception is the southwest bank of the inlet, where the waves assume an easterly wave direction. Wave focusing occurs over the old inlet's remnant ebb-shoal. A divergence in the wave angle occurs approximately 750 m northeast of the inlet, suggesting a nodal point in the associated longshore sediment transport.

LONGSHORE SEDIMENT TRANSPORT

Alongshore sediment transport estimates utilized two methods:

1. The Generalized Model for Simulating Shoreline Change (GENESIS) (Gravens, *et al*., 1991).
2. Direct application of the USACE (1984) formula (CERC Equation).

The first method integrated wave refraction, seasonal wave variations, storm events, temporal changes, shoreline change and the active beach profile height into the sediment transport estimates. It utilizes a time series of offshore waves and an external wave transformation modeling output from STWAVE. The second method estimates the maximum potential sediment transport given a few selected wave cases and a fixed shoreline. Both methods utilize the USACE (1984) formula (CERC Equation):

$$Q_\ell = K1\left(\frac{\rho\sqrt{g}}{16\kappa^{1/2}(\rho_s-\rho)(1-n)}\right)H_b{}^{5/2}\sin(2\alpha_b) \qquad \text{(Eq. 7)}$$

where

Q_ℓ = Sediment transport potential in m^3/second
K1 = Empirical sediment transport coefficient
ρ = Density of seawater = 1025 kg/m^3
g = Acceleration due to gravity = 9.81 m/s^2
κ = Breaking wave height / breaking depth
ρ_s = Density of sand grains ~ 2650 kg/m^3

n = Porosity of sand ~ 0.37
H_b = Breaking wave height in m
α_b = Breaking wave angle relative to shoreline

The coefficient K1 can be determined using the GENESIS model by trial-and-error or calculated based on the mean grain size and breaking wave height as suggested by USACE (1984), where:

$$K1 = 0.1637 \log_{10}(gH_b/w^2) - 0.0773 \quad \text{(Eq. 8)}$$

where

$$w = (\rho_s/\rho - 1)g\rho d^2/18\mu \quad \text{(Eq. 9)}$$

and

w = Fall velocity of the nearshore sediments in m/s
d = Grain size of the nearshore sediments in m
μ = Absolute viscosity of seawater kg/m·s

In the GENESIS model, an additional term is added to account for longshore variations in the breaking wave height (Gravens, *et al.* 1991). This term involves a second coefficient, K2, which may vary from 0 to K2 = K1.

Estimates of longshore sediment transport at Caravelas were calculated separately for two sections of shoreline:

(1) 3,020 m of shoreline northeast of the Boca do Tomba.
(2) 2,420 m of shoreline southwest of the Boca do Tomba.

Both sections share a common baseline, which corresponds to the northwest edge of the STWAVE grid appearing in Figures 25, 26, and 27. The northeastern section of shoreline covers the length of the island northeast of the inlet as it appeared in 1992. The southwestern section of shoreline extends between profile lines S09 and S13 (Figure 27).

GENESIS Model Calibration

Calibration of the Caravelas GENESIS model was based on the observed shoreline changes between March 2001 and August 2004 at profile lines S02, S03, S05, S06, S07, S09, S10, S11, S12, and S13 (Figure 27). Inputs to the model included the 2002-2004 offshore waves at CEPEMAR Wave Gage 106 (Figure 22), wave transformation results from the STWAVE model, March 2001 shoreline positions, the active beach profile height, and the beach mean grain size.

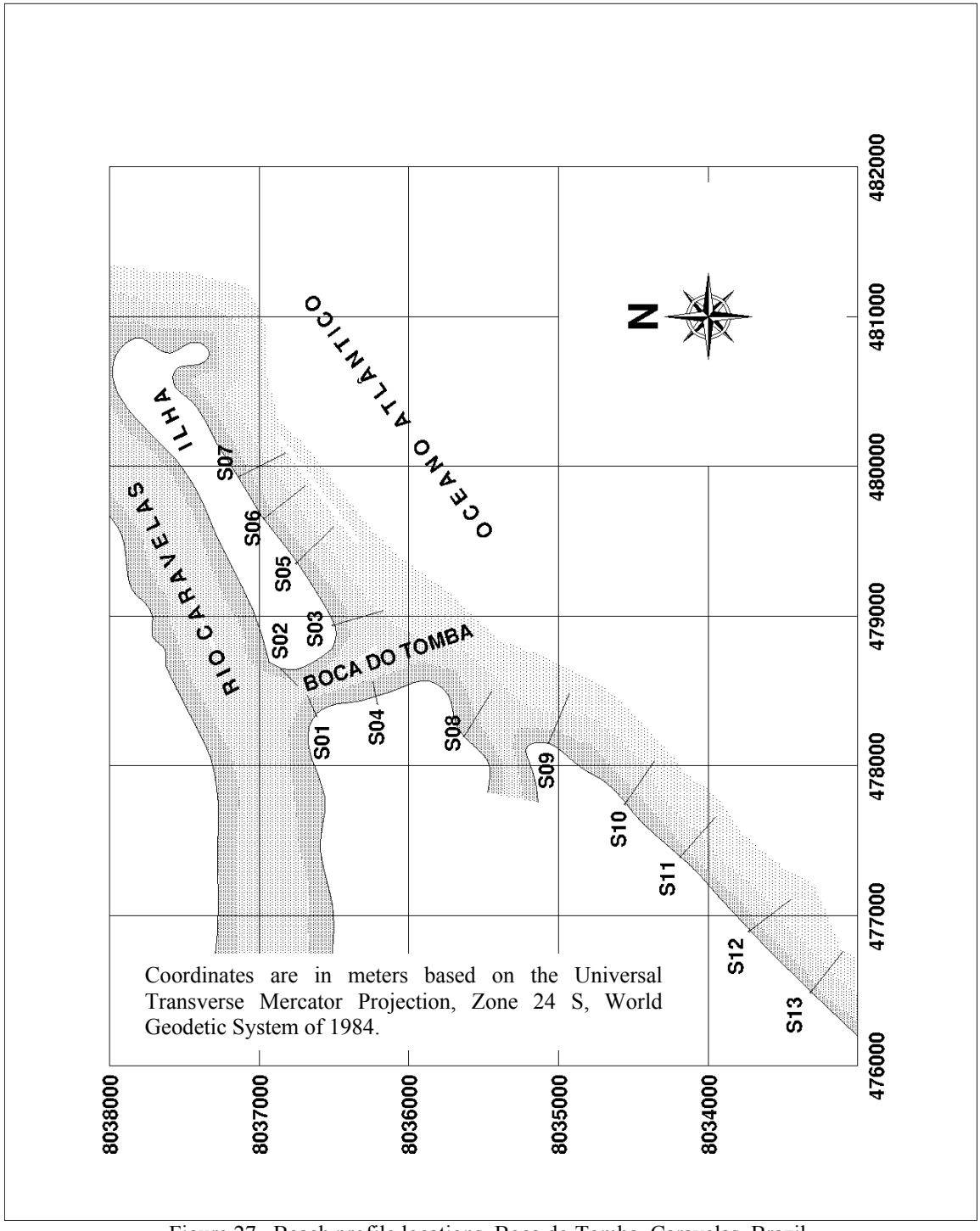

Figure 27. Beach profile locations, Boca do Tomba, Caravelas, Brazil.

Based on the field inspection and sediment sampling conducted in the areas, mean grain size on the beach was assumed to be 0.30 mm northeast of the inlet and 0.25 mm southwest of the inlet.

For this investigation, the shoreline location was defined as the position of the mean tide level contour (+1.6 m above 0 DHN or NR – *nivel de referência*) at each profile line. To determine the active profile height, shoreline and volume changes at the profile lines in Figure 28 were compared. The active profile height at each profile line was defined as the ratio of the volume change in m^3/m to the shoreline change in meters (Table 9). Excluding profiles S08-S10, whose volume changes were dominated by shoaling processes, the average active profile height was 3.5 m. The top of the active beach profile was assumed to be equal to the Mean High Water Springs contour (+2.9 m above NR). The bottom of the active beach profile was assumed to be -0.6 m NR.

The 2002-2004 wave record at CEPEMAR Wave Gage 106 provided the time series of offshore waves. To determine the nearshore waves, 52 wave angle and wave period bands were selected from the wave measurements. Each band was assigned a wave height of 1 meter and given a corresponding wave spectrum using CEDAS-NEMOS 2.01 (Veri-Tech, 2002). The 1 meter waves were then refracted to -0.6 m NR using STWAVE. Refraction coefficients were assumed to be equal to the nearshore wave heights in meters.

To determine K1 and K2 in the GENESIS model, several simulations of the March 2001 and August 2004 shoreline changes were conducted using GENESIS with the STWAVE results. The objective of the calibration procedure in the GENESIS approach is to match the average observed shoreline change to the average simulated shoreline change. Due to the lack of beach profile data northeast of profile line S07, model results northeast of profile line S07 were not included in the average shoreline changes. The resulting values of K1 and K2, along with the calibration results, appear in Table 10.

GENESIS Model Results

Longshore sediment transport rates based on the final GENESIS calibration runs appear in Figure 28. The range of uncertainty of the results displayed in Figure 28 is approximately ±36%. At most locations, the net sediment transport is towards the northeast, with very little transport towards the southwest occurring. The exception to this trend is the area between profile line S05 and the inlet. In this area, the net longshore transport is towards the southwest.

Overall, the longshore sediment transport rates in Figure 28 provide a partial explanation of the shoaling in the Boca do Tomba channel. On the updrift, or southwestern, side of the inlet, the net sediment transport rate increases from 43,000 m^3/year near profile line S13 to 59,000 m^3/year near the inlet (S09). On the downdrift side of the inlet, 16,000 m^3/year enters the inlet from the area of "reversed" sediment transport. Transport towards the northeast resumes at profile line S05, increasing to 8,000 m^3/year near profile line S07 and 14,000 m^3/year at the 1992 east end of the island. Overall, the amount of sediment entering the inlet due to wave-generated, gross longshore sediment transport along the beach is in the range of 75,000 ± 27,000 m^3/year.

Table 9. Observed beach erosion Caravelas, Brazil from March 2001 to August 2004.

Profile	Beach Length	Volume Change on the Beach		Shoreline Change	Beach Profile Height
	(m)	(m3/m)	(m3)	(m)	(m)
Northeast:					
S 2	225	-46.4	-10,400	-44.3	1.0
S 3	462	-50.0	-23,100	-46.4	1.1
S 5	421	-32.8	-13,800	-12.0	2.7
S 6	348	-32.6	-11,400	-13.2	2.5
S 7	163	-45.3	-7,400	-17.8	2.5
Total	**1,619**	**-40.8**	**-66,100**	**-27.1**	**2.0**
Channel:					
S 1	207	-35.4	-7,300	-58.6	0.6
S 4	516	-110.5	-57,000	-23.4	4.7
S 8	897	-3.0	-2,700	-0.1	N/A
Total	**1,620**	**-41.4**	**-67,000**	**-15.0**	**3.5**
Southwest:					
S 9	328	72.6	23,800	-1.7	N/A
S 10	581	-41.2	-24,000	-3.2	N/A
S 11	592	-31.4	-18,600	-16.0	2.0
S 12	630	-52.6	-33,100	-7.4	7.1
S 13	292	-53.1	-15,500	-7.0	7.6
Total	**2,424**	**-27.8**	**-67,400**	**-7.7**	**5.2**
All Profiles	**5,663**	**-35.4**	**-200,500**	**-15.3**	**3.5**

Notes:

1. Shoreline elevation = +1.6 m WGS.
2. Beach length is based on the actual shoreline shape and not the length along the GENESIS model baseline.

Table 10. Genesis model calibration march 2001 – august 2004, Caravelas, Brazil

Segment	Average Shoreline Change (m) Observed	Simulated
Northeast[+] K1 = K2 = 0.23	-27.1* -19.1**	-19.4
Southwest K1 = 0.55, K2 = 0	-7.7* -6.7**	-6.8

Notes: [+] Average shoreline changes consider profile lines S03-S07 only.
* Based on straight-line interpolation between profile lines (8).
** Based on cubic spline (curved) interpolation between profile lines.

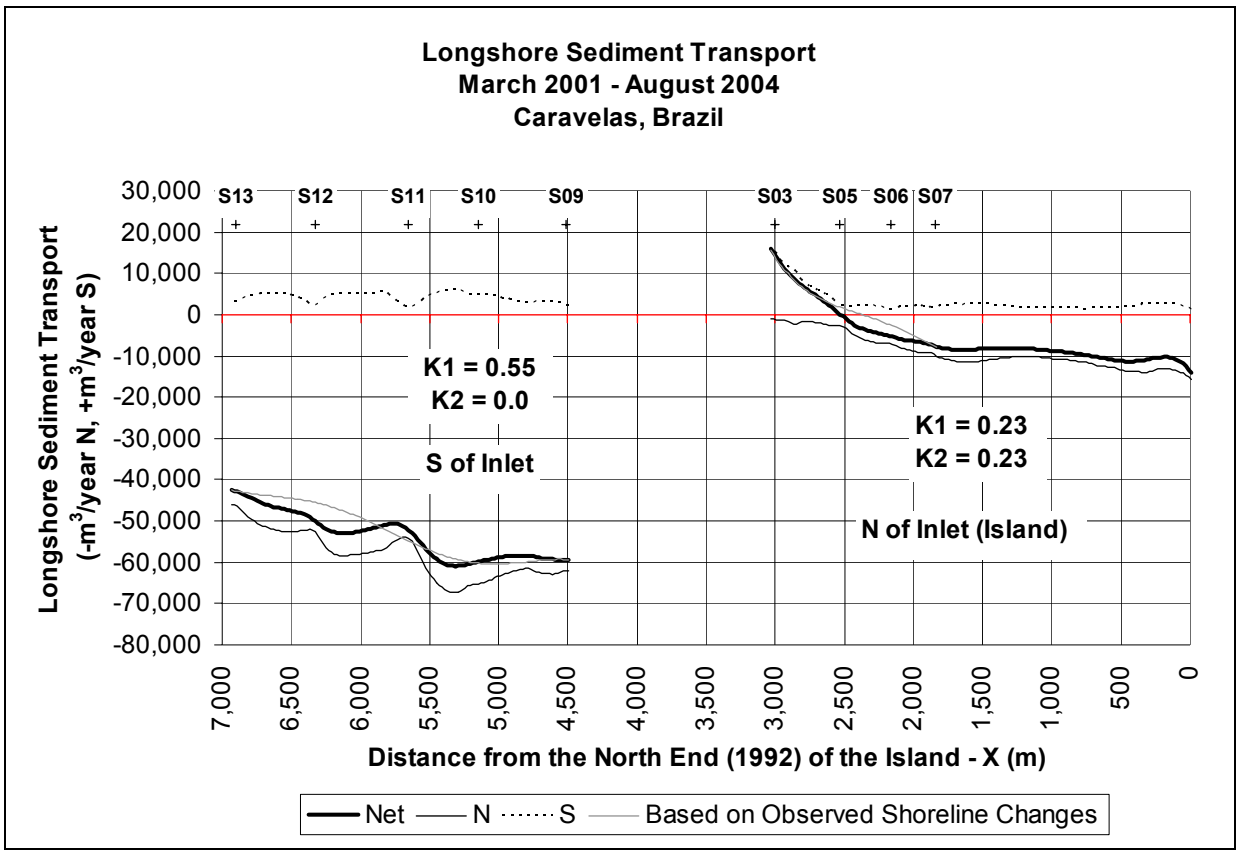

Figure 28. GENESIS longshore sediment transport, March 2001 – August 2004, Caravelas, Brazil.

Longshore Sediment Transport – USACE (1984) Formula (CERC Equation)

Longshore sediment transport rates were also calculated by direct application of the USACE (1989) formula (Eq. 7) using three average wave conditions appear in table 10. K factors in this case were not calibrated to shoreline changes but calculated from

Equation 8. Three of the wave cases previously shown in Table 8 were considered: the Average Wave, the Average Summer Wave, and the Average Winter Wave. These cases were selected to represent the net sediment transport, the sediment transport towards the southwest, and the sediment transport towards the northeast. Sediment transport estimates assumed that the breaking wave height and wave angle were equal to wave height and wave angle at -0.6 m NR (Appendix B). The value of K1, 0.40 mm, was determined using the USACE (1984) formula (eq. 8), assuming a mean grain size of 0.275 mm and a breaking wave height of 0.38 m from the Average Wave Case results at -0.6 m NR (Appendix 2). The sediment transport rates in table11 do *not* represent the actual amount of transport that occurs along the beach of the study area, but rather the maximum transport rate that could occur given the wave conditions examined and the existing shoreline orientation.

Table 11. Longshore sediment transport, based on CERC equation, Caravelas, Brazil.

	Longshore Transport (m3/year)		
	Average Wave	**Average Summer Wave**	**Average Winter Wave**
S09 to S13	-173,000	1,000	-232,000
S03 to S05	28,000	80,000	22,000
S05 to N End of Island (1992)	-59,000	57,000	-92,000

Notes: Transport is positive (+) towards southwest and negative (-) towards northeast.

Longshore Transport for the Average Wave Case

Given the Average Wave case, the longshore sediment transport is generally directed towards the northeast, except between profile lines S03 and S05. Southwest of the inlet (S13-S09), the potential sediment transport averages 173,000 m^3/year to the northeast. Between the inlet and profile line S05, the potential sediment transport averages 28,000 m^3/year into the inlet (southwest directed transport). Between profile line S05 and the east end of the island, the transport is generally towards the northeast, with an average potential value of 59,000 m^3/year to the northeast.

Longshore Transport for Average Summer Wave Case

During the summer months, transport reversals are common. Southwest of the inlet, sediment transport in both directions can occur. As a result, the average potential transport rate between profile lines S13 and S09 is 1,000 m^3/year towards the southwest. Northeast of the inlet, sediment transport is generally towards the southwest, with an average potential transport of 80,000 m^3/year between profiles lines S03 and S05, and an average potential transport of 57,000 m^3/year along the remainder of the island.

Longshore Transport for Average Winter Wave Case

During the winter months, the sediment transport is directed towards the northeast, except between profile lines S03 and S05. Southwest of the inlet (S13-S09), the potential sediment transport averages 232,000 m^3/year to the northeast. Between the inlet and profile line S05, the potential sediment transport averages 22,000 m^3/year into the inlet (southwest directed transport). Between profile line S05 and the east end of the island, the transport is generally towards the northeast, with an average potential value of 92,000 m^3/year.

Summary of Wave Modeling and Alongshore Sediment Transport

Wave activity near the Boca do Tomba is governed by the offshore wave climate, the southwest-northeast shoreline orientation, the Boca do Tomba's ebb-shoal, and the old inlet's remnant ebb-shoal. Typical offshore waves are on the order of 0.37 m, propagating from the south-southeast, resulting in a net longshore sediment transport towards the northeast. Divergent wave patterns results in a nodal point (sediment transport reversal) 0.5 km northeast of the inlet. Between this nodal point and the inlet, the net sediment transport is towards the southwest, increasing the amount of sediment brought into the inlet's channel. The net amount of sediment entering the inlet can range from 59,000 to 173,000 m^3/year from the beaches to the southwest and from 16,000 to 80,000 m^3/year from the beaches to the northeast, resulting in a combined sediment input from adjacent beaches of 75,000 m^3/yr (GENESIS Model) to 253,000 m^3/year (CERC Equation).

The modeled net sediment input into the channel, as calculated by the GENESIS model (75,000 m^3/yr), is in a similar order of magnitude than the gross littoral transport presented by DHI (2000) which was 68,000 m^3/yr. The main difference between our modeled littoral drift results and DHI (2000) results is that measured waves used by CPE indicated that most of the littoral transport is towards the north (about 80%) resulting in a net of about 59,000 m^3 to the north opposed to a net drift of 17,000 m^3 as indicated by DHI (2000). This is important from a channel maintenance perspective because when most of the transport is towards one direction (as indicated by CPE) there is an inherited need to bypass sediments around the navigation channel creating navigation problems. Littoral drift rates calculated by other methods (CERC formula and shoreline changes) indicate a higher potential for transport in this area than what was predicted by numerical modeling. Because waves have been observed to break on the offshore ebb shoals, significant sediment transport is also occurring in this zone. It must be considered that wind generated currents and tides were not incorporated in the model, the model was set-up only to verify potential transport by waves, and different results may result if wind-tide driven currents and tides are incorporated.

Additionally, tidal currents near the inlet mouth (between profiles 09 and 03) will induce erosion of channel margin banks and river banks, these sediments will be transported offshore with the ebb flow and contribute to sedimentation in the ebb-shoal/channel system. Historical inlet expansion and deepening, episodic sediment input from the river are also additional source of sediments to the offshore (ebb-shoal/channel system) that were not accounted for in the alongshore sediment transport calculations.

These combined transport mechanisms (littoral transport, inlet scouring, river input, wind and tide generated currents) have the potential to transport volumes of sediments into the Boca do Tomba area channel in the same order of magnitude as the historical ebb-shoal growth rates of 226,000 m^3/yr measured.

SEDIMENT BUDGET

A sediment budget provides a conceptual and quantitative model for sediment transport within a system (Rosati and Kraus, 1999). It summarizes the movement of sediment into, out of, and within the project area for a given time period.

In an inlet sediment budget, the difference between the sediment sources (beach erosion, river input, marine sources) and the sinks in each cell (dredging, scouring) must equal the rate of change in sediment volume occurring within that region (Eq. 10).

$$\Sigma Q_{source} - \Sigma Q_{sink} = \Delta V \qquad \text{(Eq. 10)}$$

Inlets and the adjacent beaches are connected through ebb-shoals and bypassing bars. An inlet channel/ebb shoal system has the potential to capture the left-and right-directed longshore transport. Thus, knowledge of the net and gross transport rates, as well as the potential transport behaviors of the inlet with respect to the transport pathways are investigated.

Historical Sediment Budget

A sediment budget was developed for the Boca do Tomba for the time period between 1966 and 2004 based on measured historical changes in the system (Figure 29). This "historic" sediment budget was used to determine the sources and sinks of sediment within the project over the long term. The historic sediment budget was then used to develop an estimate of recent (2001 to 2004) sediment transport within the area to aid future dredging plans.

The first step in developing a sediment budget is to identify the potential sources of sediment into the inlet/ebb shoal system. At Boca do Tomba, the following sources of sediment have been identified:

1. Littoral transport around Ponta do Catoeiro.
2. Erosion of the updrift Shoreline (the shoreline along Ilha da Caçumba south of Boca do Tomba).
3. Rio Caravelas river load and river bank erosion.
4. Boca do Tomba opening and scouring.
5. Downdrift Shoreline Erosion (the shoreline along Barra do Sul, immediately northeast of Boca do Tomba).
6. Old Rio Caravelas ebb shoal.

Sediment storage areas (sinks) identified includes:

1. Boca do Tomba ebb shoal.
2. Spit at the northern end of the downdrift island.

The magnitude and sediment pathway from each source to sink was then estimated based on literature sources (*e.g.* Andrade, 1994) and analysis of historical bathymetric and shoreline changes (this report).

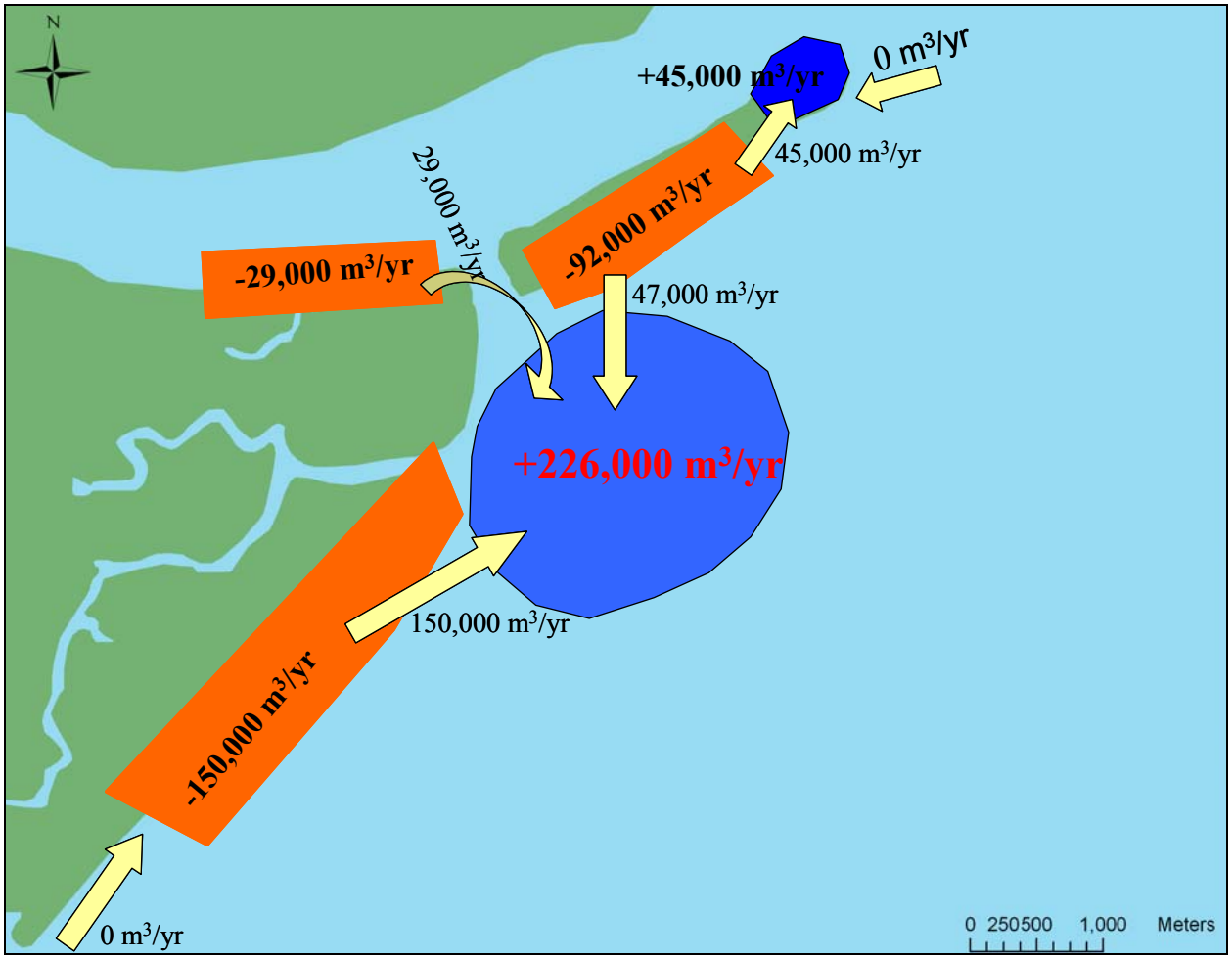

Figure 29. Historic Sediment Budget (1966 to 2004)

Littoral Transport around Ponta do Catoeiro

Sediment is transported north towards Ponta do Catoeiro at a rate of at least 125,000 m^3/year, based on its accretion rate of 25 m/year to the north (Andrade *et al.*, 1994). This study could not quantify the volume of sediment transported around and north from Ponta do Catoeiro into Ilha da Cacumba and therefore this volume was assumed to be negligible. This assumption may not be verified in the field and it must be considered that any transport around Ponta do Catoeiro will augment the supply of sediment from the

updrift shoreline and thus increase the sediment supply to the Boca do Tomba system from Ilha da Cacumba.

Updrift Shoreline (Ilha da Caçumba)

The wave modeling suggests that the sediment transport is mostly south to north, so the updrift shoreline is south of the inlet. Erosion along Ilha da Caçumba was in the order of 5.5 m/yr form 1955 to 1988, this translates to a sediment volume of about 150,000 m^3/year. The development of this estimate was discussed previously in this report. On the historical sediment budget formulation it is assumed that the sediment eroded form the updrift shoreline is transported into the ebb shoal. It is expected that this transport rate will decrease over time as the shoreline reorients itself to a more stable configuration and as sand is depleted in the beach (as indicated by recent field investigations).

Rio Caravelas River Input

The Rio Caravelas supplies some material to the Boca do Tomba ebb shoal but it is difficult to determine the quantity of the river sediment input. A comparison of two surveys collected within the river (March 2001 and November 2004) suggested that erosion of the river bed just south of the Boca do Tomba inlet. Scarping of the shoreline (river banks) was observed along the river banks south of Boca do Tomba. The erosion rate of river bank and river bed was estimated to be in the order of 29,000 m^3/year. It was assumed that this material was transported through Boca do Tomba contributing to the ebb shoal development.

Boca do Tomba Inlet

The formation of Boca do Tomba inlet resulted in the erosion of 5,567,000 m^3 of sediment from the neighboring islands, creating the current inlet throat. This material was assumed to have been transported offshore into the ebb shoal system. This volume was considered when evaluating the growth of the ebb shoal as a lump-sum sediment input into the system, it was not included in annual sediment supply estimates, because the channel is approaching a stable cross-section.

Downdrift Shoreline

The GENESIS modeling indicated that there was a nodal point on the downdrift island and that in a segment immediately north of Boca do Tomba the net sediment transport was towards the inlet. Because the ebb shoal acts as a sediment sink, southerly transport along the downdrift island will be deposited in the ebb shoal. It was observed that the north end of the downdrift island was accreting historically at an approximate rate of 45,000 m^3/year while the southern end of the island eroded at a rate of 92,000 m^3/year historically. This indicates an annual input of sediments from the downdrift island into the ebb shoal of 47,000 m^3/year.

Old Rio Caravelas Ebb Shoal

The old Rio Caravelas ebb shoal is larger than its equilibrium volume because the Boca do Tomba has diverted the majority of its tidal prism. When an inlet looses its hydraulic capacity, deflation of the existing ebb shoal is commonly observed. While this investigation was not able to determine and quantify whether that sediments from the old ebb shoal are being transported to the south and contributing to the development of the Boca do Tomba ebb shoal, we would like to indicate that it is a possibility. For example, if the accretion at the northern tip of the downdrift island (spit growth) was partially due to transport of sediment from the old ebb shoal, then the transport rate into the Boca do Tomba ebb shoal from the downdrift shoreline has been underestimated.

Ebb Shoal

The largest sink within the Boca do Tomba sediment budget cell is the offshore ebb shoal. The estimated volume contained within the ebb shoal is 14,169,000 m^3, based on a comparison of the 1966 and 2004 bathymetric surveys. The volume eroded when the inlet was created was estimated to be 5,567,000 m^3. Therefore, sediment supplied to the system from other sources is in the order of 8,602,000 m^3, which corresponds to a sediment input rate into the ebb shoal system of about 226,000 m^3/year. The existing navigation channel crosses the ebb shoal and thus the historical shoaling rate of the ebb shoal provides an indication of the potential for shoaling within the navigation channel.

Spit at the North End of the Downdrift Shoreline

The spit at the north end of the downdrift shoreline also acts as a sediment sink as it is increasing in size. The spit was estimated to be growing at 45,000 m^3/year. Sources for spit growth could not be differentiated (potential sources are the erosion of Barra do Sul and onshore transport of sediment from the ebb shoals off the old Rio Caravelas), and it was assumed herein that the predominant source is the erosion of Barra do Sul because the predominant transport direction is form north to south.

Summary from Historical Sediment Budget

Once all of the sediment sources, sinks and pathways have been identified and quantified the sediment budget can then be balanced. The balanced sediment budget presented in Figure 29 provides a regional view of sediments sources and sinks within the Boca do Tomba inlet/ebb shoal system and adjacent shorelines. However, sediment movement within the ebb shoal, and specifically into the navigation channel, requires a more refined analysis. The USACE Inlet Reservoir Model (Kraus, 2002) is a mathematical model to calculate changes in volumes of ebb-tidal shoals, and was used to model the effects of sediment transport in the navigation channel.

Recent Sediment Budget

As the inlet matures, the volume of sediment contributed by the adjacent beaches decreases because the adjacent shorelines develop a more stable planform. Observations along the adjacent beaches also suggest that sand supply may be currently limited as indicated by the beach conditions in the field (see field inspections). Furthermore, dredging of the navigation channel interrupts the natural bypassing of sand reducing sediment sources to adjacent beaches. Therefore a recent (2001 to 2004) sediment budget was developed to investigate sediment transport to the dredged navigation channel.

Nearshore wave modeling results suggests that 59,000 m^3/year were being transported north towards the inlet, while 16,000 m^3/year were being transported south into the inlet. This total transport along the beach into the inlet of 75,000 m^3/year. This estimate is in a similar order of magnitude than the gross-transport rates of DHI (2000) of 68,000 m^3/year and close to the predicted sedimentation rates within the channel of 65,000 m^3/year. However, the volume change comparison between various bathymetric surveys for the channel area suggested a channel shoaling rate of approximately 200,000 m^3/year.

The historic sediment budget suggested that about 29,000 m^3/year were being supplied by erosion of the interior river banks and river load. The sediment input into the channel from littoral transport and river load is therefore 104,000 m^3/year, approximately half of the observed sedimentation rates within the channel. Analysis of the 2004 ebb shoal survey shows that the natural channel through the inlet migrates south and north of the dredged channel and that sand sharing between the navigation channel and the ebb shoal occurs. Observed wave breaking patterns along the ebb shoal's bypassing bar also suggests that there is sediment transport from the ebb shoal into the channel due to wave action. Additionally dredging can be expected to cause slumping of the channel side slopes, and diffusion (backfilling) from the ebb-shoal to the dredged channel, all of which increase sedimentation rate within the channel.

These observations suggest that the elevated sedimentation rates within the channel are due to redistribution of sediment from the adjacent ebb shoal into the dredged channel. Therefore, the remaining 96,000 m^3/year of sedimentation within the channel was attributed to transport from the ebb shoal. The sediment contribution was divided between the north and south bars within the ebb shoal based on the ratio of littoral transport (79% from the south and 21% from the north). Figure 30 shows the sediment budget developed for the recent (post-dredging) time period.

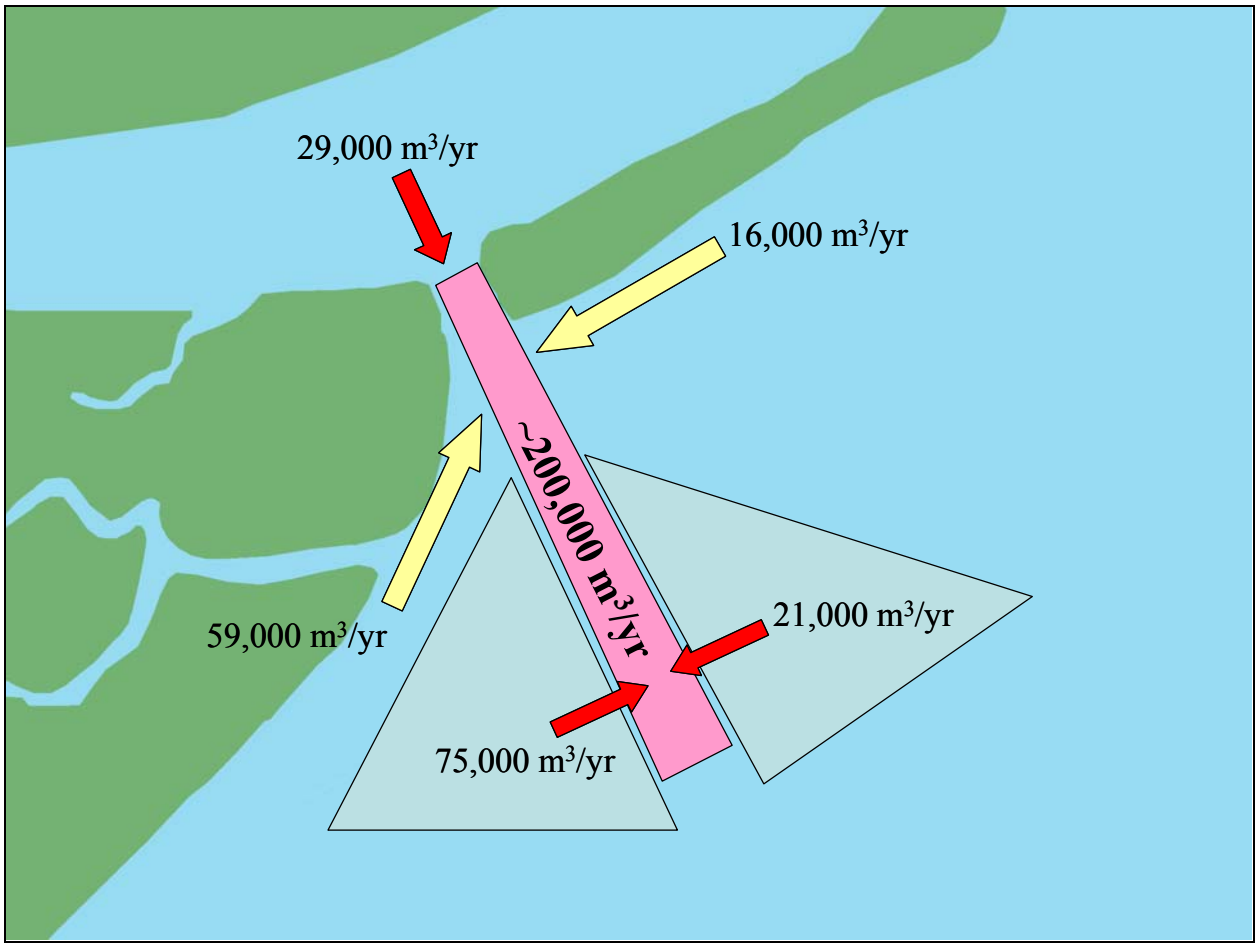

Figure 30. Recent (2001 to 2004) sediment Budget.

Previous sections of this report discussed how the sedimentation within the channel due to transport from the ebb shoal was concentrated along a 1.8 km section of the channel, where the ebb shoal bypassing bar crosses the channel. The figure above suggests that, with continuous dredging the ebb shoal sand storage will be depleted and maintenance dredging volumes can be expected to decrease with time.

INLET RESERVOIR MODEL

The USACE developed the Inlet Reservoir Model to predict the movement, storage and loss of sand from various tidal inlet features. The Reservoir Model is based on the conservation of sand volume, the existence of an equilibrium volume of morphologic features, and a "reservoir assumption (Kraus, 2002). This assumes that the inlet geomorphic features cannot form without a sufficient sediment source. A feature, such as an ebb shoal, will accrete over time but some of the material will bypass to the downdrift feature. Initially, a small volume will bypass the feature but as the feature accretes more material is transported downdrift. The model thus requires values of the input and output transport rates of each feature and their respective equilibrium volumes.

Six geomorphic features were included in the Boca do Tomba Reservoir Model (Figure 31), including:

1. the inlet,
2. the updrift shoreline,
3. the ebb shoal,
4. the channel,
5. the downdrift shoreline, and
6. the downdrift spit.

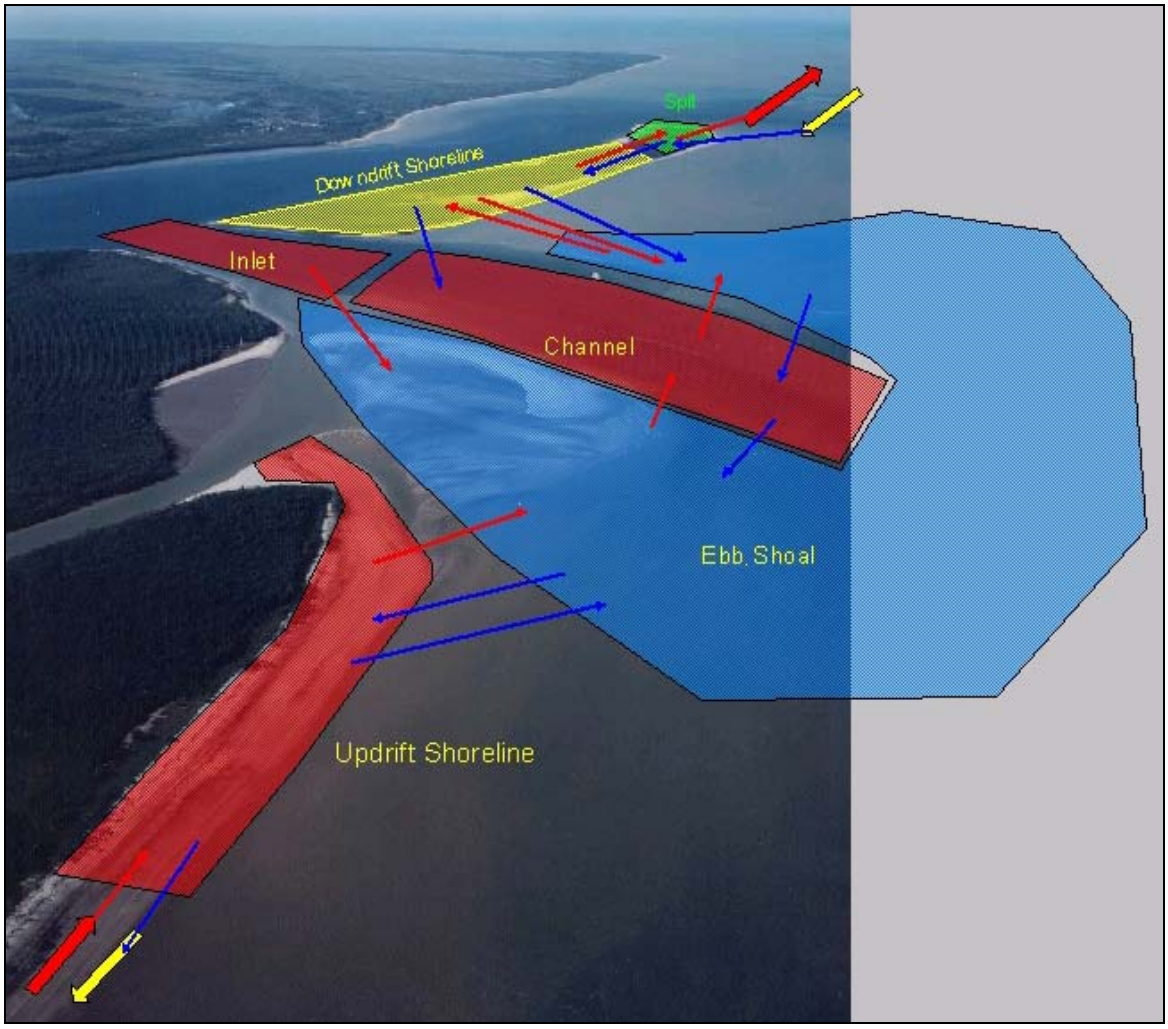

Figure 31. View of the Reservoir Model Setup for the Boca do Tomba.

The updrift and downdrift shorelines were set within the model to erode at a rate of 150,000 m^3/year and 92,000 m^3/year, respectively (historical rate). It was further assumed that the longshore transport contribution was limited to the updrift and downdrift shoreline and that there was no longshore transport into these cells. The initial volume of the inlet was 5,567,000 m^3, while the updrift shoreline and downdrift shoreline had initial input volumes of 5,674,000 $m^3$and 10,000,000 m^3, respectively. The initial

volume of the updrift shoreline was arbitrary and the model results were not sensitive to this value.

The model was calibrated using measured volume change estimates between 1966 and 2004. Ideally, several calibration points are used to calibrate and verify a model but insufficient data was available and only one calibration point was used. Model results should therefore be interpreted carefully.

The model predicts that the ebb shoal volume would have gained approximately 8,470,000 m^3 by November 2004, compared to a measured value of 8,602,000 m^3 (Figure 32). The growth of the ebb shoal is slowing but there was a distinct change in the growth of the ebb shoal following dredging event (Figure 32), caused by sediment transport (backfilling) from the ebb shoals into the channel. These modeled results reinforce the assumption of the short-term sediment budget that the adjacent ebb-shoals are a significant source of sediments into the channel.

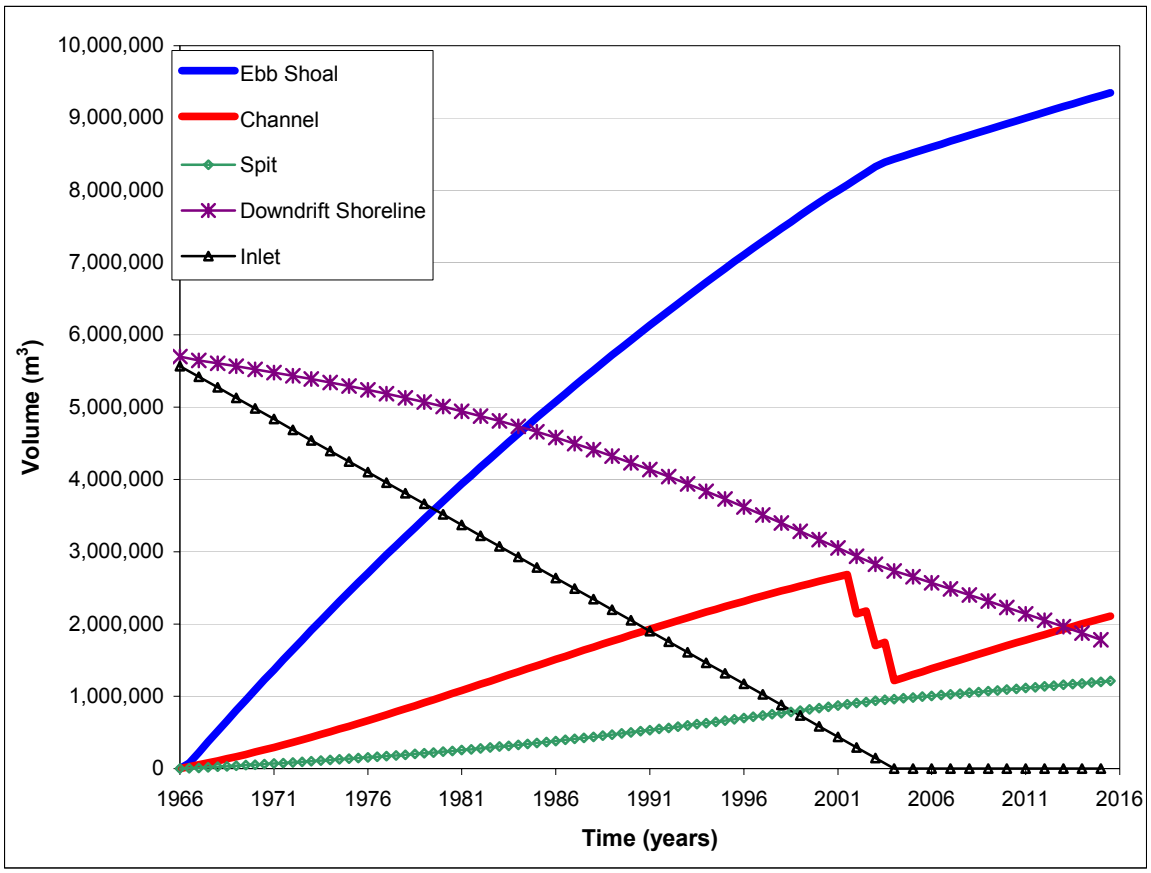

Figure 32. Reservoir Model Volumetric Output.

The model suggested that the accretion rate in the channel prior to dredging was approximately 62,000 m^3/year. While the model may not replicate the observed shoaling rates quantitatevely, it provides a useful qualitative assessment. The model illustrates that, following dredging, the shoaling rate within the channel is expected to increase, as

the modeled post dredging shoaling rate is about 85,000 m^3/year. The increased shoaling rate is from sediment entering the channel from the ebb shoal and there is an associated decrease in the ebb shoal growth rate, however it is still underestimated when compared to measured channel sedimentation rates.

The Reservoir model modeled other features within the project area. The model suggested that the volume contained in the downdrift spit was 985,000 m^3 in November 2004, compared to an observed volume of 1,697,000 m^3. The measured downdrift shoreline volume decreased from 5,674,000 m^3 to 2,178,000 m^3 between 1966 and 2004, while the model predicted a downdrift shoreline volume of 2,654,000 m^3 at the end of 2004.

Overall, the reservoir model predicted the qualitative behavior of the Boca do Tomba project area but it was not accurate quantitatively. Interpretations from model results indicate that:

1. Shoaling rates at Boca do Tomba increase following dredging events.
2. The rate of ebb shoal growth is decreasing.
3. Shoaling in the channel is not fully dependent on ebb shoal growth rate.

CHANNEL MAINTENANCE VOLUMES

Verified sedimentation rates at the Boca do Tomba channel are higher than previously estimated. Maintenance dredging is not required in the channel throat section (landward of station 2000 m) and very low requirements exist offshore of station 5000 m. From the multiple lines of evidence presented in this report we recommend that, to maintain the Tomba channel navigable for the following years, dredging maintenance volumes in the order of 200 m^3/yr (+/- 50,000) are required between channel stations 2000 m and 5000 m offshore. Intensification of dredging is required in problematic areas such as the 1 km stretch between channel stations 3000 m and 4000 m, where navigation is currently problematic. In addition to the annual maintenance volumes cited above, a capital dredging of about 103,300 m^3 is necessary to bring the channel to an elevation of – 4 m below 0 DHN (NR) and 90 meters wide, and a volume of 418,300 m^3 are necessary to bring the channel to an elevation of – 5 m below 0 DHN (NR) and 90 meters wide (see appendix 1).

Channel maintenance volumes recommended herein occur mainly due to:

(a) Dredging activities upset the channel/ebb-shoal equilibrium, resulting in greater diffusion (backfilling) of sediments from the ebb-shoal into the channel. This effect is pronounced at Boca do Tomba because the dredged channel was cut through the existing ebb-shoal and large part of the current sedimentation observed in the channel is due to sediment sharing between the dredging channel and the existing ebb-shoal (backfilling/diffusion).

(b) Wave-induced gross alongshore sediment transport.

(c) Channel migration which occurs due to the natural flow regimes or development of shoals in the deltas or spits in the mouth and is an additional source of sedimentation into the channel (promotes sand sharing between channel and adjacent shoals).

(d) Offshore channel flushing is not sufficient to remove sandy sediments from the channel as shown by the analysis channel monitoring data (bathymetry).

Sudden shoaling of navigation channels is also often related to storms, antecedent events, and channel bathymetry. Increases in expected dredging quantities and changes in shoaling patterns can occur because of an intense storm season, because of intensive rainfall over the watershed (that may increase the sediment-laden flow into the inlet) and therefore safety ranges for dredging maintenance volume estimates must be considered and incorporated into design. Channel maintenance dredging was underestimated by DHI (2000), but even though, given the circumstances of limited performance and monitoring data (dredging records, channel monitoring surveys, ebb-shoal bathymetric surveys, and wave measurements), a comprehensive and professional modeling effort was conducted by the previous consultant.

FINAL CONSIDERATIONS

The study reported herein used guidance and predictive capabilities of numerical models, supplemented by measured performance data, historical trends, and the expertise of a multi-disciplinary team to provide the second opinion recommendations. Our main findings include:

- Dredging requirements for the Boca do Tomba channel will be in the range of 200,000 m^3 (+/- 50,000 m^3) per year between channel stations 2000 m and 5000 m offshore. The sources of sedimentation into the channel are approximately divided as follows:

B. Downdrift (south) Beach ~ 30%
C. Updrift (north) Beach ~ 8%
D. Ebb shoals ~ 48%
E. Erosion of river banks and river load ~ 14%

If the channel is regularly maintained by dredging the amount contributed by the ebb shoal will decrease over time as this shoal “reservoir” of sediment is depleted. Shoaling occurs primarily in the nearshore zone of the channel, from station 2000 m to station 5000 m. Shoaling is most severe from station 3000 m to 4000 m where navigation can be negatively impacted between dredging events.

- Based on the Nov 2004 bathymetric survey Capital dredging of 103,300 would be required to establish a channel 4 m deep (below 0 DHN) and 90 meters wide, and capital

dredging of 418,300 is necessary to establish a channel 5 m deep (below 0 DHN) and 90 meters wide.

- The Boca to Tomba channel is '*stable'* (self-scouring) in its throat section (landward of channel station 2000 m) but it is not self-scouring in the nearshore zone (between stations 2000 m and 5000 m) where the channel flows reduce and sand deposits. Material shoaling in the channel between is predominantly sand.

REFERENCES

Andrade, A.C.S. 1994. Geologia da região costeira de Caravelas-Bahia: contribuição ao planejamento ambiental. Salvador-Ba, Dissertação de Mestrado, IGeo-UFBa. 152p. (Texto e mapa).

Bruun, P., Mehta, A.J., and Jonsson, I.G., 1978. Stabilityof tidal inlets; Theory and Engineering. Eslsevier, Amsterdam, pp. 1-464.

CEPEMAR, 2001. Relatório de EIA-RIMA: Terminal de barcaças para embarque e desembarque de toras de eucalipto, Caravelas-BA. Report prepared by CEPEMAR Serviços de Consultoria em Meio Ambiente Ltda. para Aracruz Celulose S.A.

CEPEMAR, 2004. Canal de Acesso ao Tomba Dragagem de Aprofundamento: Overflow de Sedimentos Arenosos. Report prepared by CEPEMAR Serviços de Consultoria em Meio Ambiente Ltda. para Aracruz Celulose S.A.

Davis, Jr. R.A. and FitzGerald, D.M., 2004.. *Beaches and Coasts*. Oxford: Blackwell Publishing, 419 pp.

Davis, Jr., R.A. and M.O. Hayes, 1984, What is a wave-dominated coast? Mar. Geol., Vol. 60, pp. 313-329.

DHI, 1998. Norsul Terminal, Caravelas Brazil: Preliminary Assessment and Numerical Wave Modeling. Report Prepared by the Danish Hydraulic Institute (DHI) for Norsul Shipping Company,

DHI, 2000. Hydraulic Investigations for Port Facilities at Caravelas. Report Prepared by the Danish Hydraulic Institute (DHI) for Aracruz Celulose S.A.

DHI 2004. Caravelas Project: Additional Hydraulic Studies. Report Prepared by the Danish Hydraulic Institute (DHI) for Aracruz Celulose S.A.

FitzGerald, D.M. (1996). "Geomorphic variability and morphologic and sedimentologic controls on tidal inlets," Journal of Coastal Research SI23, 47-71.

Gravens, Mark B. and Nicholas C. Kraus, 1991. GENESIS: Generalized Model for Simulating Shoreline Change, Report 2, Workbook and System User's Manual, Technical Report CERC-89-19, Coastal Engineering Research Center, Vicksburg, MS.

Hicks D.M. and Hume, T.M. 1996. Morphology and size of ebb tidal deltas at natural inlets on open sea and pocket-bay coasts, North Island, New Zealand. Journal of Coastal Research 12(1) p.47-64.

Hayes, M.O., 1980. General morphology and sediment patterns in tidal inlets. Sed. Geol., 26:139-156.

Hubbard, D.K. 1977. Variations in tidal inlet processes and morphology and the Georgia embayment. Technical report 14-CRD, Coastal Research Division, Geology Department., University of South Carolina, Columbia, SC, 79pp.

Jarret, J.J., 1976. Tidal-prism-inlet area relationships. GiTi report 3, U.S. Army Corps of Engineers, Waterways Experiemnt Station, Vicksburg, 31 pp.

Kraus, N.C., 2002. Reservoir model for calculating natural sand bypassing and change in volume of ebb-tidal shoals, Part I – Description. ERDC/CHL CHETN-IV-39 U.S. Army Engineer Research and Development Center, Vicksburg, MS, 14 pp.

Martin L, Bittencourt ACSP, Vilas Boas GS andFlexor J-M. 1980. Mapa geológico do quaterná-rio costeiro do Estado da Bahia – Esc. 1:250.000.Salvador-BA, SME/CPM. 60p. (Texto explicativo emapa).

Nummedal, D. and Fischer, I., 1978. Process-response models for depositional shorelines: The German and Georgian Bights. American Society of Civil Engineers, Proceedings 16th Coastal Engineeirng Conference., p. 1215-1231.

O'Brien, M.P., 1969. Equilibrium flow areas of inlets on sandy coasts. Journal of Waterways and Harbors Division, ASCE., pp. 43-52

Pope, J. (2000). "Where and why channels shoal: A conceptual geomorphic framework," ERDC/CHL CHETN-IV-12, U.S. Army Engineer Research and Development Center, Vicksburg, MS.

Rosati, J.D. (2003). "Coastal Inlet Navigation Channels Shoaling with Deepening and Widening," ERDC/CHL CHETN-IV_, U.S. Army Engineer Research and Development Center, Vicksburg, MS.

Rosati, J.D., and Kraus, N.C. (1999). "Formulation of sediment budgets at inlets," Coastal Engineering Technical Note CETN-IV-15 (Revised September 1999), U.S. Research and Development Center, Vicksburg, MS.

Smith, J. M. (2001). “Modeling nearshore transformation with STWAVE,” Coastal and Hydraulics Engineering Technical Note CHETN I-64, U.S. Army Engineer Research and Development Center, Vicksburg, MS.

USACE (U.S. Army Corps of Engineers), 1984. Shore Protection Manual. Vicksburg, Mississippi: Coastal Engineering and Research Center, Waterways Experiment Station, Vicksburg, Mississippi, Volume 1, 4th ed., US Government Printing Office, Washington, D.C., 639p.

Vincent, C.M., and Uva, L.P. (1984). "Sedimentation in dredged channels and basins -- prediction of shoaling rates," Proceedings, 19th International Conference on Coastal Engineering, American Society of Civil Engineers, 1863-1878.

Walton, T.L. and Adams, W.D., 1976. Capacity of inlet outer bars to store sand. Proc. 15th Conf. Coastal Eng., ASCE, pp. 1919-1937.

Caravelas Project

Channel Maintenance Programme

Numerical Modelling of Sedimentation Processes

Aracruz Celulose S.A.

Draft Final Report
July 2006

Caravelas Project

Channel Maintenance Programme

Numerical Modelling of Sedimentation Processes

Agern Allé 5
DK-2970 Hørsholm, Denmark

Tel: +45 4516 9200
Fax: +45 4516 9292
Dept. fax: +45 4516 8952
e-mail: dhi@dhi.dk
Web: www.dhi.dk

Client	Client's representative
Aracruz Celulose S.A.	Mário Cerqueira Junior

Project	Project No
Caravelas Project Channel Maintenance Programme Numerical Modelling of Sedimentation Processes	53880
Authors Jens Kirkegaard Anders Jensen Henrik René Jensen Ida Brøker Hans Jacob Vested	Date 28 July 2006 Approved by Jens Kirkegaard Project Director

Revision	Description	By	Checked	Approved	Date
0	Draft Final Report	ANJ/HJV	IBH	JKJ	28/07/06

Key words	Classification
Tidal Inlet Navigation Channel Sedimentation Numerical Modelling	☐ Open ☐ Internal ☒ Proprietary

Distribution	No of copies
Aracruz Celulose S.A.:	1 pdf
CPE:	1 pdf
CEPEMAR:	1 pdf
DHI: JKJ, ANJ, HRJ, HJV, IBH, JAO	1 pdf +1

CONTENTS

DRAWINGS

APPENDICES

1 INTRODUCTION

The present report describes the detailed modelling studies of sedimentation in the Caravelas Channel. The studies were proposed and a detailed proposal requested by Aracruz Celulose S.A. during a joint meeting for discussion of the 2nd Opinion Report by CPE in Vitoria-ES on 25-26 October 2005. Aracruz requested a joint effort by CPE, CEPEMAR and DHI as outlined in the Action Plan prepared at the conclusion of this meeting, see Appendix A.

Accordingly, DHI submitted a proposal on 16 December 2005, which was accepted by Aracruz Celulose Work Order 1163826 dated 22.02.2006.

The basic data required for the study was received during March-April 2006. Results of the new bathymetric soundings became available during a project meeting held in Aracruz on 3 May 2006 between Aracruz, CEPEMAR, CPE and DHI. At this meeting a preliminary presentation of the additional data was made and the data was reviewed by the participants. Lacking data and information was identified. The most important part of this data was received during the month of May.

2 CONCLUSIONS

Mathematical modelling has been used as a tool during the planning and design of the navigation channel at Caravelas. Earlier models were based on bathymetries obtained in 1998 and 2000. The depth conditions seaward of Boca do Tomba have changed significantly in recent years and much improved bathymetric information has been obtained during and after completion of the capital dredging in 2005. For this reason the mathematical model bathymetry has been updated before conducting detailed studies of sediment transport and deposition processes in the channel.

The objective of the present model is to describe the deposition of sand and mud in the channel. The modelling efforts include the application of advanced hydrodynamic models of tides, currents, waves and sediment transport.

Initially, the models have been calibrated to describe the sedimentation in the channel experienced during the period from July 2005 to February 2006. During this period the total accumulation was approx. 50,000 m^3 with about 30% being sand and 70% mud.

The calibration has described, with sufficient accuracy, the sediment distribution along the channel.

After the calibration the model was used to determine the yearly sedimentation in the present channel corresponding to depth conditions in February 2006. The average yearly sedimentation obtained by the model is 85,000 m^3 of which 27,000 m^3 is sand.

The sedimentation is a very complex process and it is generally found that results should be regarded with a very wide margin of a factor 2. Thus the results indicate that yearly sedimentation shall be expected to be within 40,000 and 170,000 m^3.

Four scenarios have been tested for comparison with the present situation, here denoted Scenario 0. The relative results of the scenario models are summarised below.

Scenario 1 - The existing channel is dredged to -5.5 m
The deepening of the channel results in a reduction of the sedimentation of mud sediments by almost 50% as compared to the existing situation. The increase of depths attracts the flow and the ebb flow deposits the sediment further south than in the existing channel. Backfilling with sand is found to be almost unchanged compared to the existing situation with an insignificant tendency for reduction of backfilling.

Scenario 2 - The channel realigns with the alternative channel
The presence of an alternative channel that follows the development of the new ebb channel is not an attractive option. The ebb flow is divided between the two channels and significant sedimentation must be expected. The modelling has shown that both sand and mud backfilling are significantly larger in the alternative channel alignment as long as the existing channel is maintained. If this option should be effective from a hydrodynamic point of view the existing channel should be filled up.

Although not confirmed by modelling, it is expected that the total sedimentation in the alternative channel, with the present channel closed, will not result in significantly lower sedimentation compared with Scenario 1.

Scenario 3 - The alternative channel is partly blocked
The simulation of closure of the alternate channel route indicates that a better flushing of the existing channel will be achieved. The sedimentation of mud is reduced for this scenario to the same level as for Scenario 1. The simulation has illustrated that alternative ebb channels which develop naturally shall preferably be backfilled, for instance with dredged material to optimise the self cleansing of the navigable channel.

Scenario 4 - Dredging a 1 m deep depression in the existing channel
This scenario clearly illustrates that overdredging in parts of the channel, which leads to depressions where the bottom level of the channel is lower than the general bottom level, leads to a significant increase of mud sedimentation.

3 STUDY APPROACH

3.1 Overall Study Objectives

The navigation channel from the open sea to Boca do Tomba has been dredged in the period from early 2002 to March 2005. The channel is dredged through the sandy ebb tidal shoals outside Boca do Tomba and through mud (lama) deposits below the sand layer and outside the ebb tidal shoals. The channel was dredged to depths deeper than 4.5 m below DHN datum with a width of more than 90 m except in the section passing the ebb tidal shoals about 2 km from Boca do Tomba, see Figure 3.1. At the end of the dredging in March 2005, the channel did not have the design width of 90 m in the central part of the channel.

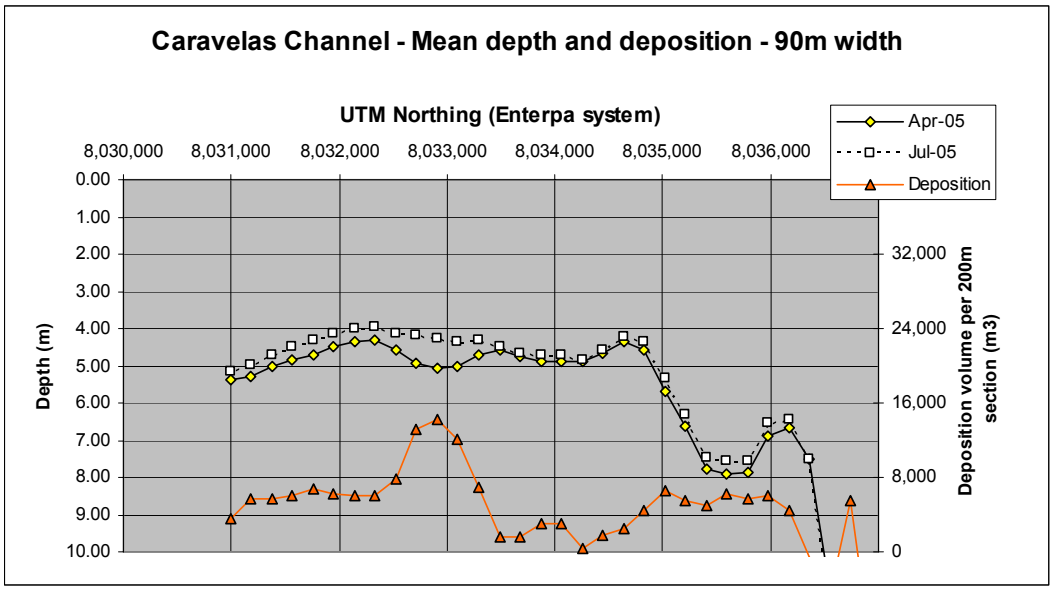

Figure 3.1 Development of the channel mean depth between April and July 2005. The offshore end of the channel is to the left in the plot. The largest deposition intensity is in the section south of the sand shoals (dredging Area 2, 1. Trecho).

As a result of wave action and currents the sand and mud are transported and deposited in the relatively calmer channel. Sediment samples and bathymetric soundings in 2005 and 2006 have shown that 70% of the deposited volume is mud for the entire channel and 50% is mud in the narrow cut through the ebb tidal shoals, Ref. /1/.

The total volume of sedimentation was 130,000 m^3 from April to July 2005, Refs. /1/ and /2/, and considerably less in the following seven months. From an earlier analysis it is expected that the total annual sedimentation is in the order of 200,000 m^3, Ref. /3/. A reassessment of this annual sedimentation is a main objective of the actual studies by CPE, CEPEMAR and DHI.

Maintenance of the channel depth needs to be planned with the aim of minimising the annual maintenance costs. For this purpose DHI, CPE and CEPEMAR have prepared an Action Plan, see Appendix A, upon request by Aracruz Celulose S.A. The plan includes

monitoring activities, numerical modelling and assessment of dredging technologies and procedures.

3.2 DHI Activities

The Action Plan (included as Appendix A) aims at recommending an optimal dredging practice by September 2006. DHI's main task of this plan is to provide updated modelling of the sediment transport and deposition in and around the navigation channel. In order to obtain the necessary basic information for the model set-up and interpretation an additional survey and monitoring programme has been carried out by CEPEMAR according to specifications prepared by DHI.

3.3 Hydrodynamics and Wave Modelling

Hydrodynamic modelling together with the wave modelling are the key tools for modelling the sediment transport and sedimentation pattern.

The hydrodynamic and wave modelling has, contrary to earlier studies, been carried out using the MIKE 21 Flexible Mesh (MIKE 21 FM) model which allows a much larger area to be included without compromising on the need for high resolution around the channel and the inlet. The 2-dimensionel model approach has been chosen due to the shallowness of the study area and the relatively small outflow of freshwater from the river compared to the large tidal flow.

The model bathymetry has been based on depth soundings made by CEPEMAR in February 2006 supplemented by data from September 2000 and November 2004 soundings. The local bathymetry data is supplemented by depth information from nautical charts to include important tide measurement stations at Cumuruxatiba to the north, Ilha de Santa Barbara (Abrolhos) to the east and Nova Viçosa to the south

The overall model mesh used in this study is shown in Figure 3.2 and an extract of the detailed mesh around the dredged channel is shown in Figure 3.3 together with centreline coordinates for the navigation channel.

The side length of the largest model mesh element is 4500 m having an area of 10,125 m^2 whereas the side length of the smallest element is 20 m having an area of 200 m^2. The total number of elements in the model is more than 86,000.

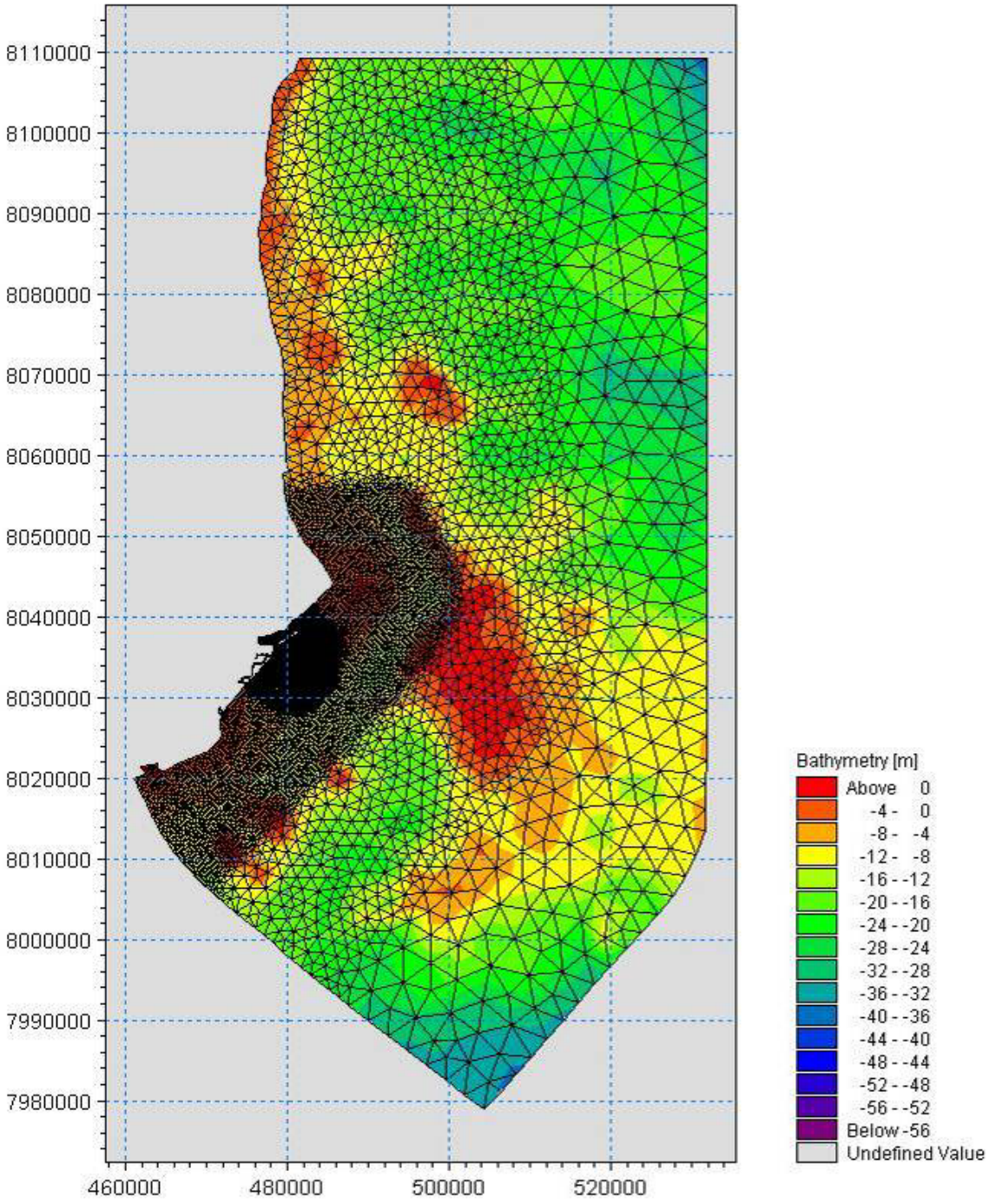

Figure 3.2 Model mesh for the hydrodynamic and sediment modelling.

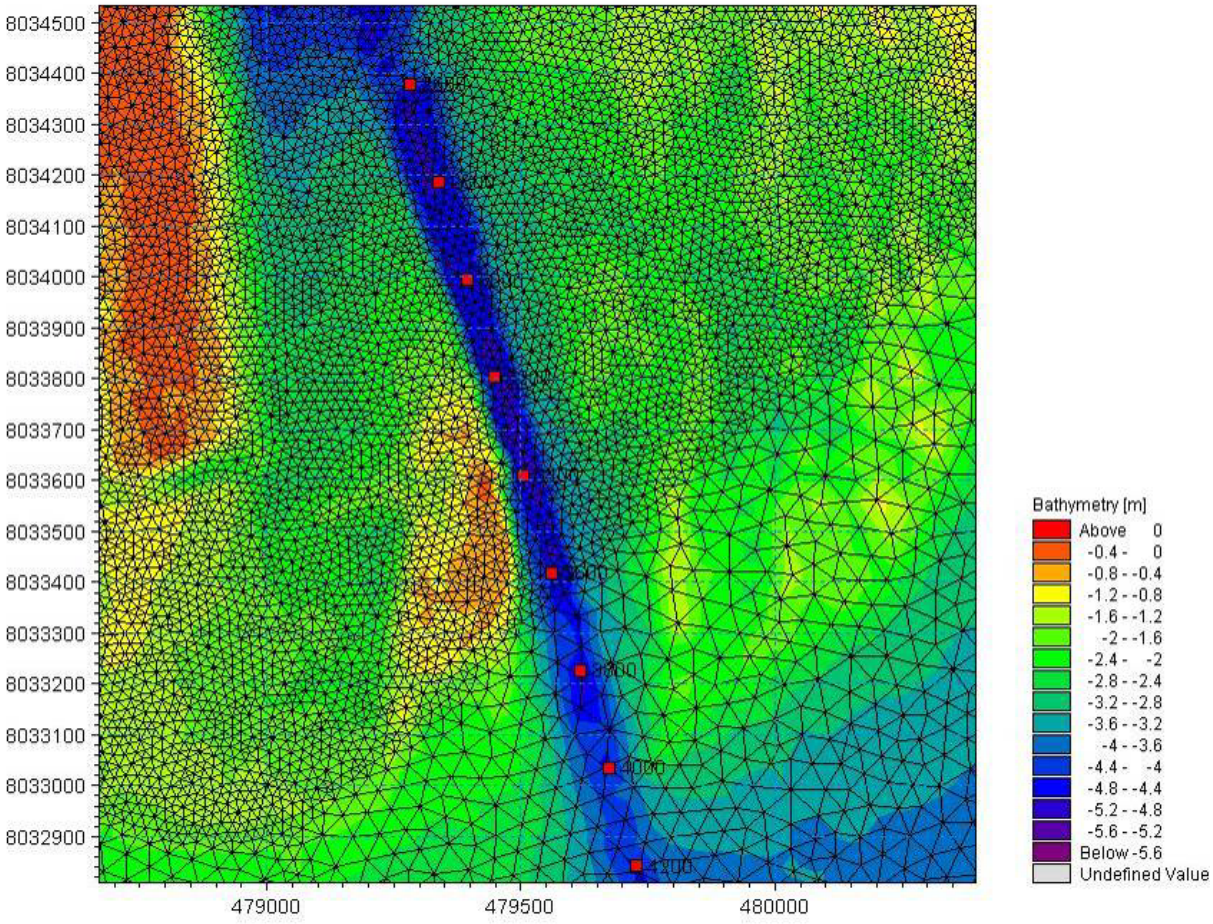

Figure 3.3 Detailed extract from an area around the dredged channel (stations 2500-4200). The red dots indicate the centreline of the channel. The bathymetry shown here represents the channel as surveyed by CEPEMAR in February 2006.

A short outline of the DHI Flexible Mesh model is given in the box below. For a detailed description reference is made to Appendix C in which a general presentation and scientific documentation are provided.

Flexible Mesh Modelling System (MIKE21-FM)

The FM 2D hydrodynamic model is a general numerical modelling system for the simulation of water levels, flows, temperature and salinity stratification in estuaries, bays and coastal areas. It simulates unsteady 2D flows using depth integrated formulations.

The FM HD includes formulations for the effects of

- Convective and cross momentum
- Bottom shear stress
- Wind shear stress at the surface
- Barometric pressure gradients
- Coriolis forces
- Momentum dispersion (through e.g. the Smagorinsky formulation)
- Sources and sinks (mass and momentum)
- Flooding and drying
- Heat exchange with atmosphere
- Vertical stratification

Hydrographic boundary conditions can be specified as a constant or variable (in time and space) level or flux at each open model boundary, as a constant or variable source or sink anywhere within the model, and as an initial free surface level map applied over the entire model.

The FM model can be applied to a wide range of hydraulic and related phenomena. This includes modelling of tidal hydraulics, wind generated currents, storm surges and flood waves. The FM HD results are also used as input for many of the other modules such as the Advection-Dispersion module (AD) and the Water Quality modules (EU).

The solution technique is based on a finite volume approach on a triangular mesh.

The FM model has the advantage that a maximum resolution can be achieved in areas of interest whereas a more coarse resolution can be applied in areas of less complexity.

3.4 Wave Modelling

A fully spectral wind wave model, MIKE 21 SW, has been used to simulate the locally generated wind waves as well as the swell. The model uses a flexible computational grid as shown in Figure 3.4.

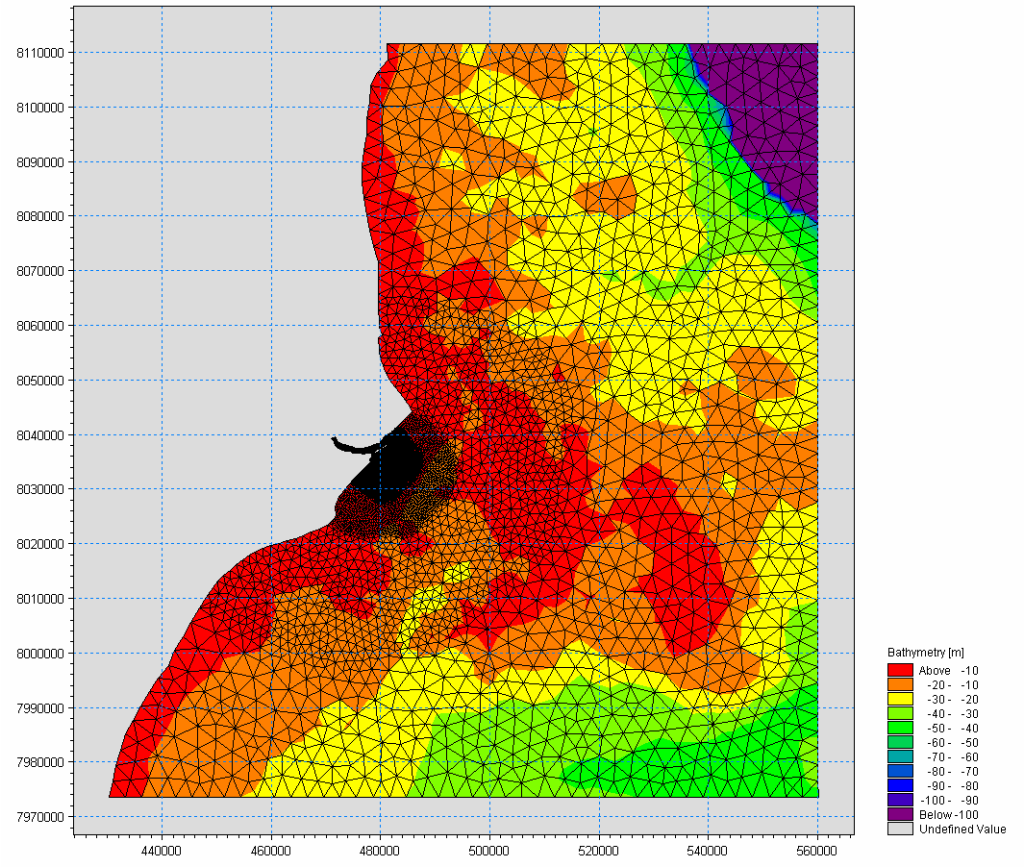

Figure 3.4 Applied model mesh for the wave modelling.

3.5 Sediment Models

Two modules of DHI's 2D Flexible Mesh modelling complex have been applied: MIKE 21 ST for sand and MIKE 21 MT for mud.

Both models use calculated fields of currents, water levels and waves as input.

MIKE 21 ST calculates the transport capacity of non-cohesive sand taking into account the grain size, water depth, current speed and direction and wave action including breaking.

The MIKE 21 MT model describes erosion and transport and deposition of mud under the action of currents and waves.

MIKE 21 MT includes the following processes:

- Sliding
- Salt flocculation
- Detailed description of the settling process
- Multiple layer description of the bed

The settling velocity varies according to the salinity, if included, and the concentration taking into account flocculation in the water column.

MIKE 21 MT (mud transport) and MIKE 21 ST (sand transport), respectively, are described in Appendix C.

4 DATA BASIS

4.1 Channel Location

The channel location is shown in Table 4.1. The centre coordinates shown in Figure 3.3 originates from this table.

Table 4.1 Channel geometry as determined based on leading light alignment, reference to Belov Drawing 2006-04-32-001-REV0 dated 04/2006.

Channel Centreline:				Channel West side				Channel East side		
station	E	N		station	E	N		station	E	N
0	478,556.7	8,036,875.9		0	478,513.5	8,036,863.4		0	478,599.9	8,036,888.4
1800	479,058.7	8,035,147.3		1800	479,015.5	8,035,134.8		1800	479,101.9	8,035,159.8
2200	479,170.3	8,034,763.1		2200	479,127.1	8,034,750.5		2200	479,213.5	8,034,775.6
2600	479,281.8	8,034,379.0		2600	479,238.6	8,034,366.5		2600	479,325.0	8,034,391.6
3000	479,393.4	8,033,994.9		3000	479,350.1	8,033,982.4		3000	479,436.6	8,034,007.5
3200	479,449.1	8,033,802.8		3200	479,405.9	8,033,790.3		3200	479,492.4	8,033,815.4
3400	479,504.9	8,033,610.8		3400	479,461.7	8,033,598.2		3400	479,548.1	8,033,623.3
3600	479,560.7	8,033,418.7		3600	479,517.5	8,033,406.2		3600	479,603.9	8,033,431.3
3800	479,616.5	8,033,226.6		3800	479,573.3	8,033,214.1		3800	479,659.7	8,033,239.2
4000	479,672.3	8,033,034.6		4000	479,629.0	8,033,022.0		4000	479,715.5	8,033,047.1
4200	479,728.0	8,032,842.5		4200	479,684.8	8,032,830.0		4200	479,771.2	8,032,855.1
4600	479,839.6	8,032,458.4		4600	479,796.4	8,032,445.8		4600	479,882.8	8,032,470.9
5000	479,951.1	8,032,074.2		5000	479,907.9	8,032,061.7		5000	479,994.3	8,032,086.8
5400	480,062.7	8,031,690.1		5400	480,019.5	8,031,677.6		5400	480,105.9	8,031,702.7
5800	480,174.2	8,031,306.0		5800	480,131.0	8,031,293.4		5800	480,217.5	8,031,318.5

The channel cross-sections (channel stations) are described by their distance from the north end of the channel inside Boca do Tomba. The relation between channel station and UTM coordinates is given by the set of equations:

Northing = 8,036,875.9-0.960331 Station

Easting = -0.290406 (Northing - 8,036,875.9)+478,556.7

This new channel geometry is in accordance with the installed leading lights. The new channel is west of the most recent channel geometries applied by the dredging contractor, Enterpa, during dredging operations (8 m and 28 m difference at the north and south ends of the channel, respectively) and east of the original channel design.

4.2 Tidal Data

Tidal predictions based on a tidal constituent database (KMS) have been used to define the open sea boundary conditions for the hydrodynamic model. The KMS database on tidal constituents consists of maps of constituents that are determined from 15 years of

satellite measurements. Tidal variations are described horizontally as well as in time. The boundaries are shown in Figure 3.1. The predicted tide at the 4 open boundaries during the entire model period is shown in Figure 4.1 and shorter sequences are shown in Figure 4.2. Figure 4.3 shows an example of the difference between the western and the eastern ends of the north boundary. Similar patterns are found along the other boundaries.

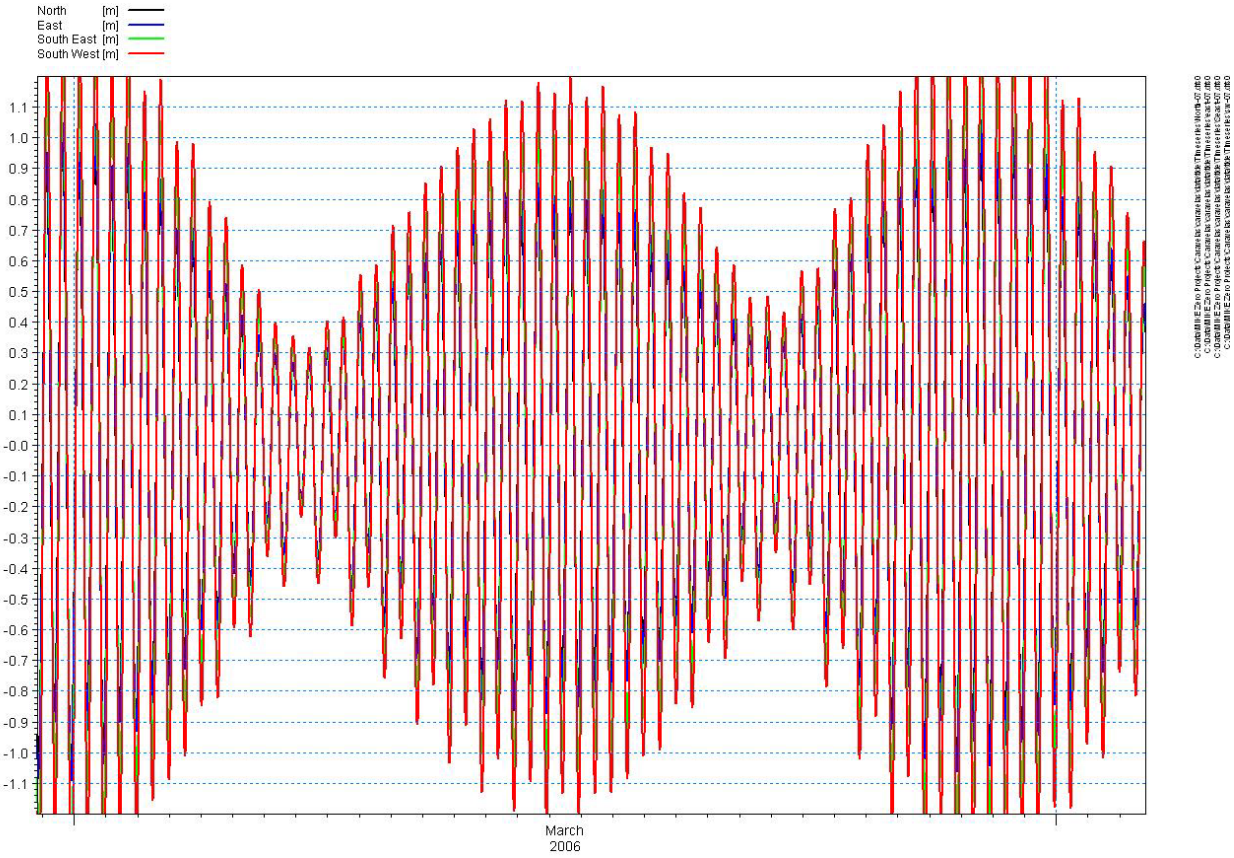

Figure 4.1 Predicted tide at the open boundaries. The curves shown are extracted from the centre of each boundary. There is an approx. difference of 0.1 m from one end to the other of each boundary.

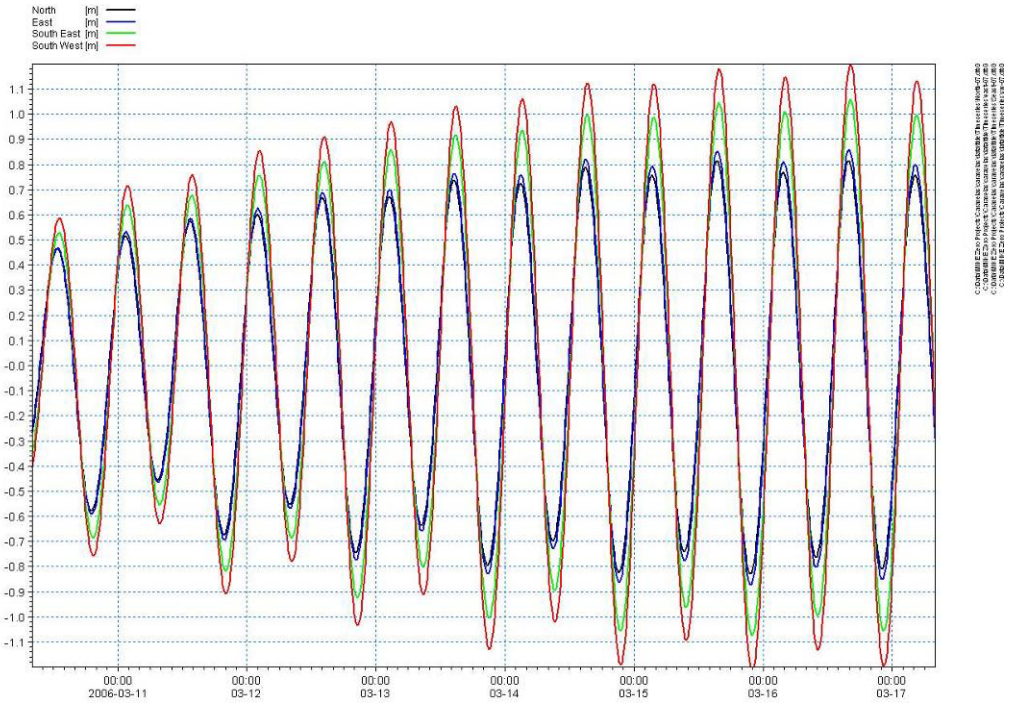

Figure 4.2 Details of Figure 4.1.

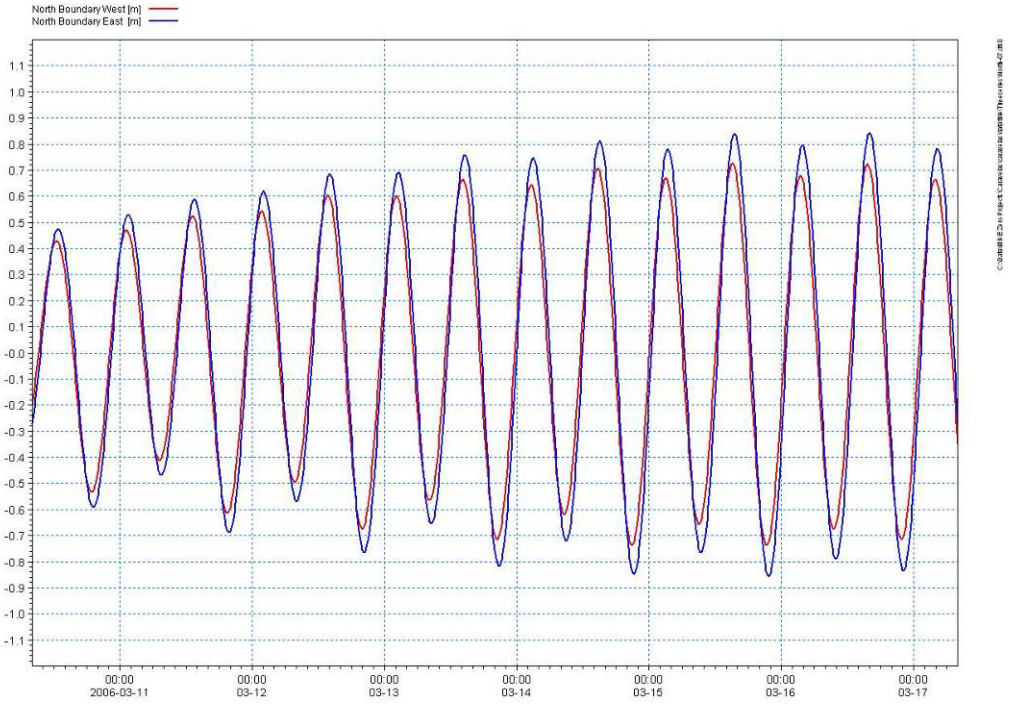

Figure 4.3 Difference between the western and the eastern ends of the north boundary.

4.3 Current Measurements and Boundary Conditions in the River

New current measurements have been made in the river in order to assess the tidal prism in Rio Caravelas and the surrounding mangrove area and to define the inland boundary conditions. The bathymetry for the river system and tidal channels west of Caravelas is

complicated and to a large extent unknown. The current measurements were carried out as depth profiling transects across the river mouth near Punta da Areia west of the terminal. The transect measurements have been repeated once every hour for a full tidal cycle one time at neap and one time at spring. The total tidal prism for each period and the flow rates have been calculated and sent to DHI. All results from the measurements were reported by CEPEMAR in April 2006, Ref. /7/.

A relation between the river discharges and the measured water levels from the Caravelas Terminal has been established and used to calculate the water flow boundary for the river. The calculated flow variation used as boundary condition is shown in Figure 4.4.

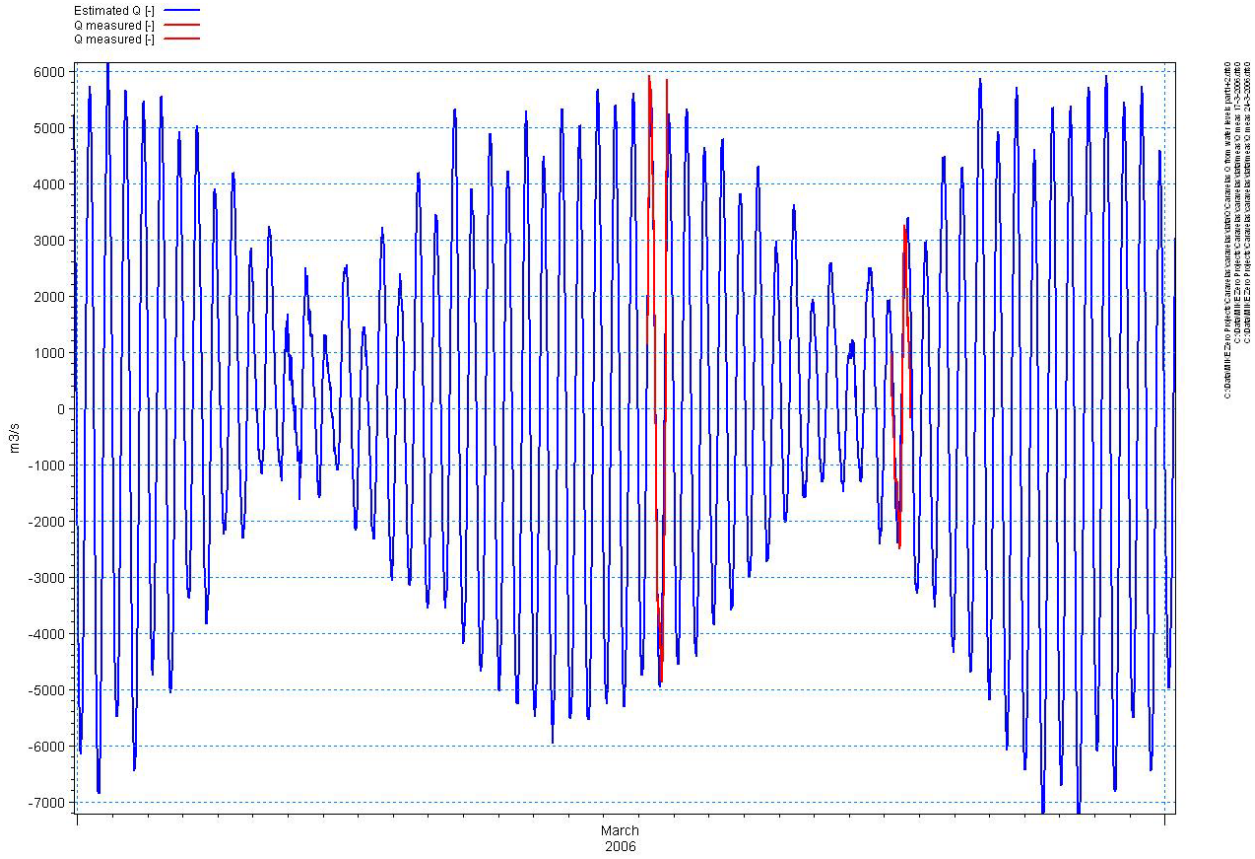

Figure 4.4 Calculated (blue line) and measured (red line) water flow.

In the figure, the red curve shows the measured discharge and the blue curve shows the river discharge as estimated from the measured water levels. The relation used is:

$$Q\ [m^3/s] = -4000\ [m^2] \times WL\ [m]$$

To get the phase correct, the phase of the discharge was shifted by -2.5 hours.

4.4 Bathymetric Soundings

The basic bathymetry of the model is based on depth soundings made by CEPEMAR in February 2006. The target for calibration of the sediment transport model is established

by subtracting the depths of the July 2005 survey from the depths of the February 2006 survey. The resulting differences in bed levels along the centreline of the bottom of the channel have been used as the target for calibration of sediment accumulation. The April 2005 survey has been used in the assessment of sedimentation and the post dredging survey of March 2006 has been used to calculate the dredged volume. All depth values are relative to chart datum. Position coordinates are in UTM-24S (WGS-84).

Note that both CEPEMAR and Belov made soundings in February 2006. The CEPEMAR bathymetry (obtained a few days after the start of dredging) is used in the model as it was available earlier than the Belov data (pre-dredging). The small differences between the two bathymetries are insignificant for the modelling. The Belov data have been used for calculation of volume changes.

4.5 Sediment Properties

Sediment grain size distribution data and characterisation was collected by CEPEMAR in July 2005 and February 2006, Ref. /6/. This data has been used in the model set-up for the definition of sediment transport model parameters.

This data was obtained from samples made by 90 cm long PVC tubes driven into the bottom by divers. The cores provide an impression of the layers of deposition and the characteristics of the layers were described by geologists. Samples were extracted from about 50% of the layers for detailed granulometric analyses. From these the average mud contents in the cores have been computed. The mud content values have been used to compute the distribution of mud and sand sedimentation along the channel.

4.6 Assessment of Sedimentation from April 2005 to April 2006

The bathymetric surveys from April 2005 (APR05), July 2005 (JUL05), February 2006 (FEB06) and April 2006 (APR06) have been transformed into digital terrain models (DTM) using ESRI Arc Map software. The x,y,z data is interpolated into a 10 m x 10 m DTM using the inverse distance weighted method which is similar to the method used by MIKE 21 to create the model bathymetry. All depth values are relative to chart datum. Position coordinates are in UTM-24S (WGS-84).

A zone along the centreline of the channel stretching from “1800” to ”6200”, which is the critical stretch of the channel, and extending 45 m on each side of the centreline has been selected for the study of sedimentation and dredging volumes. The four DTMs are shown on Dwgs. 1-4 together with profiles extracted along the centrelines.

The time gaps between the various bathymetric surveys are:

APR05 to JUL05: 3.5 months (106 days)

JUL05 to FEB06 : 6.5 months (196 days)

FEB06 to APR06: 2 months (63 days – Dredging 13/02-10/3 and 25-31/3)

Accumulation and erosion volumes calculated as JUL05-APR05, FEB06-JUL05 and APR06-FEB06 are given in Table 4.2. Accumulation is calculated separately from ero-

sion meaning that the values shown are gross values. Maps showing the accumulation/erosion patterns of JUL05-APR05, FEB06-JUL05 and APR06-FEB06 are shown on Dwgs. 5, 6 and 7.

Table 4.2 Accumulation and erosion between the four surveys. Maintenance dredging took place between surveys FEB06 and APR06. Data covers the 90 m wide channel only.

Survey	**JUL05-APR05 1000 m^3**	**FEB06-JUL05 1000 m^3**	**APR06-FEB06 1000 m^3**
Accumulation	109	50	16.0
Per month	31	8	8
Erosion	7	21	147
Per month	2	3	Dredging

The volume change from April 2005 to July 2005 is significantly higher than in the following seven months. One important reason for this is believed to be the depression created by dredging between stations 3500 and 4700, see Figure 3.1. This depression may cause increased deposition rates until filled in with sediments, in this case by mud.

According to dredging records received from Enterpa, the total dredging volumes in February-March 2006 were 410,000 m^3 of which 44,000 m^3 were characterised as sand whereas the remaining volume is mud (lama). It is seen that this volume exceeds the volume obtained from bathymetry computations by almost three times. The reason for this discrepancy is believed to be mainly the computation method for production rates. This issue has been the subject of earlier technical notes by DHI and is discussed in Section 3.2 of the new CPE-CEPEMAR report of July 2006, Ref. /9/.

The calculated volume changes depend on a number of factors which should be kept in mind when comparing volumes stated in the reports. The most important factors are:

- Computation method.
- Channel section considered.
- Accuracy of bathymetric soundings (impact of waves, horizontal and vertical control).

The *computation method* is characterized by size of cells and thus by the smoothing of the raw survey data. Small cells give rise to large variations of computed depth changes between cells and thereby account for detailed spatial variations. DHI has used two methods with cells of 10 m by 10 m and 200 m by 30 m. CPE used 50 m long cells between cross-sections. This is the reason for some differences (in the order of 10%) between volumes calculated by CPE and DHI.

The importance of *channel section* on net volume changes is clearly seen when parts of the channel erode and others accrete. Figure 4.5 shows the longitudinal distribution of

volume changes. The total deposition (positive values only) is larger than the net volume change, where all changes (positive and negative) are considered.

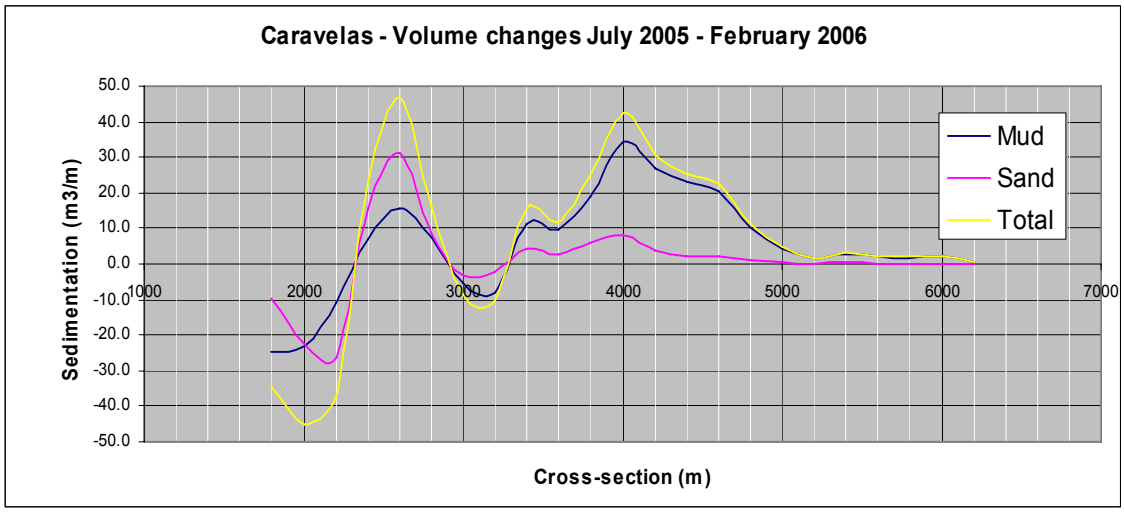

Figure 4.5 *Longitudinal distribution of volume changes. Note the large erosion figures from 1800 to 2300 and minor erosion from 2900 to 3300. In these sections there are deposition in the east side and erosion in the west side of the channel.*

Net volume changes are considered when analysing sediment infill from the surroundings, whereas the total deposition is considered when analysing maintenance dredging requirements.

The *accuracy of bathymetric soundings* is of particular importance for the calculation of volume changes. The general accuracy of vertical levels is about 0.1 m. When reading the volume changes in Caravelas reports it should be kept in mind that an offset of 0.1 m for one bathymetry plan will correspond to a volume change of 36,000 m^3 for the outer 4 km of the channel.

Variations of the horizontal control may cause inaccurate volume change figures particularly for the channel sides.

4.7 Remaining Capital Dredging

In Table 4.3 the volumes needed to be dredged to achieve a bed level of -5 m and -4.5 m within the entire channel between points 1800 and 6200 for all four bathymetries are shown. Adjustment of slopes is not included.

Table 4.3 *Volumes to be removed to achieve the -4.5 m and -5 m levels. Only volumes above these levels are included. Over-dredge and side slope dredging are not included.*

Survey	APR05 1000 m^3	JUL05 1000 m^3	FEB06 1000 m^3	APR06 1000 m^3
To -4.5 m	32.5	75.6	91.7	15.9
To -5.0 m	106.0	178.4	213.9	94.4

CPE has assumed an over-dredge by 0.3 m and dredging of the side slopes. Taking these volumes into account, the remaining capital dredging is about 220,000 m^3, which is slightly less than the volume calculated by CPE (285,000 m^3).

4.8 Distribution of Sand and Mud along the Channel

The volume changes along the channel can be divided into mud and sand based on the sediment properties described in Section 4.5. It is noted from the bathymetries that the sedimentation is not uniform across the channel width, Dwg. No. 6. For this reason, the channel was subdivided into three transverse sections, each 30 m wide, and average sedimentation rates were calculated for 200 m long subdivisions of the channel. The mud content obtained from sediment sampling was applied to each 30 x 200 m cell and the sand and mud contents were subsequently computed.

The resulting distributions for the period July 2005 to February 2006 are shown in Figure 4.6 to Figure 4.8 for the eastern, central and western sides of the channel.

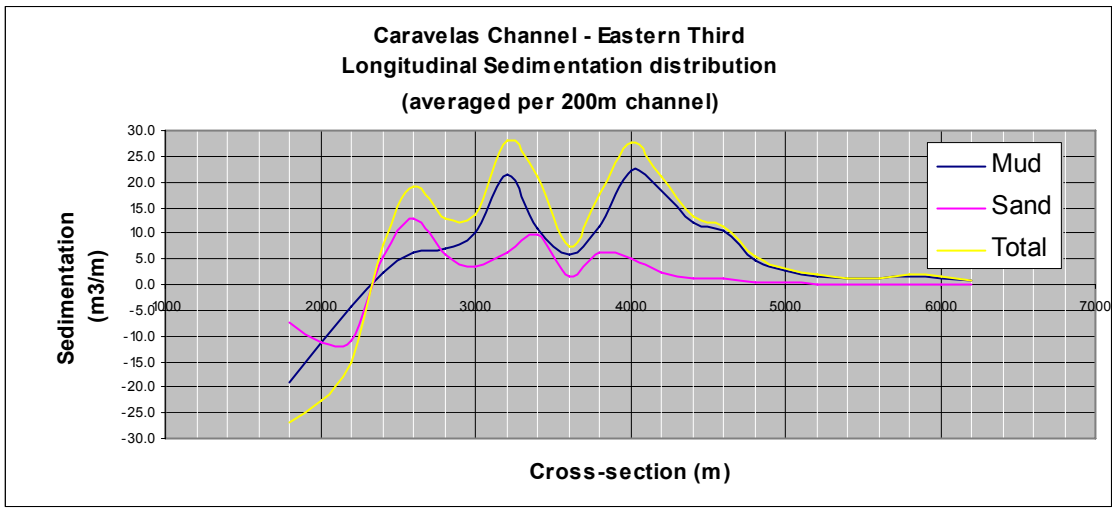

Figure 4.6 Distribution of depth changes along the channel (eastern third). The separation of negative values in mud and sand is fictitious since the properties of eroded sediments cannot be obtained from the February 2006 samples.

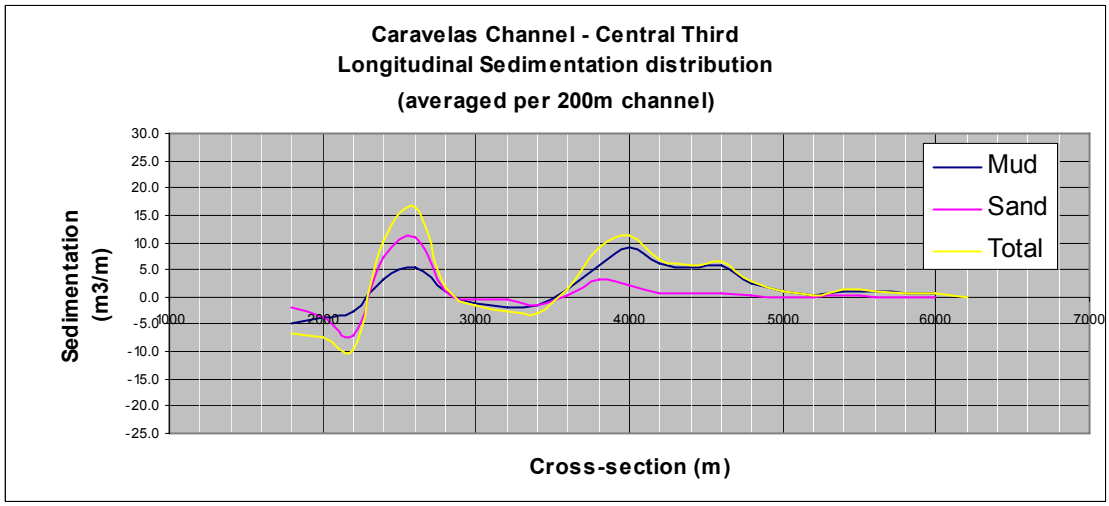

Figure 4.7 Distribution of depth changes in the central part of the channel.

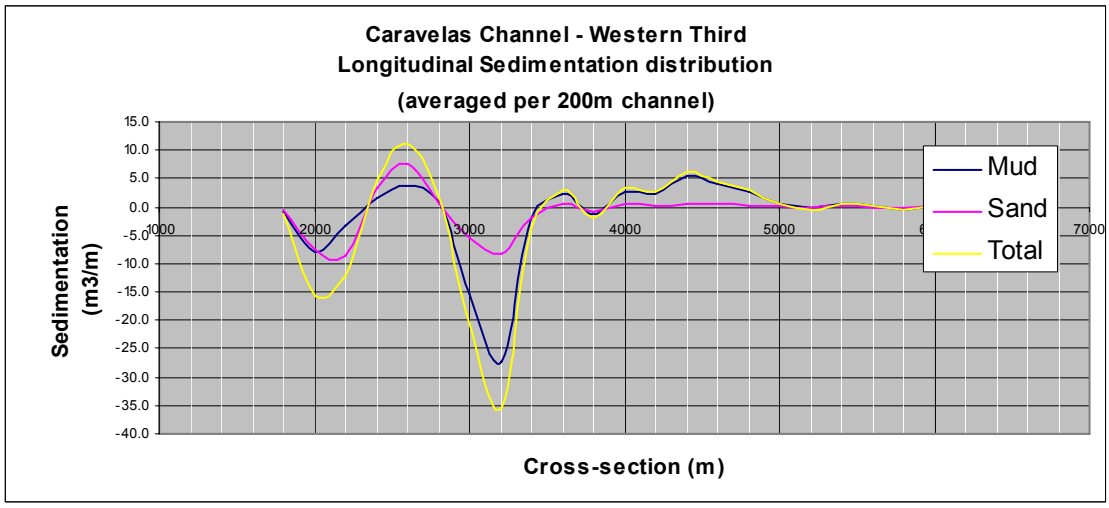

Figure 4.8 Distribution of depth changes in the western third of the channel.

This analysis shows that the sedimentation of both sand and mud is largest in the eastern side of the channel. The sand deposition is larger than the mud deposition north of station 2800 and insignificant south of station 4200. The samples made in July 2005 in the outer part of the channel typically show about 10% sand in this southern part of the channel.

The largest mud deposition occurs between stations 4000 and 4400, with a secondary peak in the east side at station 3200.

These sediment distributions serve as reference for the model calibration in Chapter 5 of this report.

5 SET-UP AND CALIBRATION OF NUMERICAL MODELS

The objective of the modelling study is to establish and calibrate a modelling complex for transport of sand and mud. The calibrated modelling complex is then used to examine alternative channel layouts. In this section the set-up and calibration of hydrodynamics, sand and mud are presented. The application of the models to test various channel layouts are presented in Section 6.

5.1 Model Set-up and Verification, Hydrodynamics

The model complex consists of a 14-day tidal hydrodynamic scenario including a net south-going current starting on 10 March 2006 and ending on 24 March 2006. In addition to this, 3 wave scenarios consisting of swell and locally generated sea waves are added. The resulting scenarios are modelled independently and the resulting sediment transport and accumulation pattern have been calculated by weighting the three scenarios according to their frequency.

The hydrodynamic model was calibrated against predicted tidal water levels and currents.

Measured currents at Station #106 were analysed and as shown in Figure 5.1 the non-tidal contribution to the current (the residual) varies over time and is of a significant magnitude.

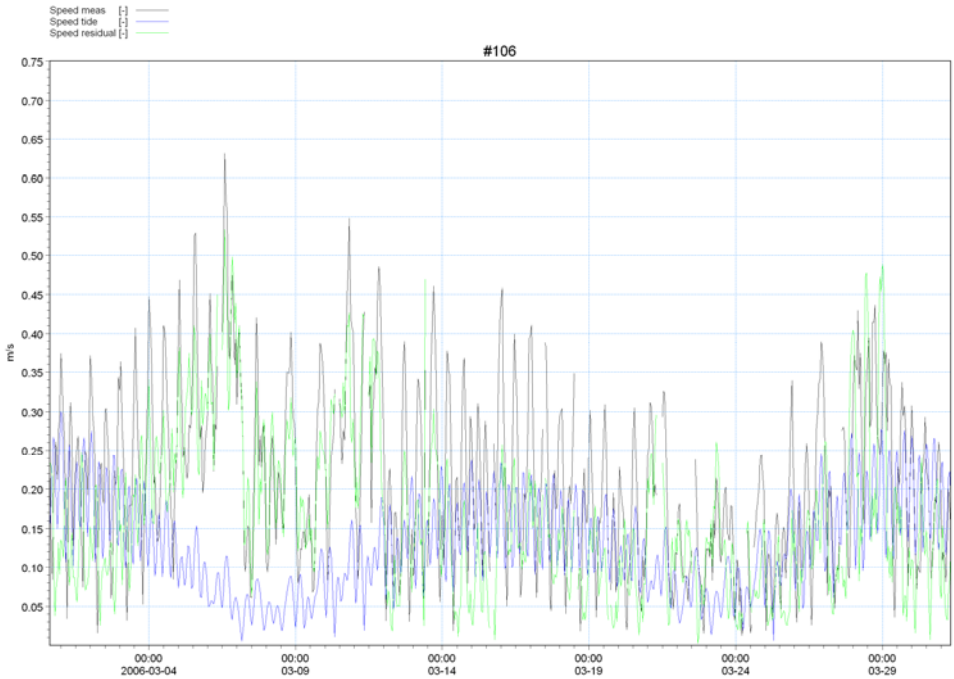

Figure 5.1 Measured (black curve), tidal (blue curve) and residual (green curve) current speeds at Station #106.

By projection of the residual currents on the main current direction (here 230 deg. N) the variability of the net currents become more clear, cf. Figure 5.2.

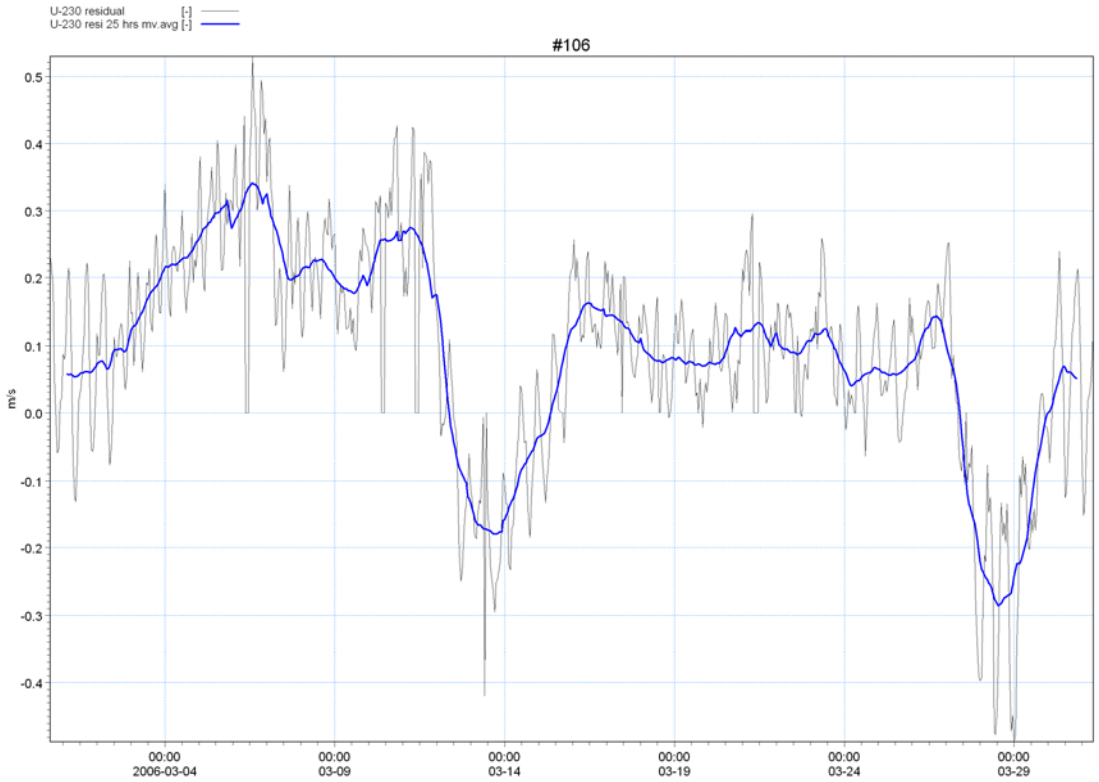

Figure 5.2 Observed residual current projected on main direction (positive is north going current). The blue curve is the 25-hour moving average current.

It is seen that the net current frequently changes orientation and that the magnitude is in the order of up to +/- 30 cm/s.

Tests with the hydrodynamic model showed that this current is not explained by local wind forcing and accordingly external (to the model) forces generate these net currents (e.g. regional winds or general circulations). Due to the time limitations of the present project it was accordingly decided to base the calibration of the hydrodynamic model on the astronomical tides (water levels and currents) and successively for the model scenarios superimpose the appropriate net current.

Based on the findings of Ref. /8/ a north-going net current of approx. 18 cm/s was used in the modelling. The net current was generated by a regional wind forcing of 10 m/s from SW.

The calibration results are shown in Figure 5.3 and Figure 5.4. In Figure 5.3 the predicted tide and the calculated tide at Caravelas are shown. In Figure 5.4 the tidal current speed and related current directions at Station #106 are shown.

Measuring station #106 was selected for the calibration due to the close vicinity of the study area. The short time schedule given it was decided not to calibrate the model against measurements from other positions.

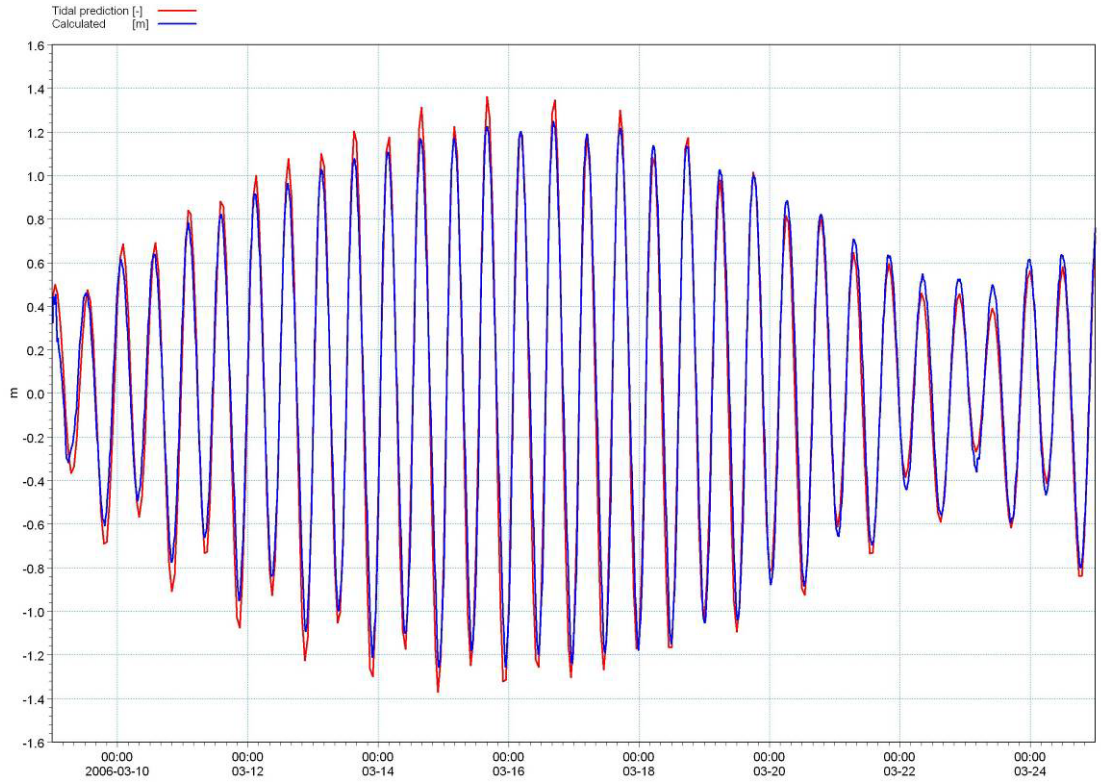

Figure 5.3 Comparison between predicted tide (red curve) and model calculated tide (blue curve) at the Caravelas terminal.

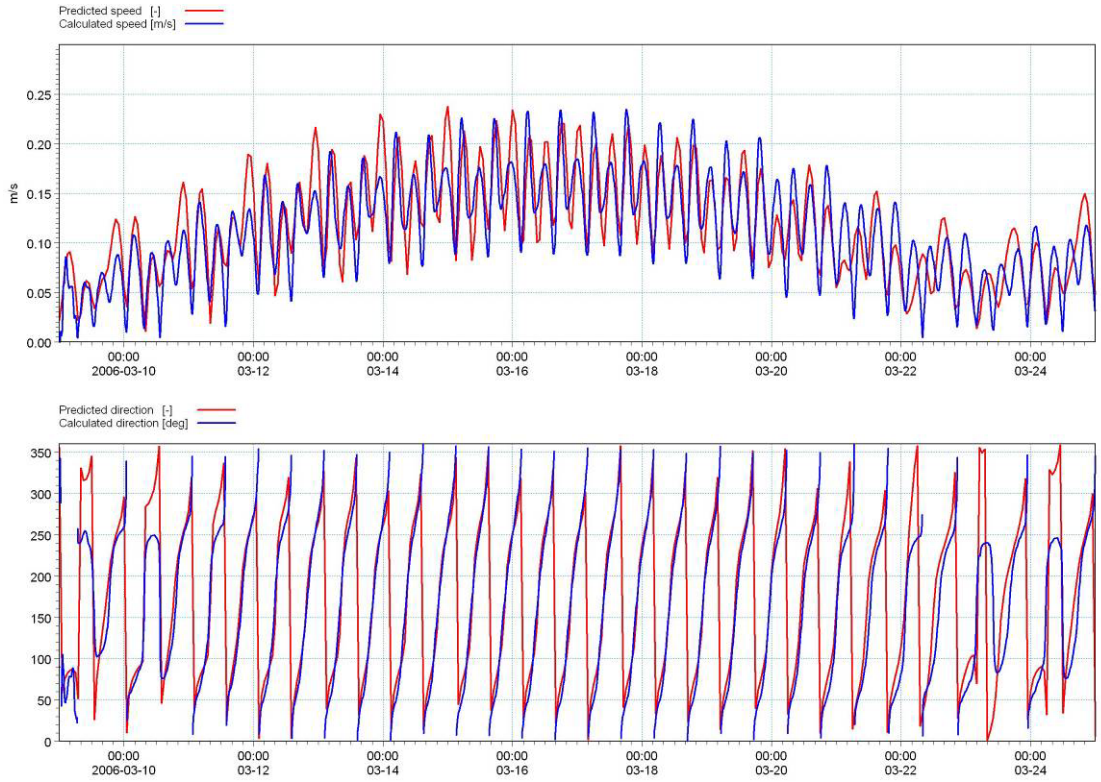

Figure 5.4 Comparison between predicted current speed and current direction (red curves) at Station #106 with model calculated values (blue curves).

The model calculated values of water levels, current speeds and directions are generally in good accordance with the measured values. The observed discrepancies between model calculated values and measured values of current speed are small (less than 5 cm(s)) and insignificant in relation to the sediment transport. The general tidal variation during spring and neap tide is well described. The information and data on the river flow are now much more accurate than during the earlier studies reported in Ref. /4/ and Ref. /5/ and together with the improved boundary conditions (tidal levels) a much better agreement between measured and modelled current direction at Station #106 has been obtained.

5.2 Calibration of the Sand Transport Model

The calibration of the sand transport model is based on the observed backfilling with sand during the period 22 July 2005 to 2 February 2006. No dredging was performed in this period and surveys were made just before and after this period. During the same period wave measurements were undertaken. The wave rose for the 195-day long period is shown in Figure 5.5 for measurement position 106. The long-term wave rose for the same position is shown as well for comparison. The long-term wave rose represents measurements for the period 6 June 2002 until 6 June 2006. The long time series has been restricted to cover full years. This is to get the best possible representation of the average yearly backfilling of the channel, see Section 6.

The comparison of the wave roses for the short calibration period and the 4-year long time series shows that during the period June to February there is a much larger representation of waves from north-easterly directions than in the yearly average wave climate.

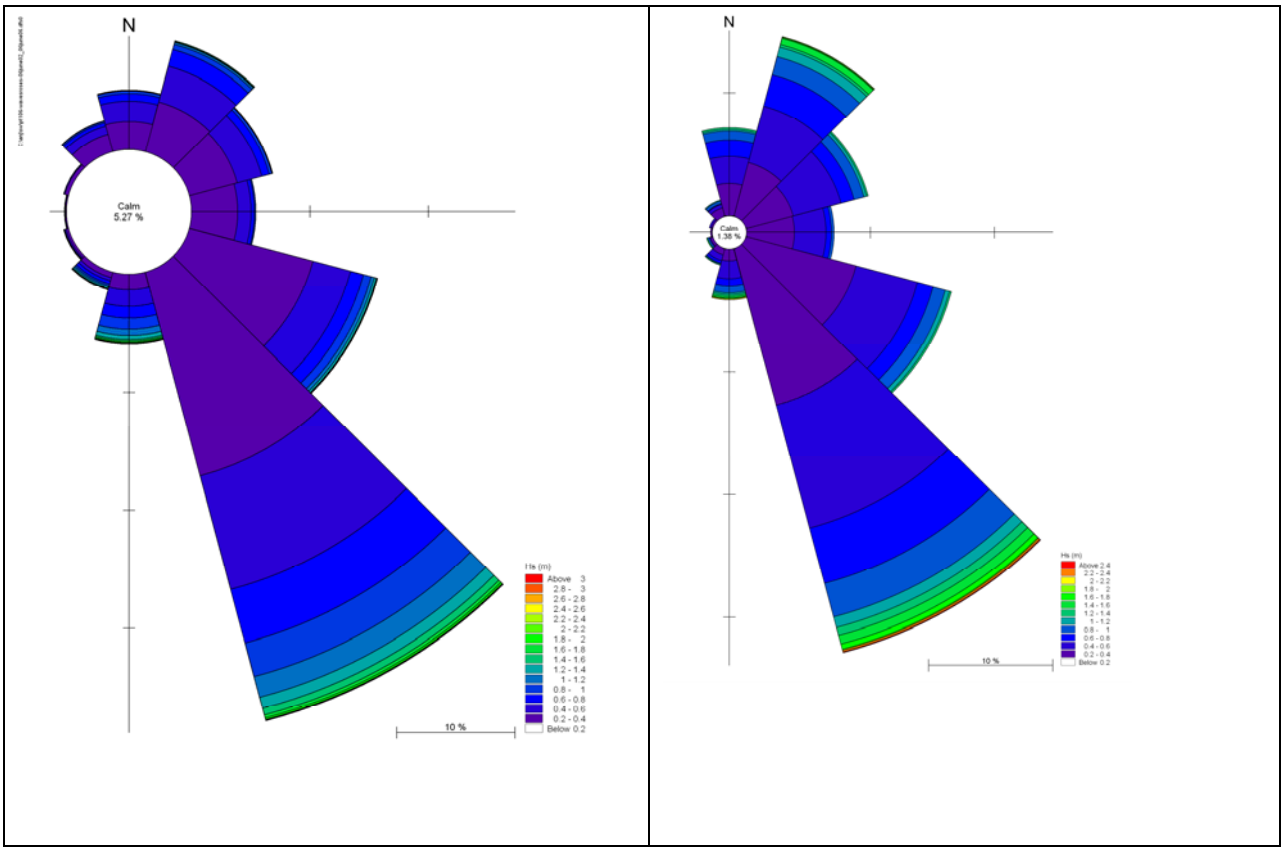

Figure 5.5 *Left: wave rose for the period 22 July 2005 to 2 February 2006.*
Right: wave rose for the period 6 June 2002 to 6 June 2006.
Both wave roses are derived from measurements at position 106.

The backfilling of the channel is a mixture of sand and mud. In this section focus is on the backfilling with sand. The majority of the backfilling with sand takes place between section 1800 and section 4200. Figure 5.6 shows an overview of the channel with the area within which the sand budget has been established based on measurements and models for the purpose of calibration of the models.

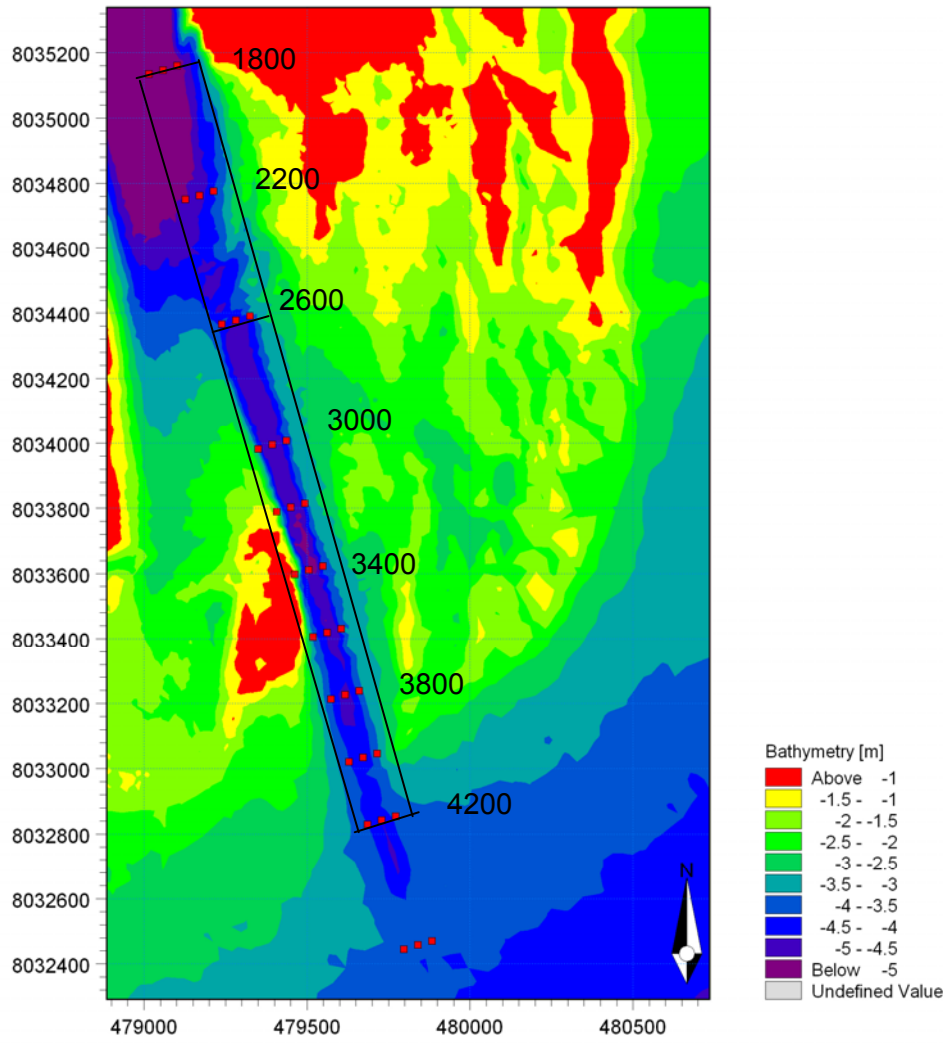

Figure 5.6 Overview of the channel with an indication of the area where the sand budget is established both from models and measurements.

Figure 5.7 shows a selection of cross sections as measured across the channel. The blue lines were measured in July 2005 and the green lines were measured in February 2006. "0" marks the centreline of the channel. The negative numbers along the x-axis represent the west side and the positive numbers represent the east side of the channel. Section 2200 shows erosion both in the channel itself and on the side of the channel. Sections 2600, 3000 and 3200 show a tendency of backfilling in the central part of the channel, the channel bottom reaches from -45 m to +45 m, and a shift to the west of the channel, i.e. deposition on the eastern side slope and erosion on the western side slope. Sections 3400 and 3600 clearly show backfilling of the trench from both sides, whereas the outer parts of the channel, sections 4000 and 4200, again show backfilling in the central part at the same time as a tendency for shifting to the west, deposition on the east side and erosion on the west side.

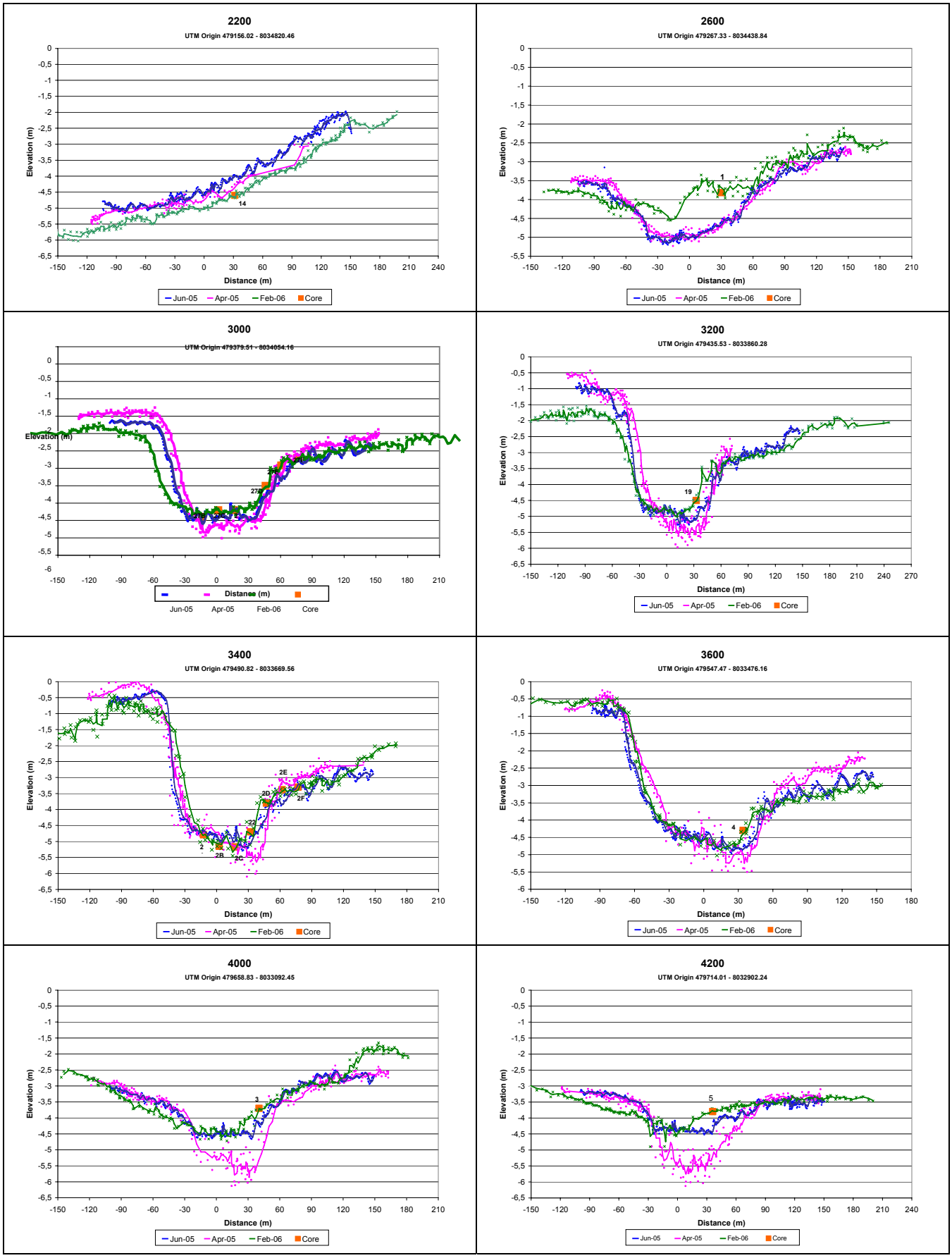
2200
UTM Origin 479156.02 - 8034820.46
Elevation (m)
Distance (m)
14
Jun-05 Apr-05 Feb-06 Core
2600
UTM Origin 479267.33 - 8034438.84
Elevation (m)
Distance (m)
1
Jun-05 Apr-05 Feb-06 Core
3000
UTM Origin 479379.51 - 8034054.16
Elevation (m)
Distance (m)
27B
Jun-05 Apr-05 Feb-06 Core
3200
UTM Origin 479435.53 - 8033860.28
Elevation (m)
Distance (m)
19
Jun-05 Apr-05 Feb-06 Core
3400
UTM Origin 479490.82 - 8033669.56
Elevation (m)
Distance (m)
2E
2D
2F
2C
2B
Jun-05 Apr-05 Feb-06 Core
3600
UTM Origin 479547.47 - 8033476.16
Elevation (m)
Distance (m)
4
Jun-05 Apr-05 Feb-06 Core
4000
UTM Origin 479658.83 - 8033092.45
Elevation (m)
Distance (m)
3
Jun-05 Apr-05 Feb-06 Core
4200
UTM Origin 479714.01 - 8032902.24
Elevation (m)
Distance (m)
5
Jun-05 Apr-05 Feb-06 Core

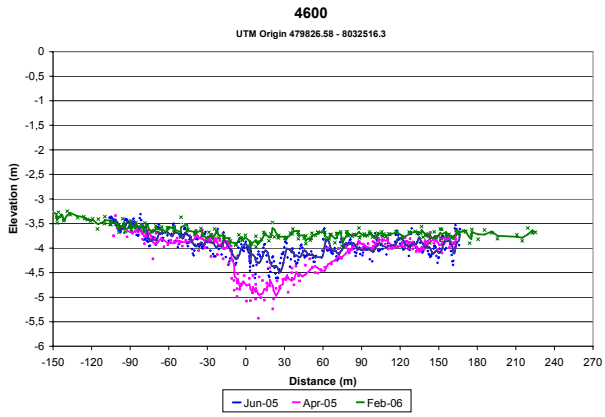

Figure 5.7 Measured cross sections along the channel. The blue lines represent measurements before and green lines after the calibration period.

Two simulations have been performed to calculate the backfilling of the trench:

1. Easterly waves and wind, offshore conditions: Hs = 1.5 m (approx. 50 km from the site) and wind corresponding to 10 m/s from northeast.

2. Southerly waves and wind, offshore conditions: Hs = 1.5 m (approx. 50 km from the site) and wind corresponding to 10 m/s from southwest.

The two cases have been run for 16 days from neap to neap for the calibration of the model. A shorter period of 24 hours has been identified which gives very close to the same sediment transport capacities around the channel. This shorter period has been used for the testing of layouts.

The wave conditions at position 106 for the two situations are the following:

Table 5.1 Wave conditions at position 106 for the two situations.

Condition	H_s [m]	Direction [deg. true north]	Duration Calibration period [days]	Duration Average year [days]
1. (East)	0.7 – 1.1	100 - 120	28	27
2. (South)	0.9 – 1.4	157 - 163	24	56

The variations in wave height and direction at position 106 are due to the tidal variations during the neap-neap period.

The approx. amount of time which shall be assigned to each of the representative conditions are estimated from the wave statistics. Assuming that all wave conditions (at position 106) from directions between 350° and 130° (over North) and wave heights larger than 0.6 m shall be represented by condition 1 the duration in the short calibration period is 28 days. Assuming that all wave conditions (at position 106) from directions between 130° and 220° and with wave heights larger than 0.6 m shall be represented by condition 2 the duration in the short calibration period is 24 days. The corresponding durations for the average year are 27 and 57 days, respectively. This indicates that the

calibration period has been a period with more easterly storms than normal for the period.

The channel backfills partly from the sides due to components of the currents perpendicular to the trench and partly due to gradients in the transport capacity along the channel. The cross-trench component of the transport capacity is significant in cases with wind, which drives a net current either to the west or to the north along the coast.

The calculated backfilling from west and east is illustrated for the two simulations with easterly and westerly winds and waves, respectively, in Figure 5.8.

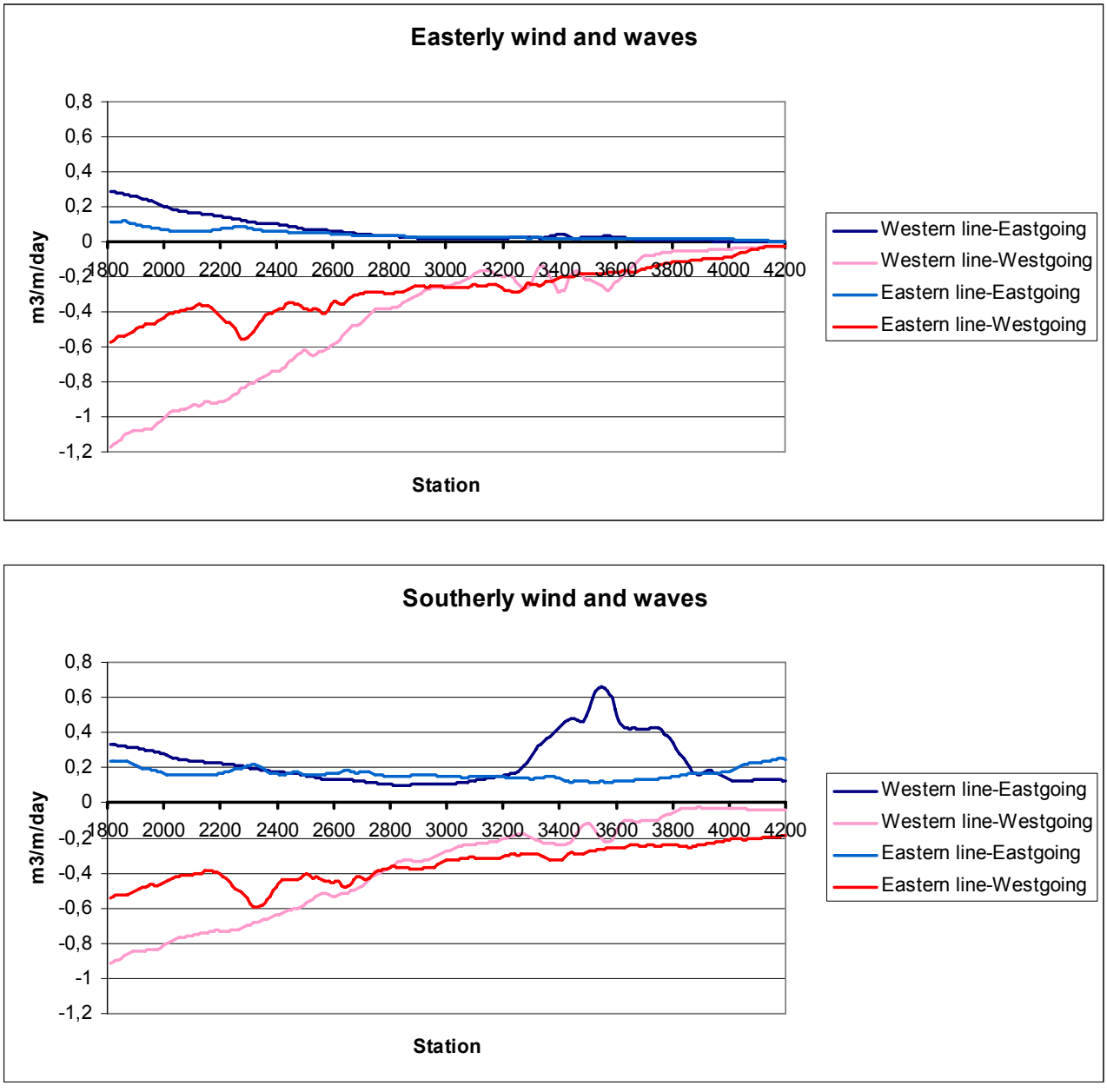

Figure 5.8 Calculated transport capacity perpendicular to the trench for easterly and southerly winds and waves, respectively. Positive values towards east.

The net transport capacities are extracted from the 16-day long simulations, conditions 1 and 2, and averaged over the simulation period along lines 100 m on either side of the centreline of the channel, see Figure 5.6. The blue lines show the east-going transport component perpendicular to the channel. Dark blue is transport across the line to the west of the channel, light blue is across the line east of the channel. The east-going transport across the line to the west of the channel enters into the channel. The east-going transport across the line to the east of the channel leaves the channel area and results in erosion on the "down-drift" side of the channel. Correspondingly, the red lines show west-going transport components across the lines to the west and east of the channel. The dark red lines illustrate transport components which backfill the channel and light red illustrates erosion on the "down drift side". The following patterns can be seen:

For easterly wind and waves:

Between section 1800 and out to 3000 the west-going transport capacity is larger on the west side than on the east side. The east-going transport component is smaller than the west-going all along the channel on both sides. The channel will therefore fill up from the east and at the same time erode on the western side, or at certain stretches even erode on both sides of the channel. Between 3000 and 4200 the west-going transport components on the east side are larger than the west-going components leading to a tendency of backfilling on the east side.

For southerly wind and waves:

It appears that also for this case erosion will take place between 1800 and 2800. Between 2800 and 4200 more sediment is coming into the channel from west than is leaving towards east (compare dark blue with light blue line), and more sediment is coming from east than is leaving towards west, (compare dark red line with light red line). This pattern corresponds to erosion on the inner part and backfilling from both sides on the outer part with a maximum around 3400-3800.

The above described backfilling is related to the "cross-channel" components only. The transport capacity parallel to the channel contributes significantly to the backfilling. The transport capacities across the selected sections for the two conditions are listed in Table 5.2:

Table 5.2 Transport capacities.

Section (Length of section: 200 m)	Net transport capacity *) [m^3/day] Easterly wind and waves	Net transport capacity *) [m^3/day] Westerly wind and waves
1800	202	134
3000	66	7
3200	62	30
4200	3	-14

*) positive values are south-going transports.

The transport capacities along the channel are significant. It appears that for the simulated conditions deposition takes place between 1800 and 3000 and between 3200 and 4200. A more detailed distribution is discussed in the following.

The modelled sedimentation for the calibration period is calculated by applying the durations derived from the wave statistics, see Table 5.1.

Figure 5.9 shows comparisons of measured depositions (green lines) on the western 1/3 of the channel and modelled backfilling from west from the two cases and of measured deposition on the eastern and central part of the channel and modelled backfilling from the east. The measured deposition in the central and eastern part has been added because the slope of the eastern side is flat and deposition mainly takes place from the eastern side. Especially the backfilling from the east along the channel from around section 2300 to 4200 is well reproduced by the model.

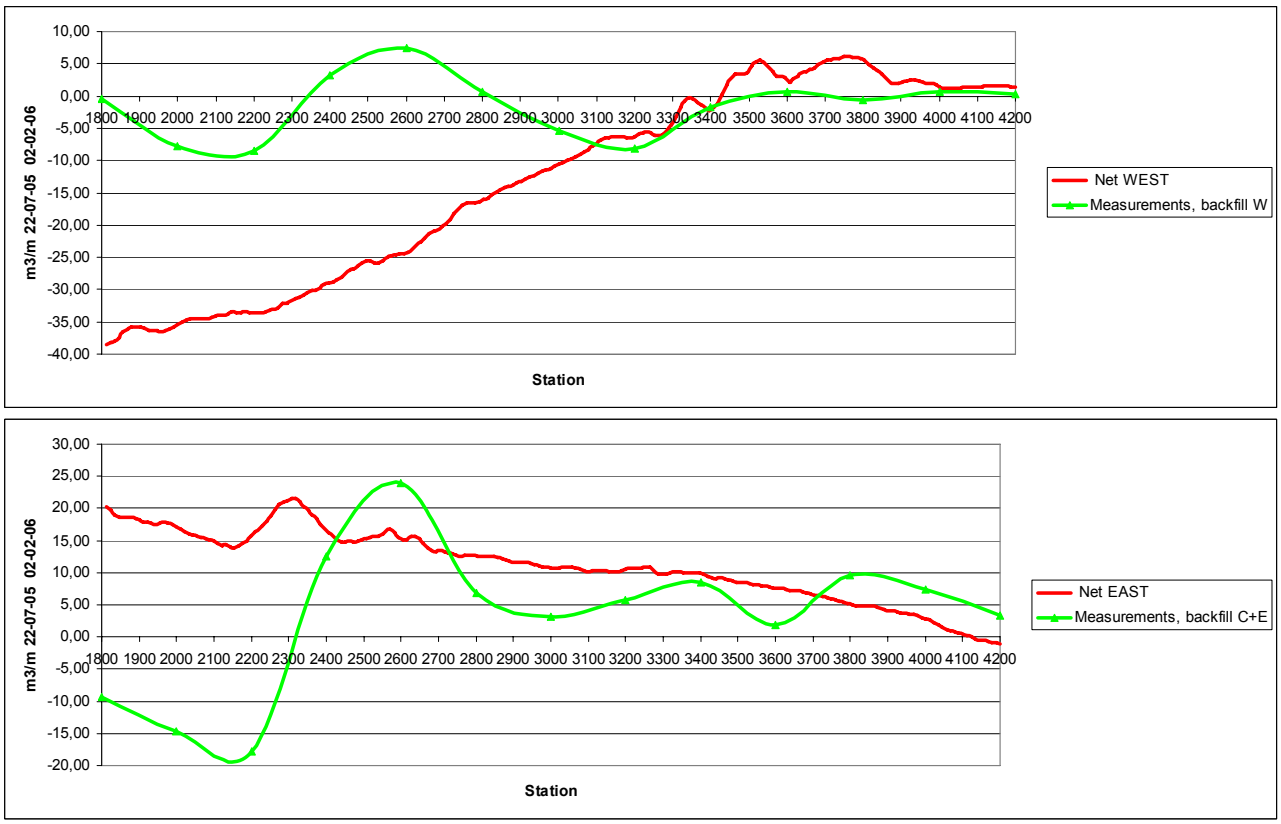

Figure 5.9 *Upper: comparison of measured deposition and erosion along the western 1/3 of the channel and the modelled backfilling from west (i.e. cross-channel transport only).*
Lower: comparison of measured deposition and erosion along the central and eastern 2/3 of the channel and the modelled backfilling from east (i.e. cross-channel transport only).

Figure 5.10 shows a comparison of the modelled and measured erosion and deposition along the channel. The green line is the measured backfilling in the period 22 July 2005 to 2 February 2006. The red line is the total calculated backfilling from east and west weighted with the durations shown in Table 5.1 and the blue line is the calculated backfilling corresponding to longitudinal gradients in the channel weighted with the same durations as the cross-channel transports. The black line is the total deposition/erosion corresponding to both cross-channel and longitudinal transport. The modelled deposition and erosion pattern clearly shows the tendency of erosion on the inner part and deposition between 2600 and 4200. The distribution of deposition is not completely in accordance with the observed distribution. This is most likely because only two charac-

teristic wave cases have been used as basis for the assessment. The total measured and modelled back-filling for the calibration period are shown in Table 5.3:

Table 5.3 Measured and modelled backfilling, 22 July 2005 to 2 February 2006.

Channel section	Measured backfilling	Modelled backfilling
1800 - 4200	3,920	4,300
2200 - 4200	10,260	10,730
2600 - 4200	13,050	12,810

It appears that with the applied durations as derived from the wave statistics the total backfilling volumes of sand are well reproduced.

The model set-up is used in the following to estimate the yearly backfilling of sand. The durations applied for the yearly average backfilling are listed in Table 5.1 and are derived from the 3-year wave statistics.

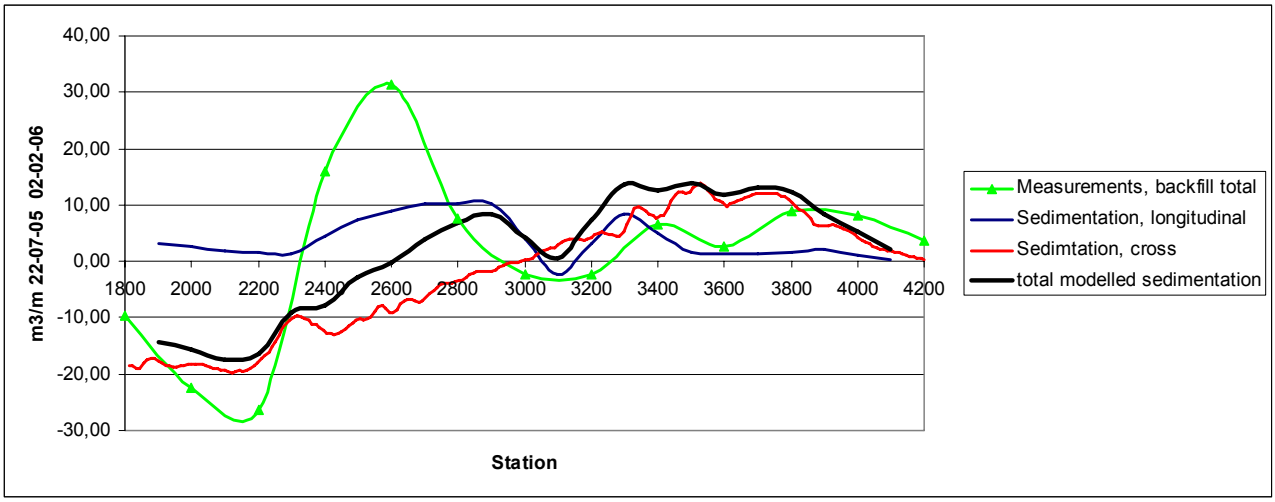

Figure 5.10 Green line: measured backfilling during the calibration period.
Red and blue lines: calculated weighted backfilling due to cross-channel and longitudinal sand transport.
Black line: calculated weighted total backfilling.

A short period has been selected from the 16 days for the testing of layouts. The period has been selected in such a way that the sediment transport pattern is as close as possible to the pattern found for the long 16-day period. The cross-channel transport components are compared in Figure 5.11 and the sedimentation due to longitudinal transport in Figure 5.12. It appears that the short period represents the longer period well for both cases. The reduction in time period has been introduced to shorten the computational time. The short period of time is sketched in Figure 5.13, which shows a time series during the long period of sediment transport across section 1800 (positive numbers south-going, negative numbers north-going).

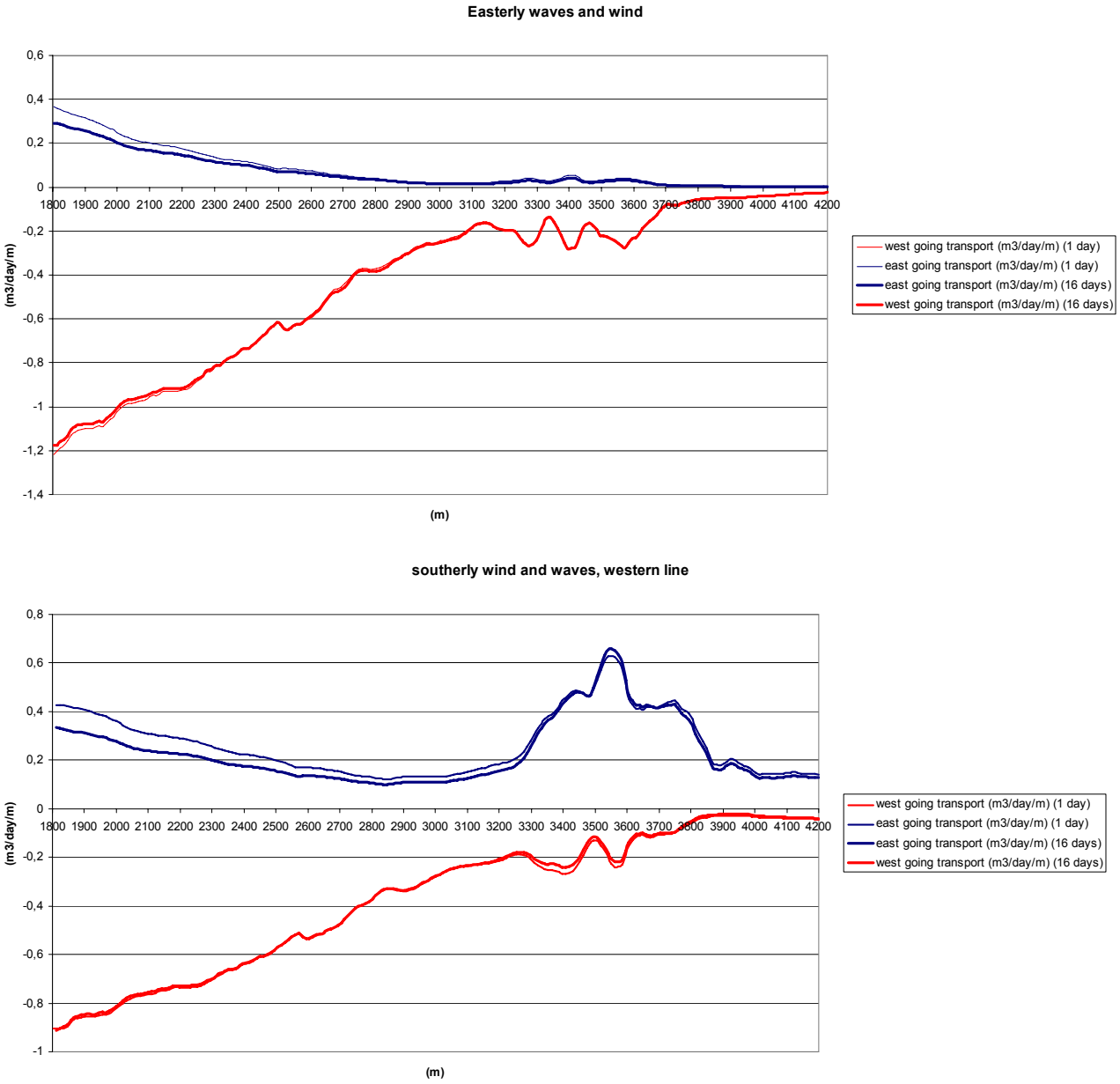

Figure 5.11 Comparison of cross-channel transport for the full 16-day period and a selected 24-hour period.

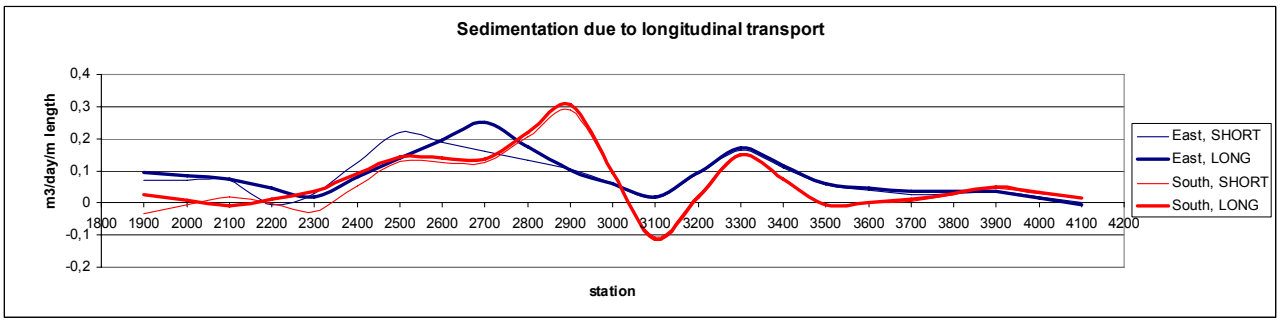

Figure 5.12 Comparison of sedimentation due to longitudinal transport presented for the two cases in m^3 /m channel/day.

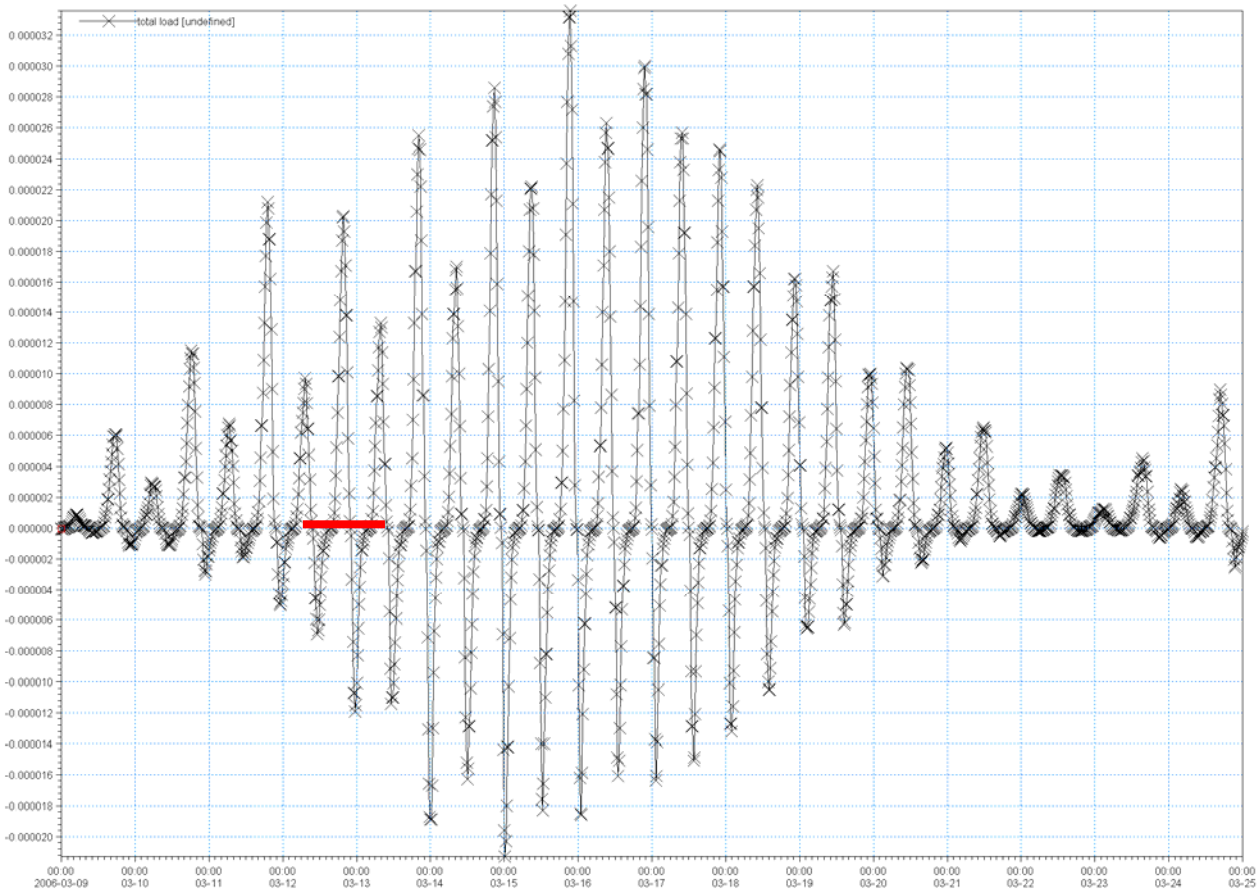

Figure 5.13 Time series during the case of easterly wind and waves of sand transport across section 1800 (positive numbers south-going, negative numbers north-going).

5.3 Calibration of the Mud Transport Model

A MIKE 21 Mud Transport (MT) model has been used to model the accumulation and erosion in the dredged channel, see also Section 3.5.

The MT module is included in this study because fine sediments with a grain size less than 64µm[1] have been accumulating in the outer part of the dredged channel from 3200 m and seaward.

As for the sand transport, the calibration of the MT model is based on the observed backfilling during the period from 22 July 2005 to 2 February 2006. An analysis has been made of the sedimentation along the channel. The sedimentation varies significantly across the channel. In order to illustrate this, the channel has been divided into three 30 m wide segments. It is further applied that the analysis of bed sediment samples shows a varying mud content of up to >90% in the outer part of the channel. This is shown in Figure 5.14 for the data that represents the calibration period of the 195 days between July 2005 and February 2006.

[1] Sediments less than 64µm are classified as silt or clay and have cohesive properties and can form colloidal particles and flocks.

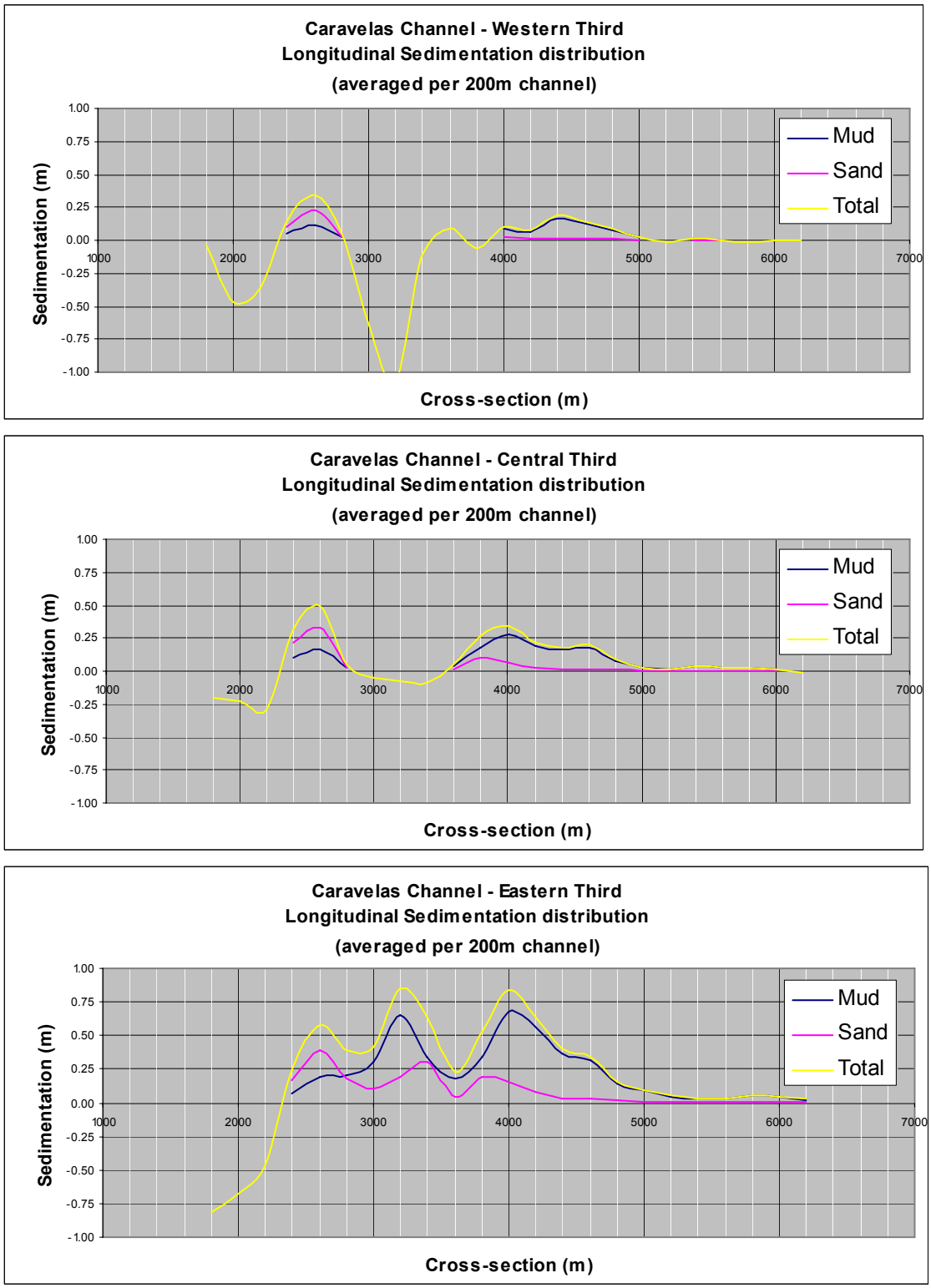

Figure 5.14 Deposition of mud at the end of the calibration simulation.

Figure 5.14 shows that mud deposits in two locations. The first location is from station 2200 to approx. 3000-3600, depending on which segment of the channel that is considered, and in a second location from station 3600 to 5000.

The observed sedimentation of mud along the channel is in the order of 38,000 m^3 for this 195-day period. 22 July 2005 to 2 February 2006.

The occurrence of mud along the coast, susceptible to sedimentation in the channel, is due to wave action that stirs up fine sediment. The sediment brought in suspension by the waves gradually settles out while it is being redistributed by the tidal flow and part of it settles in the channel.

The analysis of the wave rose for the calibration period showed that this period is different from the mean yearly wave rose. Considering wave heights, the following exceedence table is found:

Hs > 0.6 m	52 days
Hs > 0.7 m	40 days
Hs > 0.8 m	30 days

This shows, for example, that on average in the 195 days waves are larger than Hs = 0.8 m in 30 days.

The MIKE 21 MT model has been set up and calibrated to reproduce observed sedimentation along the channel in the period from 22 July 2005 to 2 February 2006.

The following sedimentation mechanism has been applied and calibrated to reproduce the observed distribution of deposition along the channel. Initially, the sediment is stirred up by waves higher than 0.8 m (measured at position 106). The initial sediment suspension is assumed to be 1000 mg/l. The hydrodynamic conditions of the simulation correspond to tidal flow and waves coming from east. Waves are included in the simulations also. The waves are with a significant wave height of about 1.5 m offshore corresponding to waves between 0.7 m and 1.1 m at position 106.

The model then simulates the redistribution and sedimentation of this sediment pool according to the hydrodynamic conditions. The simulation period is 14 days. After approx. six days the simulations show that most of the sediment is deposited and a consolidation of the sediment is taken into account as the strength of the bed increases with time and it is reinforced by the presence of sand particles.

The model calibration was made by adjusting the critical shear stress for erosion and settling velocity in order to reproduce the pattern of sedimentation along the channel.

Erosion is described following Partheniades formulation:

$$S_e = E(\frac{\tau_b}{\tau_{ce}} - 1)$$

With a critical shear stress for erosion 0.4 N/m^2 and an erosion rate E of 0.00005 $kg/m^2/s$.

Deposition follows Krone and is described as:

$$D = c_b w_s (1 - \frac{\tau_b}{\tau_{cd}})$$

Where the critical shear stress for deposition is equal to 0.1 N/m^2.

The settling velocity of the fine sediment in the model is set to be depending on the mean suspended sediment concentration in order to account for flocculation according to the following formula:

$$w_s = w_o(\frac{c}{\rho_s})^\gamma$$

Where $w_s, w_o, c, \rho_s, \gamma \ \ \rho_s$ is the settling velocity, settling scale velocity, actual sediment concentration, grain size density (2650 kg/m^3) and an empirical exponent. In the present application the following values have been applied:

$$w_s = 20[m/s](\frac{c[kg/m^3]}{2650[kg/m^3]})$$

This means that the settling velocity varies in time and space throughout the simulation

The bed property of the sediment transport model is set up with two layers of mud with sand underneath. For a concentration of 100 mg/l the settling velocity is 0.8 mm/s. Flocculation is assumed to occur when the concentration exceeds 0.01 kg/m^3.

The simulations have showed that permanent sedimentation of fine sediments can only occur during calm conditions and it was required to take into account the consolidation of the bed sediments. This was done by allowing transition of sediment from the upper layer into a second less erodable layer below.

In Figure 5.15 the horizontal distribution of deposition at the end of the calibration simulation is shown. The fine sediments settle between stations 2600-3600 and around station 4200. The bed density of dry matter is assumed to be 300 kg/m^3 corresponding to a weakly consolidated bed layer.

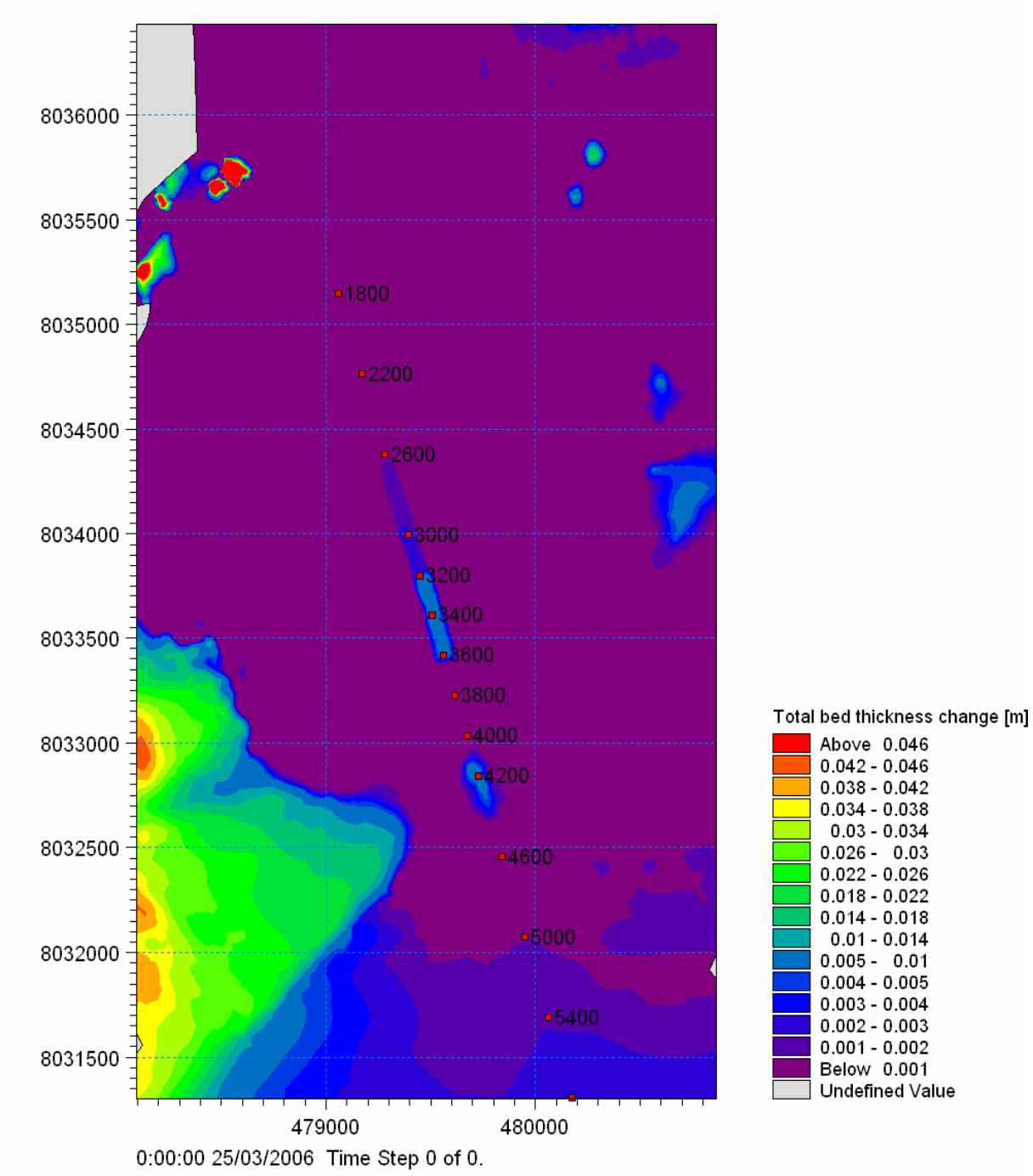

Figure 5.15 Deposition of mud at the end of the calibration simulation.

Figure 5.15 shows that mud deposits in two locations. The first location is from station 2600 to approx. 3600 the second location is from station 4100 to station 4400. This is in fairly good agreement with the observations, see Figure 5.14.

The simulated sedimentation of mud along the channel is 19,000 m^3 for the period of 195 days. Here it is assumed that a re-suspension event corresponds to 1 day where waves exceed 0.8 m. The 195 days include 30 of these events. The assessment of the measured sedimentation from July 2005 to February 2006 gives a sedimentation of 38,000 m^3 over this period.

This difference in estimates can be explained by the following factors:

- Uncertainty in the assessment of the sediment concentration after the passage of a high wave event.
- Simulation of limited wave and current conditions.
- Uncertainty in the history of events that leads to deposition.
- Formation of fluid mud over the shoals due to gravity flows into the channels from the two sides.
- Uncertainty in the assessment of the volume calculation of mud from the survey maps.

It is emphasised that the model reproduces correctly the order of magnitude of deposition and the location of the sedimentation.

In order to account for the uncertainties the simulation results must be scaled to match the observed dredging volumes. This gives that the simulated results must be multiplied by a factor of 38,000/19,000 equal to 2.0.

In Figure 5.16 below is shown the simulated sedimentation along the channel for a calibration period scaled to represent the 195-day calibration period as described above. Three lines are presented, West, Centre and East in order to illustrate the variation. The tendency for most sedimentation of mud towards east as compared to west, as seen in Figure 5.14 is also seen in the simulations and the sedimentation is in the right order of magnitude.

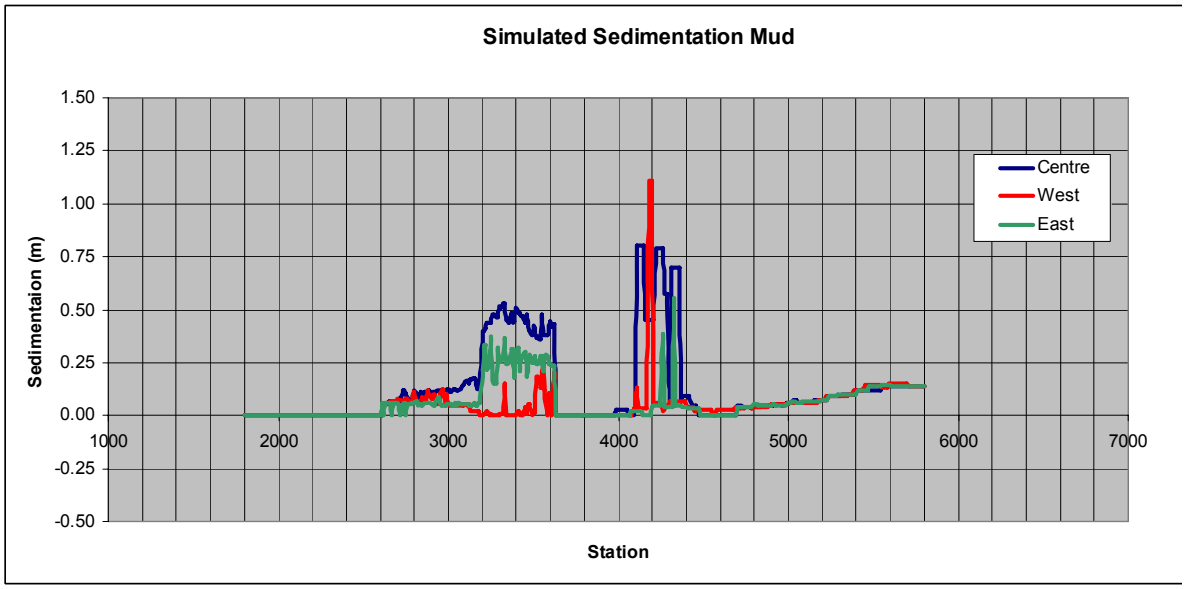

Figure 5.16 Simulated sedimentation of mud along the channel in the calibration period.

6 SCENARIO SIMULATIONS

The Action Plan, included as Appendix A, aims at recommending an optimal dredging practice by September 2006 and comprises a monitoring programme, additional studies and an assessment of alternative dredging strategies.

The objective, refer to Appendix B, for additional studies based on modelling of the sediment transport processes in and around the Caravelas channel is:

1. Traps and overdredge: evaluate the impact on total sedimentation amounts, channel sedimentation and sediment distribution for both sand and mud. This task will provide information for optimisation of dredging procedures such as the frequency of dredging and optimal channel layout.

2. Evaluate closure of alternate channel route:

    - Determine the impact of the alternate route on flow speeds and sedimentation in the navigation channel.

    - Evaluate if interventions will be beneficial and what level of intervention is needed.

In order to create reservoirs for sedimentation, so that a sufficient water depth can be maintained in periods between dredging, it may be considered to use a combination of sand traps and overdredging. Experience from the field and from model studies is that both sand traps and overdredging will result in larger total sedimentation volumes. Thus, the objective of this part of the modelling would be to reach an economically optimal dredging strategy.

Artificial closure of the alternate channel has been studied in order to describe to what extent the development of the alternate route reduces the flushing through the dredged channel and whether these effects, if any, can be mitigated either by discharging dredged sand at the bottom of the alternate channel or closing it by a permanent rock mound structure.

In order to address the above questions and optimise the dredging practice, five scenarios representing five different configurations of the entrance channel have been defined. These scenarios have been implemented in the updated hydrodynamic and sediment transport model and the corresponding sedimentation in the channel has been determined.

The five scenarios are defined in Table 6.1 below:

Table 6.1 Five scenarios.

Scenario 0	The existing channel.
Scenario 1	The existing channel is dredged to -5.5 m.
Scenario 2	The channel realigns with the alternative channel.
Scenario 3	The alternative channel is partly blocked.
Scenario 4	Dredging a 1 m deep depression in the existing channel.

The existing bathymetry and entrance channel configuration is shown in Figure 6.1. An alternative channel that turns towards west is created in parallel with the dredged channel. This alternative channel is dominated by ebb flow. This occurrence of one channel that is preferred for ebb flow is often observed in nature. The configuration is characterised by a converging flow during flood and a diverging flow during ebb. Morphologically, if not interfered by human activity, such flow conditions will often form a system of so-called ebb and flood channels separated by shoals. This is shown schematically in Figure 6.1. From a navigation point of view this is a problem since the ebb and flood channels will be separated by shoals.

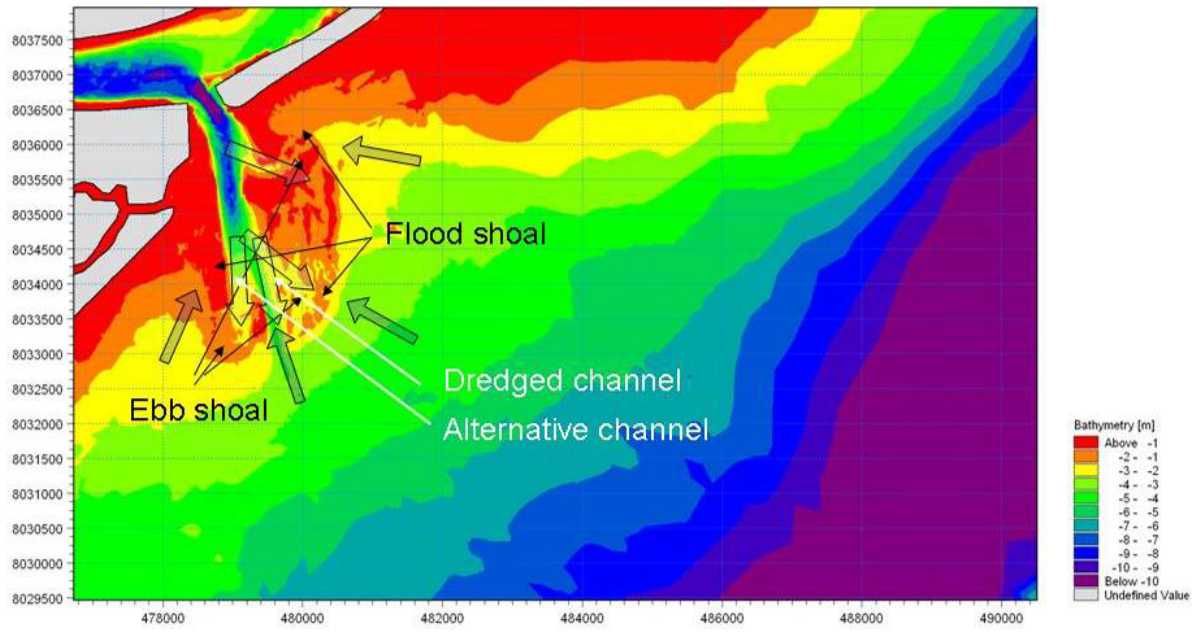

Figure 6.1 Possible idealised and simplified interpretation of the flow distribution in ebb and flood dominated channels and the formation of ebb and flood shoals.

In the following, the existing situation and Scenarios 1-4 are discussed with respect to hydrodynamics. Scenario 5 is discussed in Section 6.6, only.

6.1 Existing Channel Configuration

The bathymetry for the existing channel is shown in Figure 6.2.

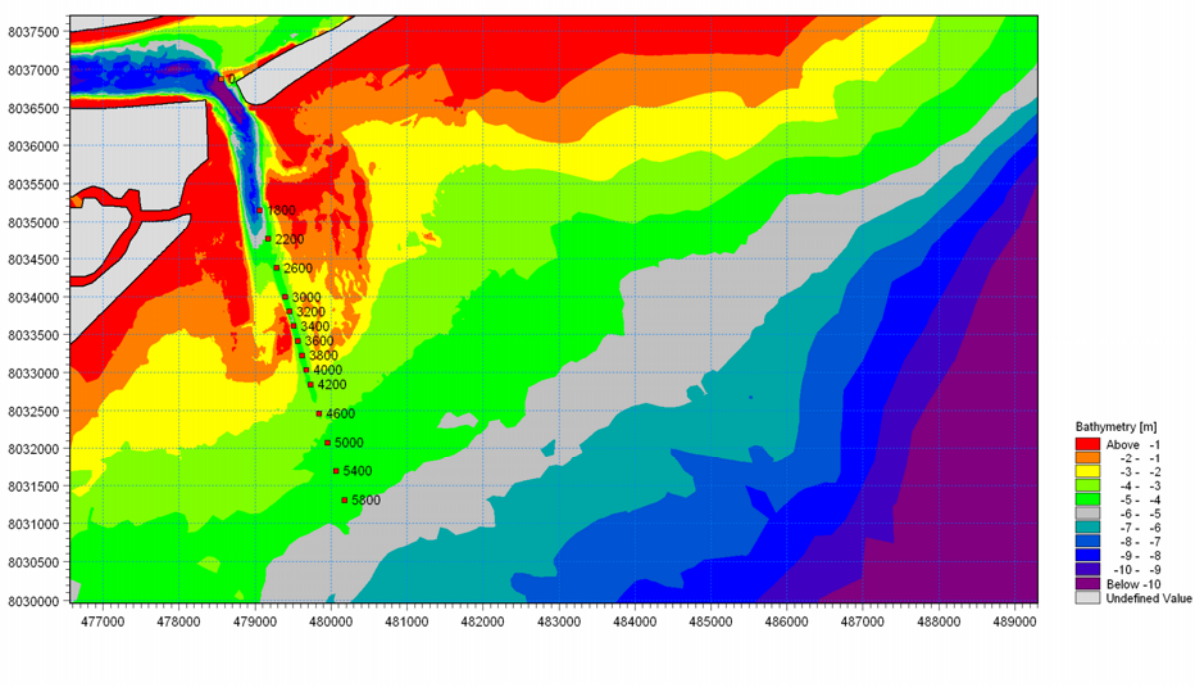

Figure 6.2 Existing channel configuration.

The current conditions are presented for four different stages of the tide: ebb, low water slack, flood and high water slack, see Figure 6.3.

The divergence of the ebb flow into the main and alternative channel is clearly seen. At low water slack the currents become very small over the main channel where the depths are significant, during flood the currents converges almost uniformly towards the entrance to the river and finally at high water slack the footprints of reduced currents over the deeper waters in the main and alternative channels are observed.

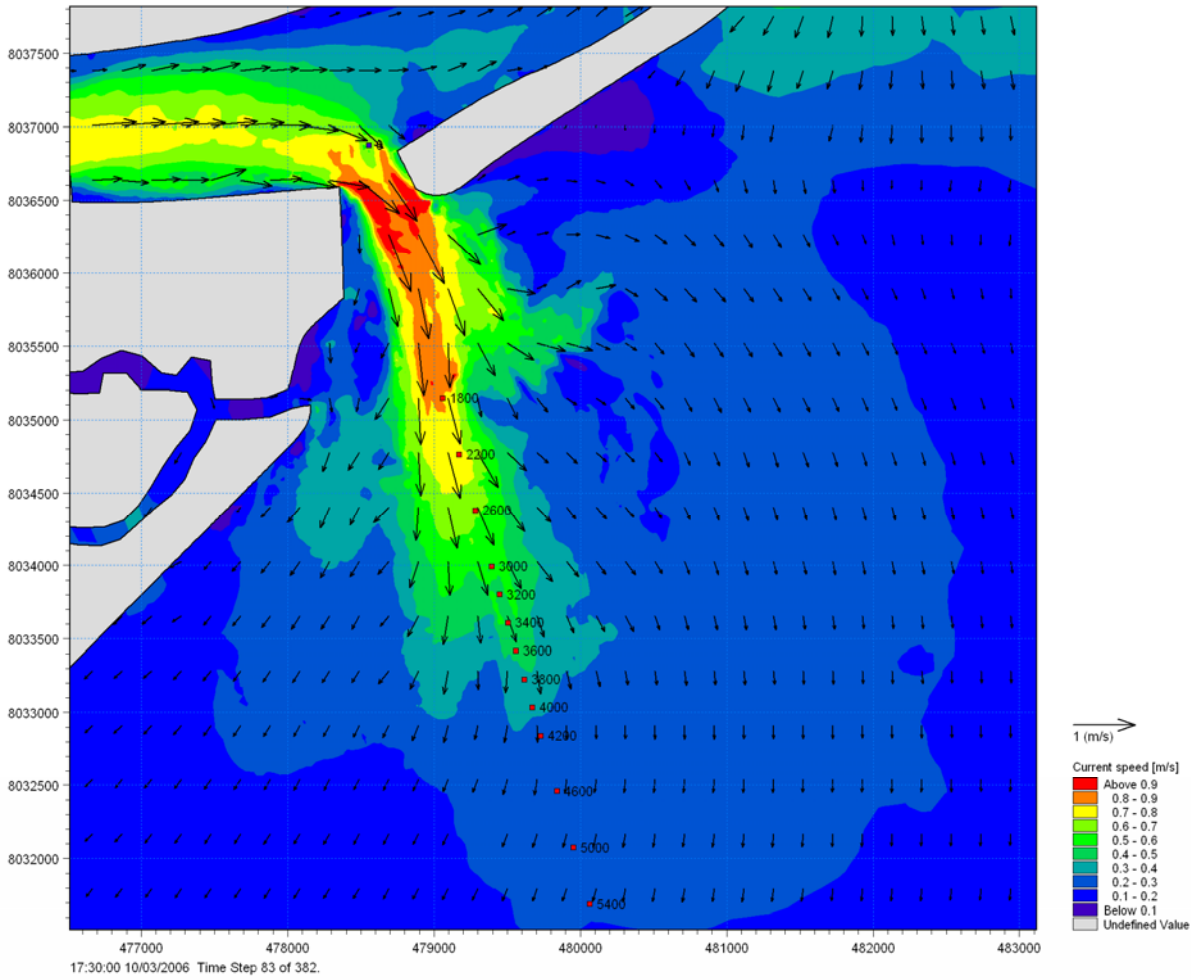

Figure 6.3a Existing channel configuration. Current speed and direction. Ebb.

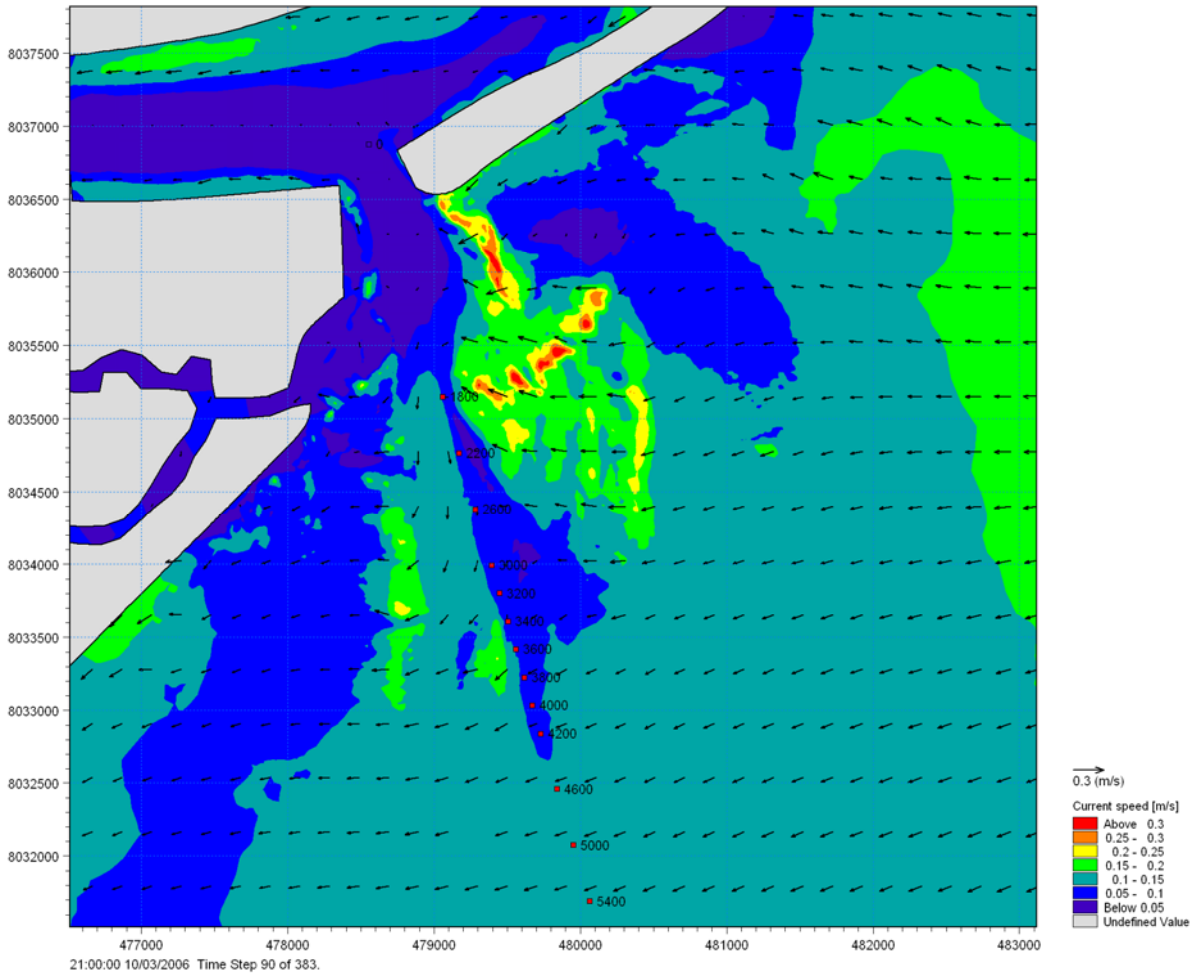

Figure 6.3b Existing channel configuration. Current speed and direction. Low water slack.

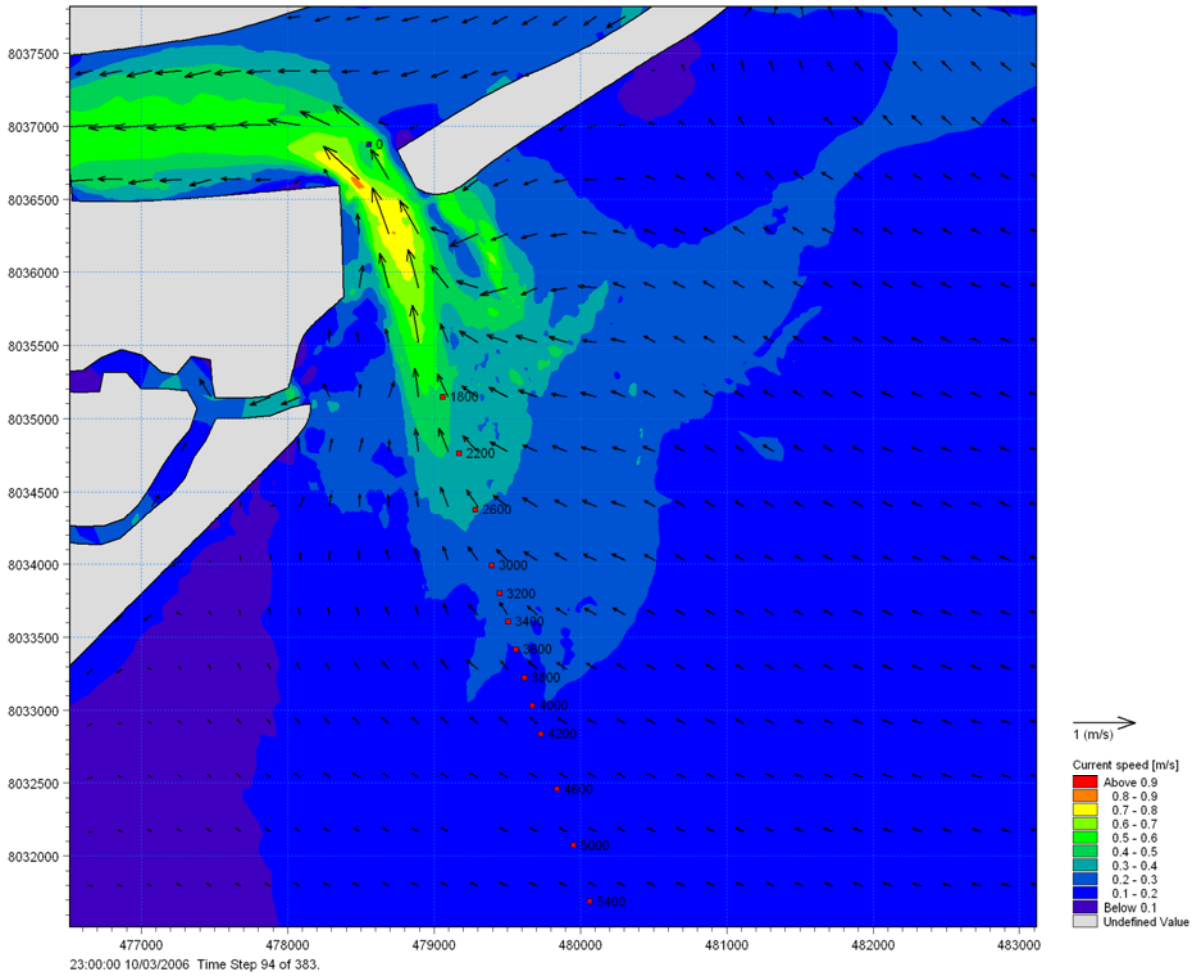

Figure 6.3c Existing channel configuration. Current speed and direction. Flood.

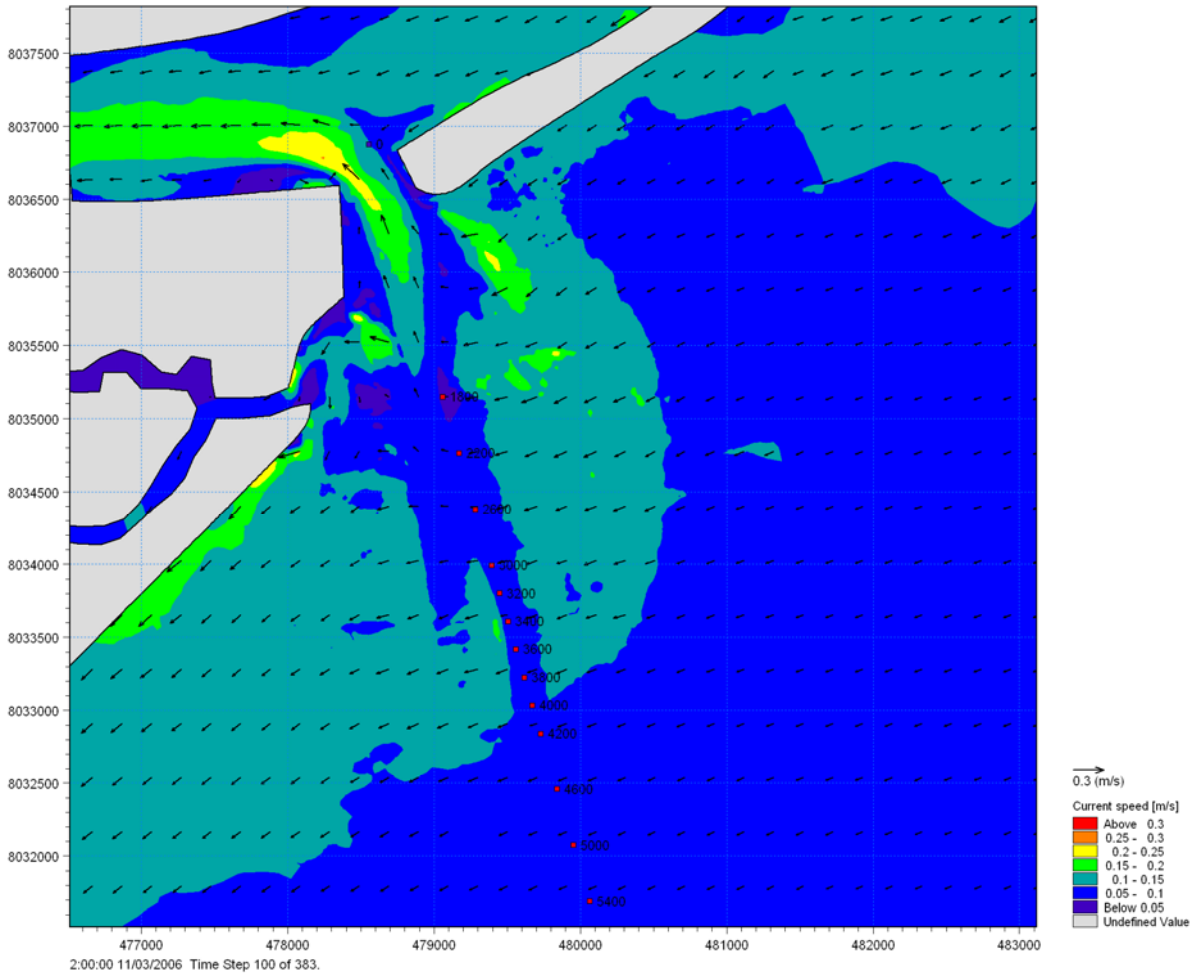

Figure 6.3d Existing channel configuration. Current speed and direction. High water slack.

6.2 Scenario 1, the Existing Channel is Dredged to -5.5 m

The bathymetry for this scenario is shown in Figure 6.4.

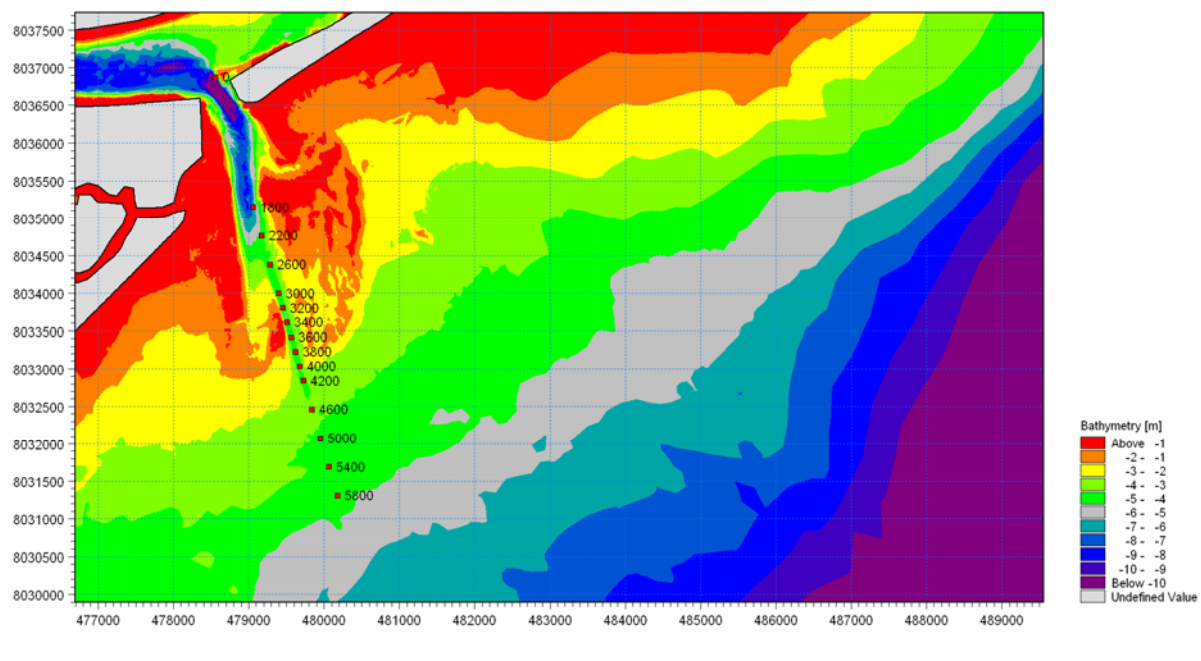

Figure 6.4 Scenario 1, the existing channel is dredged to -5.5 m.

The current conditions are presented for four different stages of the tide: ebb, low water slack, flood and high water slack, see Figure 6.5.

By comparison with the existing situation it is hardly possibly to identify any significant changes to the current fields from the four pictures of Figure 6.5.

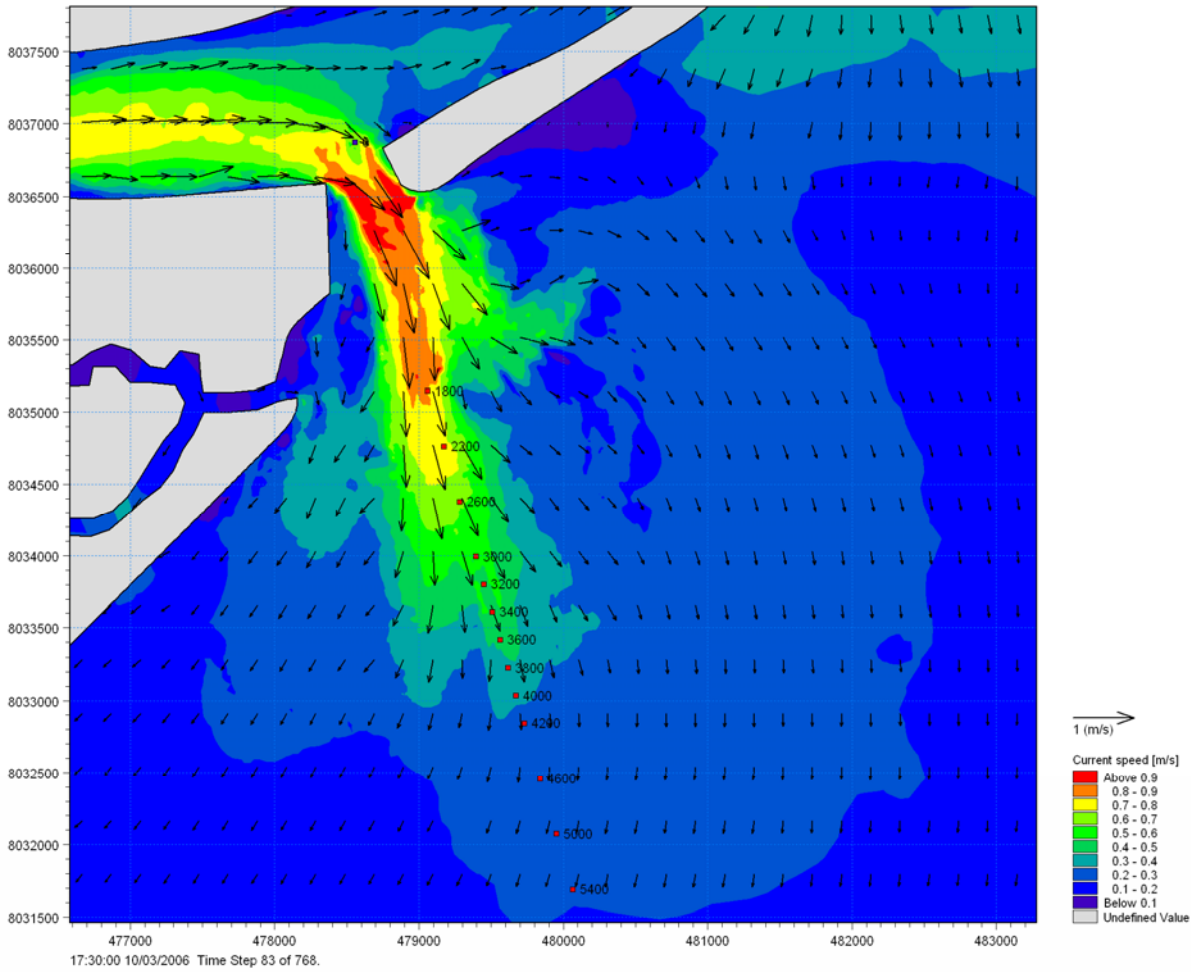

Figure 6.5a Scenario 1, the existing channel is dredged to -5.5 m. Current speed and direction. Ebb.

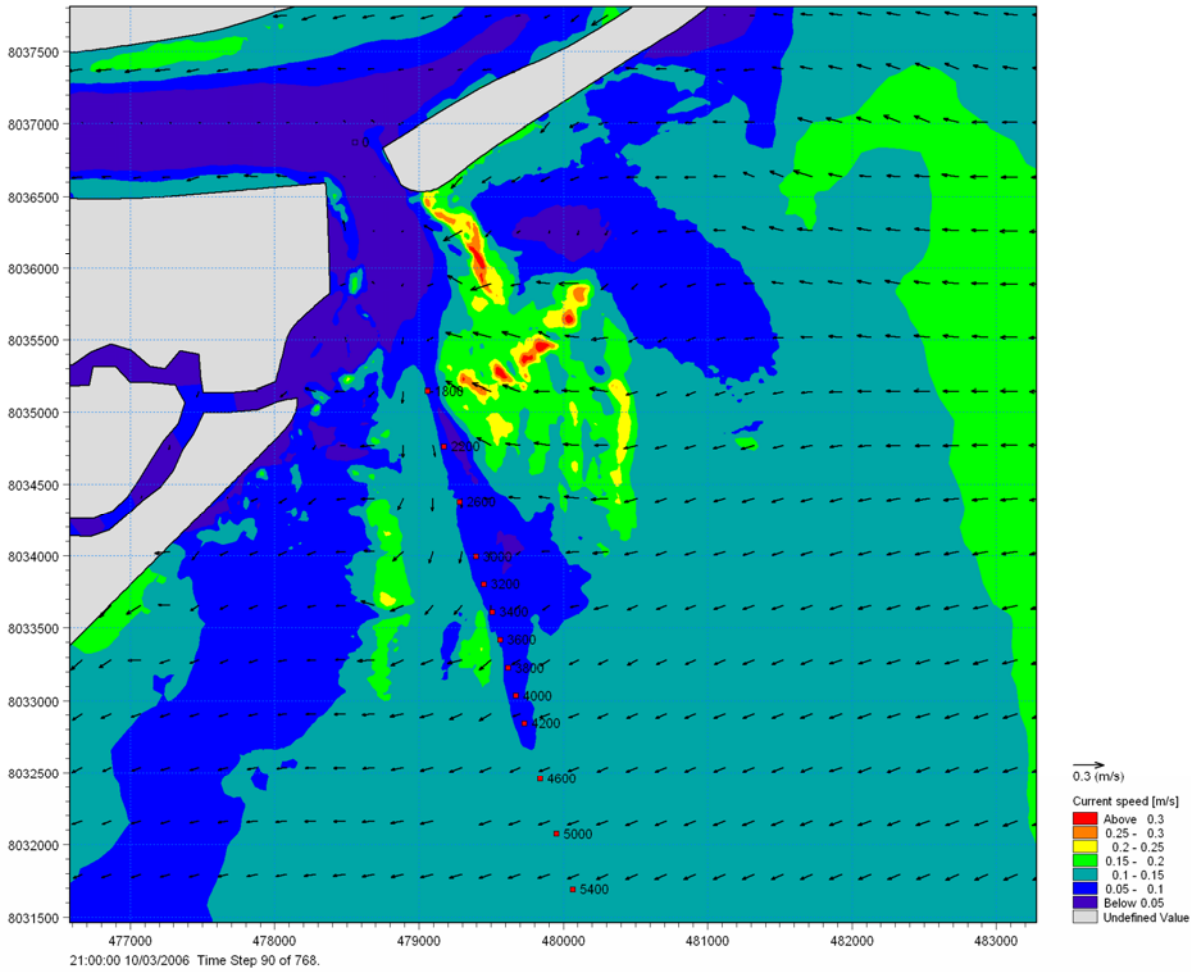

Figure 6.5b Scenario 1, the existing channel is dredged to -5.5 m. Current speed and direction. Low slack water.

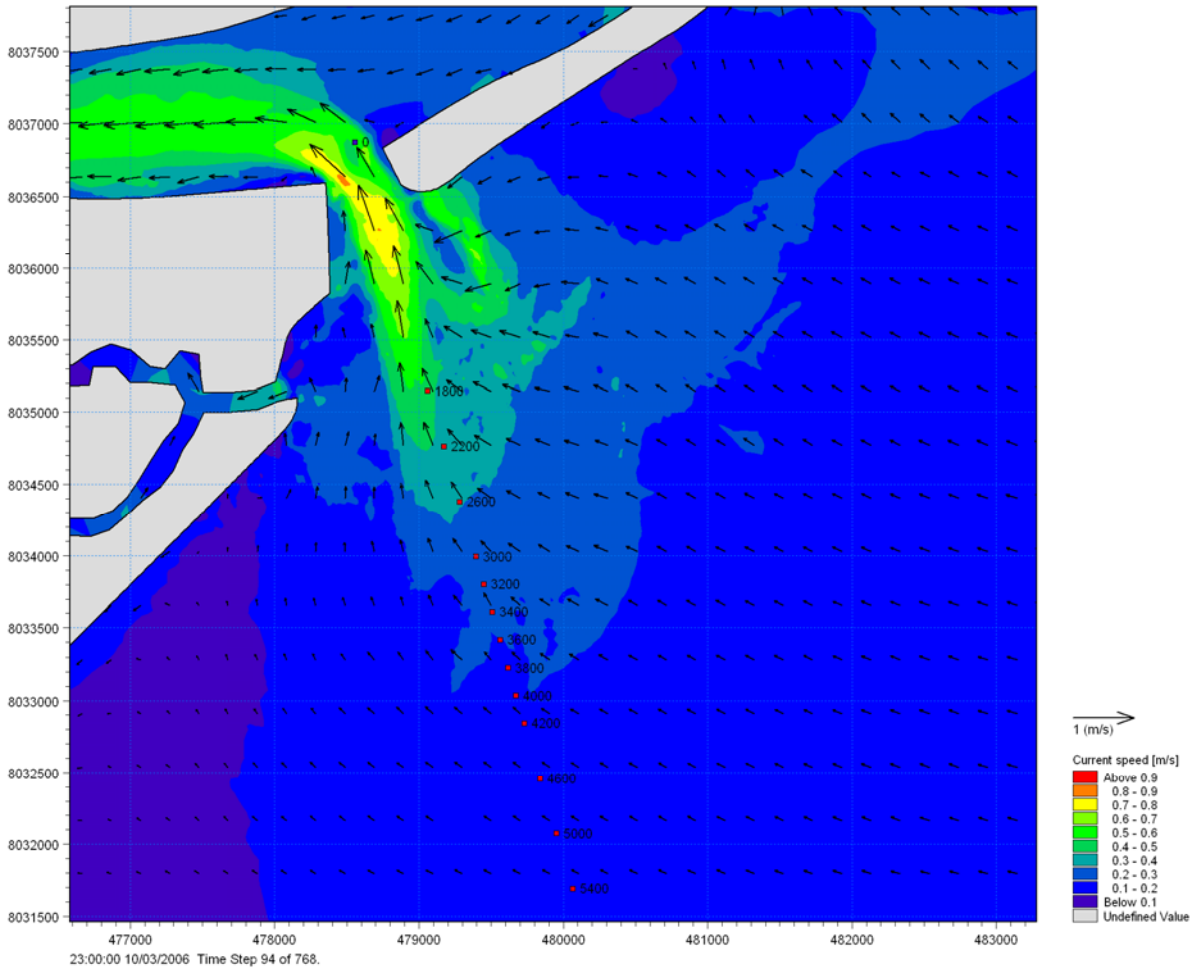

Figure 6.5c Scenario 1, the existing channel is dredged to -5.5 m. Current speed and direction. Flood.

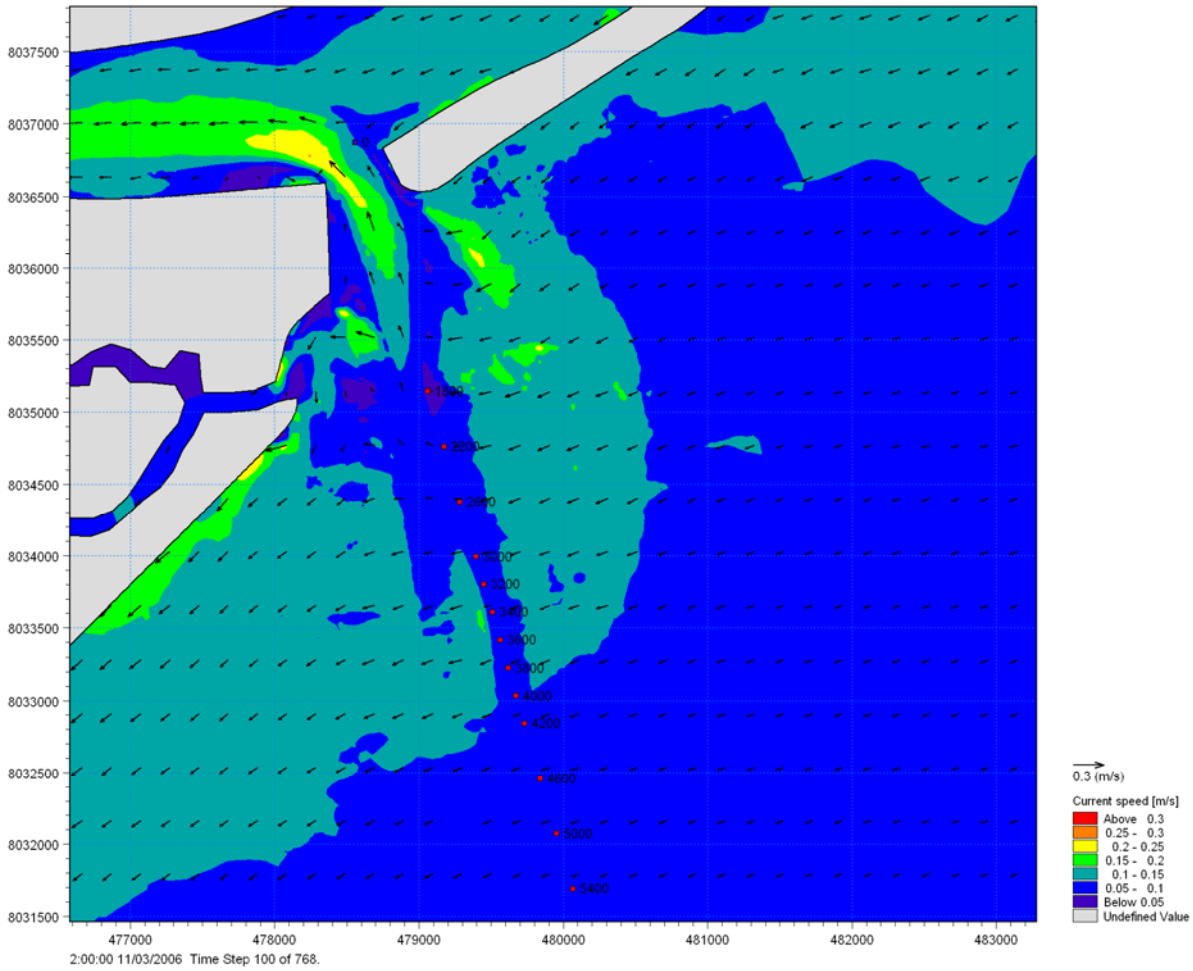

Figure 6.5d Scenario 1, the existing channel is dredged to -5.5 m. Current speed and direction. High slack water.

6.3 Scenario 2, the Channel is Realigned with the Alternative Channel

The bathymetry for this scenario is shown in Figure 6.6.

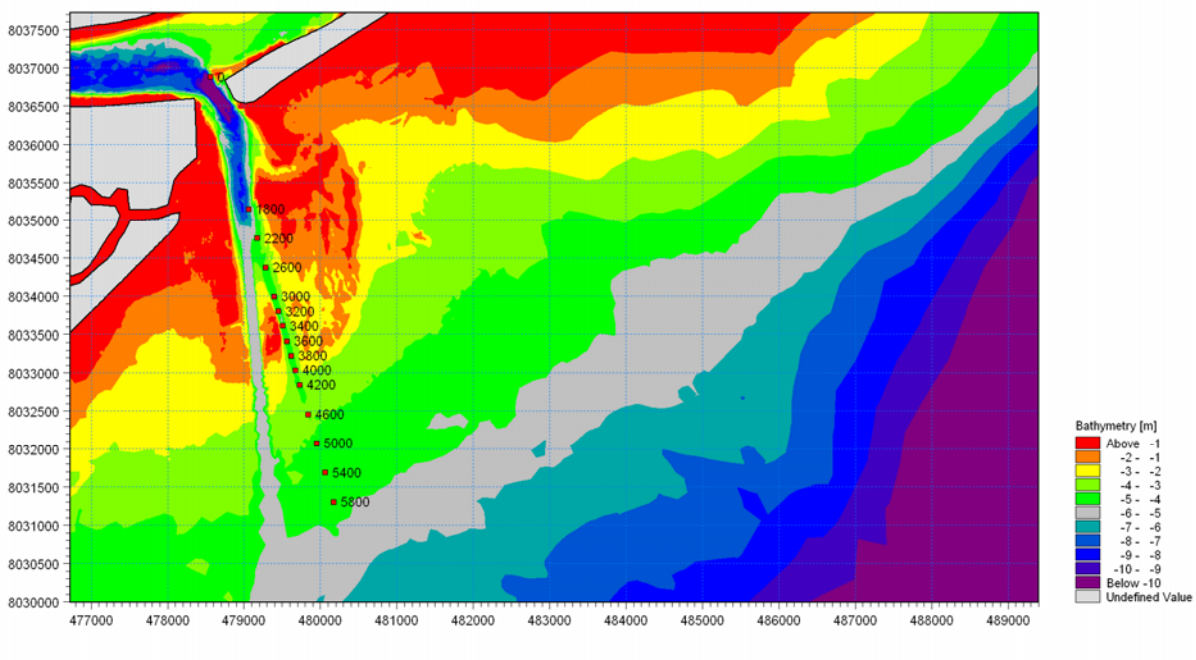

Figure 6.6 Scenario 2, the channel is realigned with the alternative channel.

The current conditions are presented for four different stages of the tide: ebb, low water slack, flood and high water slack, see Figure 6.7.

The impact of the alternative channel is significant. During ebb the flow is enhanced in the new alternative channel but also, although to a lesser degree, in the old channel that in the simulation is preserved at the existing depth. During slack waters the velocities are reduced in both channels while during flood the impact on the flow is less significant.

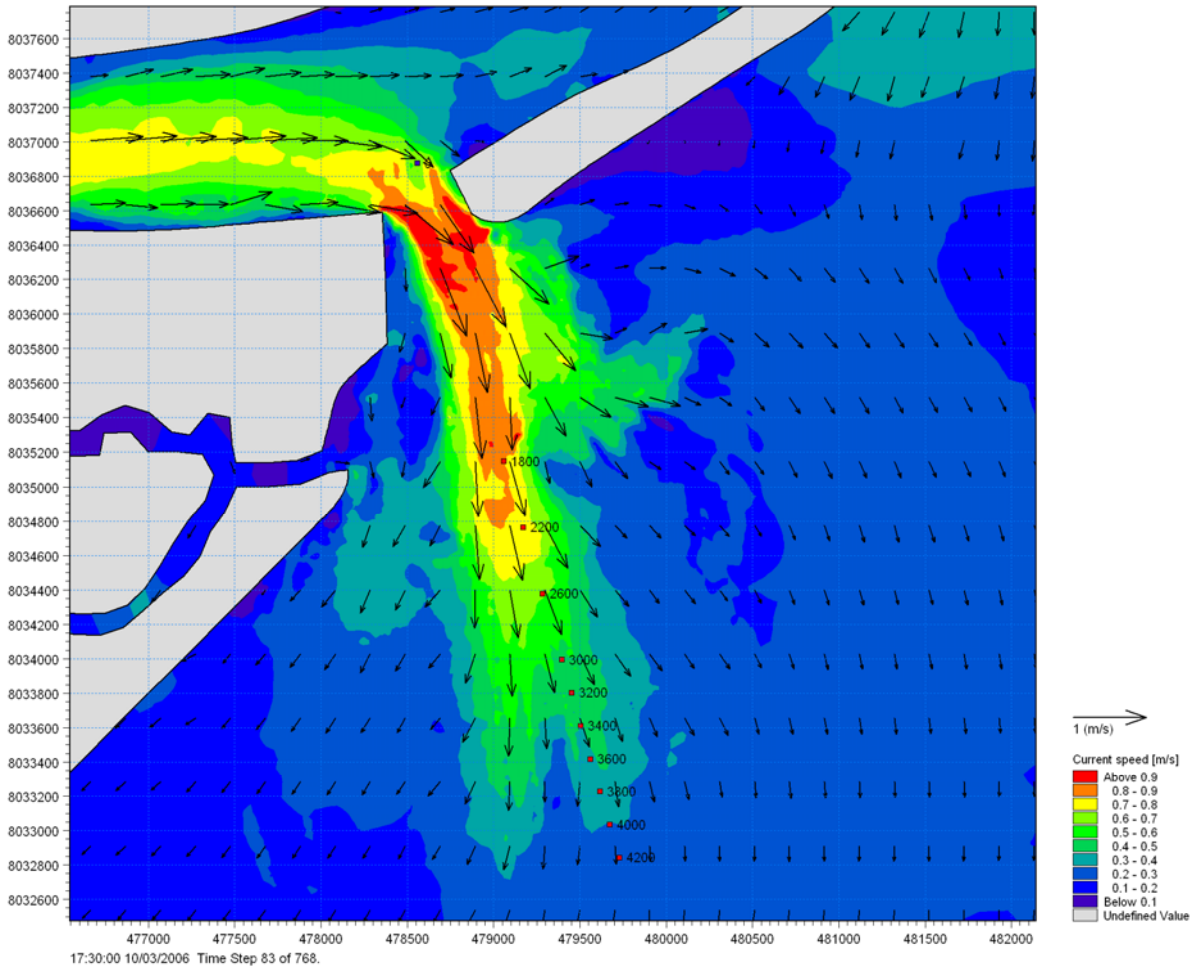

Figure 6.7a Scenario 2, the channel is realigned with the alternative channel. Current speed and direction. Ebb.

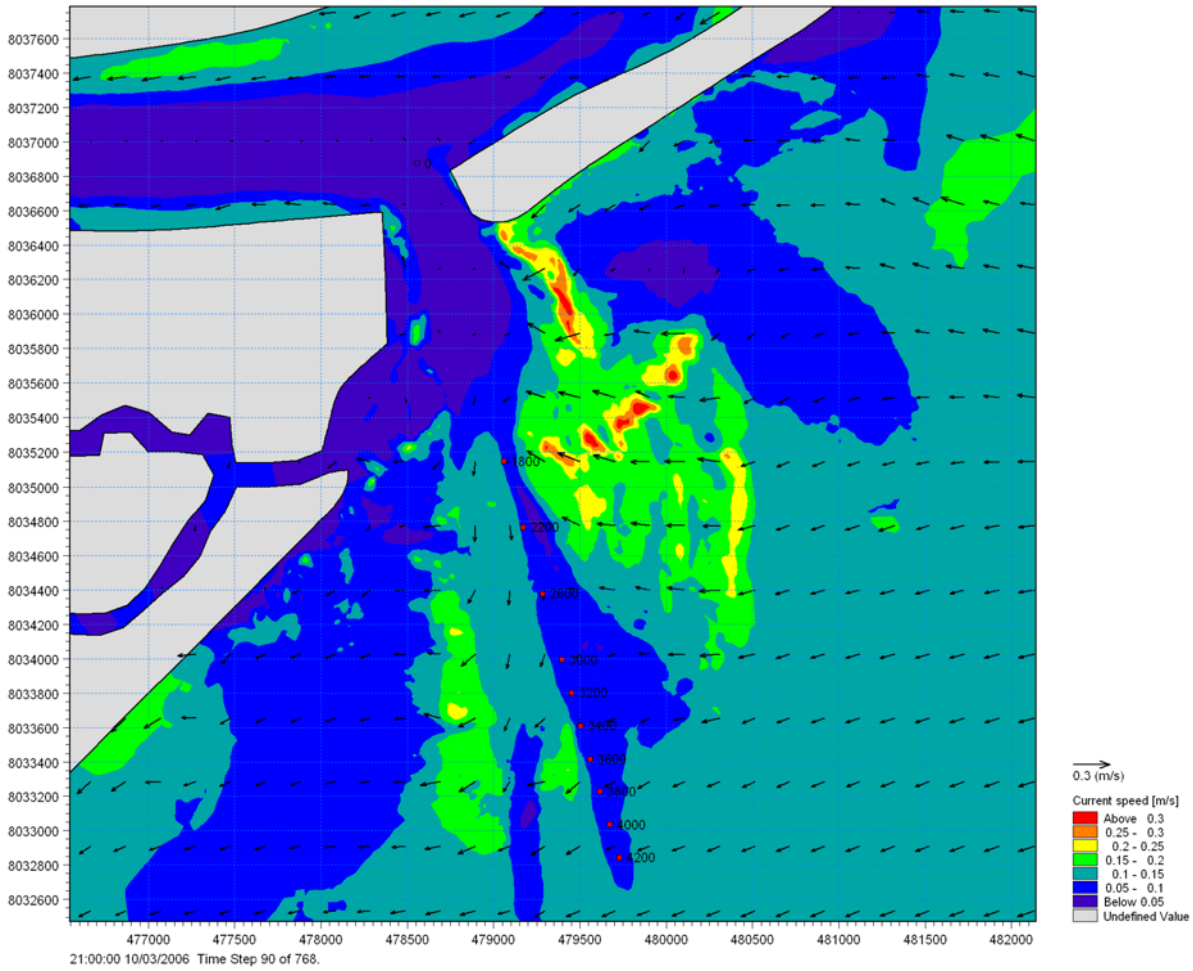

Figure 6.7b Scenario 2, the channel is realigned with the alternative channel. Current speed and direction. Low slack water.

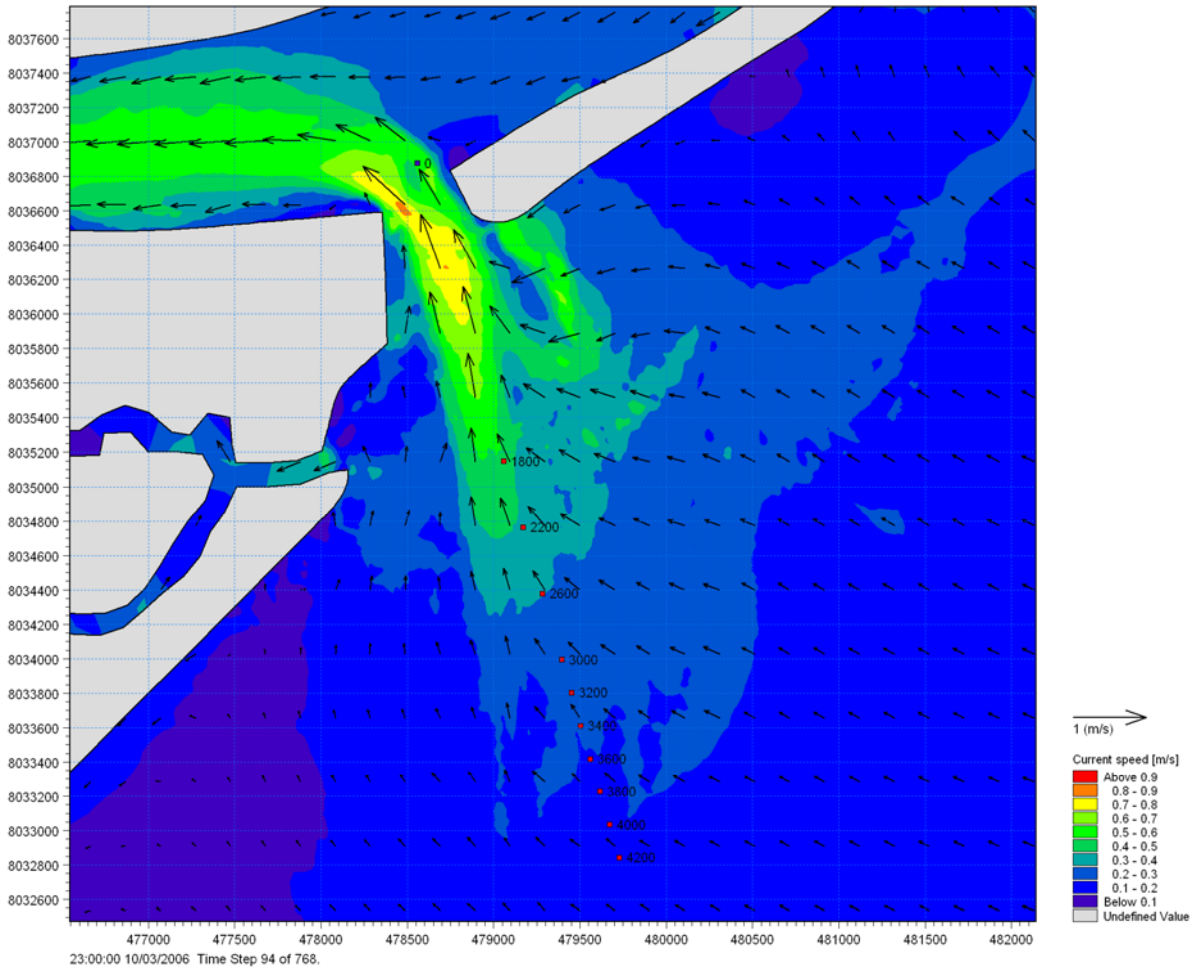

Figure 6.7c Scenario 2, the channel is realigned with the alternative channel. Current speed and direction. Flood.

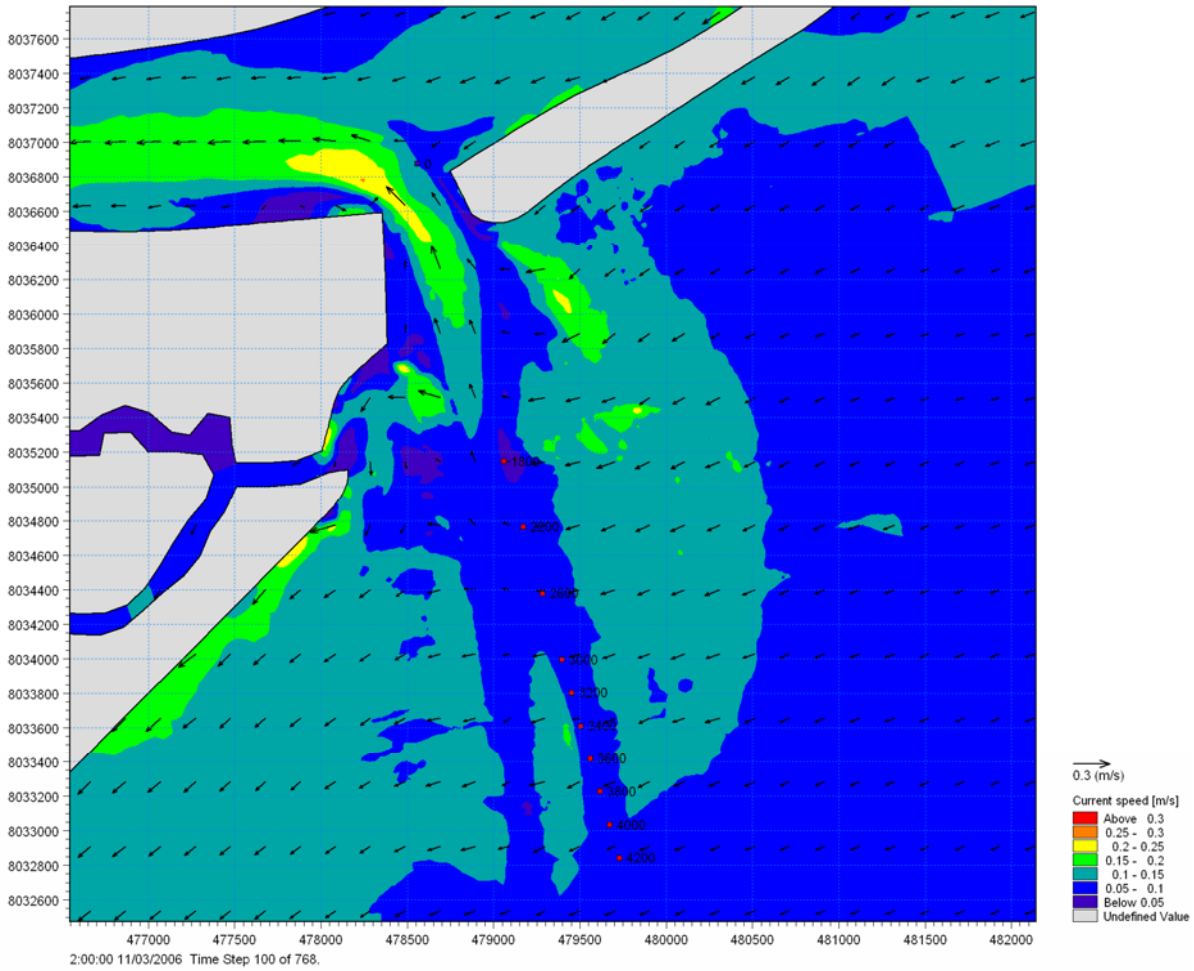

Figure 6.7d Scenario 2, the channel is realigned with the alternative channel. Current speed and direction. High water slack.

6.4 Scenario 3, the Alternative Channel is Partly Blocked

The bathymetry for this scenario is shown in Figure 6.8 and consists of a closure of the alternative channel by a submerged structure across the alternative channel. The structure has a top elevation of -1 m.

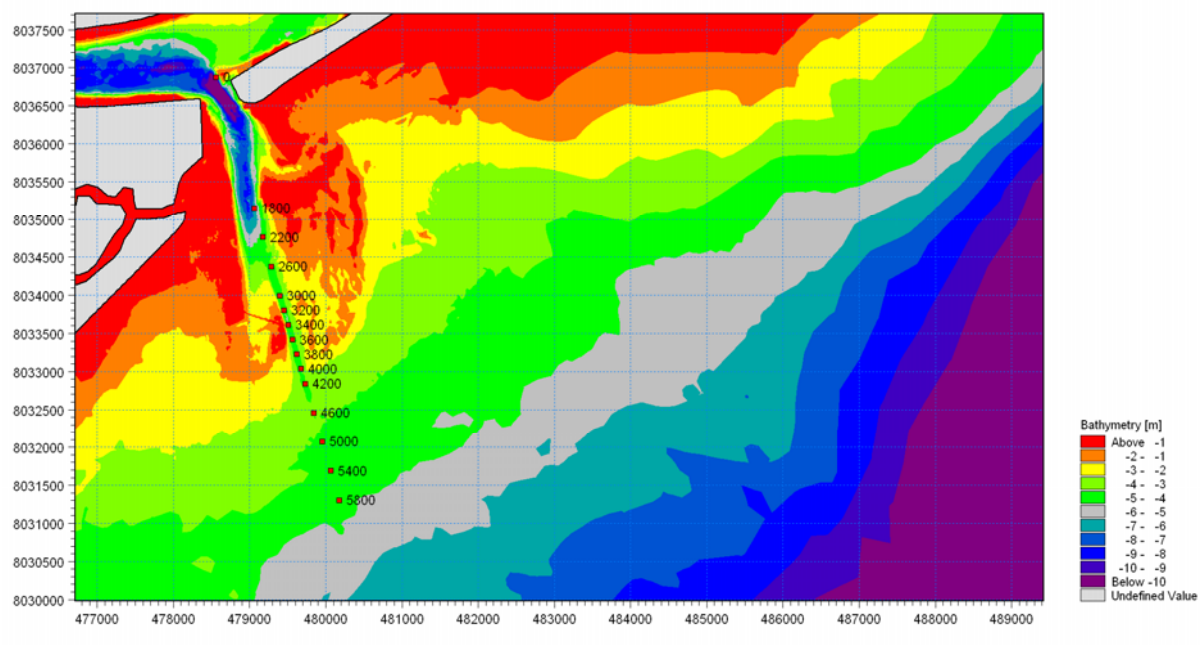

Figure 6.8 Scenario 3, the alternative channel is restricted by a sill at level -1 m close to station No. 3300.

The current conditions are presented for four different stages of the tide: ebb, low water slack, flood and high water slack, see Figure 6.9.

The impact on currents are relatively insignificant during ebb and flood although a local increase in velocity above and near the sill is observed as one would expect. At slack water the impact is less although the presence of the sill can be observed in the velocity distribution.

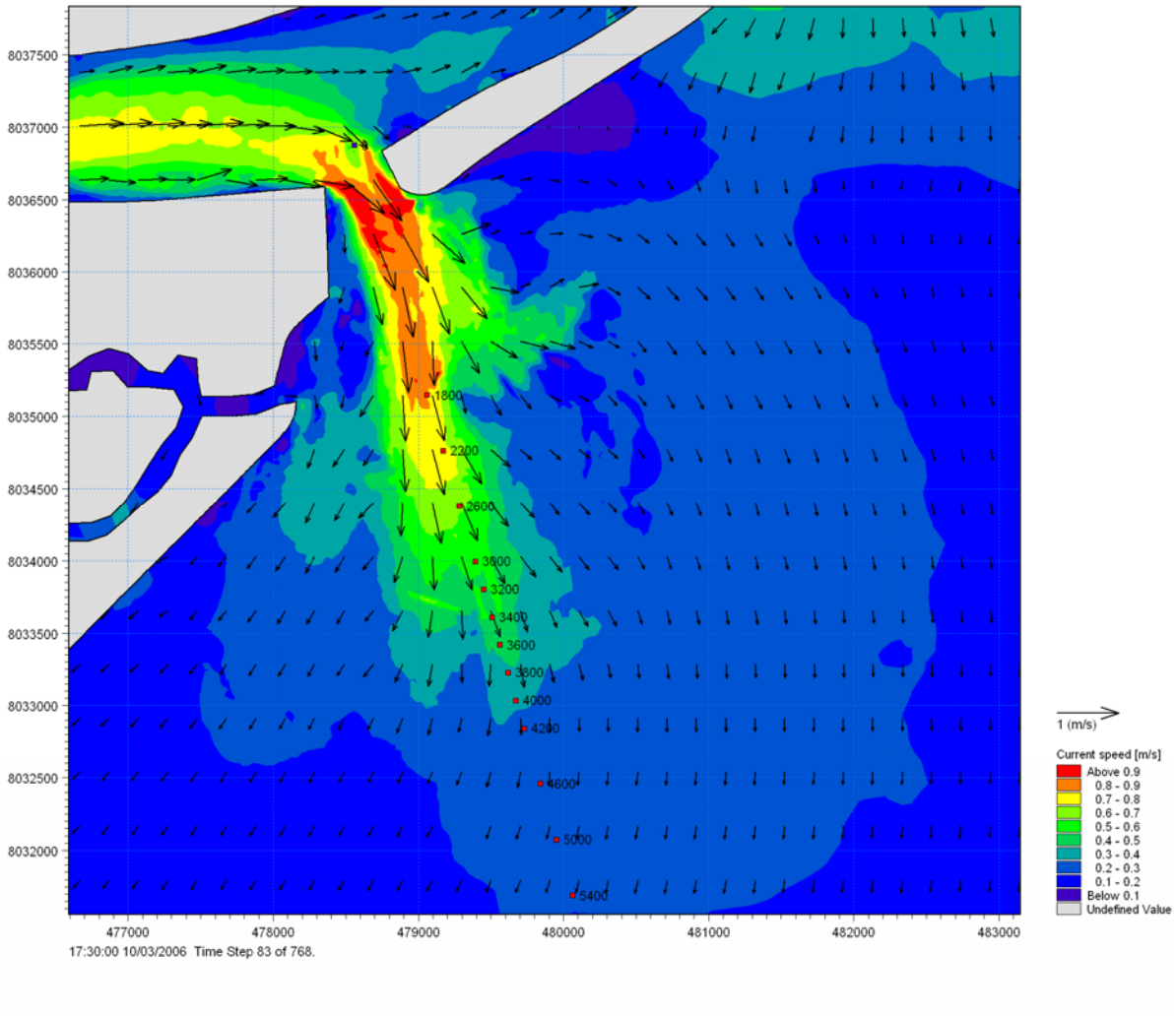

Figure 6.9a Scenario 3, the alternative channel is restricted. Current speed and direction. Ebb.

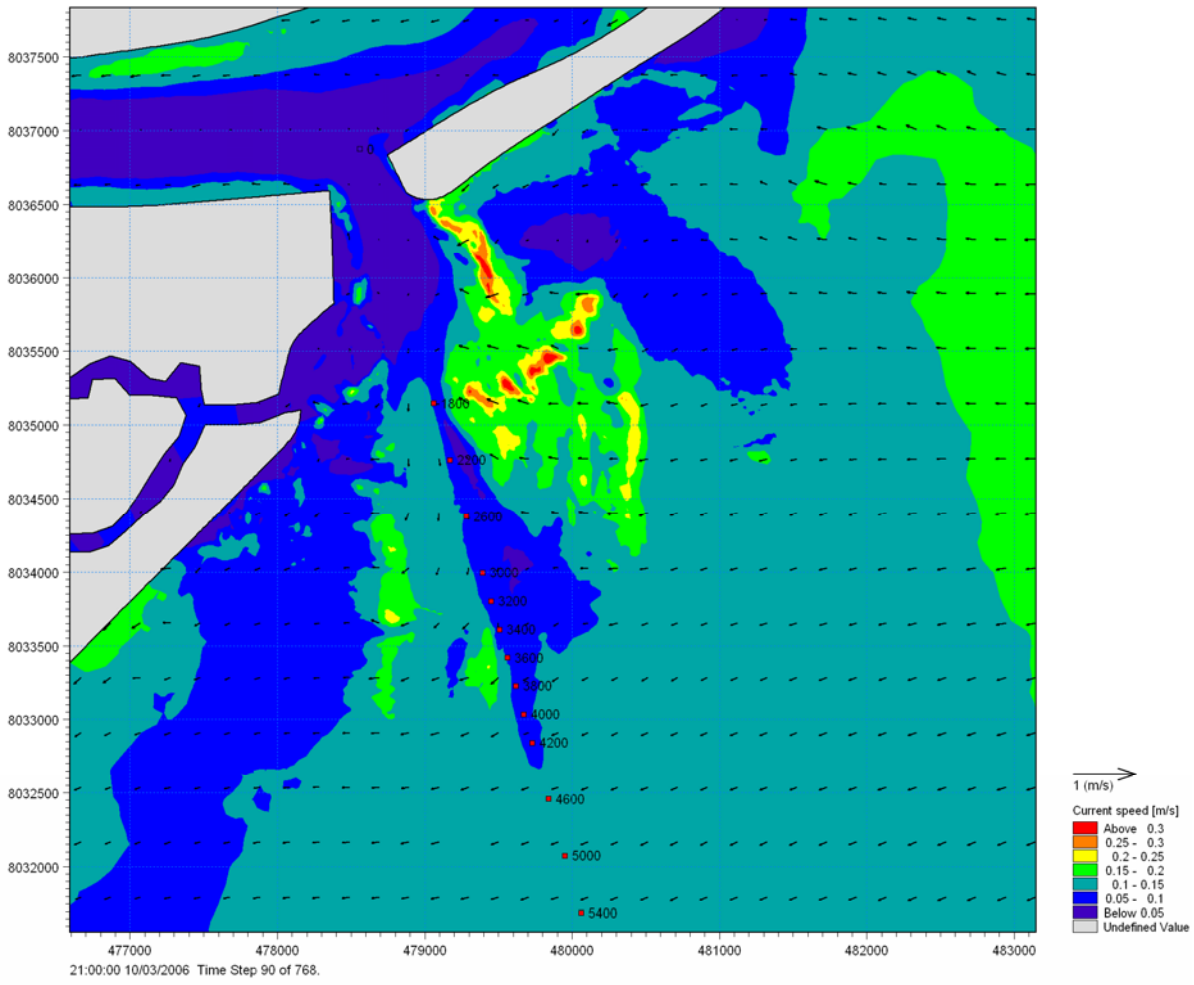

Figure 6.9b Scenario 3, the alternative channel is restricted. Current speed and direction. Low slack water.

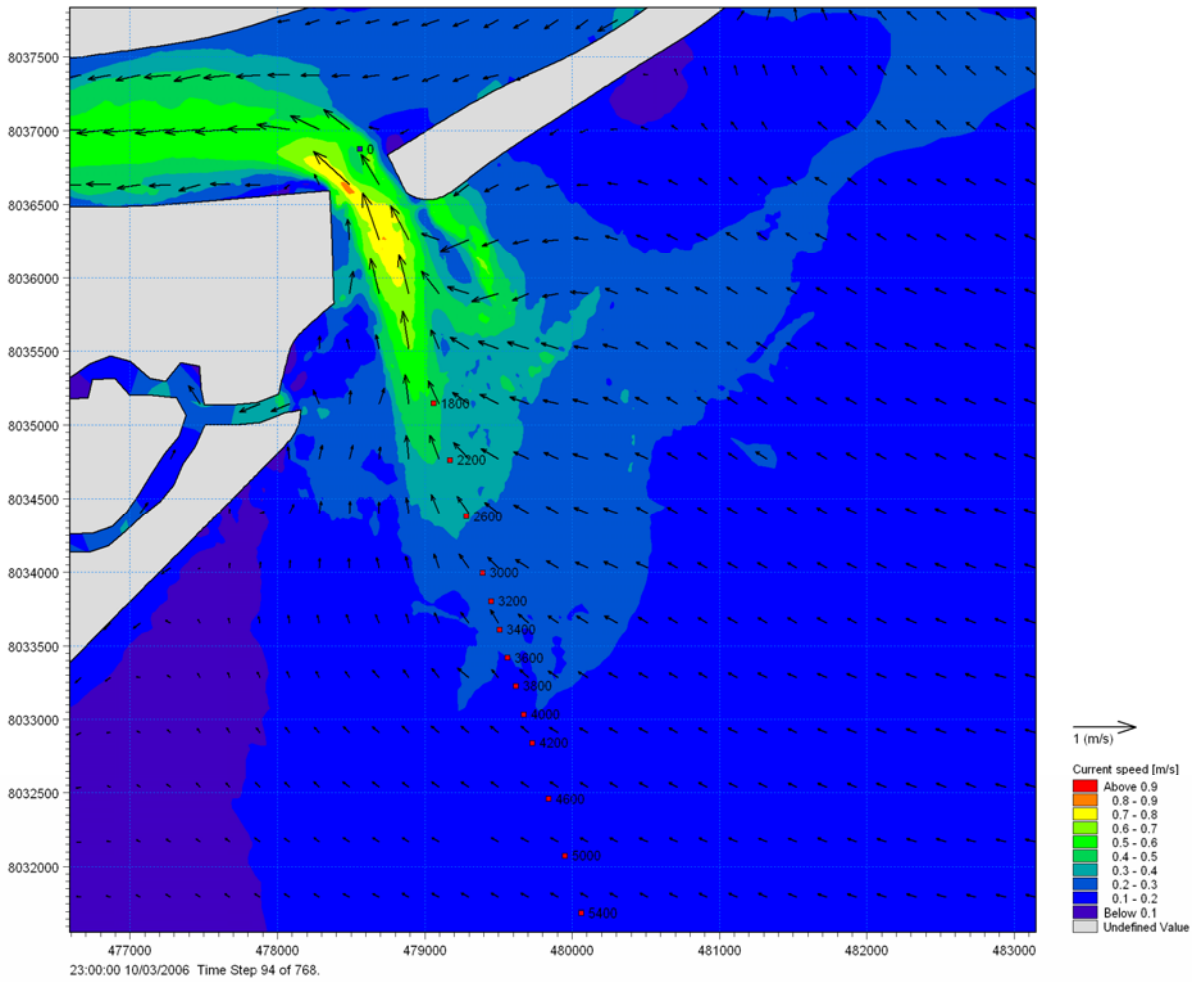

Figure 6.9c Scenario 3, the alternative channel is restricted. Current speed and direction. Flood.

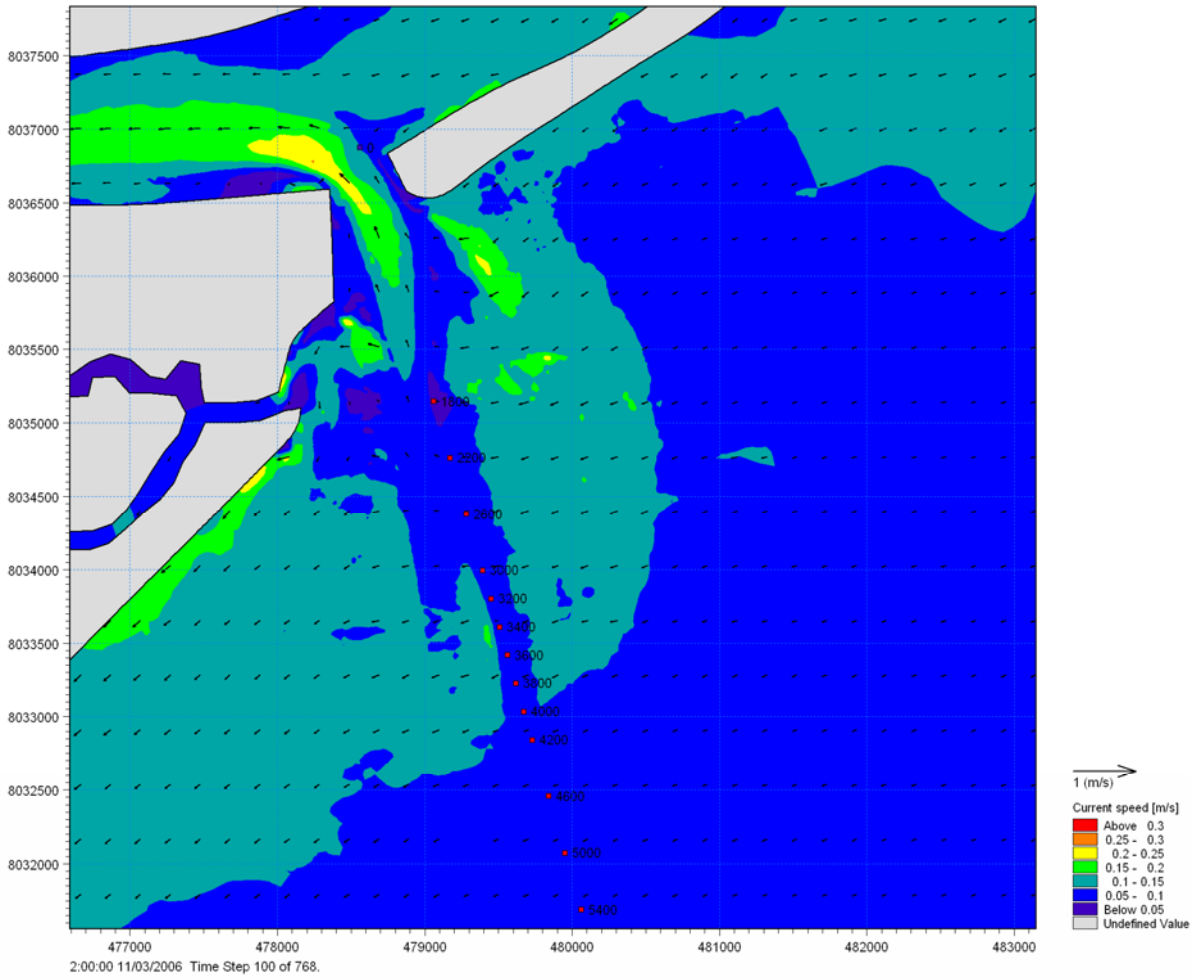

Figure 6.9d Scenario 3, the alternative channel is restricted. Current speed and direction. High water slack.

6.5 Scenario 4, Dredging a 1 m Deep Depression in the Existing Channel

The bathymetry for this scenario is shown in Figure 6.10. The overdredging between stations 3600 and 4600 in the outer parts of the channel is seen as grey on the picture.

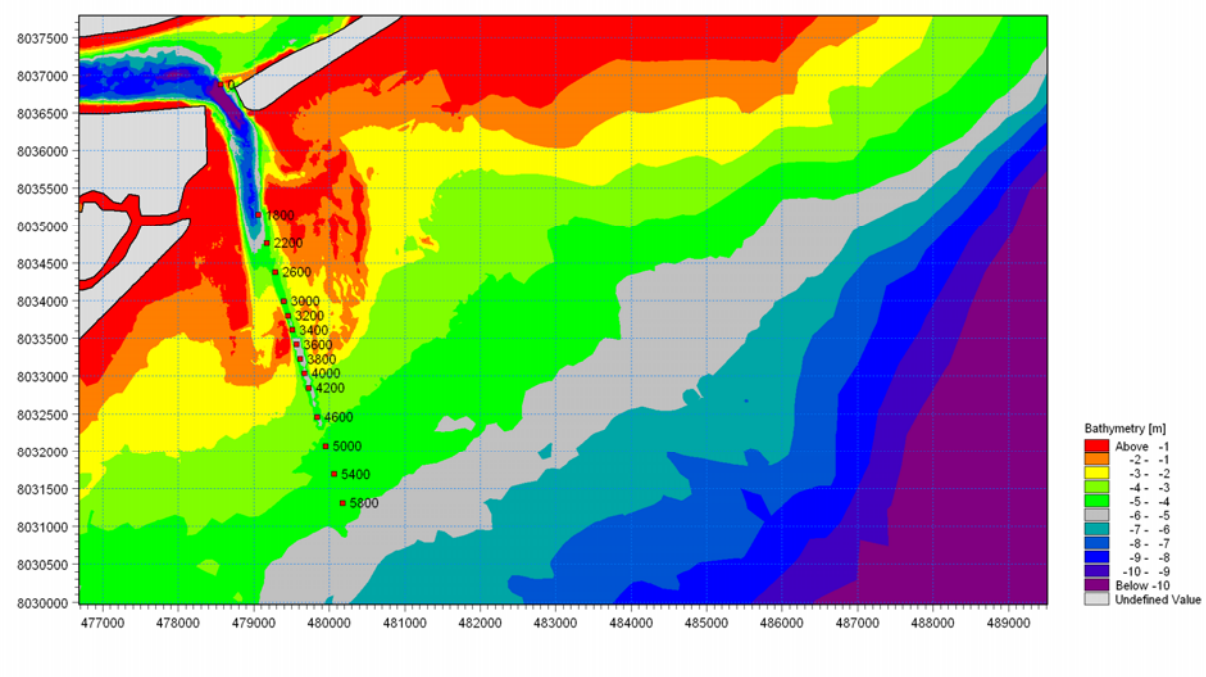

Figure 6.10 Scenario 4, dredging a 1 m deep depression in the existing channel between stations 3600 and 4600 (note the grey colour).

The current conditions are presented for four different stages of the tide: ebb, low water slack, flood and high water slack, see Figure 6.11.

The impact of the overdredging of 1 m between stations 3600 and 4600 has no discernable effect on the currents along the channel except for the low slack water situation where a reduction of currents in the channel further towards the ocean of about 500 m is observed.

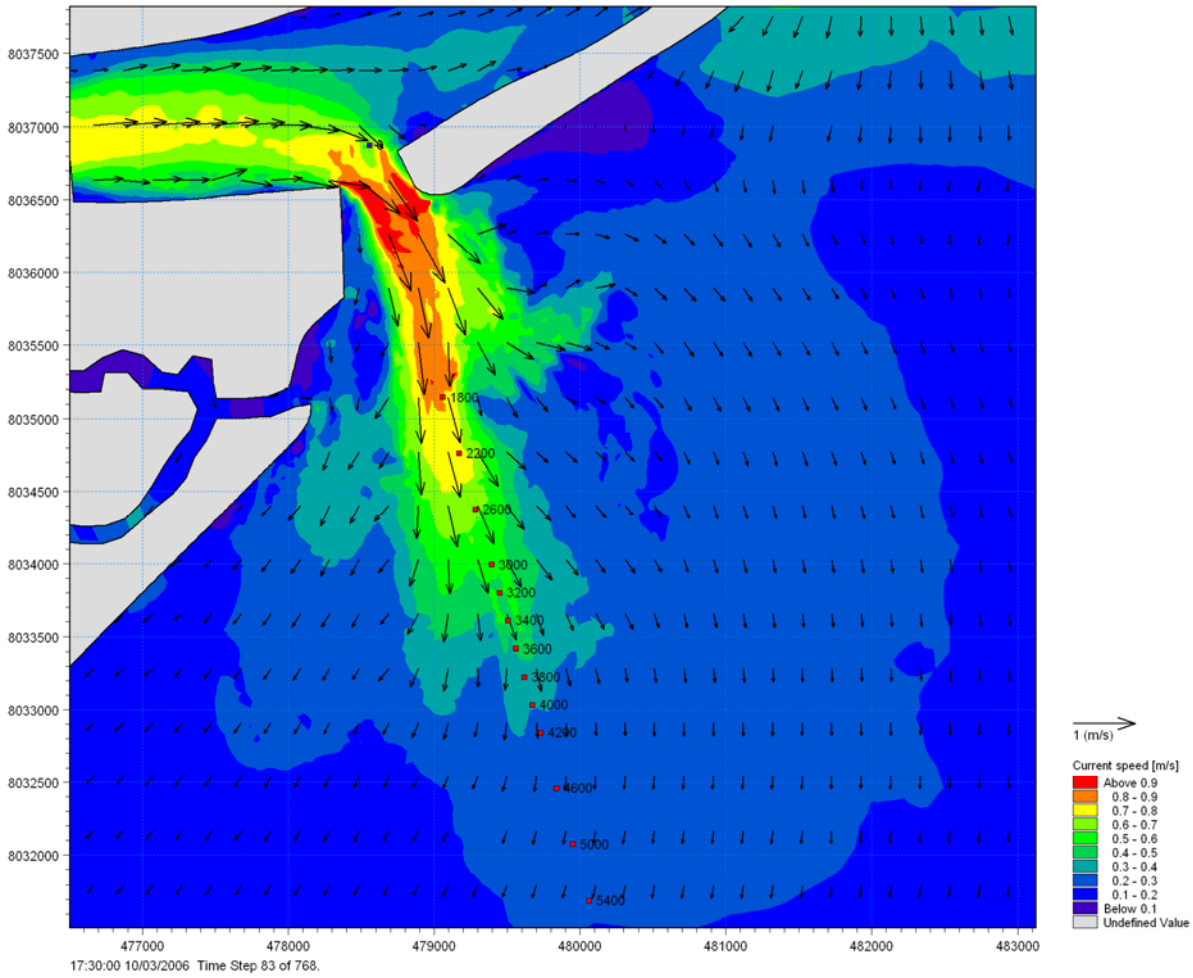

Figure 6.11a Scenario 4, dredging a 1 m deep depression in the existing channel. Current speed and direction. Ebb.

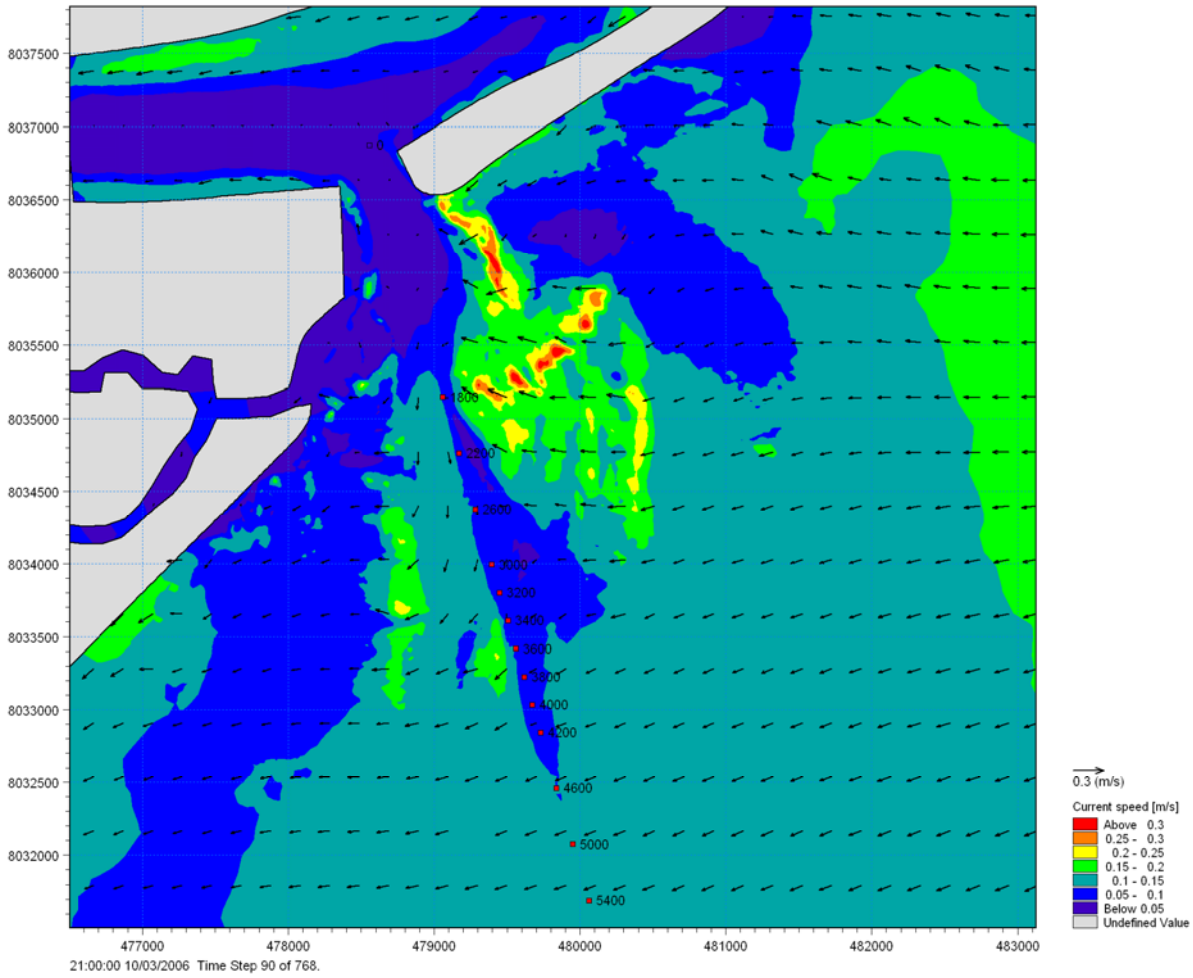

Figure 6.11b Scenario 4, dredging a 1 m deep depression in the existing channel. Current speed and direction. Low slack water.

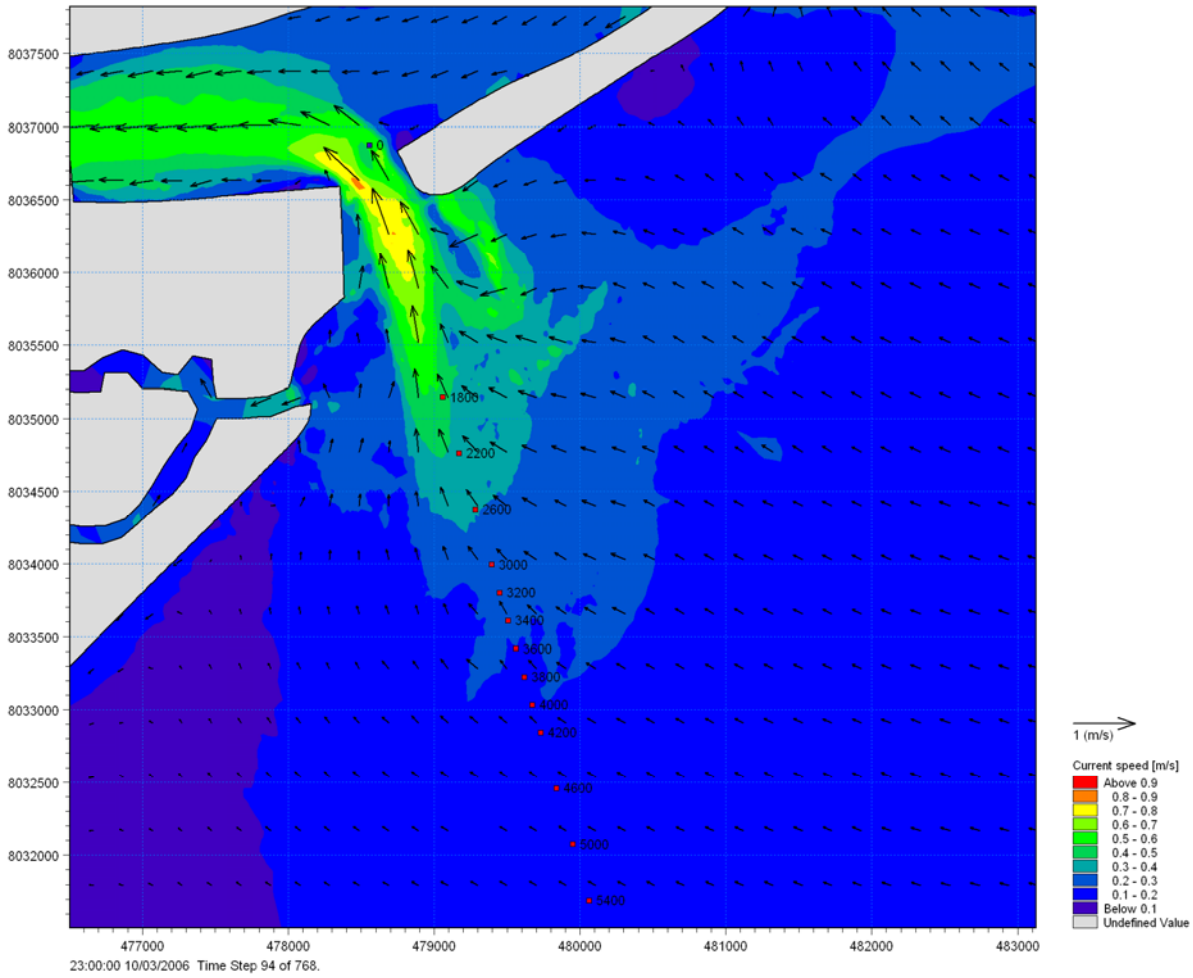

Figure 6.11c Scenario 4, dredging a 1 m deep depression in the existing channel. Current speed and direction. Flood.

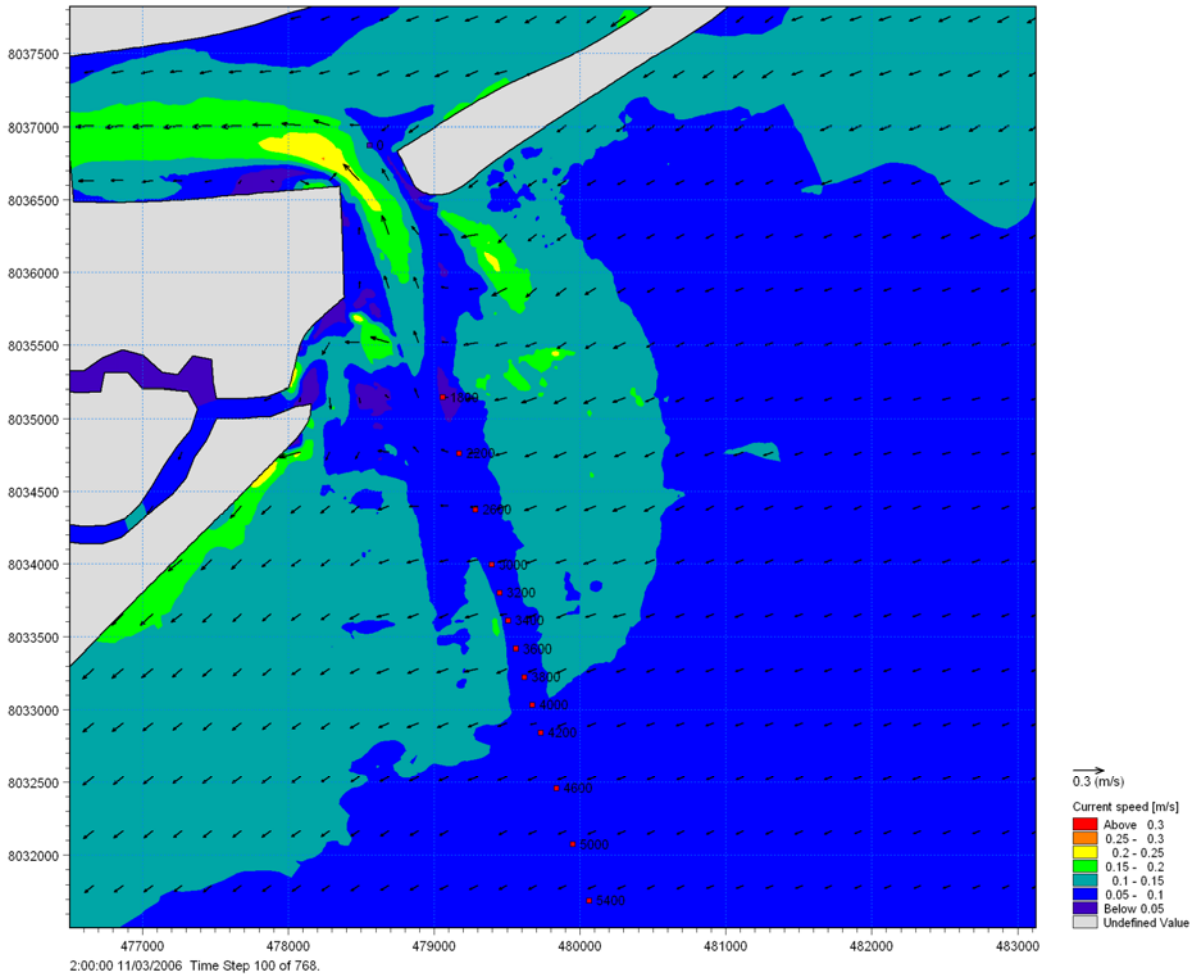

Figure 6.11d Scenario 4, dredging a 1 m deep depression in the existing channel. Current speed and direction. High water slack.

6.6 Analysis of Sedimentation

The yearly sedimentation rates for various scenarios have been estimated by the model calibrated models.

Yearly sedimentation rates of mud have been estimated for Scenarios 0 to 5. Yearly sedimentation rates of sand have been estimated for Scenarios 0 to 3. The sedimentation rates for mud are calculated for the entire channel from 1800 to 5800 whereas the sedimentation rates for sand are calculated for the stretch of 1800 to 4200 where sand is present on the sea bed.

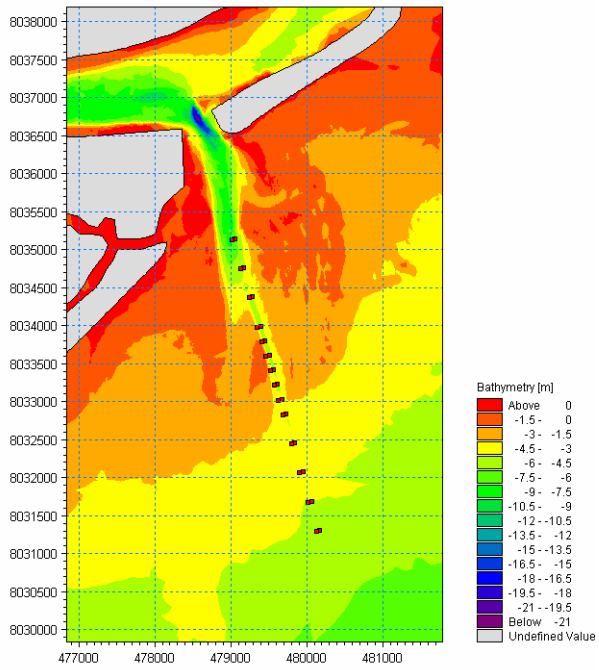

Figure 6.12 Overview of the existing channel.

6.6.1 Yearly Sedimentation, Existing Layout

The calibration of the sand showed that the two simulations undertaken for sand shall be weighted with the duration of events with significant wave height > 0.6 m from the two directional sectors giving net currents towards southwest and northeast.

The corresponding weight of the results of the mud modelling showed that the simulated results shall be tuned by a factor of two and assigned a duration corresponding to all events with a significant wave height at position 106 > 0.8 m.

The yearly durations of the two sets of simulations are derived based on the wave statistics for four years at position 106. The durations are summarised in Table 6.2:

Table 6.2 Yearly duration of the two sets of simulations.

	Duration, calibration period [days]	Duration, yearly [days]
MUD	30	46
SAND, easterly wind and waves	28	27
SAND, southerly wind and waves	24	57

Using these durations of each event leads to the following backfilling of the channel:

Table 6.3 Backfilling of the channel.

Sand [m^3]	Mud [m^3]	Total [m^3]
8,200/27,100 *)	58,000	85,100

*) 8,200 m^3 is the net deposition in the channel between 1800 and 4200. 27,100 m^3 is the sediment brought into the channel.

The yearly backfilling of the channel with sand is illustrated in Figure 6.13. The upper plot shows the weighted sedimentation from west and from east. It appears that sedimentation between 1800 and 3300 takes place from east. Between 3300 and 3900 sedimentation takes place from both sides. It is also seen that between 1800 and 3300 erosion (negative deposition) takes place on the western side of the channel. The net sedimentation due to cross-channel sediment transport is shown in the lower plot. It is thereby seen from the two plots that the channel is shifted to the west on the inner part. This is the reason for presenting two numbers in Table 6.3. The 8,200 m^3/year is the net deposition. If the channel shall be kept in place and at the original depth, the amount of dredging required corresponds to the backfilling from both sides. Furthermore, the lower plot shows the sedimentation due to longitudinal transport in the channel. It appears that the longitudinal sediment transport contributes significantly to the yearly sedimentation and that deposition due to gradients in the transport along the channel leads to deposition from around 2300 and seaward.

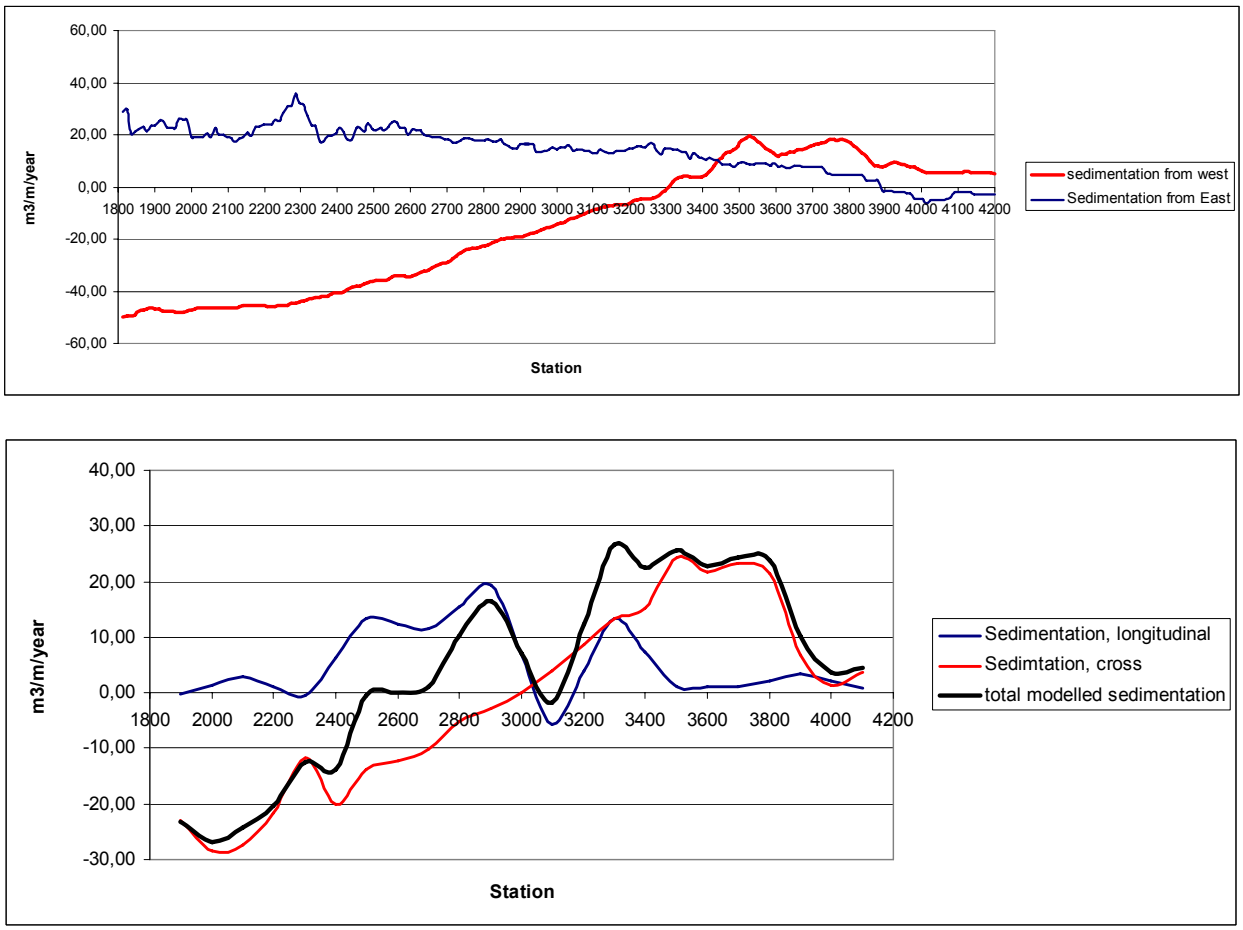

Figure 6.13 Upper plot: yearly sedimentation from west and from east due to cross-channel transport. The amounts are presented as m^3/m length of the channel. Lower Plot: sedimentation due to cross-channel transport (sum of results presented in upper plot), sedimentation due to longitudinal sediment transport which generally decreases with distance from the shore, and the total net sedimentation.

The deposition with mud is concentrated in the channel. The simulated distribution of sedimentation with mud is illustrated in Figure 6.14.

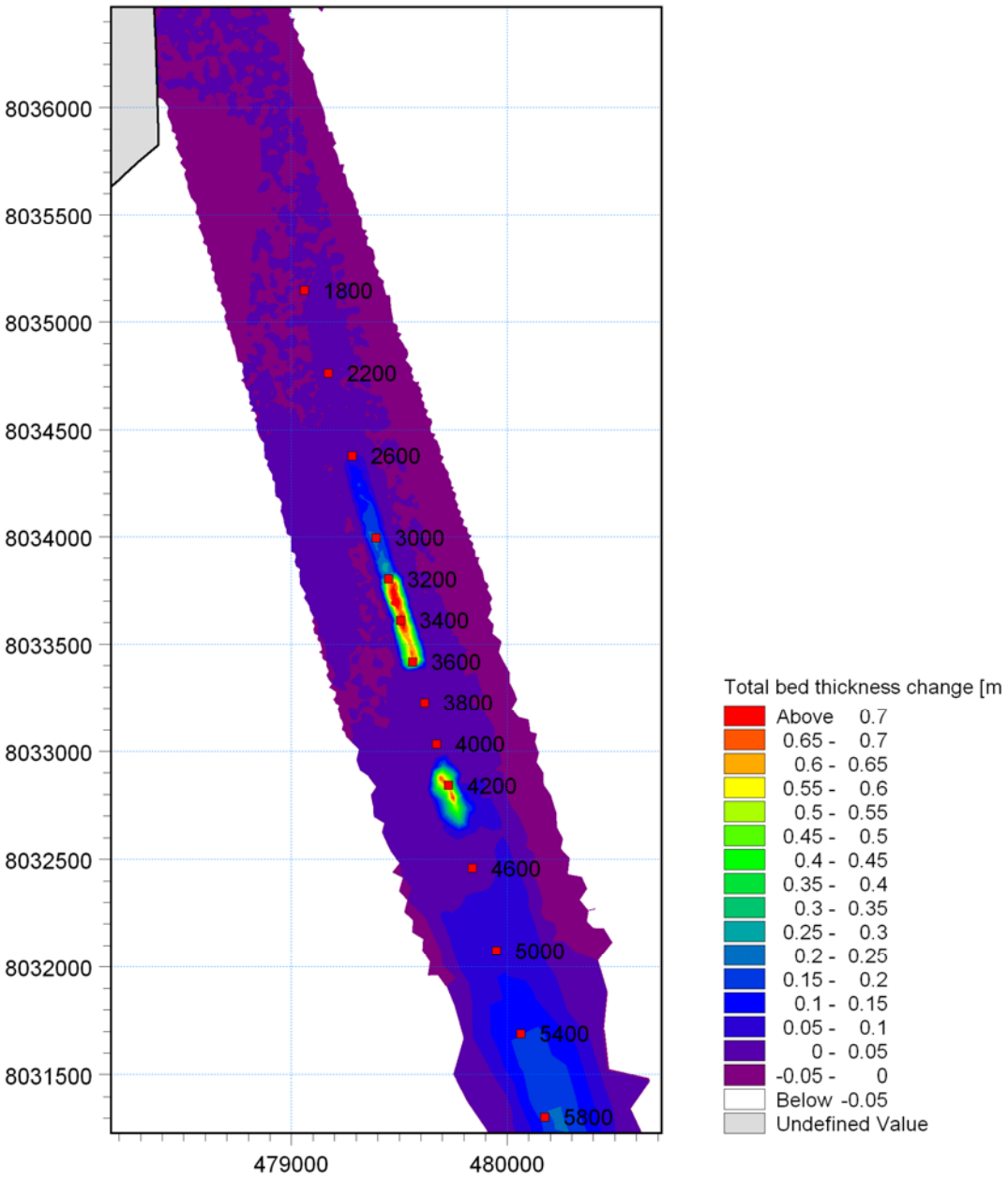

Figure 6.14 Scenario 0, simulated net sedimentation of mud, scaled to yearly sedimentation.

6.6.2 Yearly Sedimentation, Alternative Layouts

The yearly sedimentation with sand and mud has been estimated for the following alternative layouts:

Scenario 1	The existing channel is dredged to -5.5 m.	SAND	MUD
Scenario 2	The channel is realigning with the alternative channel.	SAND	MUD
Scenario 3	The alternative channel is partly blocked.	SAND	MUD
Scenario 4	Dredging a 1 m deep depression in the existing channel.		MUD

Scenario 4 has not been modelled for sand. As will be seen in the following scenario 1 and 3 give only insignificant changes to the backfilling with sand. The depression in the channel gives does not change the sand transport capacities around the channel and will therefore not lead to changes in the sand deposition. The depression is a trap for mud which will settle in areas with lower current speeds.

Backfilling with mud

The estimated yearly backfilling with mud in the entire channel from 1800 to 6200 is listed in Table 6.4.

Table 6.4 The estimated yearly backfilling with mud in the entire channel.

Layout	MUD deposition [m^3/year]
Existing	58,000
Scenario 1	31,000
Scenario 2	132,000 / 202,000 *)
Scenario 3	28,000
Scenario 4	107,000

*) original channel/alternative channel

In order to further understand the results in the above table, it is illustrative to examine the horizontal distribution of the net sedimentation of mud sediments. Figure 6.15 to Figure 6.18 show the net sedimentation of mud at the end of the 14-day simulation.

It appears that scenarios 1 and 3 are significantly more optimal than the existing layout with regards to sedimentation with mud. In both scenarios the flow is concentrated in one channel, in case of scenario 1 because the resistance in the deeper channel is smaller, which will strengthen the ebb flow in the channel, in case of scenario 3 because the naturally developed alternative channel is partly blocked.

The mud modelling has clearly illustrated that depressions in the channel have a very negative influence on the backfilling with mud.

The results from Scenario 2 show a huge increase in sedimentation with mud both in the existing channel and in the dredged, alternative channel. This is because the flow is now distributed between the two channels, the currents speeds are generally lower than if the flow is concentrated in one channel and the self cleansing effect is significantly reduced.

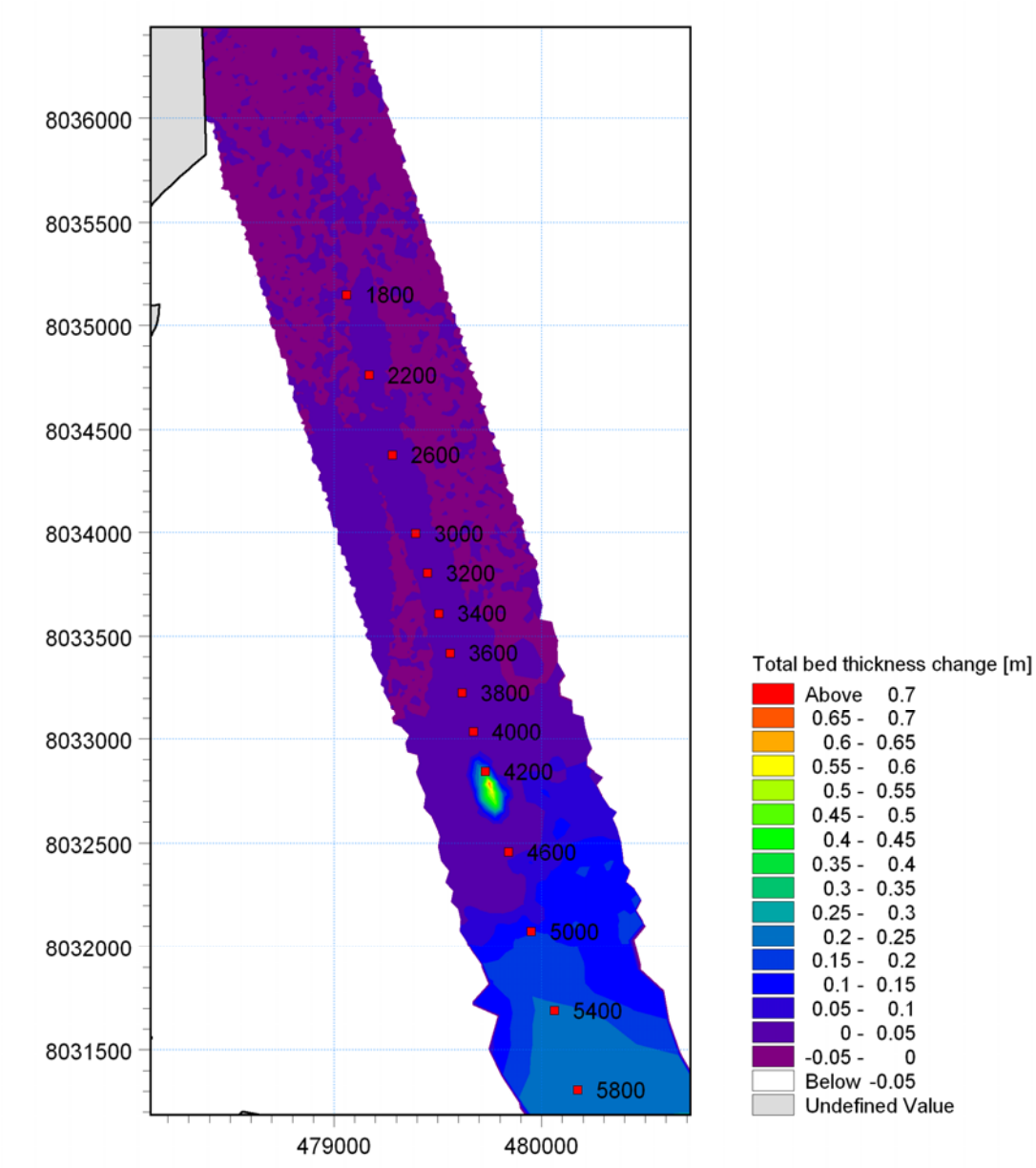

Figure 6.15 Scenario 1, simulated yearly net sedimentation of mud.

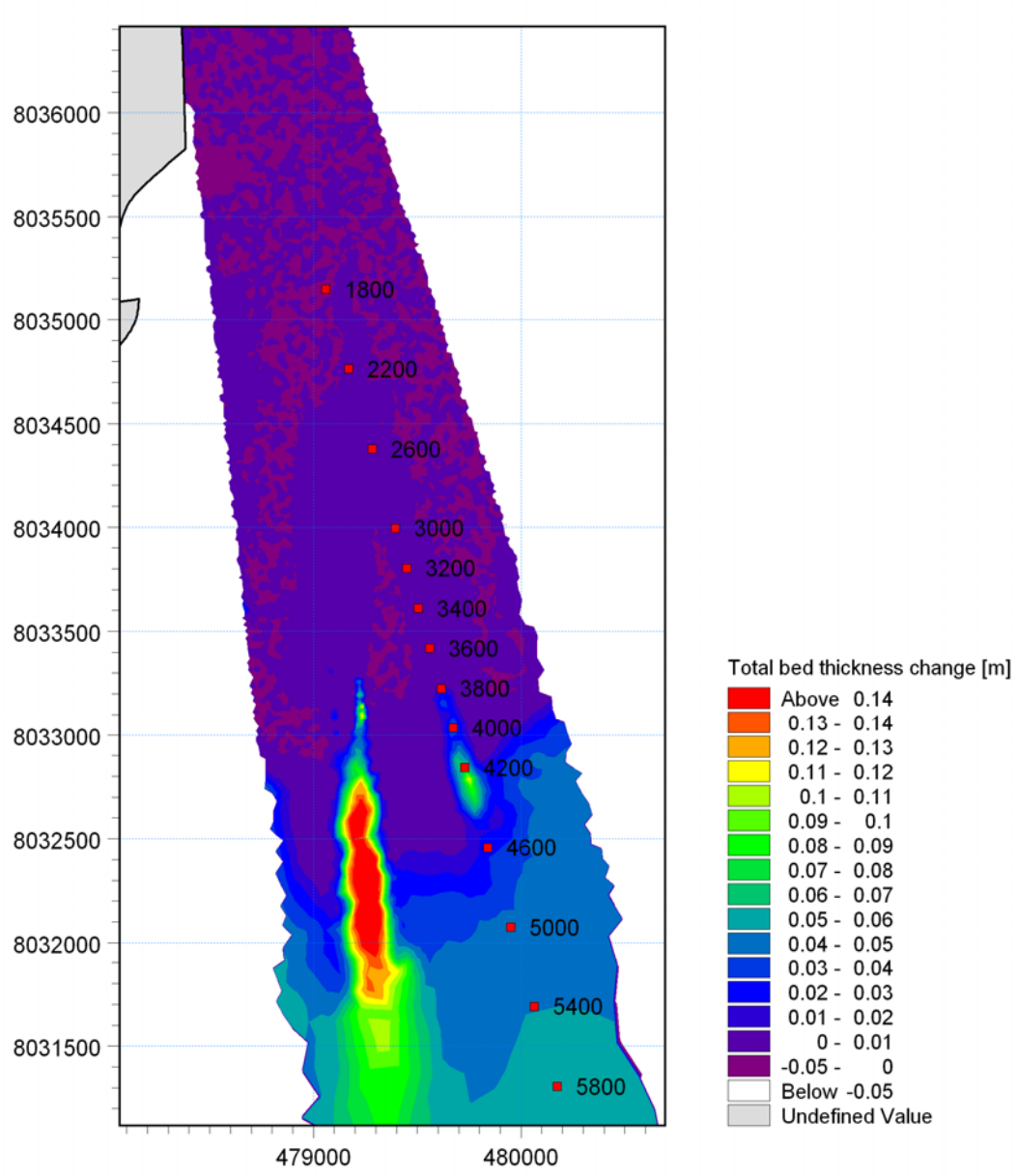

Figure 6.16 Scenario 2, simulated net sedimentation of mud. NOTE: this result is presented per re-suspension event.

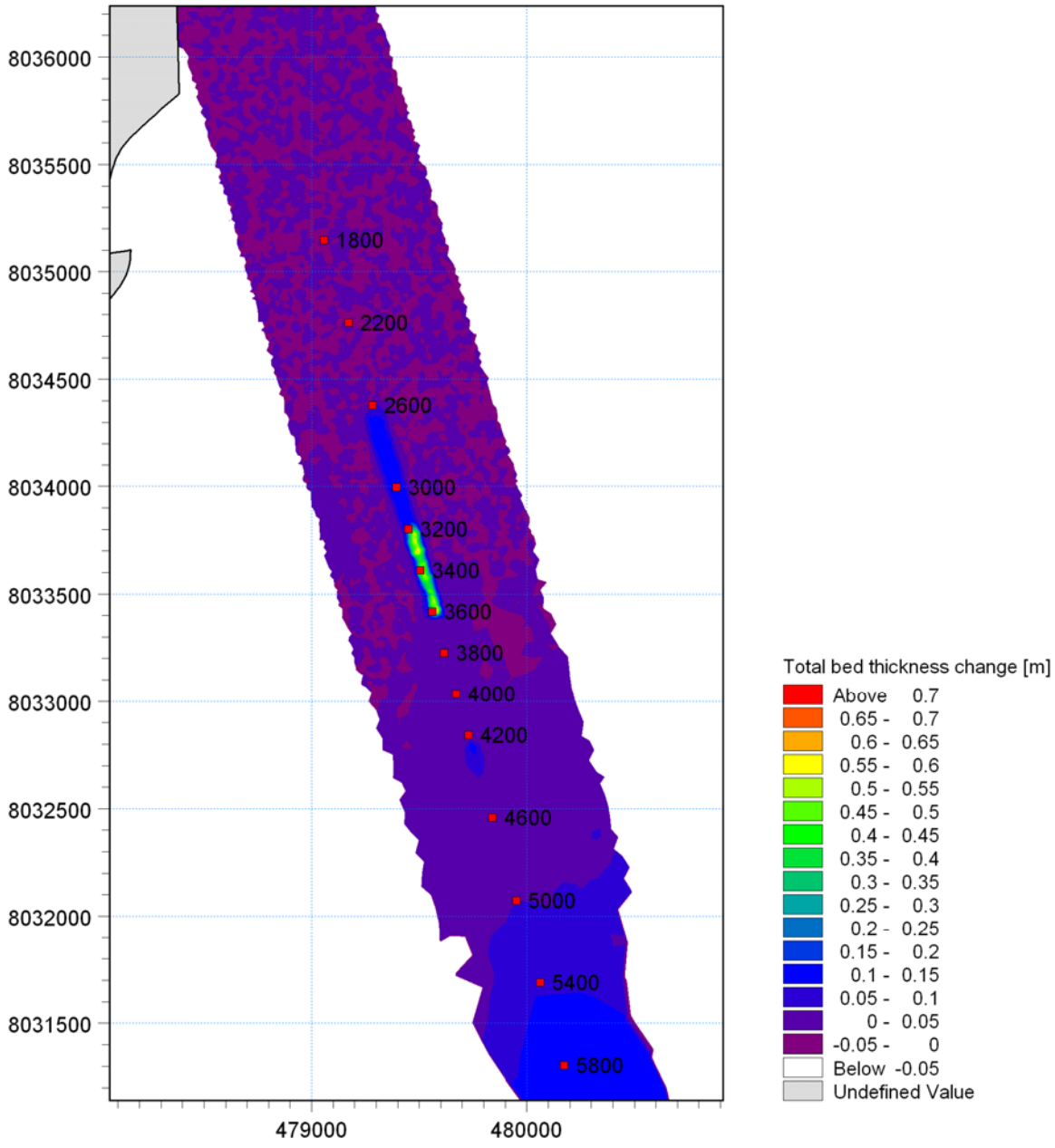

Figure 6.17 Scenario 3, simulated net yearly sedimentation of mud.

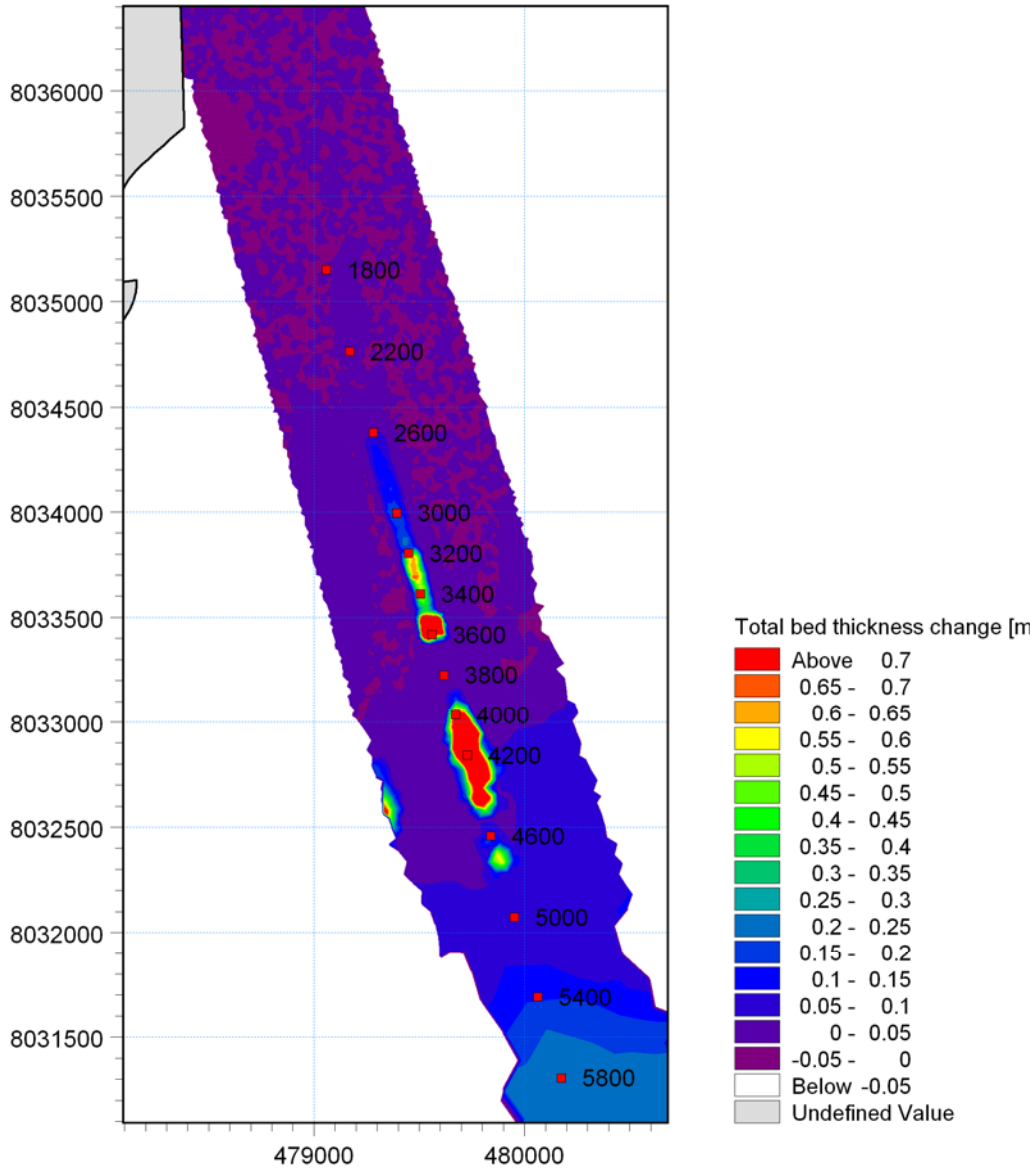

Figure 6.18 Scenario 4, simulated net yearly sedimentation of mud.

Backfilling with sand

The net deposition and the backfilling with sand have been estimated for the stretch between 1800 and 4200 for alternatives 1, 2 and 3. The results are summarised in Table 6.5

Table 6.5 Estimated yearly net deposition/backfilling with sand between 1800 and 4200.

Layout	Net deposition [m^3/year]	Backfilling [m^3/year]
Existing	8,200	27,100
1	5,070	26,300
2	13,600	32,600
3	7,500	27,900

Layouts 0, 1 and 3 result in practically the same backfilling with sand. The erosion along the inner part of the channel, mainly due to the west-going transport component away from the channel, varies slightly between the three cases and the infill from east is slightly higher in layout 3 than in the other two layouts. These very small differences lead to the small variations reflected in the results. The yearly net deposition due to cross-channel transport and due to longitudinal transport is compared with the existing layout (layout 0) in Figure 6.19.

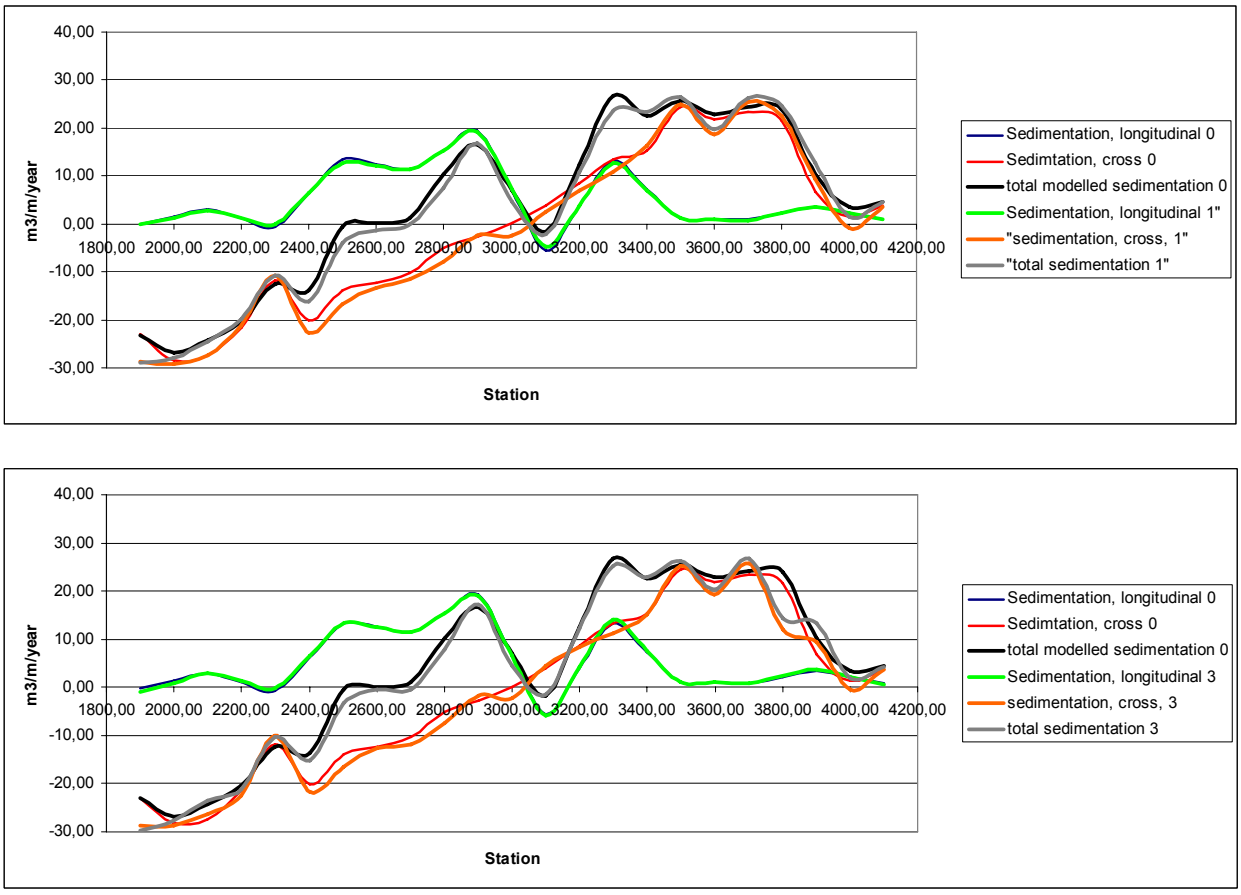

Figure 6.19 Comparison of net yearly sand deposition due to cross-channel transport and longitudinal transport for layouts 1 and 3 compared to the existing layout.

Scenario 2 gives the highest net deposition and the highest backfilling with sand of the 4 layouts. The values presented in Table 6.5 represent backfilling and net deposition in the new channel only. The below Figure 6.20 illustrates the difference between the sedimentation patterns for the existing channel and the alternative alignment, layout 2. Note that the x-axis starts in the same position but then follows the two different alignments. It appears that the alternative channel backfills significantly more from the east than the existing one on the outer part, between 2800 and 4200. It also appears that the new channel will erode on the west side on the outer part and slightly backfill on the inner part from west.

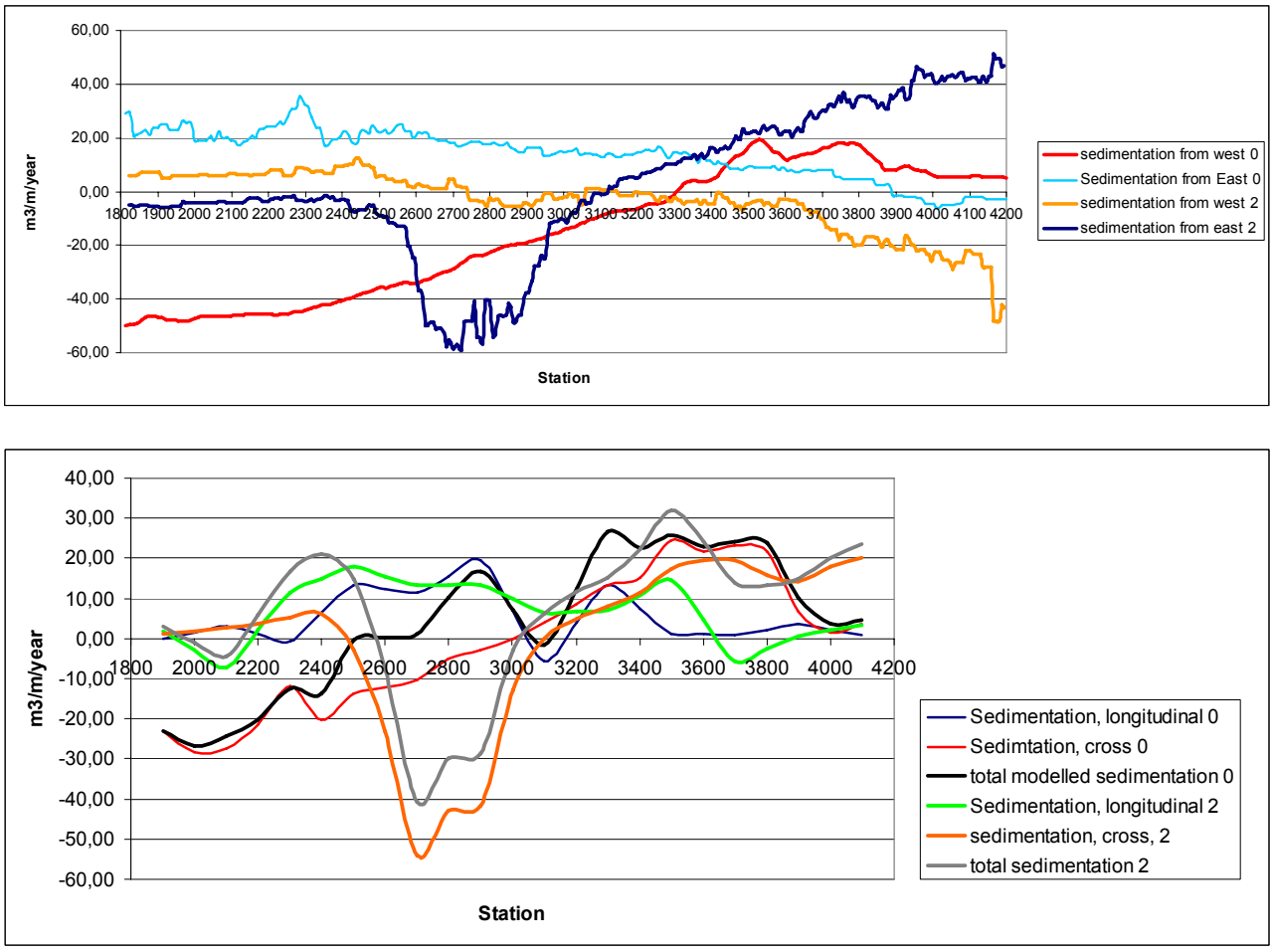

Figure 6.20 Upper plot: comparison of sedimentation from east and west for the existing channel and the alternative alignment, layout 2.
Lower plot: distribution along the existing channel and the alternative alignment, layout 2 of net sedimentation due to cross-channel transport and longitudinal transport.

The above presented results on backfilling with mud and with sand are all found using the calibrated models. The models reproduce reasonably well the backfilling during the calibration period. The wave statistics have been used as the basis for expanding the findings to cover an average year. It is emphasised that both mud and sand transport are very complicated processes and even though the models include many processes and relevant hydrographic scenarios have been simulated, the uncertainty on sediment transport modelling is known to be within a factor of 2. Furthermore, in nature variations occur from year to year due to the different frequency of storms from the two dominant di-

rectional sectors. However, the model results are deemed to represent a central estimate of backfilling rates and are well suited for inter-comparison of layouts.

6.7 Evaluation of Sedimentation

Scenario 1 - The existing channel is dredged to -5.5 m
The deepening of the channel results in a reduction of the sedimentation of mud sediments by almost 50% as compared to the existing situation. The increase of depths attracts the flow and the ebb flow deposits the sediment further south than in the existing channel. It must be emphasized that this result is a sensitive balance between the capability of the channel to flush itself and the additional sedimentation capability due to large depths. Backfilling with sand is found to be almost unchanged compared to the existing situation with an insignificant tendency for reduction of backfilling.

Scenario 2 - The channel realigns with the alternative channel
The presence of an alternative channel that follows the development of the new ebb channel is not an attractive option. The ebb flow is divided between the two channels and significant sedimentation must be expected. If this option should be effective from a hydrodynamic point of view the existing channel should be filled up. The excessive amount of dredging required does not make this option attractive. In reality, one must expect that the existing channel will gradually fill in while the new channel is maintained. The time scale for this has not been assessed. The modelling has shown that both sand and mud backfilling are significantly larger in the alternative channel alignment as long as the existing channel is maintained.

Although not confirmed by modelling, it is expected that the total sedimentation in the alternative channel, with the present channel closed, will not result in significantly lower sedimentation compared with Scenario 1.

Scenario 3 - The alternative channel is partly blocked
The simulation of closure of the alternate channel route indicates that a better flushing of the existing channel will be achieved. The sedimentation of mud is reduced for this scenario to the same level as for Scenario 1. The blockage of the alternative channel has been introduced in the model by a “sill” across the channel. However, in practical terms the simulation has illustrated that alternative ebb channels which develop naturally shall preferably be backfilled, for instance with dredged material to optimise the self cleansing of the navigable channel.

Scenario 4 - Dredging a 1 m deep depression in the existing channel
This scenario clearly illustrates that overdredging in parts of the channel, which leads to depressions where the bottom level of the channel is lower than the general bottom level, leads to a significant increase of mud sedimentation.

The effect of sand traps has been investigated in a previous study, Ref. /5/. It was found that sand traps along a long stretch of the channel have a similar influence on the overall hydrodynamics as a general deepening of the channel, i.e. the larger channel will concentrate the flow in the channel and thereby have a positive impact on the deposition with mud in the channel. The sand deposition in the channel is not very sensitive to the depth and width of the channel. However, with the sand traps in place the backfilling over the ends of the traps shall be added to the sedimentation without traps. With a wid-

ening of the channel of 20 m on either sides and additional infill of the traps in the order of 3000 m^3/year will take place.

7 COMMENTS ON DREDGING STUDY BY CPE

To come.

8 REFERENCES

/1/ DHI Water & Environment: *Sedimentation in Caravelas Channel, April - July 2005*, Note on data analysis, 18 November 2005.

/2/ DHI Water & Environment: *Analysis of channel depth changes April - July 2005*. Technical note, 21 November 2005.

/3/ CPE and CEPEMAR Servicos de Meio Ambiente*: Second Opinion on the Caravelas Channel Dredging Maintenance Assessment*, Report to Aracruz Celulose S.A., January 2005.

/4/ DHI Water & Environment: *Hydraulic Investigations for Port Facilities at Caravelas, Brazil. Phase 2* Report to Aracruz Celulose S.A., June 2000.

/5/ DHI Water & Environment: *Additional Hydraulic Studies.* Report to Aracruz Celulose S.A., February 2004.

/6/ CPE and CEPEMAR Servicos de Meio Ambiente*: Sedimentologia do Canal de Acesso a Barra do Tomba – Relatório Técnico CPM RT 101/06*, Report to Aracruz Celulose S.A., April 2006.

/7/ CPE and CEPEMAR Servicos de Meio Ambiente*: Caracterização Hidrodinâmica do Canal de Acesso a Barra do Tomba – Relatório Técnico CPM RT 106/06*, Report to Aracruz Celulose S.A., April 2006.

/8/ On the Circulation of a Coastal Channel within the Abrolhos Coral-Reef System – Southern Bahia, Brazil. Paper by G.C. Lessa and M. Cirano published in Journal of Coastal Research, Special Issue 39, 2004.

/9/ CPE and CEPEMAR Servicos de Consultoría em Meio Ambiente Ltda.: Second Opinion: Evaluation of Sedimentation Rates, Disposal Sites and Dredging Alternatives for the Caravelas Navigation Channel, Technical Report CPM RT 235/06, Rev 00, report to Aracruz Celulose S.A., July 2006.

D R A W I N G S

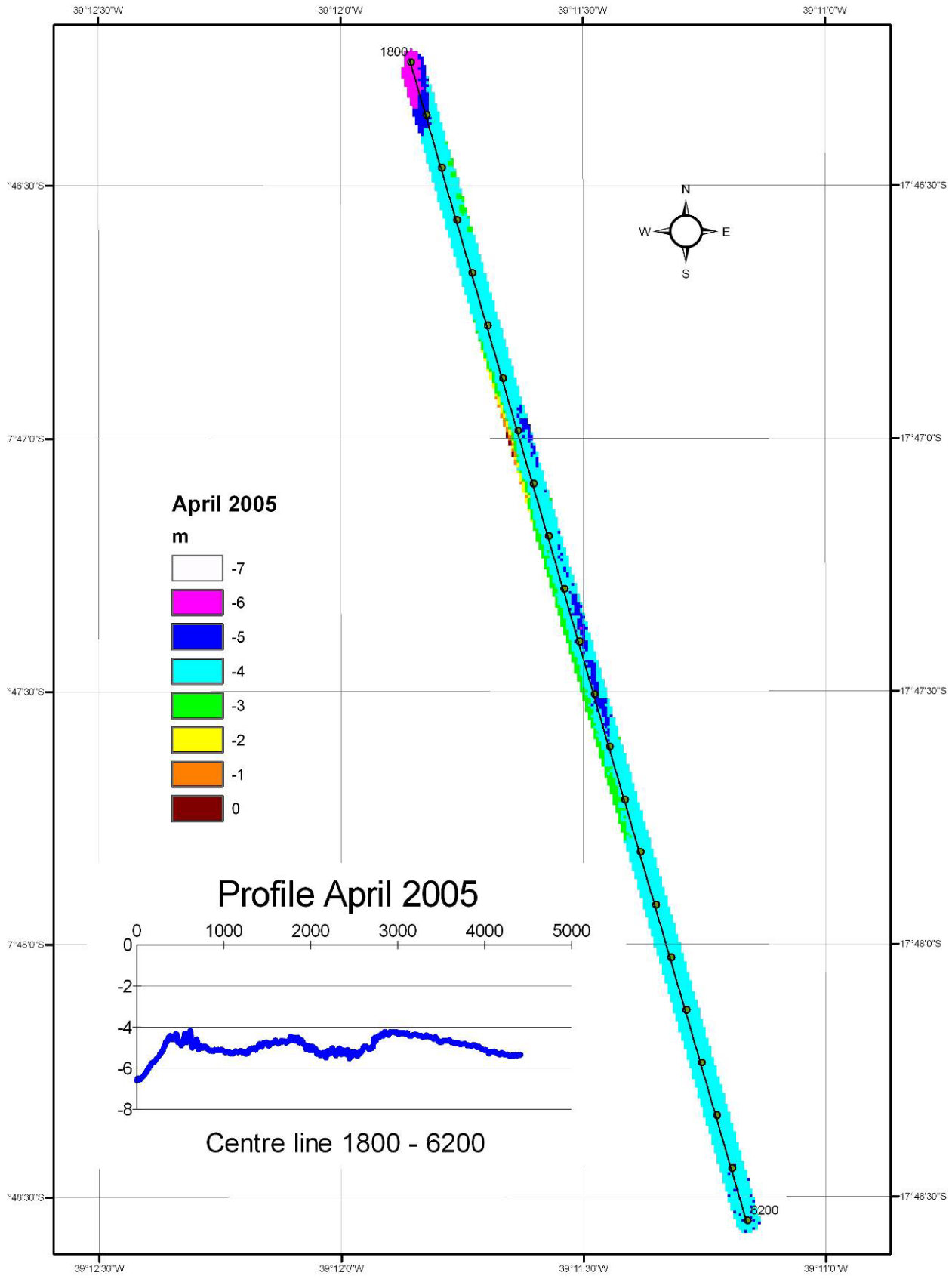

Dwg. 1 *Digital Terrain Model (DTM) of April 2005 survey. The colours indicate areas with levels above the values shown next to the legend.*

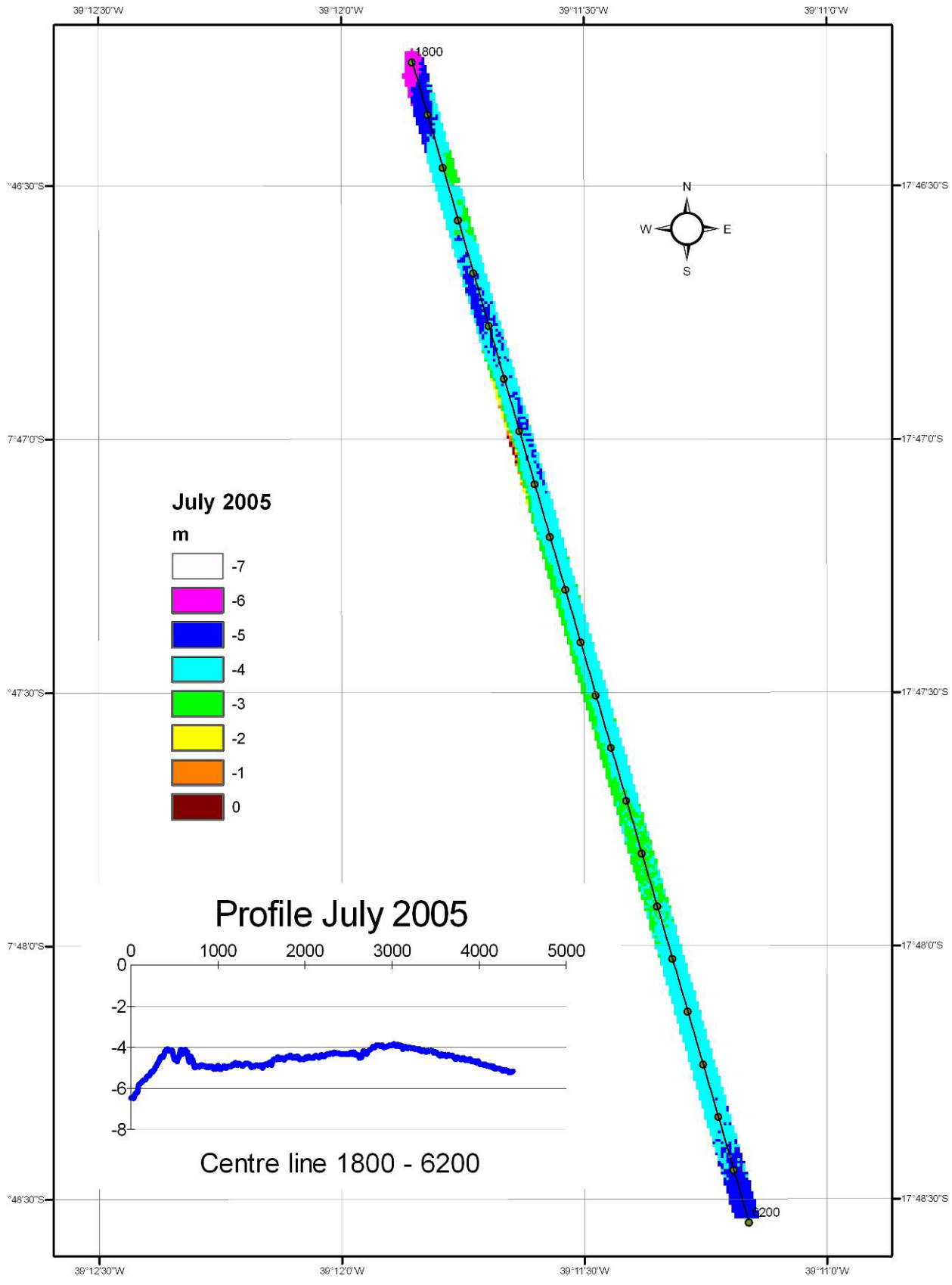

Dwg. 2 DTM of July 2005 survey.

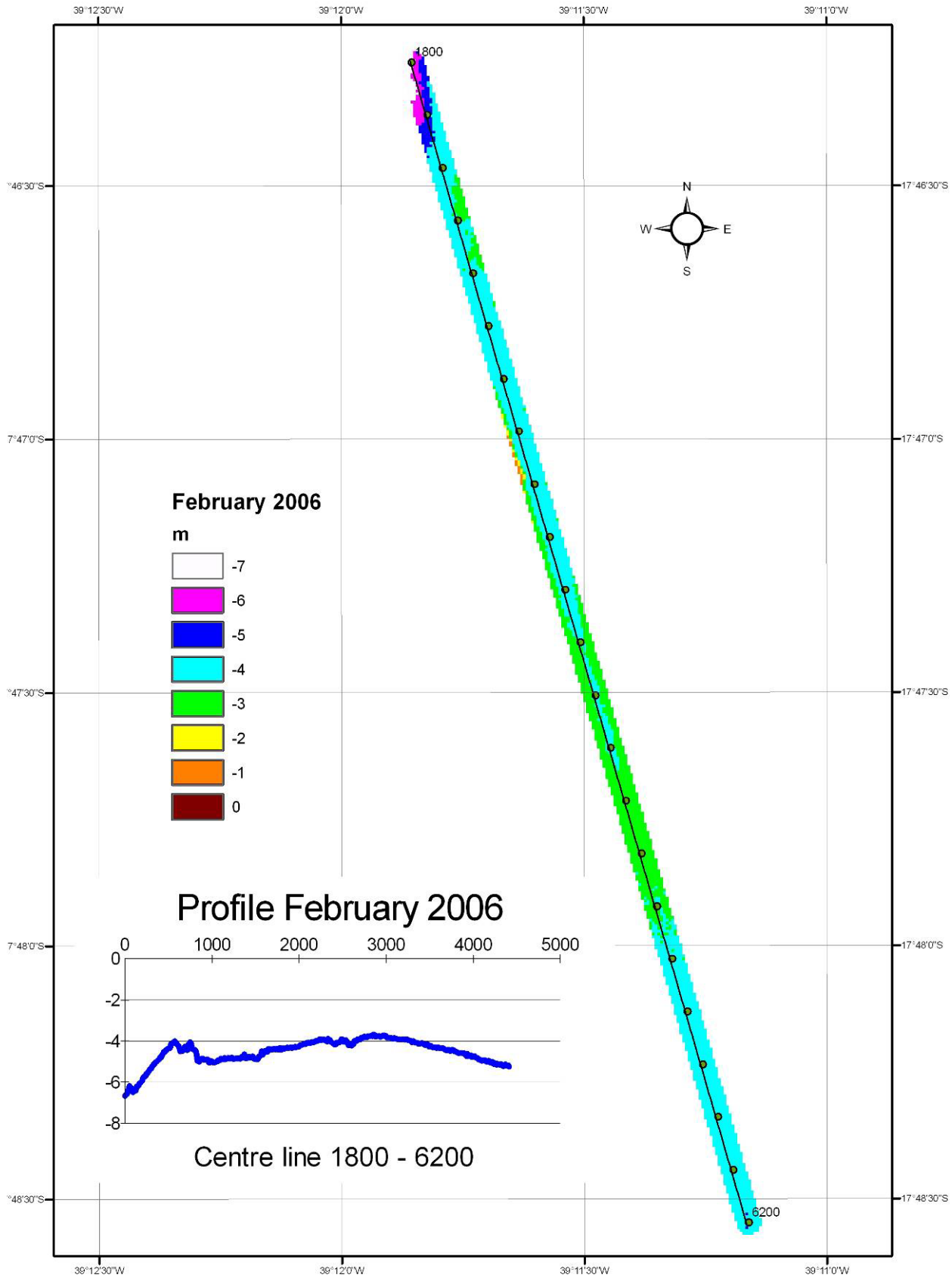

Dwg. 3 DTM of February 2006 survey.

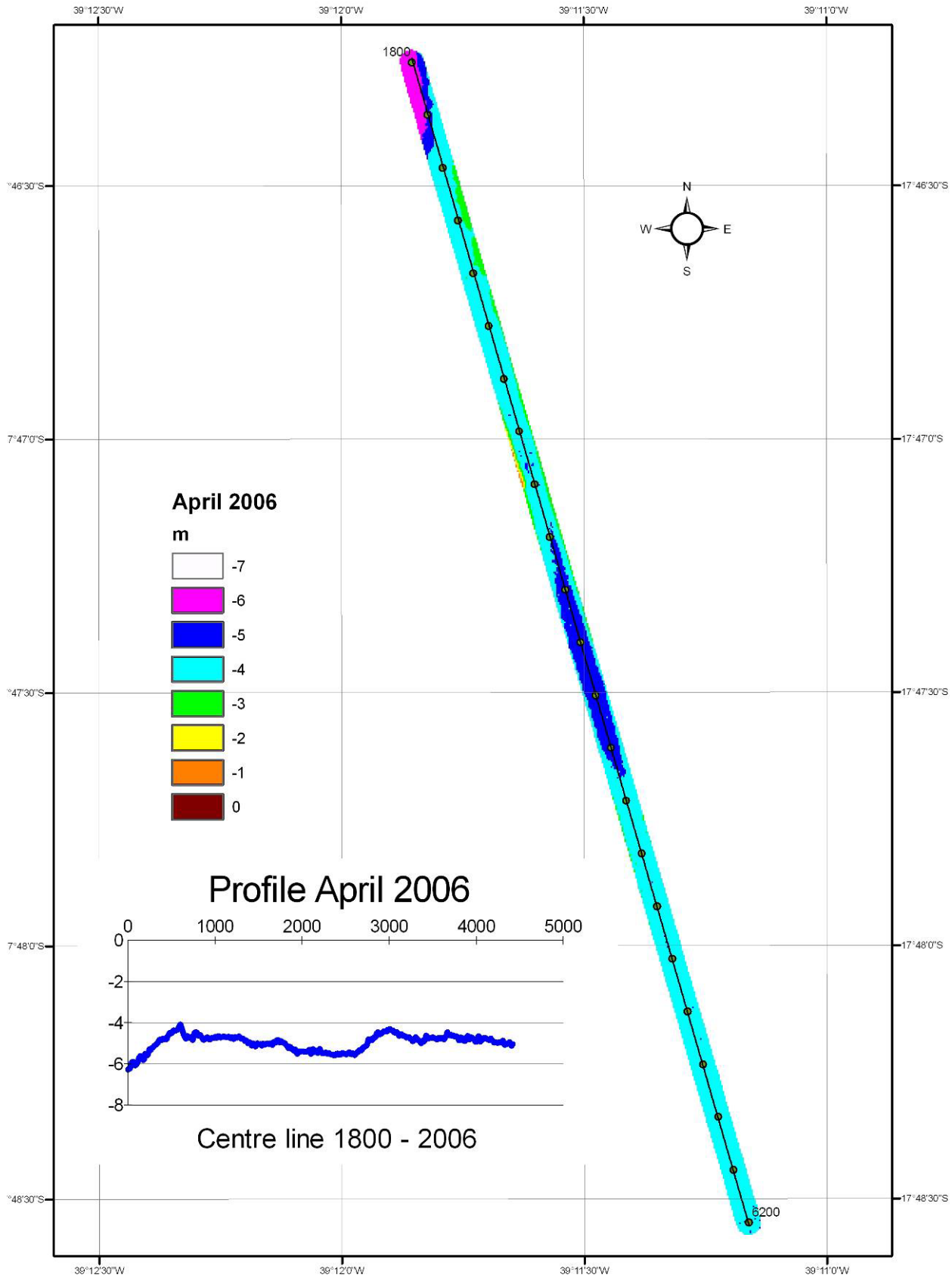

Dwg. 4 DTM of April 2006 survey.

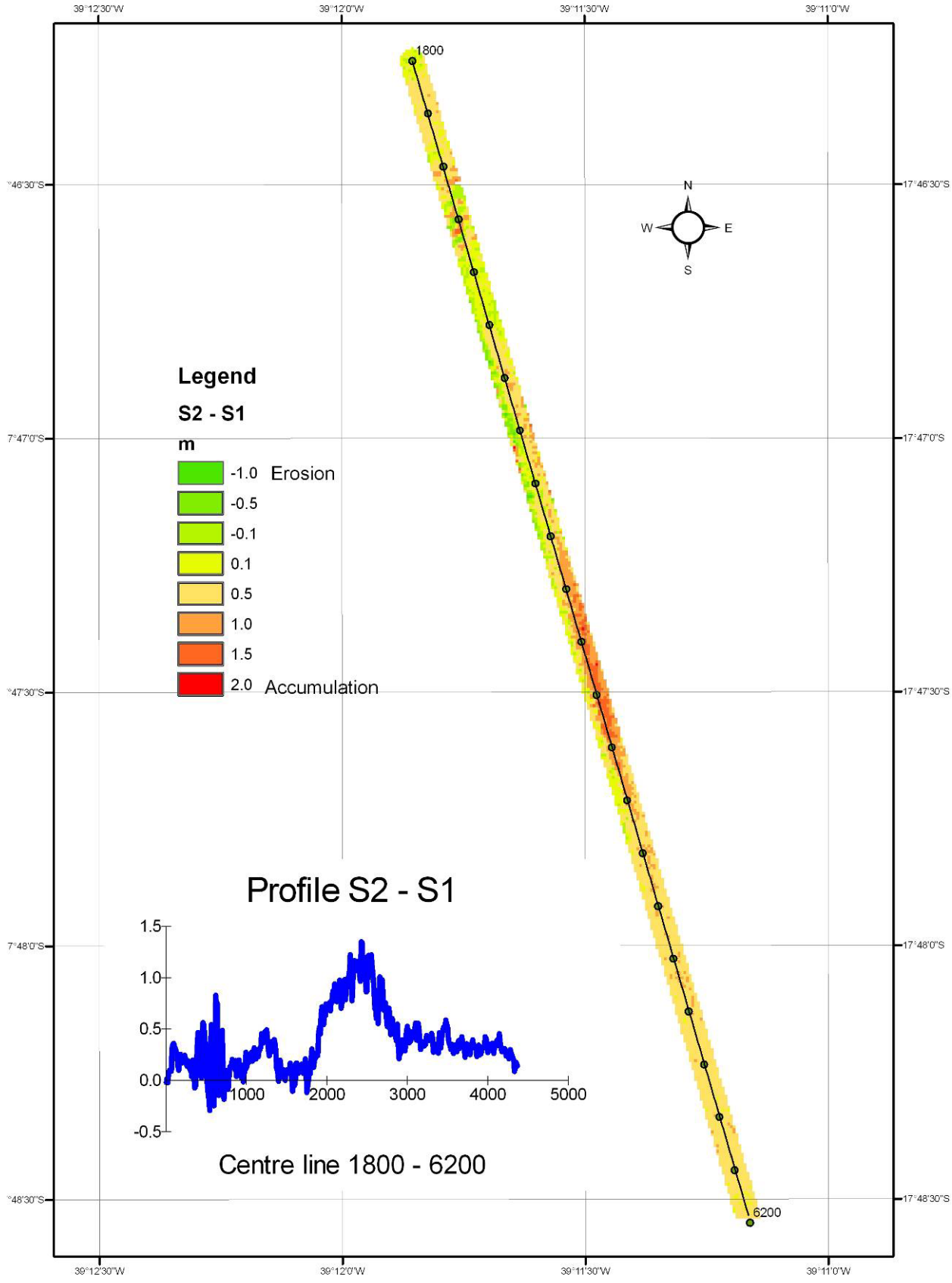

Dwg. 5 *Bathymetry S2-S1. Positive values indicate accumulation and negative erosion. The colours represent areas with level change above the indicated value (yellow represents accumulation between 0.1 and 0.5 m).*

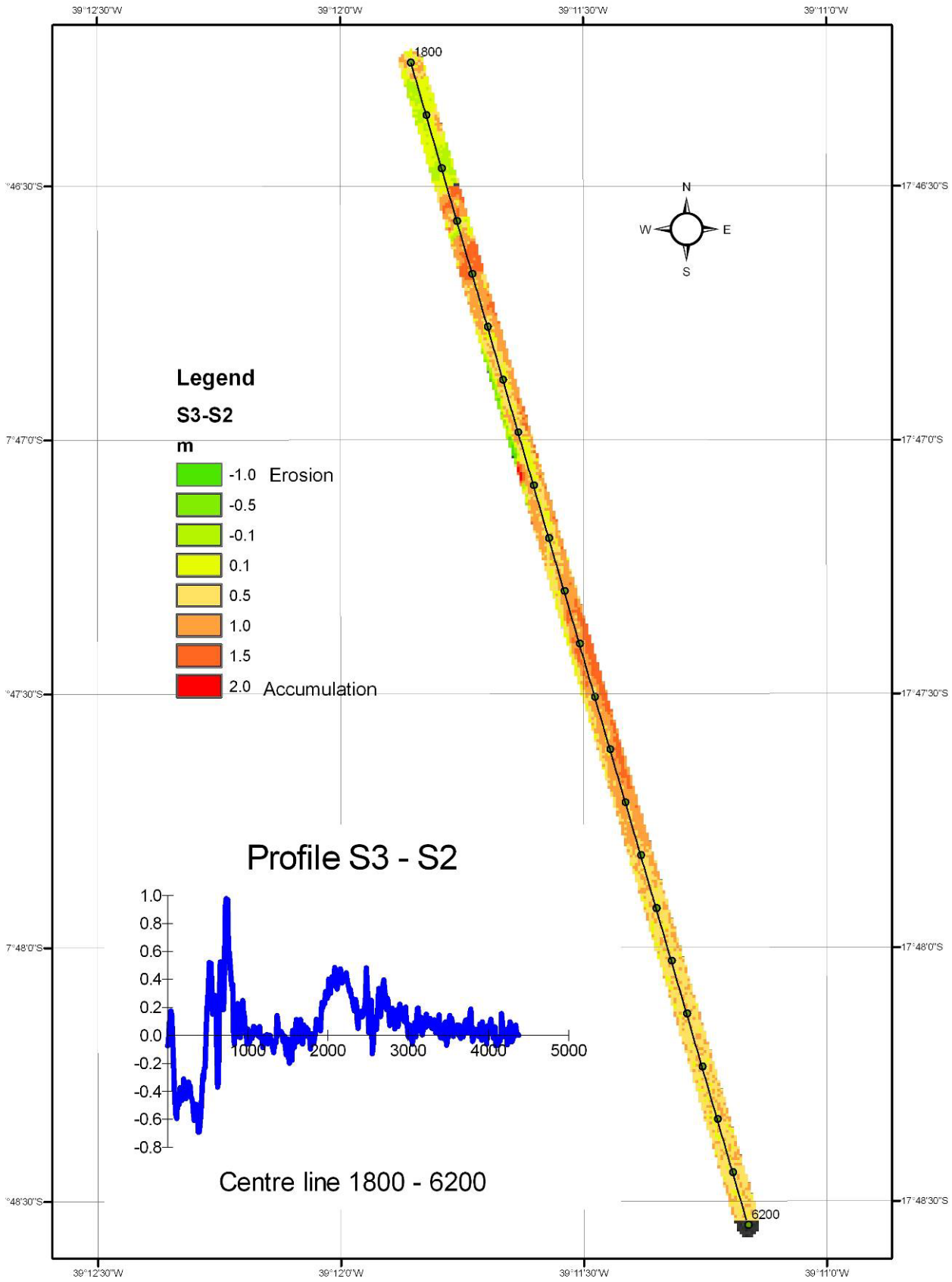

Dwg. 6 Bathymetry S3-S2. Positive values indicate accumulation and negative erosion.

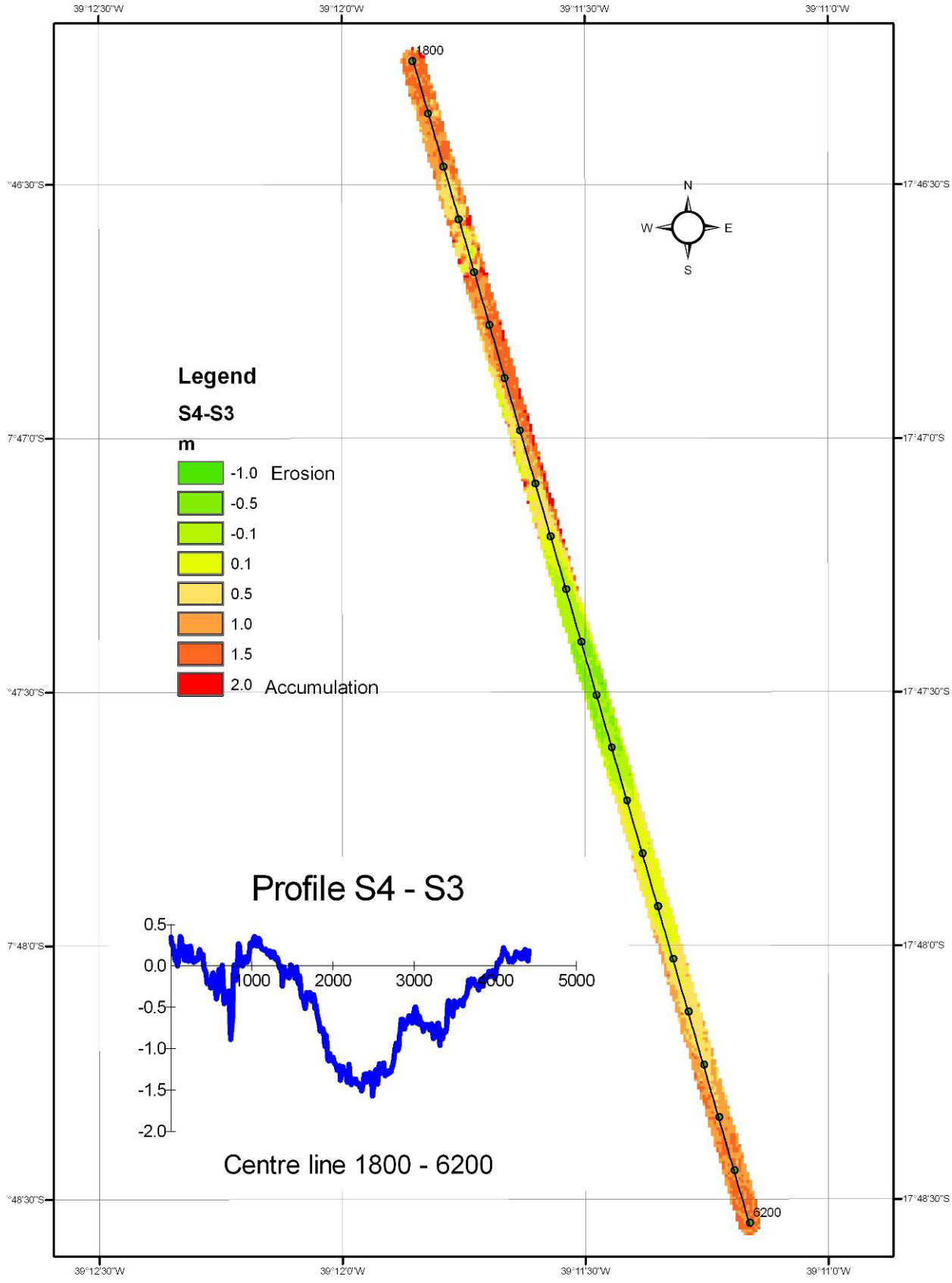

Dwg. 6 Bathymetry S4-S3. Positive values indicate accumulation and negative erosion.

A P P E N D I X A

Action Plan

Optimisation of Maintenance Dredging

Prepared by
CPE, CEPEMAR and DHI
26 October 2005

ACTION PLAN

Monitoring Program

1. Bathymetry

Frequency: 2 per year 1 before and one after annual dredging event
Spacing: Finer spacing inside channel (similar to past work, 20 m), coarser spacing outside (similar to CEPEMAR July 2005 survey, 50 m).
Coordinate System: UTM, ZONE 24S, WGS84, needs to be consistent between CEPEMAR and ENTERPA
Objective: Asses channel maintenance volumes, check dredging operations, numerical model update, shoal migration patterns & general area morphology change
Obs. Include alternate channel & shoals, refer to tide gauge (CEPEMAR exercise between gauge & S4), check positioning against Enterpa

2. Sampling

Frequency: 1 before next dredging event, samples inside the channel only
Spacing: Similar to CEPEMAR July 2005. From stations 2600 and 4200
Coordinate System: UTM, ZONE 24S, WGS84, needs to be consistent between CEPEMAR and ENTERPA.
Obs: Conduct it soon after the bathymetry
Objective: Analyze types & origin of sediments that are shoaling the channel without intervention from dredging

3. Hydrodynamic data (Waves, tides, currents)

Frequency: Continuous
Objective: Modelling verification/calibration, boundary conditions & and analysis of coastal processes in case of unexpected events (justify to IBAMA if behaviour not predicted has occurred)
Optimal Location: In front of the end of the navigation channel near buoy 2
(~UTM 8031300, 479950)

4. Wind

Frequency: Continuous
Objective: Numerical model boundary conditions

Additional Studies

1) Update of modelling with new bathymetry & sampling (select 8 to 12 model scenarios to be simulated)

2) Evaluate alternate channel route closure
   2a. Determine impact of alternate route in navigation channel flow speeds and sedimentation
   2b. Evaluate if interventions will be beneficial and what level of intervention is needed

3) Traps & Overdredge
   3a. evaluate impact on total sedimentation amounts, channel sedimentation and sediment distribution for both sand and mud (MIKE21 ST, MT)

Members involved
DHI – Numerical modelling & data verification
CEPEMAR- Supply data as required
CPE – Comment on scenarios selection and result interpretation

Alternatives

(1) Continue with current procedure (do nothing)
1a. Update maintenance volumes & costs using results from 2nd opinion and updated modelling

Members involved: DHI to provide background information to CPE/CEPEMAR, both parties to participate in results interpretation and conclusions

(2) Consider Traps + Overdredge
2a. Evaluate results of modelling in terms of capital dredging and long-term maintenance costs, navigation constraints and dredging interval optimization
2b. Compare one annual dredging event (overdredge) with multiple smaller dredging events in terms of channel sedimentation volumes

Members involved: DHI to provide background information to CPE/CEPEMAR, both parties to participate in results interpretation and conclusions

(3) Improved dredging technology

3a. Pipeline dredging (disposal one side or both sides)

- Engineering feasibility: Dimensions, dredge specs, pipeline length, and pipeline route, dredge mobility, conceptual design of spoil area,
- Discharge point selection: Modelling of behaviour of dredge spoil overflow, alongshore current reversal and seasonal current variations to select optimal discharge point location and number
- Evaluate costs: initial investment, capital dredging, long-term maintenance costs (10-20 yr perspective)

Members involved: CPE/CEPEMAR to conduct engineering feasibility, DHI to conduct modelling studies for discharge point selection, JAAKKO POYRY to provide Brazilian cost perspective for economic analysis. CPE and DHI to participate in results interpretation and conclusions

3b. **Aracruz purchase a hopper**

- Assessment of Operational practice to determine the capacity/dimensions of the dredge (1, 2 or 3 facilities)
- Assessment of Operational Costs (crew, fuel, maintenance of equipment *etc.*)
- Initial investment in dredge vessel purchase and associate land-docking facilities

Members involved: CPE/CEPEMAR to conduct engineering feasibility, DHI to conduct modelling studies for discharge point selection, JAAKKO POYRY to provide Brazilian cost perspective for economic analysis and operational issues. CPE and DHI to participate in results interpretation and conclusions

Final Report & Discussion meeting

Objective: Report study findings
Members Involved: CPE/CEPEMAR, DHI, JAKKO POYRY

a. Results Presentation meeting and discussions
Objective: Select preferred alternative

b. Prepare & present preferred alternative to IBAMA

Proposed Preliminary Schedule

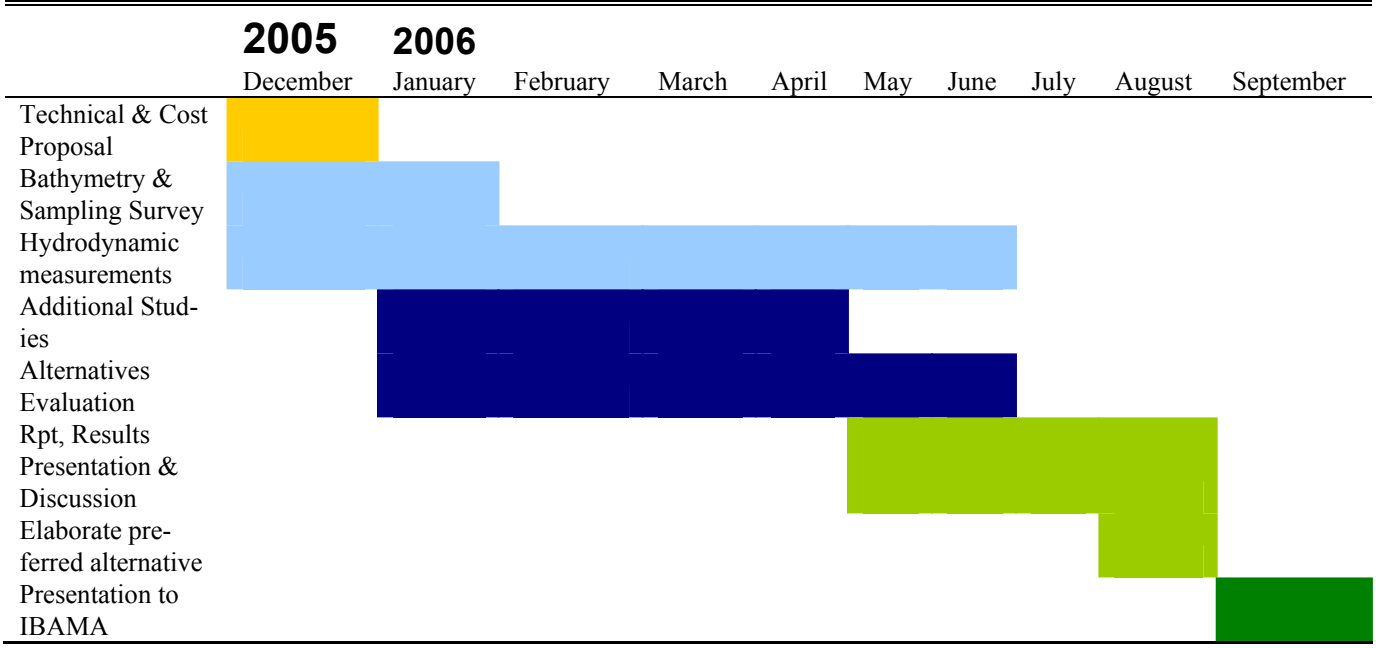

A P P E N D I X B

Scope of Work

SCOPE OF WORK

STUDY BACKGROUND

During the meeting in Vitoria on 26 October 2005 Aracruz Celulose S.A. requested DHI, CPE and CEPEMAR to prepare an Action Plan for monitoring and additional studies with the aim of presenting recommendations for the maintenance of the dredged channel for the Caravelas Terminal. The overall aim is to support the application to IBAMA of a license to maintain the required water depth in the channel. This application will be submitted to IBAMA in September 2006.

The Action Plan comprises a monitoring programme, additional studies and assessment of alternative dredging strategies.

The present proposal, prepared by DHI, presents a work programme for additional studies based on modelling of the sediment transport processes in and around the Caravelas channel.

The scope of this additional modelling is:

1. Update of modelling with new bathymetry and sediment sampling results.

2. Evaluate closure of alternate channel route:

    - Determine the impact of the alternate route on flow speeds and sedimentation in the navigation channel.

    - Evaluate if interventions will be beneficial and what level of intervention is needed.

3. Traps and overdredge: evaluate the impact on total sedimentation amounts, channel sedimentation and sediment distribution for both sand and mud. This task will provide information for optimisation of dredging procedures such as the frequency of dredging and optimal channel layout.

Re 1) For the benefit of the studies a new flexible mesh version of the MIKE 21 models will be applied for this modelling. This greatly enhances the efficiency of modelling and allows a much larger area to be included without compromising on the need for high resolution around the channel and the inlet. The model will be set up with improved tidal boundary conditions based on water level predictions at Cumuruxatiba, Nova Viçosa and Abrolhos.

The model will include the effects of wind and waves and will be calibrated and verified against water level and current data from the present measuring stations #106 and #506 as well as at the Terminal in Rio Caravelas. The model is able to describe erosion, transport and sedimentation patterns of both mud and sand. The model will be set up for these purposes and validated against information on deposition patterns from bathymetric soundings of the channel.

Re 2) After verification of the model various scenarios of artificial closure of the alternate channel will be studied. These scenarios will describe to what extent the development of the alternate route reduces the flushing through the dredged channel and

whether these effects, if any, can be mitigated either by discharging dredged sand on the bottom of the alternate channel or closing it by a permanent rock mound structure.

Re 3) Various maintenance methods have been discussed and will be subject to study by the mathematical model. In order to create reservoirs for sedimentation so that a sufficient water depth can be maintained in periods between dredging it may be considered to use a combination of sand traps and overdredging. Experience from the field and from model studies is that both sand traps and overdredging will result in larger total sedimentation volumes. Thus, the objective of this part of the modelling would be to reach an economically optimal dredging strategy.

DHI's proposal includes:

- Modelling.
- Specification of data requirements (DHI costs only).
- Results interpretation and review of CPE's dredging study.
- DHI participation in results presentation to Aracruz Celulose S.A. and IBAMA.

A P P E N D I X C

Description of applied Numerical Model MIKE 21 FM

ARACRUZ CELULOSE S. A.

TAXAS DE SEDIMENTAÇÃO E ALTERNATIVAS DE DRAGAGEM PARA O CANAL DE ACESSO A BARRA DO TOMBA, CARAVELAS, BA

Relatório Técnico

CPM RT 415/06

Novembro/06 | Revisão 00

CEPEMAR – Serviços de Consultoria em Meio Ambiente Ltda
Av. Carlos Moreira Lima, 90, Bento Ferreira, CEP 29050-650 – Vitória – ES
PABX: (27) 2121-6500 – FAX: (27) 2121-6528
E-mail: cepemar@cepemar.com

CONTEÚDO

FIGURAS

TABELAS

1
Introdução

O presente estudo foi desenvolvido em parceria pelas empresas CEPEMAR e COASTAL PLANNING ENGINEERING (CPE) com o objetivo de avaliar a natureza e as taxas de deposição dos sedimentos ao longo do canal de acesso à Barra do Tomba. Além disso, avaliaram-se novas alternativas de dragagem, incluindo a possibilidade de disposição de parte do material dragado em terra e o uso de outros tipos de equipamentos de dragagem.

2
Considerações Iniciais

A área de estudo localiza-se na foz do rio Caravelas, entre a Ponta da Baleia e Ponta do Catoeiro, no município de Caravelas, extremo sul do Estado da Bahia (Figura 2-1). O canal do Tomba tem sido dragado anualmente desde fevereiro de 2002 com o objetivo de estabilizar o canal de navegação e permitir o acesso ao terminal de barcaças oceânicas da Aracruz Celulose (ARCEL) em Caravelas.

Cabe destacar, que o presente estudo faz parte do "Projeto Segunda Opinião", o qual teve origem em 2004, quando CEPEMAR e CPE iniciaram esta parceria e realizaram a primeira avaliação do problema de assoreamento no canal. Os primeiros resultados, apresentados em CEPEMAR-CPE (2005a), sugeriam que cerca de 200.000 m^3 de sedimentos (+/- 50.000 m^3) precisavam ser removidos anualmente do canal do Tomba de forma a manter as águas navegáveis. Entretanto, questões sobre a origem dos sedimentos e os volumes anuais que se acumulam ao longo do canal ainda persistiram, tendo sido necessário a realização de uma nova análise, com levantamentos de campo adicionais. Nesta segunda etapa, cujos resultados encontram-se em CEPEMAR-CPE (2005b), confirmou-se que a taxa anual de sedimentação de 200.000 m^3 (+/- 50.000 m^3) era adequada, além disso concluiu-se que cerca de 30% do material acumulado após a dragagem era composto de areia e 70% de lama, sendo que a maior parte da areia acumula-se entre as estações 30+00 e 40+00 e que a sedimentação ativa de lama ocorre entre as estações 40+00 e 48+00 (ver Figura 2-1).

CEPEMAR-CPE (2005b) sugeriram então duas providências para melhorar o desempenho das dragagens no local: (1) modificação da estratégia de dragagem, com uso de uma draga de sucção-e-recalque e transferência de parte do material para terra; (2) avaliação da possibilidade de utilização do canal natural (alternativo) que existe a sudoeste do atual canal de navegação.

Após a realização do estudo de CEPEMAR-CPE (2005b) uma nova dragagem ocorreu entre fevereiro e março de 2006 e 4 (quatro) novos levantamentos batimétricos foram conduzidos, sendo 3 executados pela empresa Belov Engenharia (novembro de 2005, fevereiro de 2006 e abril de 2006) e 1 batimetria foi executada por CEPEMAR (2006a) em fevereiro de 2006. Adicionalmente, novas amostras de sedimentos foram coletadas ao longo do canal em fevereiro de 2006 (CEPEMAR 2006b). Realizou-se também a aquisição de dados hidrodinâmicos (CEPEMAR 2006c), os quais foram repassados ao Danish Hydraulic Institute (DHI) para execução de modelagem computacional e simulação dos processos de sedimentação ao longo do canal (ver DHI, 2006).

Com base nos novos dados de batimetria e sedimentologia, conjuntamente com a análise da modelagem computacional, a CEPEMAR e a CPE passaram para a terceira etapa do Projeto Segunda Opinião (ver CEPEMAR-CPE, 2006) e realizaram a reavaliação das necessidades de dragagem para a concretização da abertura definitiva do canal de acesso em profundidades seguras à navegação, bem como para a manutenção do canal. Além disso, realizou-se a proposição de diferentes estratégias de dragagem.

Os resultados aqui apresentados consistem, portanto, numa síntese e integração dos dados obtidos por CEPEMAR-CPE (2006) e DHI (2006), com o propósito de enfatizar as principais conclusões obtidas nos estudos realizados e os futuros rumos que a ARCEL deve seguir em relação as estratégias de dragagem ao longo do canal do Tomba.

Figura 2-1: Localização do canal de navegação, local de descarte, Ilha Barra do Sul e terminal de barcaças de Caravelas. Fonte: CEPEMAR-CPE (2006)

3
Taxas de Sedimentação e Requerimentos de Dragagem

3.1 CONDIÇÕES DO CANAL ENTRE JULHO DE 2005 E FEVEREIRO DE 2006

Dados batimétricos foram obtidos por CEPEMAR (2006a) entre os dias 14 e 20 de fevereiro de 2006 ao longo do canal do Tomba e adjacências. Estes dados foram comparados com a batimetria de julho de 2005. A Figura 3.1-1 evidencia que o canal alternativo, a sudoeste do canal de navegação, manteve-se presente e que na parte central, entre as estações 30+00 e 36+00, existem bancos, relativamente grandes, muito próximos ao canal. Estes bancos marginais ocuparam uma área maior em fevereiro de 2006 em relação a julho de 2005.

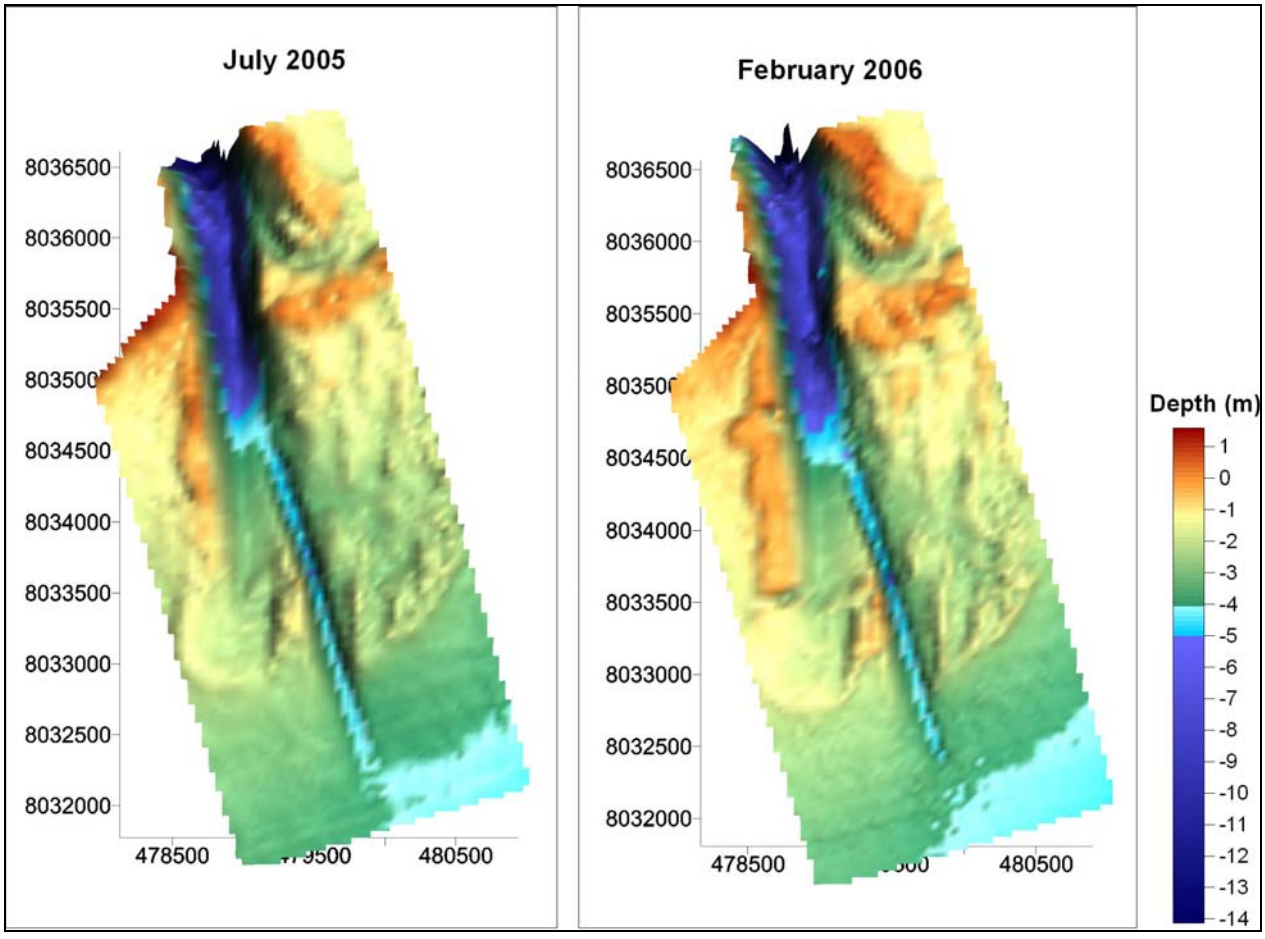

Figura 3.1-1: Mapas tridimensionais para comparação visual entre julho de 2005 e fevereiro de 2006. Fonte: CEPEMAR-CPE (2006)

3.2 CONDIÇÕES DO CANAL EM ABRIL DE 2006

De forma a avaliar quantitativamente e qualitativamente as condições do canal após a dragagem executada entre fevereiro e março de 2006 realizou-se a comparação dos dados batimétricos obtidos em abril de 2006 em relação ao projeto de dragagem concebido por CEPEMAR-CPE (2006):

- Profundidade de dragagem = 5 m abaixo do 0 da DHN;
- Overdredge = 0.3m;
- Largura do canal = 90m;
- Talude = 1 vertical: 2 horizontal.

Com base nos resultados obtidos identificaram-se 5 (cinco) distintos segmentos ao longo do canal.

♦ SEÇÕES 0 A 20+00

Este segmento possui profundidades e largura suficiente para a navegação segura.

♦ SEÇÕES 20+00 A 30+00

As profundidades neste segmento variam entre 4 m e 5 m de profundidade no eixo central do canal, mas algumas zonas marginais possuem profundidades reduzidas (3 m). Mesmo após a dragagem as profundidades continuaram baixas para a navegação segura, inferiores ao projeto conceitual, que determina profundidades de 5 m em todo canal.

♦ SEÇÕES 30+00 A 37+00

Este segmento em particular é a zona onde os bancos marginais “estrangulam” o canal, sendo a largura inferior a 90 m (Figura 3.2-1), comprometendo a navegação em qualquer situação de vento que provoque abatimento superior a 15 graus na embarcação. Sedimentos arenosos predominam nesta zona havendo uma sedimentação proveniente de sudoeste. No eixo central do canal as profundidades são geralmente de 5 m, mas extremamente baixas na margem sudoeste (1 a 3 m). Mesmo após a dragagem as profundidades e largura do canal continuaram inferiores ao projeto conceitual.

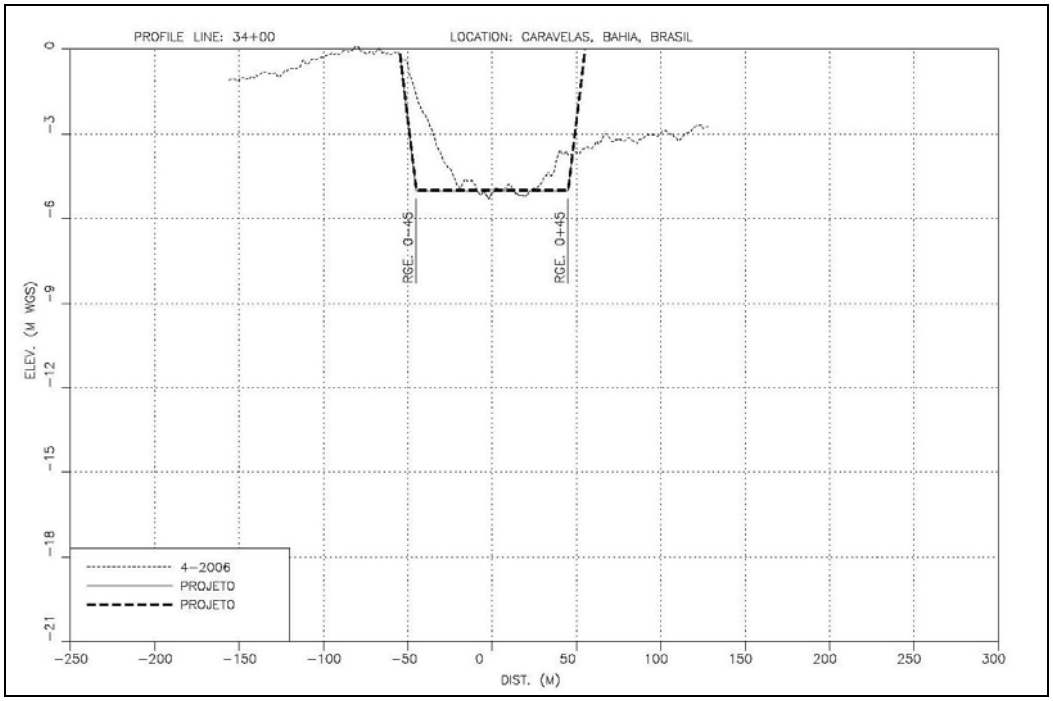

Figura 3.2-1: Comparação entre a batimetria de abril 2006 e o projeto conceitual (90 m de largura e 5 m de profundidade) ao longo da seção 34+00. Fonte: CEPEMAR-CPE (2006)

- **SEÇÕES 37+00 A 55+00**

A análise visual e volumétrica indica que a maior parte da dragagem ocorreu neste segmento. Entretanto, mesmo após a dragagem, as profundidades do canal continuaram inferiores ao projeto conceitual (entre 4,5 e 5 m). Nesta zona predomina a sedimentação de lama.

- **SEÇÕES 55+00 A 62+00**

Este segmento é caracterizado por um fundo plano, com profundidades geralmente em torno de 5 m, não havendo aparente risco a navegação.

3.3 VARIAÇÕES DE VOLUMES E TAXAS DE SEDIMENTAÇÃO

Com base nos dados extraídos dos 4 levantamentos batimétricos existentes calculou-se as alterações de volume ao longo do canal para diferentes períodos (Figura 3.3-1).

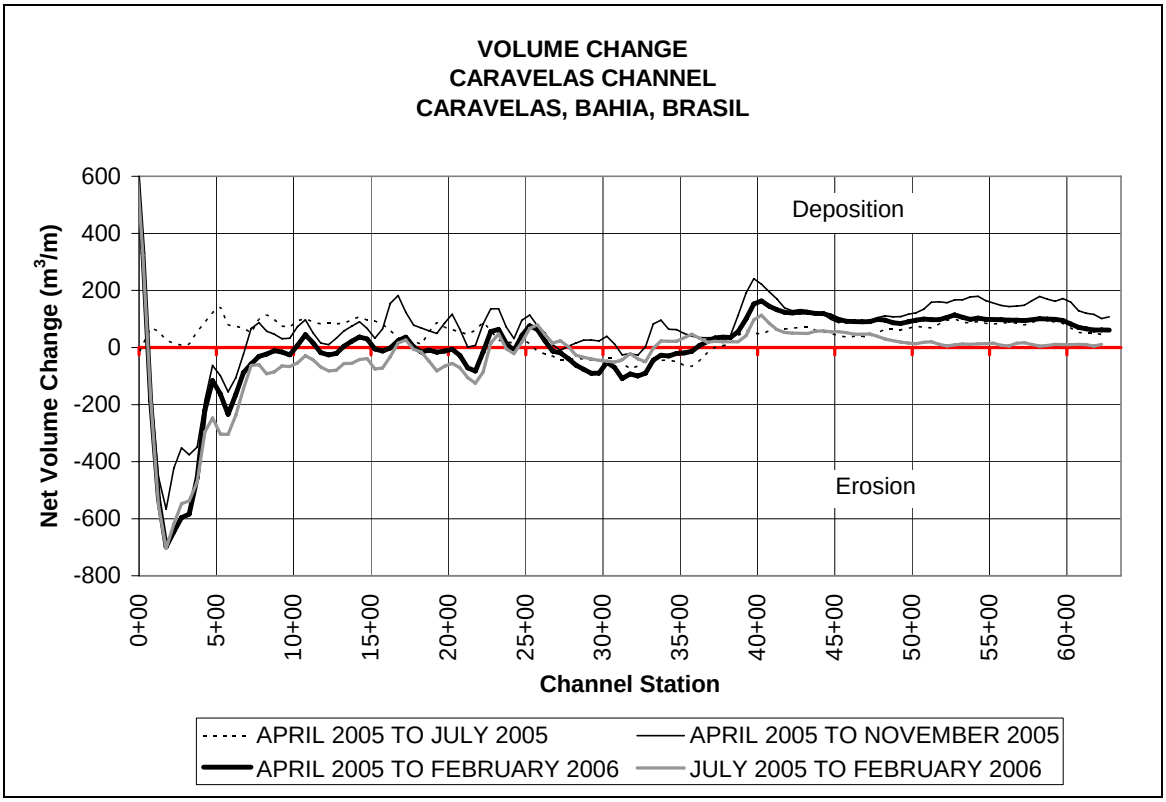

Figura 3.3-1: Variações líquidas de volume ao longo do canal em diferentes períodos. Fonte: CEPEMAR-CPE (2006)

Análises das variações de volume entre julho de 2005 e fevereiro de 2006 (Figuras 3.3-1 e 3.3-2) indicam haver maior assoreamento entre as estações 17+00 a 26+00 e 33+00 a 63+00. Estas são as zonas onde geralmente as dragagens são requeridas, mas para uma análise completa consideraram-se as variações entre as estações 17+00 e 63+00. Para este trecho, a deposição total de material ao longo do canal entre julho de 2005 e fevereiro de 2006 foi de 52.000 m^3, o que equivale a uma taxa anual de 99.300 m^3/ano. Para o período de abril de 2005 a fevereiro de 2006 a taxa de sedimentação no setor aumenta para 135.000 m^3, equivalente a uma taxa anual de 160.900 m^3/ano.

O uso do período entre abril de 2005 e fevereiro de 2006 é mais indicado, pois contabiliza também os valores de deposição imediatamente após o final da dragagem executada no ano de 2005, quando as taxas de sedimentação ainda eram elevadas, pois o canal ainda encontrava-se sob os efeitos da dragagem, buscando um “equilíbrio dinâmico”, o qual só tende a ser obtido alguns meses após o término das operações (ver Figura 3.3-3), quando então ocorre a diminuição e estabilização das taxas de sedimentação.

Observa-se, portanto, que as taxas de sedimentação encontradas para o período entre 2005 e 2006 (160.900 m^3/ano) no trecho compreendido entre as estações 17+00 e 63+00 são inferiores aos valores encontrados na primeira e segunda etapa do Projeto Segunda Opinião. Apesar disto, a taxa atualmente encontrada encontra-se na mesma ordem de grandeza do valor anterior, sendo recomendado por CEPEMAR-CPE (2006) a **manutenção do valor de 200.000 m^3/ano +/- 50.000 m^3** como forma de manter uma **margem de segurança aceitável**.

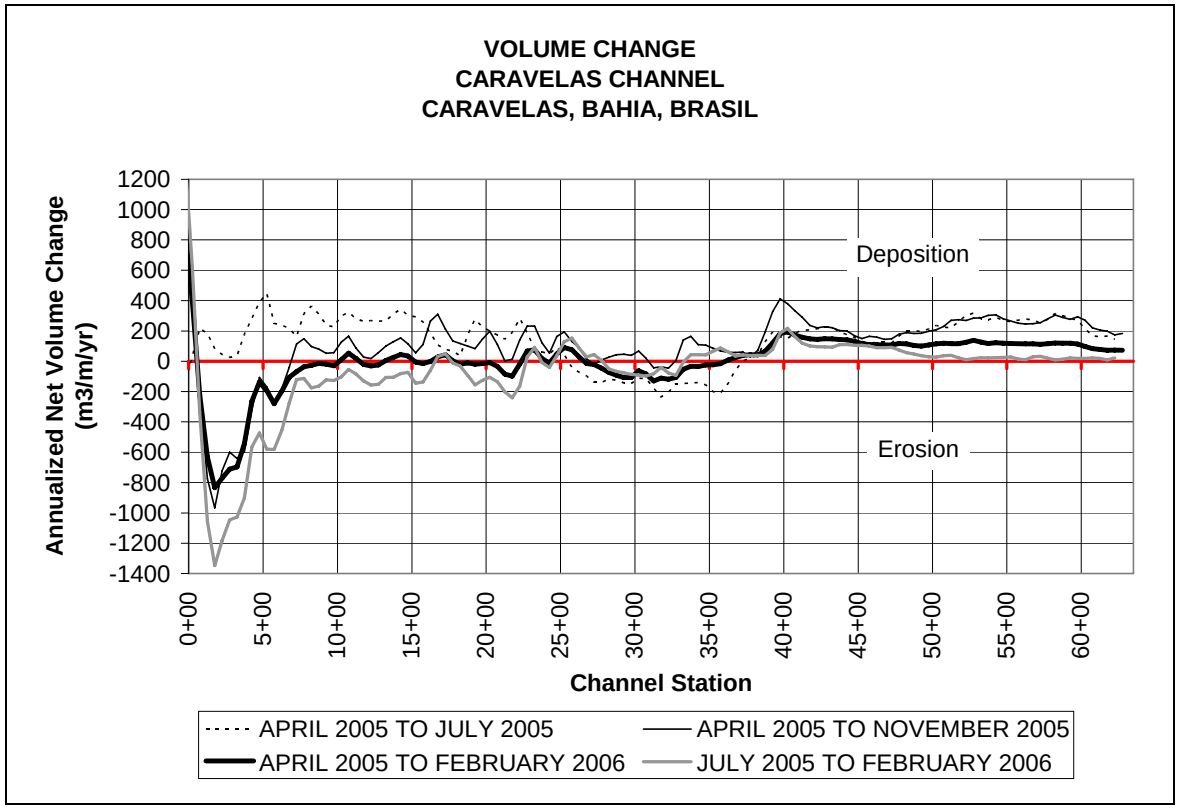

Figura 3.3-2: Variações anuais líquidas de volume ao longo do canal em diferentes períodos.
Fonte: CEPEMAR-CPE (2006)

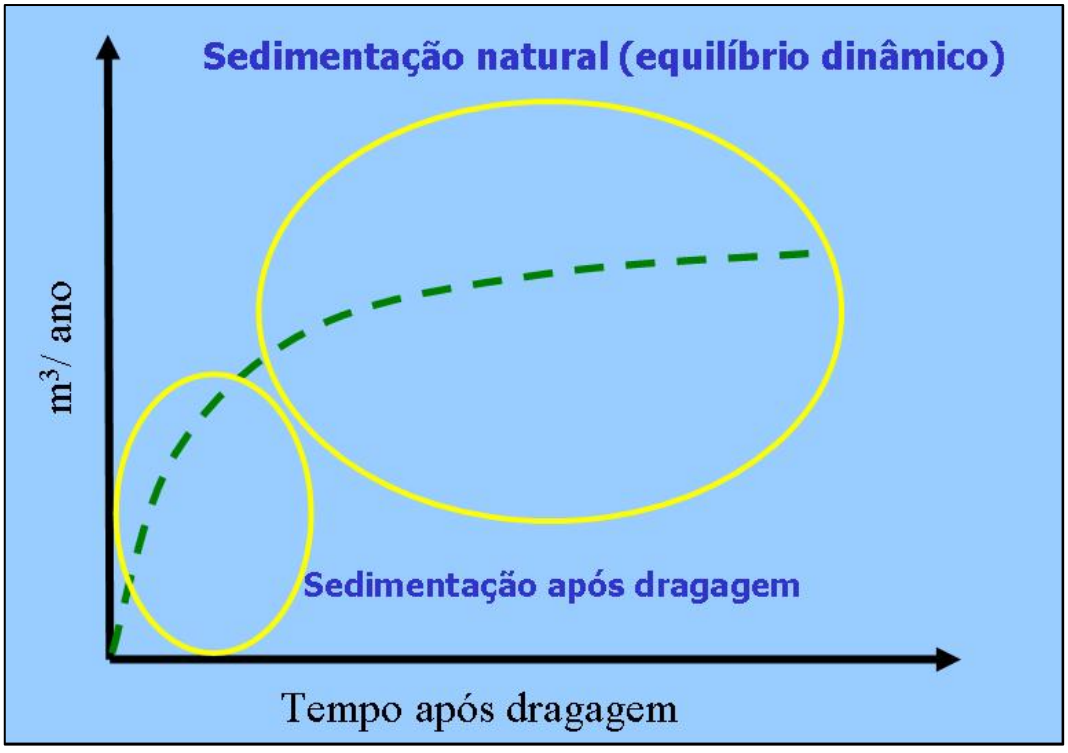

Figura 3.3-3: Evolução da taxa de sedimentação ao longo do tempo.

Os resultados acima indicam uma discrepância existente entre a situação real e o que foi inicialmente previsto no projeto conceitual de dragagem elaborado por DHI (2000), o qual previa uma taxa de sedimentação anual da ordem de 65.000 m^3/ano.

Baseando-se nas estimativas iniciais de DHI (2002) concebeu-se que haveria uma dragagem de manutenção a cada dois anos no valor de 130.000 m^3. Esta discrepância é explicável e tem sido observada em diferentes projetos de engenharia costeira, cabendo citar abaixo as principais causas que levaram a uma subestimação nas taxas de sedimentação ao longo do canal e conseqüentemente na freqüência de dragagens de manutenção:

- Os dados iniciais foram estimados com base em simulações obtidas através de modelos numéricos. Na ocasião, não existia uma série de dados que permitisse calibrar o modelo, em especial, com relação a sedimentação da lama, a qual hoje sabe-se ser muito mais ativa do que inicialmente previsto;

- As simulações de DHI (2002) foram elaboradas desconsiderando-se o talude do canal de navegação, o qual se apresenta naturalmente entre 1:6 e 1:10. Como resultado, as simulações iniciais não contemplaram as áreas adjacentes ao canal, as quais possuem uma mobilidade sedimentar tão alta quanto o próprio canal. Por conta disto os valores simulados das taxas de sedimentação apresentaram-se menores que os reais. A Figura 3.3-4 apresenta esquema do canal de navegação com diferentes taludes e profundidades projetadas.

- Desde o início dos serviços de dragagem no canal do Tomba até hoje, o projeto de engenharia vislumbra a construção de um canal com profundidade = 5 m e largura = 90 m. Tal situação nunca foi atingida por completo e, assim, o canal nunca trabalhou com a eficiência hidráulica necessária para não permitir altas taxas de assoreamento.

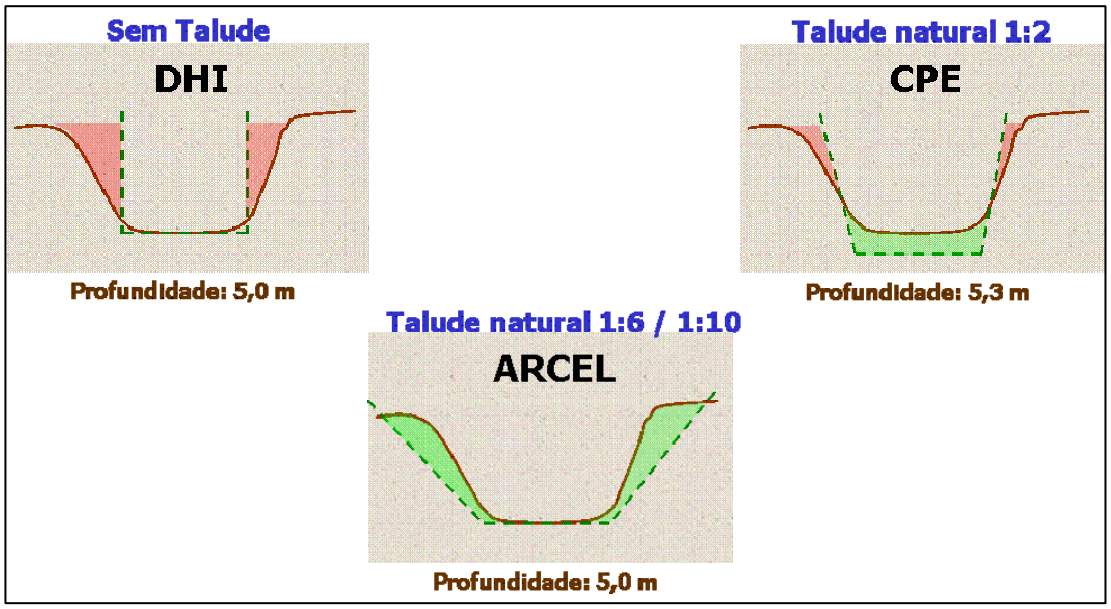

Figura 3.3-4: Esquema do canal de navegação com diferentes taludes e profundidades projetados por DHI, CPE-CEPEMAR e situação natural (ARCEL).

Cabe reforçar, que em função dos conhecimentos e dados acumulados ao longo dos últimos anos, com intenso monitoramento do local, foi possível uma modelagem mais acurada do comportamento hidrodinâmico do canal. Dessa forma, a modelagem atual (ver DHI; 2006) difere substancialmente da inicial principalmente no comportamento dos sedimentos lamosos, os quais são predominantes ao longo do canal do Tomba. À época da simulação inicial essa influencia não foi traduzida no modelo em toda sua extensão pela reduzida base de dados e conhecimento que se dispunha.

A partir dos novos conhecimentos e aprofundamento da análise é que foi possível definir que a taxa de sedimentação anual é de 200.000 m^3/ano (+/- 50.000 m^3) na cava. No entanto, como o projeto do canal jamais foi atingido o volume a ser dragado para que seja alcançado o projeto conceitual (prof. = 5 m, larg. = 90 m) é de 285.000 m^3 (incluindo talude = 1:2 e overdredge = 0,3 m). Esta estimativa baseia-se no levantamento batimétrico de abril de 2006 (pós-dragagem).

Conclui-se, portanto, a partir dos dados acima expostos que o volume a ser dragado requerido (285.000 m^3) somado a taxa anual de manutenção do canal (200.000 m^3/ano) nos fornece o volume real necessário a ser dragado **(485.000 m^3)**.

Este último número é o volume total aproximado que deverá ser dragado na próxima campanha de dragagem, a ser realizada no ano de 2007 (Tabela 3.3-1).

Tabela 3.3-1: Resumo do volume total aproximado a ser dragado no canal do Tomba, Caravelas (BA).

Requerimentos de dragagem	Volume
Taxa de sedimentação anual	200.000 m^3/ano
Volume a ser dragado para alcançar o projeto	285.000 m^3
Volume total aproximado a ser dragado em 2007	485.000 m^3

3.4 DISTRIBUIÇÃO DOS TIPOS DE SEDIMENTOS AO LONGO DO CANAL

Em fevereiro de 2006, realizou-se ao longo do canal a amostragem de 28 testemunhos (Figura 3.4-1) com o objetivo de obter amostras de sedimentos não-perturbadas, as quais posteriormente passaram por uma criteriosa descrição e análise sedimentológica. Maiores detalhes sobre metodologia de coleta e análise encontram-se em CEPEMAR (2006b) e CEPEMAR-CPE (2006).

Os dados de 2006 foram comparados a dados anteriores (julho/2005) e permitiram estimar a sedimentação recente nos locais de coleta. Os resultados encontrados são semelhantes aos dados obtidos em CEPEMAR-CPE (2005b), evidenciando que o maior percentual de lama ocorre nas partes mais distais do canal, enquanto que as areias ocorrem predominantemente no setor central. Os resultados de CEPEMAR-CPE (2006) mostram que no setor central a sedimentação de areia entre 2005 e 2006 foi da ordem de 46%, valor diferente do apontado para a totalidade do canal que é de apenas 30%. Assim, de forma geral, podemos assumir que para a porção central do canal do Tomba a

distribuição de sedimentos é de 50% de areia + 50% de lama, enquanto que na totalidade do canal a composição de sedimentos é de 30% de areia + 70% de lama.

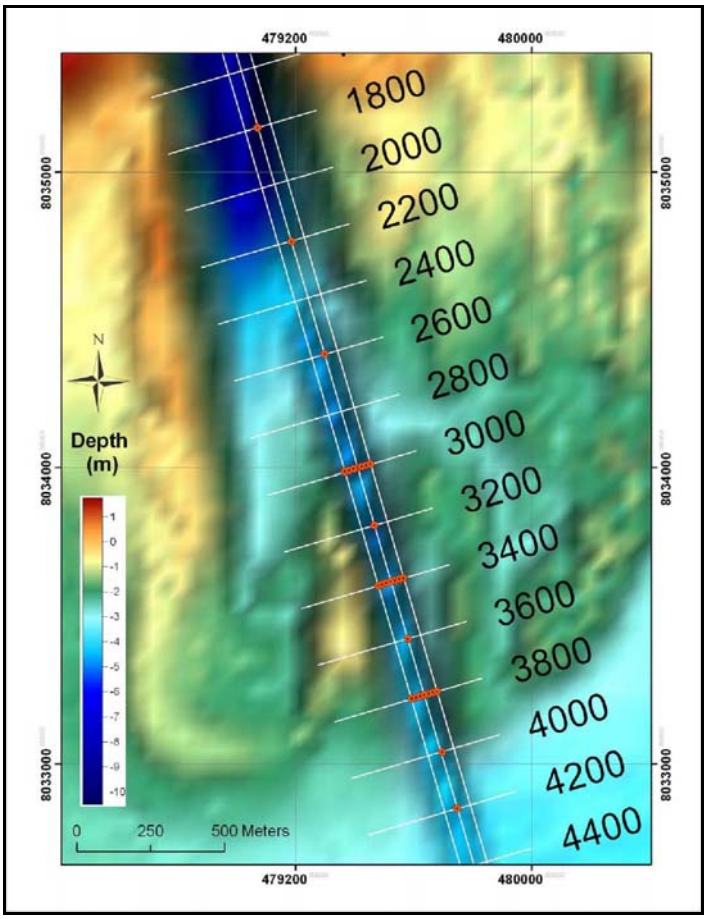

Figura 3.4-1: Localização das amostragens (em vermelho) com testemunhos (Datum: WGS 84)

3.5 A DRAGAGEM DE 2006

De acordo com os registros da empresa de dragagem foram dragados cerca de 410.330 m^3 de sedimentos ao longo do canal do Tomba entre os meses de fevereiro e março de 2006 (estimativas realizadas com base em medições na cisterna das dragas).

Análises das batimetrias de pré e pós-dragagem evidenciam que "*in situ*" o volume dragado foi da ordem 158.000 m^3 (**38% do volume na cisterna**) as possíveis razões para esta discrepância são:

- Variações naturais de volume do material dragado na cisterna das dragas em virtude da sua grande desagregação durante o processo de dragagem;
- Assoreamento durante a operação de dragagem;
- Imprecisões inerentes ao processo de levantamento batimétrico.

A análise dos levantamentos batimétricos revelou que os dados são consistentes, dentro das margens de precisão aceitáveis. A identificação das taxas de assoreamento durante operações de dragagem é um processo difícil de mensurar. O processo de "empolamento" há tempos é reconhecido durante dragagens e, no caso específico de Caravelas, possui grande importância para a comparação de volumes dragados, medidos na cisterna, com os volumes medidos *in situ* através de sondagens batimétricas, em função da maior variabilidade na desagregação e maior tempo de decantação dos materiais finos que compõe o sedimento lamoso no canal.

Não obstante, as imprecisões inerentes aos processos de medição utilizados (que estão em conformidade com os mais aceitos no mundo todo) demonstra-se a concordância entre os volumes dragados medidos na cisterna e *in situ* com base nas batimetrias, conforme evidenciou o "Relatório de Acompanhamento da Dragagem - Fevereiro e Março de 2006", encaminhado ao IBAMA em junho/06.

4
Avaliação das Alternativas de Dragagem

4.1 ANÁLISE DOS EQUIPAMENTOS DE DRAGAGEM

Uma comparação entre diferentes equipamentos de dragagem foi realizada de forma a elucidar melhor as alternativas de dragagem existentes. Adicionalmente procedeu-se avaliação da possibilidade de disposição de parte do material dragado em terra, sendo o sítio recomendado para esta disposição a ilha Barra do Sul.

♦ DRAGA DE SUCÇÃO-E-RECALQUE COM EMPREGO DE TUBULAÇÕES

As principais vantagens do uso de uma draga de sucção-e-recalque (Figura 4.1-1) são:

- Capacidade de escavar diferentes tipos de materiais (desde materiais compactos até lama fluida) e disposição direta nos sítios de descarte através das tubulações;
- Operação contínua o que resulta numa maior produtividade e eficiência, com redução dos custos e otimização do tempo;
- Maior precisão no posicionamento da boca da draga.

As principais limitações são:

- Capacidade limitada de trabalhar sob condições de mar adversas;
- Necessidade do uso de sistemas especiais de ancoragem;
- As tubulações flutuantes podem causar perigos a navegação, requerendo procedimentos especiais para instalação.

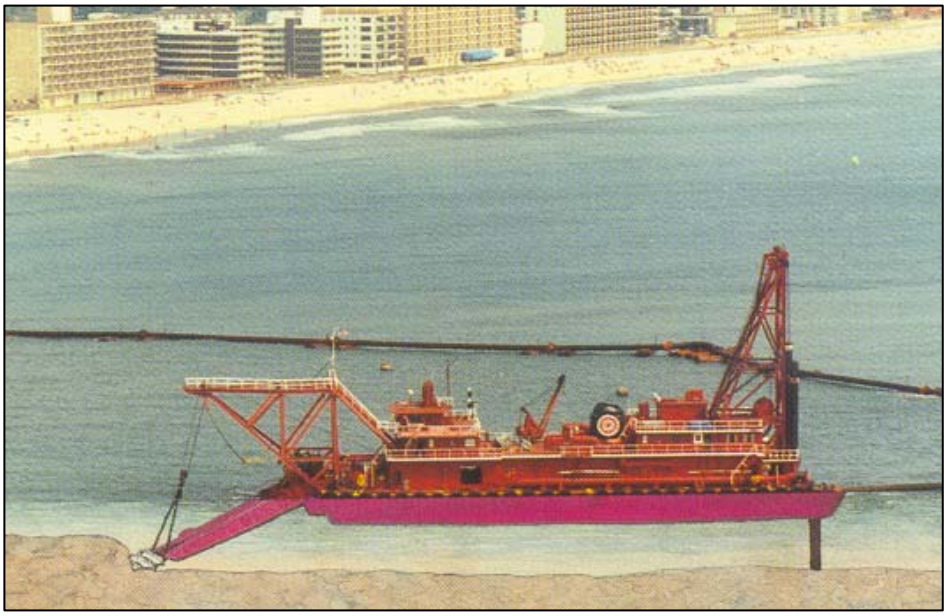

Figura 4.1-1: Desenho esquemático de uma draga de sucção-e-recalque de grande porte concebida para a execução de serviços marítimos.

Cabe mencionar, que estas dragas podem operar com tubulações para conduzir o material da área de dragagem até a área de disposição, com batelões lameiros e até mesmo combinando estas duas opções, dependendo da condição de mar e distancia do ponto de dragagem ao ponto de disposição.

♦ DRAGA AUTOTRASNPORTADORA DO TIPO HOPPER

As principais vantagens do uso de uma draga do tipo hopper (Figura 4.1-2) são:

- Capacidade de trabalho em condições de mar adversas;
- Alta mobilidade, com poder de mover-se facilmente e evitar a obstrução do tráfego de embarcações;
- Pode ser mais econômico quando comparado com dragas de sucção-e-recalque caso as áreas de disposição sejam muito longes (distância superior a 10 km do local de dragagem).

As principais limitações são:

- As restrições de acesso para dragagem e disposição em áreas de baixa profundidade;
- Não podem operar continuamente, necessitando deslocar-se para transporte do material até o descarte, interrompendo o "ciclo de dragagem";
- Escavam com menos precisão que as dragas de sucção-e-recalque;
- A eficiência e ganhos econômicos são reduzidos quando o "*overflow*" é proibido;
- Apresentam dificuldades em executar dragagens nos taludes, especialmente quando os acessos são restritos devido às baixas profundidades nas áreas marginais.

Em Caravelas, a maior vantagem das dragas do tipo hopper é a possibilidade de dragar durante condições de mar agitado, por outro lado, as principais desvantagens incluem baixa produtividade (devido à baixa densidade de sólidos e proibição de *overflow* na maior parte do canal) e as profundidades muito baixas que limitam a execução dos serviços, o que é uma das principais razões porque no setor central do canal (entre as estações 30+00 e 37+00) até hoje não se alcançou as profundidades requeridas no projeto.

Figura 4.1-2: Vista aérea de uma draga hopper operando em Caravelas.

♦ SUMÁRIO DA EFICIÊNCIA DOS TIPOS DE DRAGAS

As dragas do tipo hopper, usualmente empregadas na dragagem ao longo do canal do Tomba, não operam com total eficiência devido às limitações impostas pelas baixas profundidades locais e restrições para o emprego de *overflow*.

As áreas rasas e estreitas do canal nunca foram devidamente dragadas, por conta disto, até hoje ainda não se construiu o canal com a profundidade e largura projetado (5 e 90 metros, respectivamente). Além disso, a proibição do uso de *overflow* nas áreas onde predominam sedimentos lamosos no canal promove diminuição na eficiência da dragagem.

De acordo com CEPEMAR-CPE (2006) o emprego de uma draga de sucção-e-recalque com uso de tubulações para o descarte de parte do material dragado em terra apresenta-se com uma das alternativas técnicas mais indicadas para a execução dos serviços de dragagem em Caravelas, uma vez que será possível dragar em águas rasas e de forma contínua, propiciando maior rapidez na conclusão dos serviços e o cumprimento de prazos impostos por restrições ambientais, tais como o “defeso do camarão” e as “condições de inverno”, que restringem as operações de dragagem no local ao longo do ano.

4.2 DISPOSIÇÃO DO MATERIAL EM TERRA

A escolha do local de disposição do material dragado é um dos fatores de maior relevância em um projeto de dragagem. Considera-se, que quanto mais perto for o sítio de disposição, menor será o custo dos serviços. Obviamente, a motivação para escolha do local não pode apenas basear-se sob a ótica econômica, tendo também que atentar para os impactos ambientais gerados pela disposição. Com base nestes dois preceitos, aliado ainda à análise da capacidade do equipamento de dragagem recomendado (sucção-e-recalque) para a execução do descarte em terra avaliou-se a possibilidade de descarte de parte do material dragado na ilha Barra do Sul. Esta ilha, localizada na desembocadura da Barra do Tomba vêm sofrendo nas últimas décadas um acelerado processo de erosão da linha de costa (ver Figura 4.2-1).

O processo de erosão acelerou significativamente a partir da abertura do canal na década de 1960. Com a abertura do canal, o suprimento de sedimentos vindos das praias adjacentes localizadas a SW foi interrompido pelo “efeito hidráulico” imposto pelo fluxo do canal, interrompendo o transpasse de sedimentos que passaram a depositar-se na forma de bancos marginais. Esta retenção de sedimentos alterou o balanço sedimentar e desencadeou o processo de erosão costeira, associado também ao aumento do regime hidrodinâmico no local. Uma análise das alterações na linha de costa entre os anos de 1966 e 1992 é apresentada na Figura 4.2-2.

A acentuada erosão na ilha Barra do Sul motivou a escolha deste local para disposição do material arenoso dragado e assim dar uma destinação benéfica ao material. Este local poderá vir a receber as areias da parte central do canal do Tomba, as quais são muito semelhantes às das praiais da ilha Barra do Sul, ou mesmo, uma parcela de sedimentos lamosos (acima de 80% de lama). A estratégia proposta para esta dragagem seria o engordamento das praias hoje em erosão com o material arenoso proveniente da dragagem (Figura 4.2-3), deixando que a ação das ondas e correntes promova a seleção do material fino (argilas e siltes) misturado com a areia.

Caso os sedimentos lamosos, porventura, viessem a ser descartados em terra (Figura 4.2-4) haveria a necessidade de criação de diques de contenção (Figura 4.2-5), ou o descarte na zona de surfe onde ondas e correntes podem naturalmente selecionar o material, transportando os grosseiros em direção a praia e dispersando os finos ao largo.

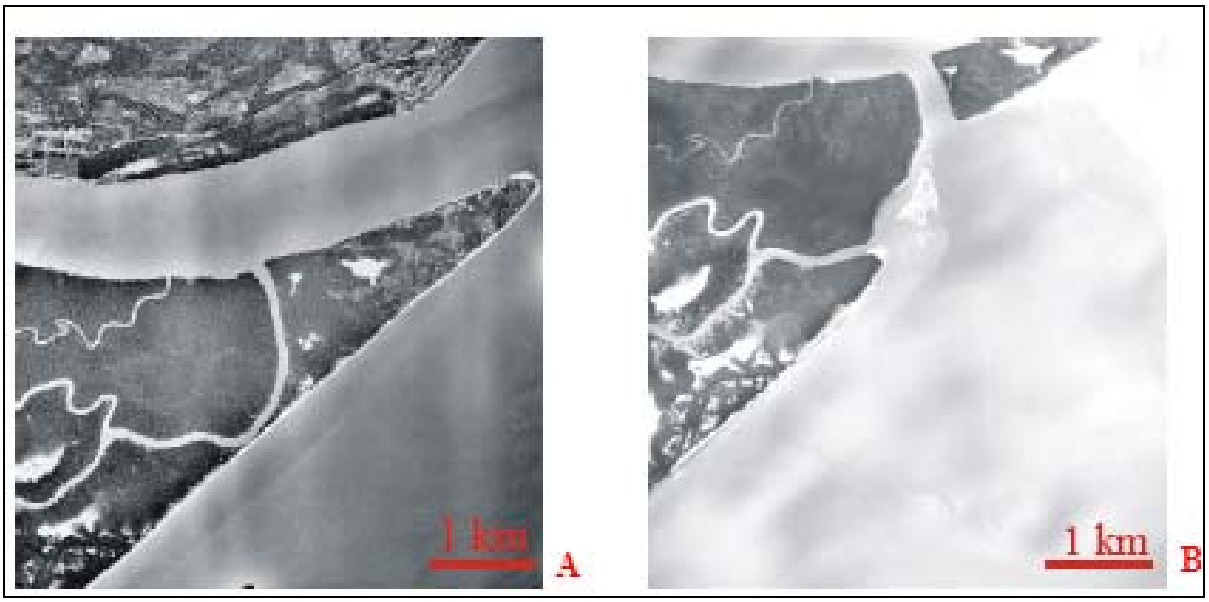

Figura 4.2-1: Fotos aéreas da ilha Barra do Sul em 1966 (A) e 1992 (B). Fonte: CEPEMAR (2001)

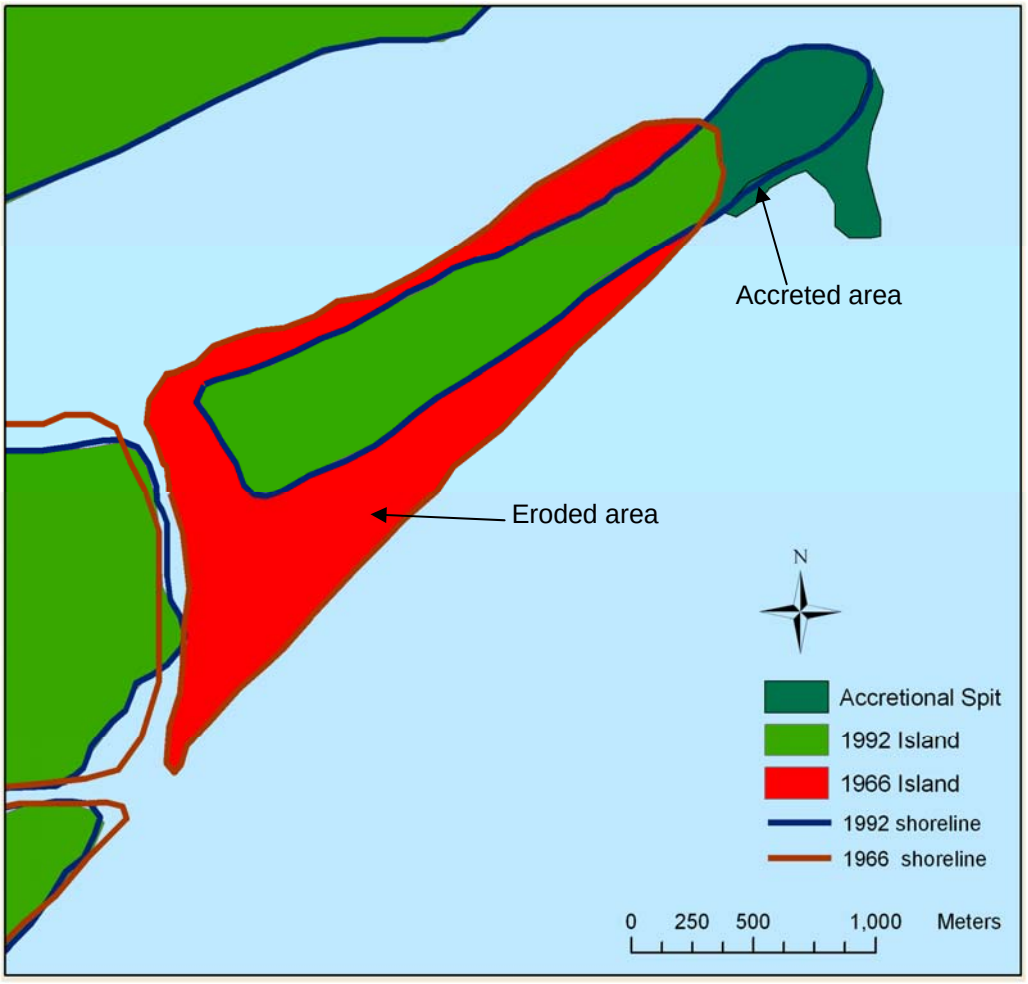

Figura 4.2-2: Alterações ocorridas entre 1966 e 1992 na linha de costa da ilha Barra do Sul. Observar a grande erosão (áreas em vermelho) após a abertura do canal. Fonte: CEPEMAR-CPE (2005b)

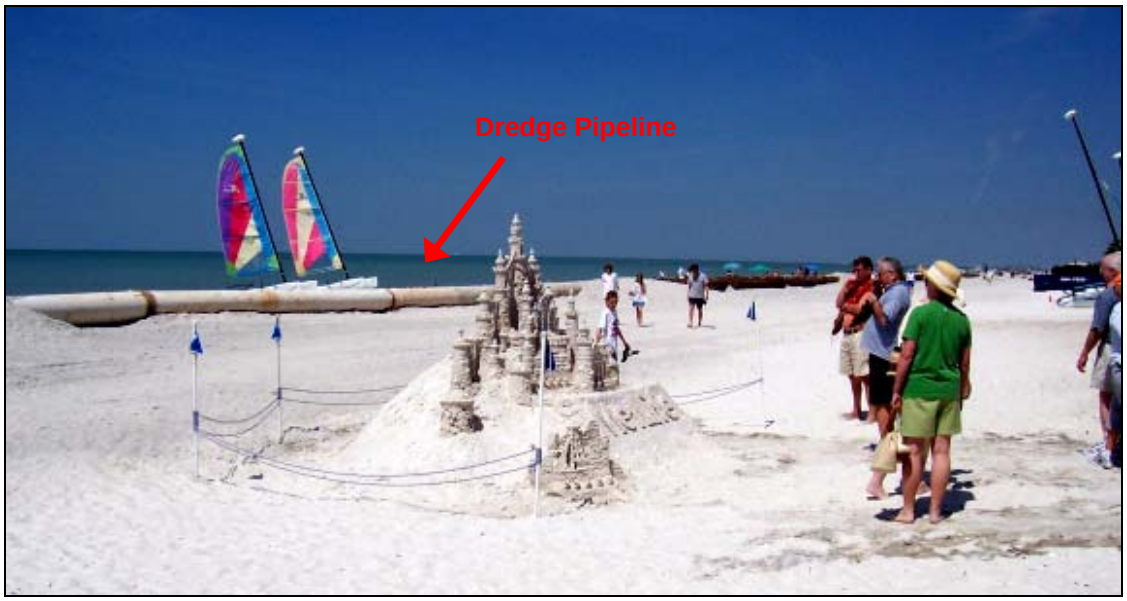

Figura 4.2-3: Tubulação utilizada para o engordamento de uma praia turística da Austrália.

Figura 4.2-4: Operação de descarte de material numa praia localizada na Lousiana (EUA). Cerca de 1 milhão de metros cúbicos de sedimentos foram descartados.

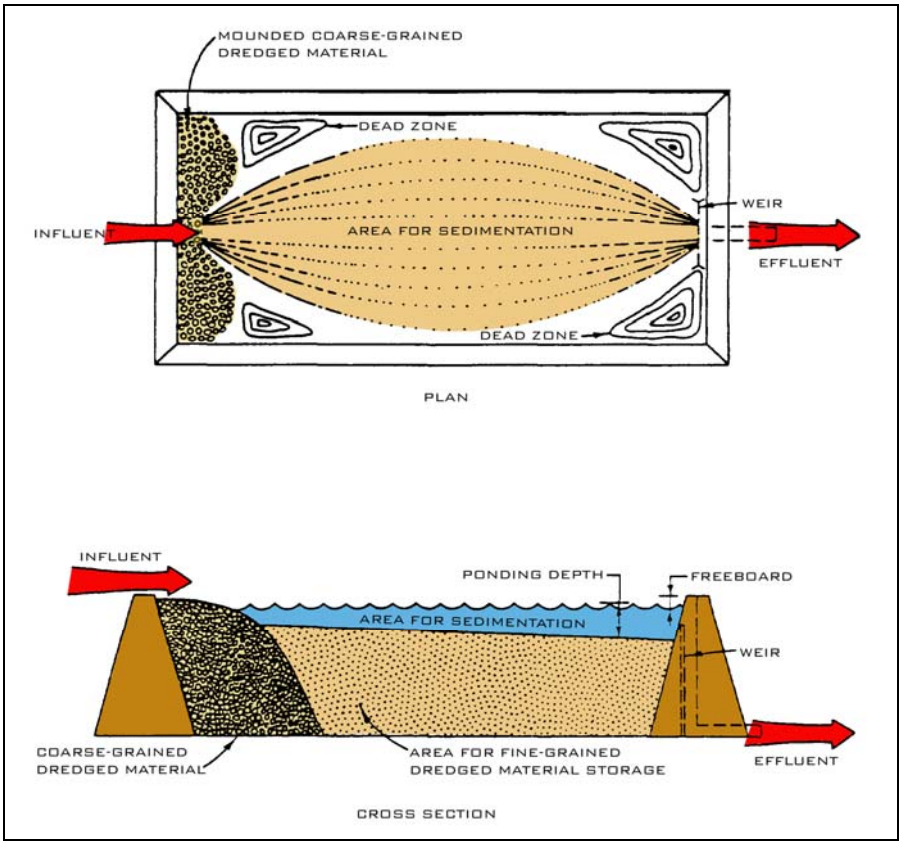

Figura 4.2-5: Esquema conceitual de um dique de contenção.

Após criteriosa análise das alternativas de disposição do material dragado em Caravelas, CEPEMAR-CPE (2006), recomendaram como principal opção o uso de uma draga de sucção-e-recalque com tubulações para realização do descarte em terra em conjunto com a disposição em mar aberto. Desta forma, utilizar-se-iam as areias e misturas de areia e lama para o engordamento das praias na ilha Barra do Sul e os sedimentos lamosos continuariam a ser descartados no bota-fora oceânico, historicamente utilizado nas operações de dragagem em Caravelas (Figura 4.2-6). Embora tenha se avaliado a alternativa de construção de diques de contenção, sob o aspecto técnico e econômico esta alternativa mostrou-se menos apropriada do que o lançamento direto sobre a praia.

A decisão pelo uso de descarte em terra conjuntamente com descarte em mar aberto baseou-se nas facilidades de descarte do material arenoso na ilha Barra do Sul, uma vez que esta se encontra próxima à parte central do canal (onde predominam sedimentos que podem ser utilizados para o engordamento da praia) e porque a atual área de bota-fora encontra-se relativamente perto das partes mais distais do canal, onde predominam sedimentos lamosos. Este cenário, sob o aspecto econômico e técnico, se apresenta como melhor alternativa, já que reduzir distâncias entre o local de dragagem e os sítios de disposição é uma eficiente estratégia para redução de custos e melhoria do desempenho das dragagens.

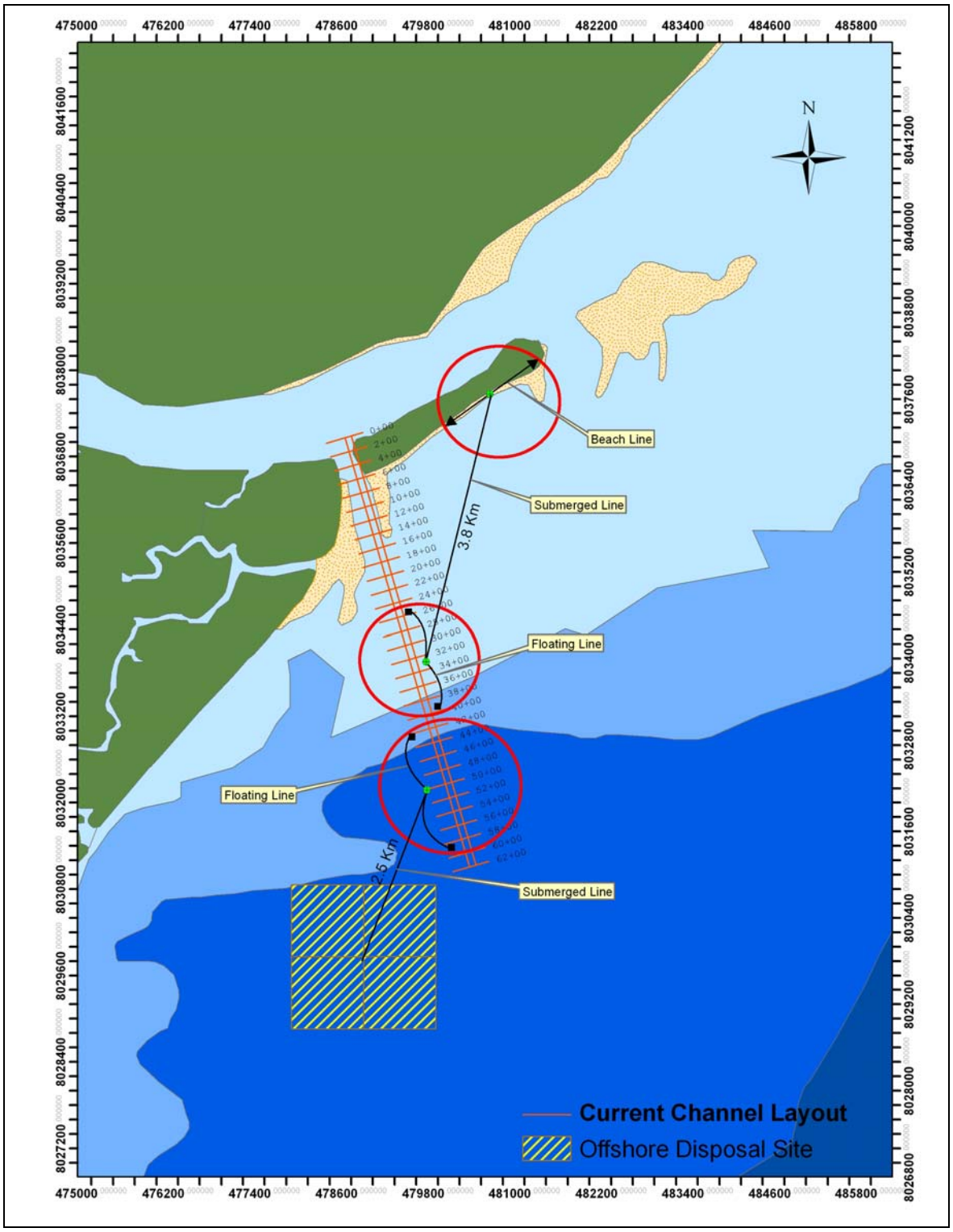

Figura 4.2-6: Esquema de operação da draga de sucção-e-recalque com tubulações mostrando as áreas de dragagem e disposição, tubulações flutuantes e submersas. Fonte: CEPEMAR-CPE (2006)

Cabe ressaltar também, os aspectos ambientais considerados na análise, sendo possível citar abaixo as principais vantagens identificadas na adoção desta nova estratégia de dragagem:

- Recomposição das áreas erodidas na ilha Barra do Sul, incrementando a proteção costeira contra eventos tempestuosos;

- Destinação benéfica de parte do material dragado (areias), indo de encontro a "Boa Prática" ambiental e aos conceitos atuais em gestão de dragagens, onde o uso benéfico é extremamente aceito e recomendado (Protocolo do *London Convention*, o qual o Brasil é país signatário);

- Aumento da eficiência dos serviços, permitindo a realização de dragagens em espaços de tempo mais curtos, revertendo-se em menor interferência no meio;

- Diminuição da necessidade de descarte de grandes quantidades de material em mar aberto, reduzindo a magnitude dos impactos ambientais.

A definição da posição exata onde deverá ser realizado o descarte na ilha Barra do Sul demandará maiores estudos sobre a hidrodinâmica do local e simulações do comportamento do material arenoso na praia e a dispersão do material fino em suspensão. Durante a disposição de material na praia a fração de sedimentos finos será transportada em suspensão pela corrente litorânea, entretanto aumentos na concentração de sólidos em suspensão tendem a permanecer confinados próximos ao local de disposição.

CEPEMAR-CPE (2005a), demonstraram que na região da ilha Barra do Sul, a partir da porção central da ilha, a tendência do transporte de sedimentos é de SW para NE, em sentido reverso ao observado predominantemente na região de Caravelas. Esta peculiaridade no transporte de sedimentos é que faz com que ano após ano, o material erodido tenda a depositar-se a NE da ilha, formando um esporão arenoso (ver Figuras 4.2-2 e 4.2-3). Após tal análise, CEPEMAR-CPE (2006) sugerem que o descarte do material arenoso em terra se dê na parte central da porção NE da ilha, conforme Figura 4.2-7, a partir deste ponto os sedimentos deverão ser redistribuídos até as praias a serem engordadas por tubulações mais curtas.

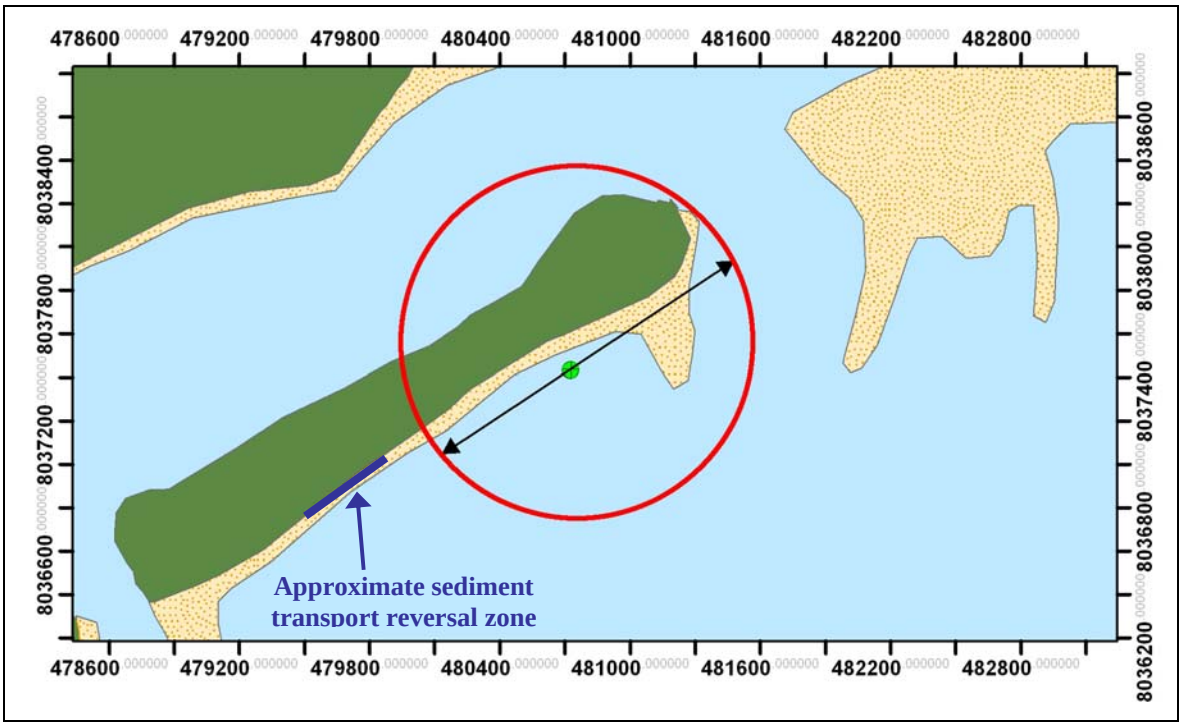

Figura 4.2-7: Localização do potencial ponto de descarte na ilha Barra do Sul.
Fonte: CEPEMAR-CPE (2006)

5
Análise da Configuração do Canal do Tomba através de Modelagem Numérica

O DHI (2006), através do uso da ferramenta de modelagem numérica (MIKE21HD) analisou 5 (cinco) diferentes cenários de configuração do canal do Tomba quanto a profundidade e largura, bem como, quanto ao fechamento e/ou abertura do canal alternativo a sudoeste do canal de navegação existente.

A análise destes cenários evidenciou que dentre as cinco opções testadas, duas mostraram-se bastante favoráveis na redução das taxas de sedimentação e incremento do fluxo hidrodinâmico do canal existente (Figura 5-1a), se consideradas em relação à configuração do projeto (profundidade = 5m e largura = 90m) também simulada. São estes cenários:

- Dragagem do canal existente de forma homogênea para 5,5 metros de profundidade (Figura 5-1b);
- Fechamento do canal alternativo (Figura 5-1c).

De forma resumida, o que o DHI (2006) demonstra em suas análises é que a implementação de quaisquer destas duas opções reduziria significativamente a acumulação de lama ao longo do canal. Considerando que os dados de CEPEMAR-CPE (2006) demonstram que quase 70% do assoreamento do canal decorre de acumulações de lama, tais alternativas teriam grande potencial em reduzir as necessidades de dragagens de manutenção.

Entende-se que tais alternativas produziriam poucas alterações nos padrões de corrente (velocidade e direção), mas teriam grande eficácia na redução das taxas de acumulação de lama.

Os resultados demonstraram que o primeiro cenário (dragagem uniforme de um canal com 5,5 metros de profundidade) tem potencial de **reduzir cerca de 50%** a acumulação de lama, pois o incremento das profundidades e a homogeneidade (inexistência de armadilhas de sedimentos) aumentam a eficiência do fluxo hidrodinâmico. Tais resultados, entretanto, devem ser vistos com cautela devido o balanço “crítico” entre capacidade de fluxo e incremento na sedimentação, o qual pode vir a ser induzido pelo aprofundamento do canal, pois gera maiores espaços para acomodação de sedimentos (ampliação da capacidade de estoque).

O segundo cenário (fechamento do canal alternativo) tem potencial para reduzir as taxas de acumulação de lama em **cerca de 45%**. Para o fechamento parcial do canal alternativo, entretanto, recomenda-se o emprego de sedimentos arenosos da porção central do canal. Esta prática incrementaria o fluxo no canal existente.

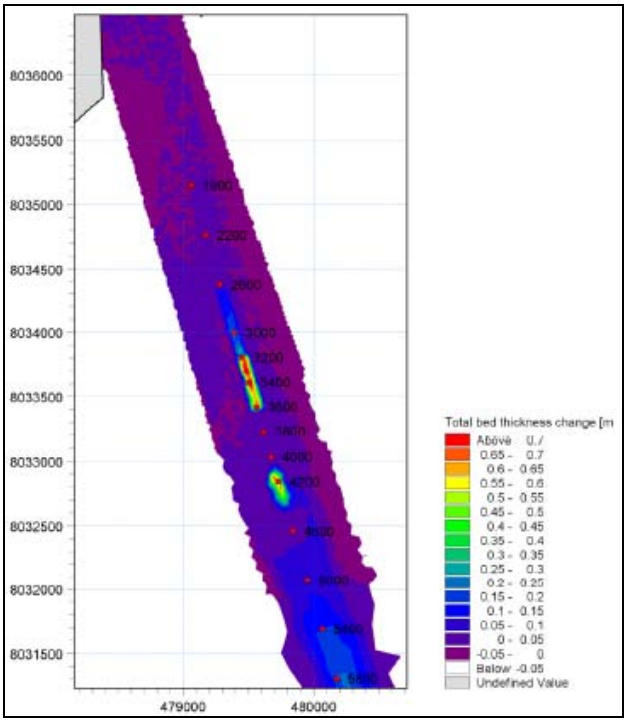

A) Canal existente.

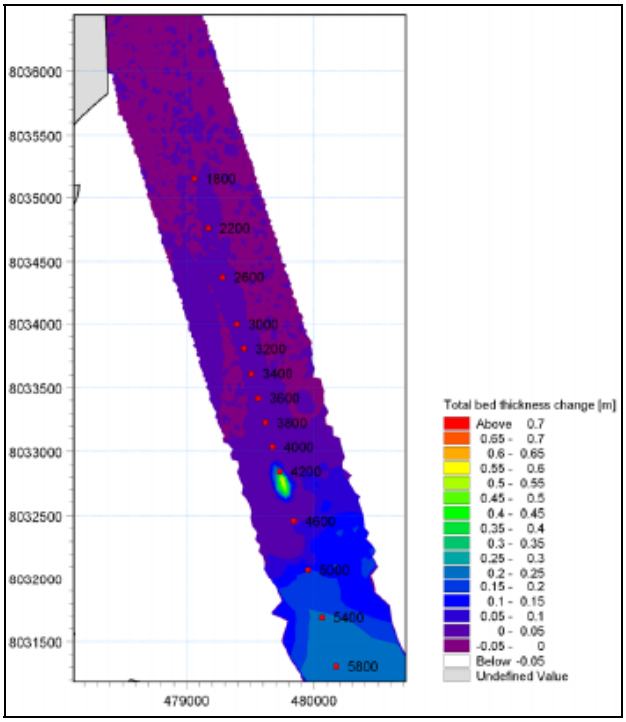

B) Canal com 5,5 metros de profundidade.

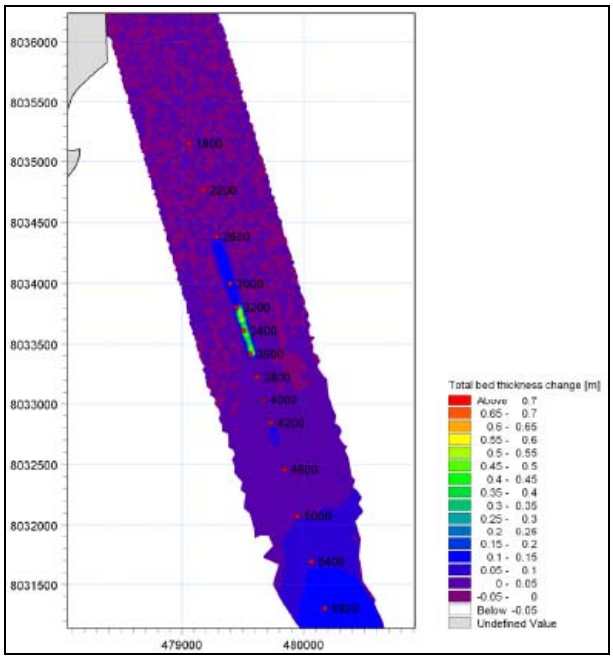

C) Fechamento canal alternativo.

Figura 5-1: Cenários da acumulação líquida de lama no canal do Tomba.

Cabe destacar que o estudo do DHI (2006) não explorou mais detidamente os cenários acima quanto à sedimentação de areia, ficando para *posteriori* o detalhamento destes resultados, bem como a análise dos dois cenários acima descritos em conjunto, o que supostamente poderia trazer reduções ainda mais significativas das taxas de sedimentação ao longo do canal do Tomba.

6
Cronograma

A Aracruz Celulose S.A, em prospecção preliminar no mercado nacional, verificou que não há disponibilidade de um equipamento do tipo sucção-e-recalque de grande porte que pudesse ser considerado para atender às recomendações do presente estudo.

Além disso, as recomendações, embora apresentem um cenário conceitual preciso, demandam ainda de avaliações tecnológicas e um extenso trabalho de detalhamento traduzindo-o em um projeto executivo para implementação pela ARCEL.

A CEPEMAR-CPE procederá à elaboração de um projeto conceitual dos equipamentos de dragagem bem como sua operação, baseados nas conclusões dos trabalhos apresentados neste relatório, bem como de eventuais outras informações que sejam obtidas.

Estima-se que essa etapa levará em torno de 4 (quatro) meses para ser concluída. Posteriormente, a ARCEL. conduzirá o detalhamento de um projeto executivo e buscará opções para contratação desse serviço ou mesmo a construção dos equipamentos.

A estimativa é de que todo o processo leve em torno de 2 (dois) anos para ser concluído. Durante esse período a Aracruz Celulose S.A. pretende continuar a atuar na manutenção do canal com a mesma operação hoje vigente. Ressalta-se, que o extenso monitoramento ambiental da atividade de dragagem, a base de dados existente e os diferentes estudos realizados ao longo destes anos de operação em Caravelas indicam que não ocorrem impactos ambientais diferentes e/ou fora das magnitudes daqueles previstos no processo de licenciamento ambiental.

Vale destacar que, embora preserve-se a tecnologia de dragagem para o período de detalhamento do projeto de um novo equipamento de dragagem, o processo de gestão e controle das operações de dragagem têm passado por melhorias contínuas, já atendendo a todas as recomendações relativas a esse tema propostas no estudo da CEPEMAR-CPE para contratação das operações, e ainda diversas outras relativas à fiscalização e otimização de processos aumentando o controle e conseqüentemente a eficiência da operação de dragagem no canal do Tomba.

7
Conclusões

As conclusões dos estudos no escopo do Projeto Segunda Opinião, conduzidos CEPEMAR-CPE e DHI, foram apresentadas nesse relatório e indicam que as taxas de sedimentação ao longo do canal do Tomba calculadas para projeto (5 m de profundidade e 90 de largura) demandam manutenção por dragagem de 200.000 m^3/ano ± 50.000 m^3 como forma de manter o canal em condições seguras para navegação.

Em função do canal ainda não estar nas dimensões de projeto, e baseado nas condições de abril de 2006 (pós-dragagem) calcula-se que o volume a ser dragado para alcançar as especificações do projeto conceitual de dragagem é de 285.000 m^3. Tal valor somado a taxa anual de manutenção do canal (200.000 m^3/ano) resulta em um volume total necessário de dragagem na cava de 485.000 m^3 para a próxima campanha de dragagem, a ser realizada no início de 2007. A ratificação deste último número somente será possível após realização da batimetria pré-operacional, a ser realizada antes do início dos serviços de dragagem.

Os resultados evidenciam que existe uma diferença entre a necessidade de dragagem atual e o que foi inicialmente previsto no projeto conceitual de dragagem elaborado por DHI (2000), que estimava a necessidade de uma dragagem de manutenção a cada dois anos no valor de 130.000 m^3. Tal diferença levou a uma subestimação nas taxas de sedimentação ao longo do canal e conseqüentemente na freqüência de dragagens de manutenção, o que implicou na não implantação efetiva do canal de projeto. Destacam-se como principais motivos para as diferenças ora observadas nas taxas de sedimentação em relação à originalmente prevista: (i) A inexistência, na época, de uma série de dados para calibração do modelo numérico e; (ii) A não conclusão do canal na profundidade e largura projetada, fazendo com que o canal nunca atingisse a eficiência hidráulica necessária para reduzir o assoreamento.

O emprego de uma draga de sucção-e-recalque com uso de tubulações ou mesmo batelões lameiros para o descarte de parte do material dragado em terra apresenta-se com alternativa técnica mais indicada para a execução dos serviços de dragagem no canal do Tomba, uma vez que será possível dragar com maior precisão em águas rasas e de forma contínua, propiciando maior rapidez na conclusão dos serviços e o cumprimento de prazos impostos por restrições ambientais, tais como o “defeso do camarão” e as “condições de inverno”, que restringem as operações de dragagem no local ao longo do ano.

O sítio de disposição recomendado para o descarte em terra foi a ilha Barra do Sul, que a partir de então, receberia o material arenoso proveniente do setor central do canal enquanto que a atual área de bota-fora continuaria a receber sedimentos lamosos das partes mais distas do canal. Este cenário, sob o aspecto econômico, técnico e ambiental mostrou-se o mais favorável, cabendo citar as principais vantagens identificadas sob o aspecto ambiental: (i) Recomposição das áreas erodidas na ilha Barra do Sul, incrementando a proteção costeira; (ii) Destinação benéfica de parte do material dragado (areias); (iii) Aumento da eficiência dos serviços, permitindo a realização de dragagens em espaços de tempo mais curtos, revertendo-se em menor interferência no meio; (iv) Diminuição da necessidade de descarte de grandes quantidades de material em mar aberto, reduzindo a magnitude dos impactos ambientais.

A modelagem numérica evidenciou que dois cenários podem ser bastante favoráveis na redução das taxas de sedimentação e incremento do fluxo hidrodinâmico do canal existente, são estes: (i) Dragagem do canal existente de forma homogênea para 5,5 metros de profundidade; (ii) Fechamento do canal alternativo. A implementação de quaisquer destas duas opções reduziria significativamente a acumulação de lama ao longo do canal (45% a 50%). Uma vez que, quase 70% do assoreamento do canal decorre de acumulações de lama, tais alternativas teriam grande potencial em reduzir as necessidades de dragagens de manutenção.

Em função do tempo necessário para elaboração de um projeto conceitual dos equipamentos de dragagem e posterior detalhamento e construção ou contratação desse equipamento/sistema a Aracruz Celulose S.A manterá a operação com a tecnologia de dragagem atual durante esse período. Continuará, porém, como ora têm feito com notável êxito, a implementar melhorias operacionais e técnicas para garantia de fiscalização, controle, segurança e eficiência na atividade de dragagem.

8
Referências Bibliográficas

CEPEMAR. 2001. **Estudo de Impacto Ambiental do Terminal de Barcaças para Embarque e Desembarque de Toras de Eucalipto da Aracruz Celulose S.A.; Caravelas-BA**. CPM RT 033/01. 550p.

CEPEMAR. 2006a. **Batimetria Detalhada do Canal de Acesso e Adjacências da Barra do Tomba.** Relatório Técnico RT CPM 089/06 preparado para Aracruz Celulose S.A. 12pp.

CEPEMAR. 2006b. **Sedimentologia do Canal de Acesso a Barra do Tomba.** Relatório Técnico RT CPM 101/06 preparado para Aracruz Celulose S.A. 14pp

CEPEMAR. 2006c. **Caracterização Hidrodinâmica do Canal de Acesso a Barra do Tomba**. Relatório Técnico RT CPM 106/06 preparado para Aracruz Celulose S.A. 11pp.

CEPEMAR-CPE. 2005a. **Second Opinion on the Caravelas Dredging Maintenance Assessment**. Relatório Técnico preparado para Aracruz Celulose S.A. 63pp.

CEPEMAR-CPE. 2005b. **Follow up Assessment of Sedimentology and Morphology Changes on the Caravelas Channel.** Relatório Técnico preparado para Aracruz Celulose S.A. 74pp.

CEPEMAR-CPE. 2006. **Evaluation of Sedimentation Rates, Disposal Sites and Dredging Alternatives for the Caravelas Navigation Channel.** Relatório Técnico preparado para Aracruz Celulose S.A. 56pp.

DHI. 2000. **Hydraulic Investigations for Port Facilities at Caravelas.** Relatório Técnico preparado para Aracruz Celulose S.A. 101pp.

DHI. 2006. **Channel Maintenance Programme: Numerical Modelling of Sedimentation Processes.** Relatório Técnico preparado para Aracruz Celulose S.A. 100pp.

9
Equipe Técnica

Profissional	Mauricio de Carvalho Torronteguy
Registro no Conselho de Classe	-
Cadastro Técnico Federal de Atividades e Instrumentos de Defesa Ambiental	IBAMA nº 1451476
Responsabilidade	Coordenador do Estudo; Elaboração relatório
Assinatura	

Profissional	Marcelo Poças Travassos
Registro no Conselho de Classe	-
Cadastro Técnico Federal de Atividades e Instrumentos de Defesa Ambiental	IBAMA nº 38793
Responsabilidade	Revisão relatório
Assinatura	

ANEXO T

Composição do microfitoplâncton durante as campanhas de amostragem em Caravelas - BA

	2001	2003			2004		2005		
	OUT	FEV	JUL	OUT	MAI	OUT	FEV	MAR	ABR
	1	2	3	4	5	6	7	8	9
DIVISÃO BACILLARIOPHYTA (diatomáceas)									
Classe Fragilariophyceae									
Complexo *Licmosphenia/Climacosphenia*		•							
*** Ordem Fragilariales**	•	•	•	•					•
Família Fragilariaceae		•				•		•	•
**Asterionellopsis glacialis* (Castracane) Round	•	•	•	•	•	•	•	•	•
Bleakeleya notata (Grunow) Round								•	
Diatoma tenue Agardh	•								
Podocystis sp.			•						
Synedra formosa Hantzsch			•						
Synedra spp.	•	•	•						
Ordem Licmophorales									
Família Licmophoraceae									
Licmophora cf. *gracilis* var. *minor* Kützing	•								
Licmophora lyngbyei Kützing	•								
Licmophora spp.			•	•				•	
Ordem Rhaphoneidales									
Família Rhaphoneidaceae									
Rhaphoneis surirella (Ehrenberg) Grunow in Van Heurck	•								
Raphoneis spp.	•								
Ordem Toxiriaceae									
Família Toxiriaceae									
Toxarium undulatum Bailey	•								
Ordem Thalassionematales									
Família Thalassionemataceae			•	•		•		•	•
Lioloma pacificum (Cupp) Hasle*	•		•			•			
Thalassionema cf. *bacillare* (Heiden) Kolbe			•	•	•				
Thalassionema frauenfeldii (Grunow) Grunow		•				•	•	•	•

**Thalassionema nitzschioides* Grunow	•	•	•	•	•	•	•	•	•
Thalassiothrix longissima Cleve & Grunow	•								
Ordem Rhabdonematales									
Família Rhabdonemataceae									
Rhabdonema adriaticum Kützing	•								
Ordem Striatellales									
Família Striatellaceae									
Grammatophora oceanica cf. *vulgaris communs Ehrenberg*	•								
Classe Bacillariophyceae	•	•	•	•	•	•	•	•	•
Ordem Lyrellales									
Família Lyrellaceae									
Lyrella cf. *lyra* Karayeva	•								
Lyrella spp.	•								
Ordem Mastogloidales									
Família Mastogloiaceae									
Mastogloia cf. *meisteri* Hustedt									
Mastogloia spp.	•								
Ordem Cymbellales									
Família Cymbellaceae									
cf. *Cymbela* sp.		•							
Ordem Achnanthales									
Família Cocconeidaceae									
Cocconeis cf. *scutellum* Ehrenberg	•								
Cocconeis spp.	•								
Ordem Naviculales									
Família Diploneidaceae									
Diploneis bombus Ehrenberg	•								
Diploneis didyma Ehrenberg	•								
**Diploneis* spp.	•	•	•	•	•	•	•	•	•
***Familia Naviculaceae**		•			•	•	•	•	
Amphiprora cf. *pulchra* Smith*	•								

Haslea wawrikae Simonsen	•	•		•	•	•		•	•
**Meuniera membranacea* (Cleve) P.C. Silva*		•	•	•	•	•	•		•
Navicula cf. *transitans*							•		•
Navicula cf. *transitans* var. *derasa* (Grunn Cleve & Grunow) Cleve					•	•			•
Navicula cf. *vanhoefenii* Kützing	•								
Navicula spp.	•	•	•	•		•			
**Trachyneis aspera* Ehrenberg	•								
Complexo *Tropidoneis*		•				•			
Tropidoneis spp.		•	•	•					
Família Pleurosigmataceae									
Donkinia sp.			•						
Gyrosigma cf. *balticum* Cleve	•								
** Pleurosigma angulatum* W. Smith	•		•						
Pleurosigma elongatum Smith	•								
**Pleurosigma naviculaceum* Brébisson	•								
**Pleurosigma/Gyrosigma* spp.	•	•	•	•	•	•	•	•	•
Família Plagiotropidaceae									
Plagiotropis sp.		•							
Ordem Thalassiophysales									
Família Catenulaceae									
Amphora cf. *angusta* var. *ventricosa* Gregory	•								
Amphora cf. *arenaria* Donkin	•		•						
Amphora biggiba Grunow ex A. Schmidt	•								
Amphora decussata Grunow	•								
Amphora cf. *labuensis* Cleve				•					
Amphora ostrearia Kützing	•								
Amphora cf. *ovalis* (Kützing) Kützing		•							
Amphora spp.	•	•	•	•	•				•
*** Ordem Bacillariales**									
Família Bacillariaceae							•	•	
** Bacillaria paxillifera* Hendey	•	•	•	•	•	•	•	•	•

* *Cylindrotheca closterium* Reimann	•	•	•	•	•	•	•	•	•
* Complexo *Cylindrotheca closterium/Nitzschia longissima*	•	•	•	•		•	•	•	•
Fragilariopsis doliolus (Wallich) Medlin & Sims	•		•						
Nitzschia acicularis Smith	•								
Nitzschia bicapitata Cleve			•						
Nitzschia cf. *incerta* Grunow	•			•			•		
**Nitzschia* cf. *longissima* Grunow	•	•	•			•			
Nitzschia cf. *lorenziana* Grunow	•						•	•	
Nitzschia cf. *majuscula* Grunow	•								
Nitzschia cf. *panduriformis* Gregory	•					•			•
Nitzschia cf. *ventricosa* Kitton	•								
Nitzschia sigma Smith	•					•			
Nitzschia spp.	•	•	•	•		•	•	•	•
* *Pseudonitzschia "delicatissima"*	•	•	•	•	•	•		•	•
Pseudo-nitzschia "seriata"	•	•			•	•	•		•
Pseudo-nitzscia multistriata Takano				•					
Pseudo-nitzschia pungens Grunow ex Cleve			•						
Ordem Rhopalodiales									
Família Rhopalodiaceae									
Epithemia cistula (Ehrenberg) Ralfs	•								
Ordem Surirellales									
Família Entomoneidaceae									
**Entomoneis* spp.		•	•	•		•	•	•	•
Família Surirellaceae									
Campylodiscus cf. *biangulatus* Greville	•								
Campylodiscus rutilus Skvortzow	•								
Surirella cf. *comis* Schmidt	•								
Surirella cf. *elongata* (Pantocsek) Crosby & Wood	•								
Surirella fastuosa (Ehrenberg) Kützing	•								
Surirella spp.	•								
Classe Coscinodiscophyceae		•	•	•	•	•	•	•	•

Ordem Thalassiosirales									
Família Thalassiosiraceae									
Planktoniella muriformis (Loeblich, Wight & Darley) Round	•			•					
Thalassiosira eccentrica Cleve	•								
Thalassiosira leptopus Fryxell	•								
Thalassiosira cf. *punctigera* (Grunow) Fryxell	•								
* *Thalassiosira* spp.			•	•	•	•	•		
Família Skeletonemataceae									
cf. *Detonula pumila* (Castracane) Gran			•						
**Skeletonema costatum* Greville		•	•	•	•	•	•	•	•
Skeletonema cf. *tropicum* Cleve	•							•	
Skeletonema spp.						•			
Família Stephanodiscaceae									
Cyclotella cf. *litoralis* Lange & Syvertsen	•								
Cyclotella stylorum Brightwell	•								
Cyclotella spp.	•	•			•	•			
Família Lauderiaceae									
Lauderia cf. *annulata* Cleve		•							
Ordem Melosirales									
Família Melosiraceae									
**Melosira moniliformis* (O. F. Müller) Agardh	•								
Melosira spp.	•								
Família Stephanopyxidaceae									
Stephanopyxis turris (Arnott) Ralfs	•								
Família Hyalodiscaceae									
Podosira stelliger (Bailey) Mann	•								
Ordem Paraliales									
Família Paraliaceae									
**Paralia sulcata* (Ehrenberg) Cleve	•	•	•	•	•	•	•	•	•
Ordem Coscinodiscales									
Família Coscinodicaceae									

Coscinodiscus centralis Ehrenberg		•		•					
Coscinodiscus granii Gough		•					•		
Coscinodiscus cf. *marginatus* Ehrenberg	•								
Coscinodiscus cf. *perforatus* Ehrenberg		•							
Coscinodiscus radiatus Ehrenberg	•			•					
Coscinodiscus cf *stellaris* Roper	•								
Coscinodiscus spp.	•	•		•	•	•	•	•	
Palmeria hardmaniana Greville			•						
Família Aulacodiscaceae									
Aulacodiscus cf. *kittonii* Arnott ex Ralfs	•								
Família Hemidiscaceae									
Actinocyclus sp.		•							
Hemidiscus sp.		•							
Roperia tesselata (Roper) Grunow ex Pelletan	•								
Família Heliopeltaceae									
Actinoptychus senarius (Ehrenberg) Ehrenberg	•			•		•			
Actinoptychus splendens (Shadbolt) Ralfs ex Pritchard	•								
Actinoptychus vulgaris Schumann	•								
Actinoptychus spp.				•		•			•
Actinoptychus undulatus	•								
Ordem Asterolamprales									
Família Asterolampraceae									
Asteromphalus sp.						•			•
Ordem Triceratiales									
Família Triceratiaceae									
Auliscus cf. *coelatus* Bailey	•								
Cerataulus turgidus (Ehrenberg) Ehrenberg	•								
Odontella cf. *aurita* (Lyngbye) Agardh			•	•		•	•		
Odontella cf. *granulata* (Roper) Ross		•							
Odontella longicruris (Greville) Hoban			•		•	•	•		
Odontella mobiliensis Grunow	•	•	•	•	•		•	•	•

Odontella regia (Schultze) Simonsen				•					
Odontella rhombus (Ehrenberg) Kützing	•		•						
Odontella sinensis (Greville) Grunow		•	•	•			•	•	
Odontella tuomeyi	•								
Odontella spp.				•			•		•
Triceratium favus Ehrenberg	•			•			•		
Triceratium favus var. *quadrata* Ehrenberg	•				•				
Família Plagiogrammaceae									
Dimeregramma cf. *marinum* Gregory	•								
***Ordem Biddulphiales**									
Família Biddulphiaceae									
Biddulphia biddulphiana (Smith) Boyer	•								
Biddulphia tuomeyi (Bailey) Roper	•					•	•	•	
Isthmia enervis Ehrenberg	•								
Terpsinoe musica Ehrenberg	•								
Ordem Hemiaulales									
Família Hemiaulaceae									
Cerataulina pelagica Hendey	•	•	•	•				•	
Eucampia cf. *zodiacus* Ehrenberg			•	•					
Eucampia cornuta (Cleve) Grunow	•		•						
Hemiaulus hauckii Grunow in Van Heurck		•	•	•	•			•	
Hemiaulus membranaceus Cleve	•	•	•			•	•	•	•
Hemiaulus sinensis Greville		•	•				•		•
Ordem Bellerocheaceae									
Família Bellerocheaceae									
Bellerochea horologicalis Von Stosch	•	•							
Bellerochea malleus Van Heurck	•					•	•	•	•
Ordem Lithodesmiaceae									
Família Lithodesmiaceae									
Ditylum brightwelli (West) Grunow	•		•		•	•	•	•	•
Helicotheca tamesis (Shrubsole) Ricard*		•	•	•			•		

Lithodesmium undulatum Ehrenberg		•							
Ordem Corethrales									
Família Corethraceae									
* *Corethron criophilum* Castracane			•	•				•	•
Corethron sp.	•								
Ordem Cymatosirales									
***Familia Cymatosiraceae**	•				•	•	•	•	•
* *Campylosira cymbelliformis* (A. Schmidt) Grunow	•	•				•	•	•	
Campylosira sp.			•				•		
Cymatosira lorenziana Grunow	•								
Ordem Rhizosoleniales									
Familia Rhizosoleniaceae			•						
Dactyliosolen cf. *phuketensis* (Sundström) Hasle		•	•	•		•			
Dactyliosolen fragilissimus (Bergon) Hasle	•		•			•		•	•
cf. *Guinardia cylindrus* (Cleve) Hasle					•				
* *Guinardia delicatula* (Cleve) Hasle	•	•		•		•			
Guinardia flaccida (Castracane) H. Peragallo		•	•					•	
Guinardia striata (Stolterfoth) Hasle	•	•		•	•	•	•	•	•
Proboscia alata (Brightwell) Sundström	•	•	•	•				•	•
Pseudosolenia calcar-avis (Schultze) Sundström	•	•		•	•			•	•
Rhizosolenia cf. *fallax* Sundström				•					•
Rhizosolenia hebetata (Bailey) Gran		•	•					•	•
Rhizosolenia imbricata Brigthwell	•	•		•				•	•
* *Rhizosolenia pungens* Cleve-Euler		•	•	•		•		•	•
Rhizosolenia robusta Norman in Pritchard	•		•	•		•			
Rhizosolenia setigera Brightwell	•	•	•	•	•	•	•	•	•
Rhizosolenia cf. *styliformis* Brightwell		•	•	•		•			•
Ordem Chaetocerales									
Família Chaetoceraceae									
Bacteriastrum delicatulum Cleve	•		•						
Bacteriastrum cf. *hyalinum* Lauder			•	•		•			•

Bacteriastrum spp.		•				•			
Chaetoceros aequatorialis Cleve						•			
Chaetoceros cf. *affinis* Lauder		•	•	•		•			
Chaetoceros cf. *affinis* var. *affinis*	•								
Chaetoceros cf. *atlanticus* Cleve		•							
Chaetoceros cf. *brevis* Schütt				•		•		•	
Chaetoceros coarctatus Lauder		•		•		•	•	•	•
Chaetoceros concavicornis Mangin			•						
Chaetoceros contortum Schütt									•
Chaetoceros cf. *constrictus* Gran				•		•			
Chaetoceros curvisetus Cleve			•		•	•	•	•	•
Chaetoceros cf. *dadayi* Pavillard		•							
Chaetoceros danicus Cleve		•	•	•		•			
Chaetoceros decipiens Cleve		•	•	•		•	•	•	
Chaetoceros didymus Ehrenberg						•		•	
Chaetoceros eibenii Grunow			•	•					
Chaetoceros cf. *laciniosum* Schütt									•
Chaetoceros lorenzianus Grunow	•	•	•			•		•	•
Chaetoceros pendulus Karsten			•						
Chaetoceros peruvianus Brightwell			•			•		•	•
Chaetoceros subtilis Cleve								•	
**Chaetoceros subtilis* var. *abnormis*								•	•
Chaetoceros cf. *tenuissimus* Meunier						•			
Chaetoceros cf. teres Cleve				•					
**Chaetoceros* cf. *tetrastichon* Cleve		•						•	•
Chaetoceros spp.	•	•	•	•	•	•	•	•	•
Ordem Leptocylindrales									
Família Leptocylindraceae									
* *Leptocylindrus danicus* Cleve		•	•	•	•	•	•	•	•
* *Leptocylindrus minimus* Gran		•	•	•	•	•	•	•	•
DIVISÃO DINOPHYTA (dinoflagelados)									

Classe Dinophyceae		•	•	•		•	•	•	•
*** Ordem Gymnodianiales**	•	•	•	•	•	•	•	•	
Família Gymnodiniaceae									
cf. *Cochlodinium* sp.					•				
Gymnodinium spp.	•								
Gyrodinium spp.	•	•				•		•	
Ordem Gonyaulacales									
Família Ceratiaceae									
Ceratium breve (Ostenfeld & Schmidt) Schröder		•	•	•		•			
Ceratium cf. *deflexum* (Kofoid) Jorgensen		•	•						
Ceratium extensum (Gourret) Cleve	•								
**Ceratium furca* (Ehrenberg) Claparède & Lachmann	•	•	•			•	•	•	•
Ceratium fusus (Ehrenberg) Dujardin	•	•	•			•	•	•	•
Ceratium cf. *macroceros* (Ehrenberg) Vanhöffen			•						•
Ceratium cf. *massiliense* (Gourret) Jorgensen	•		•				•	•	
Ceratium setaceum Jorgensen						•			
Ceratium symmetricum Pavillard	•								
Ceratium teres Kofoid							•		
Ceratium trichoceros (Ehrenberg) Kofoid			•	•		•	•	•	•
Ceratium cf. *tripos* (O. F. Müller) Nitzsch	•	•	•				•	•	
Ceratium sp.			•			•		•	
Família Goniodomataceae									
Alexandrium cf. *tamarensis* (Lebour) Balech	•								
Alexandrium sp.		•						•	
Ordem Peridiniales									
Família Peridiniaceae									
Scrippsiella cf. *trochoidea* (Stein) Loeblich III		•	•						
Scrippsiella cf. *spinifera* Honsell & Cabrini		•	•	•					
Scripsiella sp.						•			
Família Congruentidiaceae									
Protoperidinium cf. *depressum* (Bailey) Balech		•		•		•	•	•	

Protoperidinium cf. *hirobis* Abé			•						
**Protoperidinium* cf. *laticeps* (Gronteved & Seidenfaden)		•							
Protoperidinium cf. *leonis* (Pavillard) Balech			•			•			
Protoperidinium cf. *obtusum* (Karsten) Parke & Dodge	•								
Protoperidinium cf. *ovatum* Pouchet	•								
Protoperidinium cf. *pallidum* (Ostenfeld) Balech	•								
Protoperidinium cf. *pellucidum* Bergh			•	•					
Protoperidinium cf. *pentagonum* (Gran) Balech		•					•	•	
Protoperidinium cf. *steinii* (Jörgensen) Balech	•	•		•					
* *Protoperidinium* spp.	•	•	•	•	•	•	•	•	
Família Podolampaceae									
Podolampas bipes Stein	•								
Podolampas elegans Schütt						•			
Podolampas sp.						•			
Ordem Incerta									
Família Oxytocaceae									
Oxytoxum caudatum Schiller	•								
Oxytoxum gracile Schiller									•
Oxytoxum sceptrum (Stein) Schröder							•		
Oxytoxum spp.	•				•	•		•	
Ordem Dinophysales									
Família Dinophysiaceae									
Dinophysis caudata Saville-Kent	•			•		•		•	
Dinophysis tripos Gourret			•						
Família Oxyphysiaceae									
Oxyphysis oxytoxoides Kofoid	•								
Ordem Prorocentrales									
Família Prorocentraceae									
Prorocentrum cf. *balticum* (Lohmann) Loeblich III			•						
Prorocentrum gracile Schütt	•	•	•	•					
Prorocentrum cf. *mexicanum* Tafall			•	•					

**Prorocentrum micans* Ehrenberg	•	•	•	•	•	•		•	•
Prorocentrum spp.		•	•	•					
Classe Noctiluciphyceae									
Ordem Noctilucales									
Família Noctilucaceae									
Noctiluca scintilans (Macartney) Kofoid & Swezy						•			
Pronoctiluca pelagica Fabre- Domergue**		•							
DIVISÃO CYANOPHYTA (cianobactérias)									
Classe Cyanophyceae									
*** Ordem Chroococcales**		•		•			•	•	•
Família Microcystaceae									
Johannesbaptistia pellucida Taylor & Drouet	•								
Merismopedia sp.	•								
*** Ordem Oscilatorialles**	•	•	•	•	•	•	•	•	•
Família Oscillatoriaceae									
** Katagnymene* sp.	•								•
Oscillatoria cf. *limosa* (Dillwyn) C. Agardh									•
Ordem Nostocales		•		•		•	•	•	•
Família Nostocaceae									
Anabaena cf. *oryzae* Fritsch									•
** Anabaena* spp.		•			•		•		•
Rhichelia sp.									•
Spirulina spp.								•	•
DIVISÃO CHROMOPHYTA									
Classe Dictyochophyceae (silicoflagelados)									
Ordem Dictyochales									
Família Dictyochaceae									
Dictyocha fibula Ehrenberg	•	•	•	•	•	•	•		•
Mesocena polymorpha Lemmermann			•						
Classe Prymnesiophyceae (cocolitoforídeos)	•								
cf. *Michaelsarsia* sp.									•

Calciosolenia murrayi Gran								•	
DIVISÃO CHLOROPHYTA									
Classe Euglenophyceae (euglenofíceas)			•	•		•		•	•
Ordem Euglenales									
Família Euglenaceae									
Euglena cf. *acus* Ehrenberg	•								
Euglena cf. *ascusformis* Schiller		•	•	•					
Classe Prasinophyceae (prasinofíceas)									
Halosphaera viridis Schnaitz	•								
Classe Chlorophyceae (clorofíceas)									
Ordem Chlorocoocales									
Família Hydrodictyaceae									
Pediastrum duplex Meyen			•						
Ordem Zygnemales									
Família Desmidiaceae									
Cosmarium sp.1			•						
Staurastrum cf. *iotanum* Wolle			•						

ANEXO U

Composição do ictioplâncton coletado nas sete estações de amostragem durante as nove campanhas realizadas na área de construção do Terminal de Barcaças Luciano Villas Boas Machado, em Caravelas - BA

SUBFILO VERTEBRATA
SUPERCLASSE GNATHOSTOMATA
CLASSE ACTINOPTERYGII
SUBCLASSE NEOPTERYGII
DIVISÃO TELEOSTEI
SUBDIVISÃO Elopomorpha
ORDEM Anguilliformes
FAMÍLIA Ophichthidae
SUBDIVISÃO Clupeomorpha
ORDEM Clupeiformes
SUBORDEM Clupeoidei
FAMÍLIA Engraulidae
GÊNERO *Anchoa*
ESPÉCIE *A. filifera* (Fowler, 1915) - Manjuba
ESPÉCIE *A. spinifer* (Valenciennes, 1848) - Manjuba-savelha
GÊNERO *Anchoviella*
ESPÉCIE *A. lepidentostole* (Fowler, 1911) - Manjuba
FAMÍLIA Pristigasteridae
SUBFAMÍLIA Pristigasterinae
GÊNERO *Odontognathus*
ESPÉCIE *O. mucronatus* Lacepède, 1800
SUBFAMÍLIA Pelloninae
GÊNERO *Pellona*
ESPÉCIE *P. harroweri* (Fowler, 1917) - Sardinha-grande
FAMÍLIA Clupeidae
GÊNERO *Platanichthys*

ESPÉCIE *P. platana* (Regan, 1917)
SUBDIVISÃO Euteleostei
SUPERORDEM Ostariophysi
ORDEM Siluriformes (Nematognathi)
FAMÍLIA Ariidae (Tachysuridae)
GÊNERO *Bagre*
ESPÉCIE *B. bagre* (Linnaeus, 1766) - Bagre-bandeira
SUPERORDEM Acanthopterygii
SÉRIE Atherinomorpha
ORDEM Atheriniformes
SUBORDEM Atherinoidei
FAMÍLIA Atherinopsidae
SUBFAMÍLIA Menidiinae
GÊNERO *Atherinella*
ESPÉCIE *A. brasilienesis* (Quoy & Gaimard, 1825) - Mamarreis
SÉRIE Atherinomorpha
ORDEM Beloniformes
SUBORDEM Belonoidei (=Exocoetoidei)
FAMÍLIA Hemiramphidae
GÊNERO *Hyporhamphus*
ESPÉCIE *H. unifasciatus* (Ranzani, 1842) - Agulha-branca
SUPERFAMÍLIA Exocoetoidea
FAMÍLIA Exocoetidae
GÊNERO *Cypselurus*
ESPÉCIE *Cypselurus* sp. - Voador
SÉRIE Percomorpha

ORDEM Syngnathiformes
SUBORDEM Syngnathoidei (Solenichthyes)
INFRAORDEM Syngnatha
SUPERFAMÍLIA Syngnathoidea (Lophobranchii)
FAMÍLIA Syngnathidae
GÊNERO *Syngnathus* (= *Dermatostethus*)
ESPÉCIE *S. folletti* Herald, 1942 - Peixe-cachimbo
SUBFAMÍLIA Hippocamphinae
GÊNERO *Hippocampus*
ESPÉCIE *H. reidi* Ginsburg, 1933 - Cavalo-marinho
ORDEM Scorpaeniformes
FAMÍLIA Triglidae
GÊNERO *Prionotus*
ESPÉCIE *Prionotus* sp. - Cabrinha
ORDEM Perciformes
SUBORDEM Percoidei
SUPERFAMÍLIA Percoidea
FAMÍLIA Serranidae - Mixole, Cherne
FAMÍLIA Carangidae
SUBFAMÍLIA Caranginae
GÊNERO *Caranx*
ESPÉCIE *Caranx* sp.
GÊNERO *Chloroscombrus*
ESPÉCIE *C. chrysurus* (Linnaeus, 1766) - Palombeta
GÊNERO *Oligoplites*
ESPÉCIE *Oligoplites* sp. - Guaivira

FAMÍLIA Gerreidae
GÊNERO *Eucinostomus*
ESPÉCIE *Eucinostomus* sp. - Carapicu
FAMÍLIA Haemulidae (Pomadasydae) - Roncador
FAMÍLIA Sciaenidae
GÊNERO *Stellifer*
ESPÉCIE *S. rastrifer* (Jordan, 1889) - Cangoá
ESPÉCIE *S. stellifer* (Bloch, 1790) - Canguá
ESPÉCIE *Stellifer* sp.
GÊNERO *Menticirrhus*
ESPÉCIE *M. americanus* (Linnaeus, 1758) - Papa-terra
GÊNERO *Cynoscion*
ESPÉCIE *Cynoscion* sp. - Pescada
GÊNERO *Macrodon*
ESPÉCIE *M. ancylodon* (Bloch & Schneider, 1801) - Pescada-foguete
GÊNERO *Umbrina*
ESPÉCIE *U. canosai* Berg, 1895 - Corvina-riscada
FAMÍLIA Kyphosidae
SUBFAMÍLIA Kyphosinae
GÊNERO *Kyphosus*
ESPÉCIE *K. sectatrix* (Linnaeus, 1758) - Pirajica
SUBORDEM Labroidei
FAMÍLIA Pomacentridae
SUBFAMÍLIA Pomacentrinae
GÊNERO *Abudefduf*
ESPÉCIE *A. saxatilis* (Linnaeus, 1758) - Sargento

SUBORDEM Blennioidei
FAMÍLIA Blenniidae
GÊNERO *Parablennius*
ESPÉCIE *P. pilicornis* (Cuvier, 1829) - Peixe-macaco
GÊNERO *Hypleurochilus*
ESPÉCIE *H. fissicornis* (Quoy &Gaimard, 1824) - Peixe-macaco
SUBORDEM Gobioidei (Xenopterygii)
FAMÍLIA Gobiesocidae
GÊNERO *Gobiesox*
ESPÉCIE *G. strumosus* Cope, 1870 - Peixe-ventosa
SUBORDEM Gobioidei (Xenopterygii)
FAMÍLIA Gobiidae
GÊNERO *Microgobius*
ESPÉCIE *M. meeki* Evermann & Marsh, 1899 - Maria-da-toca
SUBORDEM Scombroidei
FAMÍLIA Scombridae – Cavalinhas, Bonitos Atuns e afins
FAMÍLIA Trichiuridae
SUBFAMÍLIA Trichiurinae
GÊNERO *Trichiurus*
ESPÉCIE *T. lepturus* Linnaeus, 1758 - Peixe-espada
SUBORDEM Kurtoidei
FAMÍLIA Ephippidae
GÊNERO *Chaetodipterus*
ESPÉCIE *C. faber* (Broussonet, 1782) - Enxada
FAMÍLIA Nomeidae
ORDEM Pleuronectiformes

SUBORDEM Pleuronectoidei
FAMÍLIA Paralichthyidae
GÊNERO *Paralichthys*
ESPÉCIE *Paralichthys* sp. - Linguado
GÊNERO *Etropus*
ESPÉCIE *E. crossotus* Jordan & Gilbert, 1882 – Linguado
FAMÍLIA Cynoglossidae
GÊNERO *Symphurus*
ESPÉCIE *Symphurus* sp. - Língua de mulata
FAMÍLIA Achiridae
GÊNERO *Achirus*
ESPÉCIE *A. lineatus* (Linnaeus, 1758) - Tapa
GÊNERO *Trinectes*
ESPÉCIE *T. paulistanus* (Ribeiro, 1915) – Linguado
ORDEM Tetraodontiformes
SUBORDEM Tetraodontoidei
SUPERFAMÍLIA Balistoidea
FAMÍLIA Monacanthidae
GÊNERO *Stephanolepis*
ESPÉCIE *S. hispidus* (Linnaeus, 1766) - Peixe-porco
SUPERFAMÍLIA Ostracioidea (Ostracodermi)
FAMÍLIA Ostraciidae (Ostraciontidae) - Peixe-cofre
SUPERFAMÍLIA Tetraodontoidea
FAMÍLIA Tetraodontidae - Baiacu

ANEXO V

Lista das espécies e densidade (número de indivíduos/0,04 m^2) encontradas em cada ponto coletado por *corer*. Campanha: Abril/2002

GRUPO	ESPÉCIE	ESTAÇÕES																				
		Canal										Descarte										
		C1	C2	C3	C4	C5	C6	C7	C8	C9	C10	D1	D2	D3	D4	D5	D6	D7	D8	D9	D10	TOTAL
	Harmothoe macginitei	1	0	0	0	0	0	0	0	0	0	0	0	0	1	0	0	0	0	0	0	2
	Linopherus ambigua	0	0	0	0	0	0	0	0	1	0	0	0	0	0	0	0	0	0	0	0	1
	Gyptis callithrix	1	0	0	0	0	1	0	0	1	0	1	1	0	0	0	0	0	0	0	0	5
	Eusyllinae gen. sp. A	0	1	0	0	0	0	0	0	0	0	0	0	0	0	0	0	0	0	0	0	1
	Neanthes bruaca	2	1	0	0	0	0	0	1	2	1	0	0	0	1	0	6	0	1	1	0	16
	Aglaophamus juvenalis	0	0	0	0	0	0	1	0	0	0	0	0	0	0	0	0	0	0	0	0	1
	Glycera cf. convoluta	0	0	0	0	0	0	0	0	0	0	0	0	0	0	0	0	0	0	0	0	0
	Glycera sp. A	0	0	1	0	0	0	0	0	0	0	0	0	0	0	0	0	0	0	0	0	1
	Goniada brunnea	0	0	0	0	0	0	0	0	0	0	0	0	0	0	0	0	0	0	0	0	0
	Glycinde multidens	0	0	0	0	0	0	0	0	0	0	0	0	0	1	0	1	0	0	0	0	2
	Parandalia tricuspis	0	0	0	0	0	1	0	1	0	0	0	1	0	0	0	0	0	0	1	0	4
	Sigambra grubei	1	0	0	0	0	0	0	0	0	1	0	0	0	0	0	0	0	0	0	0	2
	Diopatra cuprea	0	0	0	0	0	0	0	0	0	0	0	0	0	0	0	0	0	0	0	0	0
POLYCHAETA	*Nematonereis schamardae*	0	0	0	0	0	0	0	0	0	0	0	0	0	0	1	0	0	0	0	0	1
	Lumbrineris sp.	0	0	0	0	0	0	0	0	0	0	0	0	0	1	0	0	0	0	0	0	1
	Ninoe brasiliensis	0	0	0	0	0	0	0	0	0	0	0	0	0	0	0	0	0	0	0	0	0
	Scoloplos (Scoloplos) sp. A	0	1	0	0	0	0	0	0	0	0	0	0	0	0	0	0	0	0	0	0	1
	Scoloplos (Leodamas) rubra	3	0	0	3	0	0	0	0	0	0	0	0	0	0	0	0	0	0	0	0	6
	Paraprionospio pinnata	0	0	0	0	0	6	4	1	0	0	0	0	0	0	1	0	0	3	0	0	15
	Prionospio sp. A	0	0	0	0	0	0	0	0	0	0	0	0	0	0	0	0	0	0	0	0	0
	Spiochaetopterus sp. A	0	0	0	0	0	0	0	0	0	0	0	0	0	0	0	0	0	0	0	0	0
	Capitellidae gen. sp.	1	0	0	0	0	0	0	0	0	0	0	0	0	0	0	0	0	0	0	0	1
	Magelona variolamellata	0	0	0	0	0	0	1	1	0	1	0	2	0	0	2	0	0	1	1	1	10
	Magelona posterolongata	0	0	0	0	0	0	0	1	0	0	1	0	0	0	0	0	0	1	2	0	5
	Owenia fusiformis	0	0	0	0	0	0	0	0	0	0	0	0	0	0	0	0	0	0	0	0	0
	Loimia medusa	1	0	0	0	0	0	0	0	0	0	0	0	0	0	0	0	0	0	0	0	1
	Thelepus setosus	2	0	0	0	0	0	0	0	0	0	0	0	0	0	0	0	0	0	0	0	2
	Caecum someri	0	0	0	0	0	0	0	0	0	0	0	0	0	0	0	0	0	0	0	0	0
	Vitrinelidae spp.	0	0	1	1	0	0	0	0	0	0	0	0	0	0	0	0	0	0	0	0	2
	Finella dubia	1	1	2	3	2	2	4	1	5	3	0	0	0	0	0	0	0	0	0	0	24
	Natica pusilla	0	0	3	8	0	0	0	0	0	0	0	0	0	0	0	0	0	0	0	0	11
	Eulima sp.	0	0	2	0	0	0	0	0	0	0	0	0	0	0	0	0	0	0	0	0	2
	Nassarius vibex	0	1	0	0	0	0	0	0	0	3	0	0	0	0	0	0	0	0	0	0	4
	Olivella minuta	1	9	5	21	12	9	6	4	3	3	4	4	0	4	6	4	2	3	1	4	105
	Terebra sp.	0	0	1	1	0	0	0	0	0	0	0	0	0	0	0	0	0	0	0	0	2
	Odostomia sp.	1	1	8	13	0	1	1	2	5	2	0	0	0	0	0	0	0	0	0	0	34
	Odostomia virginae	3	1	10	9	6	1	2	16	25	22	6	2	1	4	5	1	4	7	3	7	135
	Eulimastoma surinamense	0	0	9	3	0	0	0	0	0	0	0	0	0	0	0	0	0	0	0	1	13
	Chrysalida jadisi	0	0	0	1	0	0	0	0	0	0	0	0	0	0	0	0	0	0	0	0	1
	Turbonilla spp.	2	0	6	5	2	0	1	1	2	4	0	0	0	0	0	0	0	0	0	0	23
	Iselica anomala	0	0	0	0	0	0	0	0	0	0	0	0	0	0	0	0	0	0	0	0	0
	Acteon sp.	0	0	0	0	0	0	0	0	0	0	0	0	0	0	0	0	0	0	0	0	0
	Acteocina bidentata	1	0	4	0	0	0	0	0	0	0	0	0	0	0	0	0	0	0	0	0	5
	Acteocina bullata	0	0	0	1	0	0	0	2	3	4	2	2	4	1	2	2	2	0	1	2	28
	Haminoea sp.	0	0	0	0	0	0	0	0	0	0	0	0	0	0	0	0	0	0	0	0	0
MOLLUSCA	*Volvulella texasiana*	0	0	0	0	0	0	0	0	0	0	0	0	0	1	0	0	0	0	0	0	1
	Melampus coffeus	0	8	2	0	0	0	0	0	0	0	0	0	0	0	0	0	0	0	0	0	10
	Nucula semiornata	3	4	9	6	8	12	16	25	22	7	21	20	5	28	38	9	27	33	11	23	327
	Anadara ovalis	3	0	1	4	1	0	0	0	0	0	0	0	0	1	0	0	0	0	0	0	10
	Leptopecten bavayi	0	0	1	1	0	0	0	0	0	0	0	0	0	0	0	0	0	0	0	0	2
	Trachycardium murictum	0	1	0	0	0	0	0	0	0	0	0	0	0	0	0	0	0	0	0	0	1
	Mulinia cleryana	0	0	0	0	0	0	0	0	0	0	0	0	0	0	0	0	0	0	0	0	0
	Mulinia aff. branneri	0	0	0	0	0	0	0	0	0	0	0	0	0	0	0	0	0	0	0	0	0
	Solen obliquus	0	0	0	0	0	0	0	0	0	0	0	0	0	0	0	0	0	0	0	0	0
	Tellina trinitatis	0	0	2	1	0	0	1	0	1	2	0	2	1	2	1	2	2	0	1	0	18
	Strigilla sp.	0	1	7	6	1	0	0	0	0	0	0	0	0	0	0	0	0	0	0	0	15
	Temnoconcha brasiliana	0	0	0	0	1	1	0	3	0	1	0	0	0	0	0	0	0	0	0	0	6
	Abra equalis	1	2	2	1	1	2	1	1	2	5	1	0	1	0	1	1	0	2	1	0	25
	Donax gemmula	0	1	8	5	1	0	2	0	4	1	0	0	0	0	0	0	0	0	0	0	22
	Chione cancellata	0	0	1	4	5	12	2	4	1	3	0	0	0	0	2	0	0	0	0	0	34
	Corbula caribaea	0	5	9	2	1	0	0	0	1	4	1	0	1	1	0	1	1	1	0	1	29
	Pandora bushiana	0	0	0	0	0	0	0	0	0	0	0	0	0	0	0	0	0	0	0	0	0
	Cardiomya perrostrata	0	0	0	0	0	0	0	0	0	1	0	0	0	0	0	0	1	0	0	0	2
	Dentalium cf. americanum	1	4	5	2	2	1	1	6	2	1	0	2	0	3	6	2	2	1	0	2	43

(Continuação)

CRUSTACEA	Harpacticoida *gen sp*	0	0	0	1	0	0	0	0	0	0	0	0	0	0	0	0	0	0	0	1
	Cypridina sp	0	0	0	0	0	0	0	0	0	0	0	0	0	0	0	0	0	0	0	0
	Podocopa *gen sp*	0	0	0	0	0	0	0	0	0	0	0	0	0	0	0	0	0	0	0	0
	Cytherella sp	0	0	0	0	0	0	0	0	0	0	0	0	0	0	0	0	0	0	0	0
	Bithocypris sp A	0	0	0	0	0	0	0	0	0	0	0	0	0	0	0	0	0	0	0	0
	Bithocypris sp B	0	0	0	0	0	0	0	0	0	0	0	0	0	0	0	0	0	0	0	0
	Macropyxis sp	0	0	0	0	0	0	0	0	1	0	0	0	0	0	0	0	0	0	0	1
	Cytheracea *sp A*	0	0	0	0	0	0	0	0	4	0	0	0	0	0	3	0	0	0	0	7
	Cytheracea *sp B*	0	0	0	0	0	0	0	0	0	0	0	0	0	0	0	0	0	0	0	0
	Neomonoceratina mediterranea	0	0	0	0	0	0	0	0	1	0	0	0	0	0	0	0	0	1	0	2
	Puriana sp	0	0	0	0	0	0	0	0	0	0	0	0	0	0	0	0	0	0	0	0
	Ampelisca paria	0	0	0	0	0	0	0	0	0	0	0	0	0	0	0	0	0	0	0	0
	Ampelisca pugetica	0	0	0	0	0	0	2	0	0	0	9	0	1	4	0	0	0	0	0	16
	Metharpinia sp	0	0	1	0	0	0	0	0	0	0	0	0	0	0	0	0	0	0	0	1
	Cirolana parva	0	0	0	1	2	0	0	0	0	0	0	0	0	0	0	0	0	0	0	3
	Excorallana oculata	0	0	0	0	0	0	0	0	0	0	0	1	0	0	0	0	0	0	0	1
	Alpheus sp	0	0	0	0	0	0	0	0	1	0	0	0	0	0	0	0	0	0	0	1
	Pinixia cristata	0	0	0	0	0	0	0	0	0	0	0	0	0	0	0	0	0	0	0	0
ECHINODERMATA	Ophiuroidea *sp*	6	5	0	0	0	0	1	0	0	0	0	0	0	0	0	0	0	0	0	12
	Mellita quinqueperforata	0	0	0	0	2	0	0	0	0	0	0	0	0	0	0	0	0	0	0	2
	TOTAL	**35**	**47**	**100**	**103**	**47**	**49**	**46**	**70**	**87**	**69**	**46**	**37**	**14**	**53**	**68**	**29**	**41**	**54**	**23**	**41**

(Continuação)

GRUPO	ESPÉCIE	Pluma																	Controle								
		P1	P3	P5	P7	P9	P11	P13	P15	P17	P18	P19	P21	P23	P25	P27	P29	A1	A2	A3	A4	A5	A6	A7	A8	A9	A10	TOTAL
	Harmothoe macginitei	0	0	0	0	0	0	0	0	0	0	0	0	0	0	0	0	0	0	0	0	0	0	0	0	0	0	**0**
	Linopherus ambigua	0	0	0	0	0	0	0	0	0	0	0	0	0	0	0	0	1	0	0	0	0	0	0	0	0	0	**1**
	Gyptis callithrix	1	0	0	0	0	0	0	0	0	0	0	0	0	0	0	0	0	0	0	0	0	0	0	0	0	0	**1**
	Eusyllinae gen. sp. A	0	0	0	0	0	0	0	0	0	0	0	0	0	0	0	0	0	0	0	0	0	0	0	0	0	0	**0**
	Neanthes bruaca	2	0	2	2	3	0	0	0	0	0	1	3	1	0	2	0	3	1	1	0	1	1	3	3	2	0	**31**
	Aglaophamus juvenalis	0	0	0	0	0	0	0	0	0	0	0	0	0	0	0	0	0	0	0	0	0	0	0	0	0	0	**0**
	Glycera cf. convoluta	0	0	0	0	1	0	0	0	0	0	0	0	0	0	0	0	0	0	0	0	0	0	0	0	0	0	**1**
	Glycera sp. A	0	0	0	0	0	0	0	0	0	0	0	0	0	0	0	0	0	0	0	0	0	0	0	0	0	0	**0**
	Goniada brunnea	0	0	0	0	0	0	0	0	0	0	0	0	1	0	0	0	0	0	1	0	0	0	0	0	0	0	**2**
	Glycinde multidens	0	0	0	0	0	0	0	1	0	0	0	0	1	0	0	0	0	0	0	0	0	0	0	0	0	0	**2**
	Parandalia tricuspis	0	0	0	0	0	1	0	0	0	0	0	0	0	0	0	0	0	0	0	0	0	0	1	0	0	0	**2**
	Sigambra grubei	1	0	0	0	0	0	0	0	0	0	0	0	0	0	0	0	0	0	0	0	0	0	0	0	0	0	**1**
	Diopatra cuprea	0	0	0	0	0	0	0	0	0	0	0	2	0	0	0	0	0	0	0	0	0	0	0	0	0	0	**2**
POLYCHAETA	*Nematonereis schamardae*	0	0	0	0	0	0	0	0	0	0	0	0	0	0	0	0	0	0	0	0	0	0	0	0	0	0	**0**
	Lumbrineris sp.	0	0	0	0	0	0	0	0	0	0	0	0	0	0	0	0	0	0	0	0	0	0	0	0	0	0	**0**
	Ninoe brasiliensis	0	0	0	0	0	0	0	0	0	0	0	0	1	0	0	0	0	0	0	0	0	0	0	0	0	0	**1**
	Scoloplos (Scoloplos) sp. A	0	0	0	0	0	0	0	0	0	0	0	0	0	0	0	0	1	0	0	0	0	0	0	0	0	0	**1**
	Scoloplos (Leodamas) rubra	0	0	0	0	0	0	0	0	0	0	0	0	0	0	0	0	0	0	0	0	0	0	0	0	0	0	**0**
	Paraprionospio pinnata	0	0	0	1	0	3	0	0	3	0	2	1	0	2	0	0	0	1	0	1	0	0	0	0	0	0	**14**
	Prionospio sp. A	0	0	0	0	0	0	0	0	0	0	0	0	0	0	0	0	0	0	0	1	0	0	0	0	0	0	**1**
	Spiochaetopterus sp. A	0	0	0	0	0	0	0	0	0	0	0	0	0	0	0	1	0	0	0	0	0	0	0	0	0	0	**1**
	Capitellidae gen. sp.	0	0	0	0	0	0	0	0	0	0	0	0	0	0	0	0	0	0	0	0	0	0	0	0	0	0	**0**
	Magelona variolamellata	0	0	0	1	5	0	0	1	0	0	0	1	1	1	1	0	1	1	0	4	0	1	1	0	1	0	**20**
	Magelona posterolongata	0	0	2	1	9	1	0	1	0	0	1	0	0	0	0	0	1	2	2	0	0	0	0	0	1	0	**21**
	Owenia fusiformis	0	0	0	0	0	0	0	0	0	0	0	0	0	0	0	0	0	0	0	1	0	0	0	0	0	0	**1**
	Loimia medusa	0	0	0	0	0	0	0	0	0	0	0	0	0	0	0	0	0	0	0	0	0	0	0	0	0	0	**0**
	Thelepus setosus	0	0	0	0	0	0	0	0	0	0	0	0	0	0	0	0	0	0	0	0	0	0	0	0	0	0	**0**
	Caecum someri	0	0	0	0	0	0	0	0	0	0	0	0	0	0	0	0	1	0	0	0	0	0	0	0	0	0	**1**
	Vitrinelidae spp.	0	0	1	3	1	0	0	0	0	0	0	0	3	6	9	0	0	0	0	0	0	0	0	0	0	0	**23**
	Finella dubia	1	1	2	4	1	0	1	0	0	0	1	2	3	3	5	0	0	0	0	0	0	0	0	0	0	0	**24**
	Natica pusilla	0	0	2	7	0	0	0	0	0	0	1	2	3	5	11	0	1	4	7	3	2	5	0	6	0	0	**59**
	Eulima sp.	0	0	0	0	0	0	0	0	0	0	0	1	1	3	3	0	0	0	0	0	0	0	0	0	0	0	**8**
	Nassarius vibex	0	0	0	0	0	0	0	0	0	0	0	0	0	0	0	0	0	0	0	0	0	0	0	0	0	0	**0**
	Olivella minuta	8	10	6	10	3	3	4	4	5	4	2	1	2	2	0	1	2	14	13	2	9	4	6	8	2	0	**125**
	Terebra sp.	0	0	0	0	0	0	0	0	0	0	0	0	0	0	0	0	2	2	0	0	1	0	0	0	0	0	**5**
	Odostomia sp.	0	1	1	5	3	0	0	0	0	0	0	0	1	1	0	0	1	3	0	0	1	0	0	0	0	0	**17**
	Odostomia virginae	5	14	17	28	7	9	11	15	16	27	14	12	7	5	6	2	3	4	11	5	7	6	1	3	1	0	**236**
	Eulimastoma surinamense	0	0	0	1	1	0	0	0	0	1	2	1	1	0	0	0	0	0	0	0	0	1	0	0	0	0	**8**
	Chrysalida jadisi	0	0	1	1	1	0	0	1	0	0	0	1	1	2	3	0	2	1	0	1	0	1	0	0	0	0	**16**
	Turbonilla spp.	1	3	8	8	3	0	0	1	2	2	2	4	10	16	10	4	5	8	12	6	3	2	0	3	1	0	**114**
	Iselica anomala	0	0	0	0	0	0	0	0	0	0	0	0	0	0	0	0	0	0	1	0	0	0	0	0	0	0	**1**
	Acteon sp.	0	0	0	1	1	0	0	0	0	0	0	0	0	0	1	0	0	0	0	8	0	0	0	0	0	0	**11**
	Acteocina bidentata	0	1	2	3	2	0	0	0	0	0	0	0	2	1	2	3	2	7	21	9	6	8	1	4	1	0	**75**
	Acteocina bullata	4	15	7	6	4	2	3	0	2	3	12	29	23	21	22	3	1	5	11	3	4	6	4	7	3	0	**200**
	Haminoea sp.	0	1	2	0	0	0	0	0	0	0	0	0	0	0	1	0	0	0	0	0	0	0	0	0	0	0	**4**
	Volvulella texasiana	1	0	2	1	1	0	0	0	0	0	1	1	2	3	2	1	2	2	3	1	0	1	1	0	0	0	**25**
MOLLUSCA	*Melampus coffeus*	0	0	0	0	0	0	0	0	0	0	0	0	0	0	0	0	0	1	0	0	0	0	0	0	0	0	**1**
	Nucula semiornata	23	47	15	17	7	13	27	26	45	44	32	13	6	13	7	6	4	20	14	3	2	3	3	5	2	0	**397**
	Anadara ovalis	0	0	2	5	1	0	0	0	0	2	0	1	1	1	2	0	0	0	0	0	0	0	0	0	0	0	**15**
	Leptopecten bavayi	0	0	0	2	1	0	0	0	0	0	0	0	1	1	1	0	0	0	0	0	0	0	0	0	0	0	**6**
	Trachycardium muricтum	0	1	0	0	1	0	0	0	0	0	0	1	0	0	0	0	0	0	0	0	0	0	0	0	0	0	**3**
	Mulinia cleryana	1	0	0	1	0	0	0	0	1	0	0	0	0	0	0	0	0	0	0	0	1	0	0	0	0	0	**4**
	Trachycardium muricтum	0	1	0	0	1	0	0	0	0	0	0	1	0	0	0	0	0	0	0	0	0	0	0	0	0	0	**3**
	Mulinia cleryana	1	0	0	1	0	0	0	0	1	0	0	0	0	0	0	0	0	0	0	0	1	0	0	0	0	0	**4**
	Mulinia aff. branneri	0	0	0	0	0	0	0	1	1	1	0	0	0	0	0	0	0	0	0	0	0	0	0	0	0	0	**3**
	Solen obliquus	0	0	0	0	1	0	0	0	0	0	0	0	0	0	0	0	0	0	0	0	0	0	0	0	0	0	**1**
	Tellina trinitatis	0	0	3	2	0	0	0	1	2	1	1	0	1	1	3	1	2	2	2	1	0	1	2	2	1	0	**29**
	Strigilla sp.	0	0	0	0	0	0	0	0	0	0	0	0	0	0	0	0	0	1	1	0	0	0	0	0	0	0	**2**
	Temnoconcha brasiliana	0	0	1	8	3	0	1	0	1	0	0	1	1	1	0	0	0	1	0	0	1	0	1	0	1	0	**21**
	Abra equalis	4	3	7	18	11	0	1	1	2	0	4	10	12	14	12	2	2	3	5	1	2	3	3	4	2	0	**126**
	Donax gemmula	0	0	0	0	0	0	0	0	0	0	0	0	0	0	0	0	0	0	0	0	0	0	0	0	0	0	**0**
	Chione cancellata	0	0	3	2	1	0	0	0	0	0	1	1	1	2	2	2	2	1	4	2	1	1	1	0	1	0	**28**
	Corbula caribaea	0	4	7	11	3	0	0	0	1	2	3	6	8	14	11	4	2	2	15	1	4	1	5	1	3	0	**108**
	Pandora bushiana	0	1	0	0	0	0	0	0	0	0	0	0	0	0	0	0	0	1	0	0	0	0	0	0	0	0	**2**
	Cardiomya perrostrata	1	1	1	1	0	0	0	0	0	0	0	1	1	0	0	0	1	0	0	0	1	0	1	0	0	0	**9**
	Dentalium cf. americanum	6	9	17	18	7	2	0	2	2	9	5	6	5	4	6	5	10	12	9	6	4	7	8	6	4	0	**169**
	Harpacticoida *gen sp*	0	0	0	0	0	0	0	0	0	0	0	0	0	0	0	0	0	0	0	0	0	0	0	0	0	0	**0**
	Cypridina sp	0	0	0	0	0	0	0	0	0	0	0	0	0	0	0	0	0	0	0	0	0	0	1	0	0	0	**1**
	Podocopa *gen sp*	0	0	0	3	0	0	0	0	0	0	0	0	0	0	0	0	0	0	0	0	0	0	0	0	0	0	**3**
	Cytherella sp	0	0	1	2	0	0	0	0	0	0	0	0	0	0	1	0	0	0	0	0	0	0	0	0	0	0	**4**
	Bithocypris sp A	0	0	1	0	0	0	0	0	0	0	0	0	0	0	2	0	0	0	0	0	0	0	0	0	0	0	**3**
	Bithocypris sp B	0	0	0	0	0	0	0	0	0	0	0	0	0	0	2	0	0	0	0	0	0	0	0	0	0	0	**2**
	Macropyxis sp	0	0	0	2	0	0	0	0	0	0	0	0	0	0	1	1	0	0	0	0	0	0	0	0	0	0	**4**
	Cytheracea *sp A*	0	0	9	2	0	0	0	0	0	0	0	0	0	0	0	0	0	0	0	0	0	0	0	0	0	0	**11**
CRUSTACEA	Cytheracea *sp B*	0	0	2	0	0	0	0	0	0	0	0	0	0	0	0	1	0	0	0	0	0	0	0	0	0	0	**3**
	Neomonoceratina mediterranea	0	0	12	23	0	0	0	0	0	0	0	0	0	0	6	0	0	0	0	0	0	0	0	0	0	0	**41**
	Puriana sp	0	0	0	3	0	0	0	0	0	0	0	0	0	0	0	0	0	0	0	0	0	0	0	0	0	0	**3**
	Ampelisca paria	0	0	0	0	1	0	0	0	0	0	0	0	0	0	0	0	0	0	0	0	0	1	1	0	0	0	**3**
	Ampelisca pugetica	0	0	0	8	0	0	0	0	0	0	0	0	0	0	0	0	0	0	0	0	0	0	0	0	0	0	**8**
	Metharpinia sp	0	0	0	0	0	0	0	0	0	0	0	0	0	0	0	0	0	0	0	0	0	0	0	0	0	0	**0**
	Cirolana parva	0	0	0	0	0	0	0	0	0	0	0	0	0	0	0	0	0	0	0	0	0	0	0	0	0	0	**0**
	Excorallana oculata	0	0	0	0	0	0	0	0	0	0	0	0	0	0	0	0	0	0	0	0	0	0	0	0	0	0	**0**
	Alpheus sp	0	0	0	0	0	0	0	0	0	0	0	0	0	0	0	0	0	0	0	0	0	0	0	0	0	0	**0**
	Pinixia cristata	0	0	0	0	0	0	0	0	0	0	0	0	0	0	0	0	0	0	0	0	0	0	0	0	0	0	**0**
ECHINODERMATA	Ophiuroidea *sp*	0	0	0	0	0	0	0	0	0	0	0	0	0	0	0	0	0	0	0	0	0	0	0	0	0	0	**0**
	Mellita quinquеperforata	0	0	0	0	0	0	0	0	0	0	0	0	0	0	0	0	0	0	0	0	0	0	0	0	0	0	**0**
	TOTAL	**59**	**112**	**136**	**211**	**83**	**34**	**48**	**55**	**83**	**96**	**85**	**101**	**99**	**123**	**135**	**37**	**50**	**98**	**136**	**57**	**51**	**53**	**45**	**52**	**26**	**0**	

ANEXO X

- Lista taxonômica das espécies registradas durante as campanhas de monitoramento, entre Março/2006 e Março/2007.
- Dados de captura total entre as diferentes estações analisadas, ao longo das campanhas, 1 (Mar/2006), 2 (Jun/2006), 3 (Set/2006) e 4 (Mar/2007), separados por espécie.

Lista taxonômica das espécies registradas durante as campanhas de monitoramento, entre Março/2006 e Março/2007

Classe Elasmobranchii
Ordem Carcharhiniformes
Família Carcharninida
Rhizoprionodon porosus (Poey, 1861)
Ordem Rajiformes
Família Dasyatidae
Dasyatis guttata (Bloch & Schneider, 1801)
Família Myliobatidae
Aetobatus narinari (Euphrasen, 1790)
Classe Actinopterygii
Ordem Anguiliformes
Família Ophichthidae
Ophichthus parilis (Richardson, 1848)
Ordem Clupeiformes
Família Engraulidae
Anchoa filifera (Fowler, 1915)
Anchoa januaria Hildebrand, 1943
Anchoa lyolepis (Evermann & Marsh, 1092)
Anchoa marinii Hildebrand, 1943
Anchoa spinifera (Valenciennes, 1848)
Anchoa tricolor (Agassiz, 1829)
Anchoa phrygiatus
Centrengraulis edentulus (Cuvier, 1829)
Lycengraulis grossidens (Agassiz, 1829)
Família Pristigasteridae
Chirocentrodon bleekerianus (Poey, 1867)

Odontognathus mucronatus (Lacépéde, 1800)
Pellona harroweri (Fowler, 1919)
Família Clupeidae
Opisthonema oglinum (Lesueur, 1818)
Ordem Siluriformes
Família Ariidae
Arius phrygiatus (Valenciennes, 1840)
Aspistor luniscutis (Valenciennes, 1840)
Bagre bagre (Linnaeus, 1758)
Bagre marinus (Mitchill, 1815)
Cathorops spixii (Agassiz, 1829)
Genidens barbus (Lacépéde, 1800)
Genidens luteus
Genidens genidens (Cuvier, 1829)
Notarius grandicassis (Valenciennes, 1840)
Sciades proops (Valenciennes, 1840)
Ordem Aulopiformes
Família Synodontidae
Synodus foetens (Linnaeus, 1766)
Ordem Lophiiformes
Família Ogcocephalidae
Ogcocephalus vespertilio (Linnaeus, 1758)
Ordem Scorpaeniformes
Família Triglidae
Prionotus punctatus (Bloch, 1793)
Família Dactylopteridae

Dactylopterus volitans (Linnaeus, 1758)
Ordem Perciformes
Família Serranidae
Diplectrum radiale (Quoy & Gaimard, 1824)
Rypticus randalli Courtenay, 1967
Família Carangidae
Chloroscombrus chrysurus (Linnaeus, 1766)
Carangoides bartholomaei (Cuvier, 1833)
Selene vomer (Linnaeus, 1758)
Selene setapinnis (Mitchill, 1815)
Família Gerreidae
Diapterus rhombeus (Cuvier, 1829)
Diapterus radiale (Cuvier, 1829)
Eucinostomus argenteus Baird & Girard, 1855
Eucinostomus gula (Quoy & Gaimard, 1824)
Família Haemulidae
Conodon nobilis (Linnaeus, 1758)
Genyatremus luteus (Bloch, 1790)
Pomadasys corvinaeformis (Steindachner, 1868)
Família Sparidae
Calamus pennatula Guichenot, 1868
Família Polynemidae
Polydactylus virginicus (Linnaeus, 1758)
Família Sciaenidae
Ctenosciaena gracilicirrhus (Metzelaar, 1919)
Cynoscion acoupa (Lacépéde, 1801)

Cynoscion jamaicensis (Vaillant & Bocourt, 1883)
Cynoscion microlepidotus (Cuvier, 1830)
Cynoscion leiarchus (Cuvier, 1830)
Isopisthus parvipinnis (Cuvier, 1830)
Larimus breviceps Cuvier, 1830
Macrodon ancylaman (Bloch & Schneider, 1801)
Menticirrhus americanus (Linnaeus, 1758)
Menticirrhus littoralis (Holbrook, 1847)
Micropogonias furnieri (Desmarest, 1823)
Nebris microps (Curvier, 1830)
Paralonchurus brasiliensis (Steindachner, 1875)
Stellifer brasiliensis (Schultz, 1945)
Stellifer rastrifer (Jordan, 1889)
Stellifer stellifer (Bloch, 1790)
Stellifer sp.
Família Ephippidae
Chaetodipterus faber (Broussonet, 1782)
Família Scaridae
Nicholsina usta (Valenciennes, 1840)
Família Stromateidae
Peprilus paru Linnaeus, 1758
Família Trichiuridae
Trichiurus lepturus Linnaeus, 1758
Ordem Pleuronectiformes
Família Paralichthyidae
Citharichthys macrops (Dresel, 1885)

Etropus crossotus Jordan & Gilbert, 1882
Syacium papillosum (Linnaeus, 1758)
Família Achiridae
Achirus declivis Chabanaud, 1940
Trinectes microphthalmus Chabanaud, 1928
Trinectes paulistanus (Miranda-Ribeiro, 1915)
Família Cynoglossidae
Symphurus plagusia (Bloch & Schneider, 1801)
Symphurus tesselatus (Quoy & Gaimard, 1824)
Ordem Tetraodontiformes
Família Tetraodontidae
Lagocephalus laevigatus (Linnaeus, 1766)
Sphoeroides testudineus (Linnaeus, 1766)
Cyclichthys spinosus (Linnaeus, 1758)
Família Diodontidae
Cyclichthys spinosus (Linnaeus, 1756)
Sphoeroides spengleri (Bloch, 1785)
Sphoeroides testudineus (Linnaeus, 1758)
Lagocephalus laevigatus (Linnaeus, 1766)

Dados de captura total entre as diferentes estações analisadas, ao longo das campanhas, 1 (Mar/2006), 2 (Jun/2006), 3 (Set/2006) e 4 (Mar/2007), separados por espécie

	Controle				Canal				Pluma A				Pluma B				Descarte				Total			
Espécie	**1**	**2**	**3**	**4**	**1**	**2**	**3**	**4**	**1**	**2**	**3**	**4**	**1**	**2**	**3**	**4**	**1**	**2**	**3**	**4**	**1**	**2**	**3**	**4**
Achirus declivis	0	0	0	0	0	0	0	0	0	4	0	0	0	2	0	0	0	0	0	0	0	6	0	0
Aetobatus narinari	0	0	0	0	0	1	0	0	0	0	0	0	0	0	0	0	0	0	0	0	0	1	0	0
Anchoa filifera	0	0	2	1	0	0	7	0	1	0	2	0	3	0	5	1	1	0	1	0	5	0	17	2
Anchoa januaria	1	0	0	0	0	0	0	0	1	0	0	0	0	0	0	0	1	0	2	0	3	0	2	0
Anchoa lyoleps	0	0	0	0	0	0	5	0	4	0	1	0	0	0	2	0	3	0	3	0	7	0	11	0
Anchoa marinii	0	0	0	0	1	0	0	0	0	0	0	0	0	0	0	0	0	0	0	0	1	0	0	0
Anchoa spinifera	0	0	5	0	41	1	40	0	16	5	7	1	6	1	1	0	56	2	18	2	119	9	71	3
Anchoa tricolor	2	0	0	0	0	0	0	0	0	0	0	0	0	0	0	0	0	0	0	0	2	0	0	0
Arius phrygiatus	0	0	0	0	0	2	0	0	1	0	0	0	0	0	0	0	0	0	0	0	1	2	0	0
Aspistor luniscutis	1	10	11	24	3	38	10	8	8	12	7	3	0	8	7	14	4	8	4	3	16	76	39	52
Bagre bagre	0	2	4	0	0	2	5	0	3	0	3	0	0	2	5	0	1	0	1	1	4	6	18	1
Bagre marinus	0	0	1	1	2	1	0	0	9	0	1	0	1	0	0	0	0	1	0	1	12	2	2	2
Calamus pennatula	0	0	0	0	0	0	0	0	0	0	0	0	0	0	0	1	0	0	0	0	0	0	0	1
Carangoides bartholomaei	0	0	0	0	0	0	0	2	0	0	0	0	0	0	0	0	0	0	0	0	0	0	0	2
Cathorops arenatus	0	0	0	0	0	0	9	0	0	0	9	0	0	0	3	0	0	0	2	0	0	0	23	0
Cathorops spixii	0	0	0	0	0	68	19	0	0	8	9	0	0	36	4	0	0	0	11	0	0	112	43	0
Cetengraulis edentulus	0	1	1	0	0	1	0	0	1	0	0	0	0	0	0	0	1	0	2	0	2	2	3	0
Chaetodipterus faber	0	5	0	4	4	0	0	0	2	0	0	4	10	3	2	3	7	1	0	9	23	9	2	20
Chirocentrodon bleekerianus	0	1	1	18	34	0	0	0	5	0	4	0	2	3	8	0	16	1	0	0	57	5	13	18
Chloroscombrus chrysurus	2	0	0	0	0	0	0	2	0	0	1	26	0	0	2	2	0	0	0	9	2	0	3	39
Conodon nobilis	0	0	2	4	0	0	0	0	1	0	3	0	2	0	5	1	0	0	0	0	3	0	10	5
Ctenosciena gracilicirrhus	0	0	0	5	2	0	0	0	0	0	0	1	39	0	0	0	1	0	0	1	42	0	0	7
Citharichthys macrops	0	1	0	0	0	0	0	0	0	0	0	0	0	1	0	0	0	0	0	0	0	2	0	0
Cyclichthys spinosus	0	2	0	0	0	0	0	0	0	0	0	0	0	3	0	2	0	4	0	0	0	9	0	2
Cynoscion acoupa	0	0	0	0	0	2	0	0	0	0	0	0	0	0	0	0	0	0	0	0	0	2	0	0
Cynoscion jamaicensis	1	0	0	0	0	3	0	2	0	3	1	1	5	0	0	0	0	0	4	0	6	6	5	3
Cynoscion leiarchus	0	0	0	12	0	0	0	7	0	0	0	16	0	0	0	28	0	0	0	19	0	0	0	82
Cynoscion microlepidotus	0	0	6	0	0	3	1	0	0	0	3	7	0	1	4	0	0	0	5	0	0	4	19	7
Cynoscion virescens	0	0	0	0	0	0	1	0	0	0	0	0	0	0	0	0	0	0	0	0	0	0	1	0
Dactylopterus volitans	0	0	0	0	0	0	0	1	0	0	0	0	0	0	0	0	0	0	0	0	0	0	0	1
Dasyatis guttata	0	1	0	2	1	1	0	1	3	0	0	4	0	0	0	0	3	0	0	3	7	2	0	10

(Continuação)

	Controle				Canal				Pluma A				Pluma B				Descarte				Total			
Espécie	**1**	**2**	**3**	**4**	**1**	**2**	**3**	**4**	**1**	**2**	**3**	**4**	**1**	**2**	**3**	**4**	**1**	**2**	**3**	**4**	**1**	**2**	**3**	**4**
Diapterus rhombeus	4	0	0	5	1	0	0	5	0	0	0	1	3	0	0	0	0	0	0	2	8	0	0	13
Diplectrum radiale	1	0	0	1	0	0	0	5	0	0	0	1	1	0	0	0	0	0	0	0	2	0	0	7
Etropus crossotus	4	10	1	11	12	0	0	9	18	0	0	21	45	2	2	4	0	0	0	4	79	12	3	49
Eucinostomus argenteus	8	0	0	7	0	0	0	338	0	0	0	40	1	0	0	138	0	0	0	5	9	0	0	528
Eucinostomus gula	1	0	0	0	0	0	0	5	0	0	0	62	0	0	0	4	0	0	0	0	1	0	0	71
Genidens barbus	0	0	0	0	0	0	0	0	3	0	0	0	0	0	0	0	0	0	0	0	3	0	0	0
Genidens genidens	0	0	0	0	0	1	0	0	0	0	0	0	0	0	0	0	0	0	0	1	0	1	0	1
Genyatremus luteus	0	0	0	0	0	0	0	0	0	0	0	8	0	0	0	0	2	0	0	3	2	0	0	11
Isopisthus parvipinnis	0	1	76	1	11	1	19	0	32	4	56	0	17	5	32	0	20	5	49	0	80	16	232	1
Lagocephalus laevigatus	0	2	0	0	0	0	0	1	2	1	0	2	0	0	0	1	0	0	0	0	2	3	0	4
Larimus breviceps	0	24	21	4	13	5	0	0	42	2	1	0	79	6	6	0	37	3	1	4	171	40	29	8
Lycengraulis grossidens	4	0	0	11	1	0	0	2	0	0	1	1	0	0	0	0	0	1	0	2	5	1	1	16
Macrodon ancylaman	0	3	23	0	1	2	5	0	1	2	9	0	2	1	4	0	0	6	12	1	4	14	53	1
Menticirrhus americanus	0	6	1	1	0	1	0	2	0	2	0	24	13	2	1	3	2	1	0	32	15	12	2	62
Menticirrhus litoralis	0	0	0	2	5	0	1	4	1	0	0	15	0	0	0	6	0	0	0	1	6	0	1	28
Micropogonias furnieri	0	0	0	0	0	0	0	0	0	0	0	1	0	0	0	0	0	0	0	0	0	0	0	1
Nebris microps	0	1	4	0	0	1	6	0	9	4	9	0	18	6	5	0	0	1	13	0	27	13	37	0
Nicholsina usta	0	0	0	0	0	0	0	1	0	0	0	1	0	0	0	0	0	0	0	0	0	0	0	2
Notarius grandicassis	0	1	0	0	0	0	0	0	0	0	0	0	1	0	0	0	0	0	0	0	1	1	0	0
Odontognathus mucronatus	0	1	124	0	4	1	56	0	14	1	88	0	45	1	35	0	13	2	66	0	76	6	369	0
Ogcocephalus vespertilio	0	0	0	0	0	0	0	0	0	0	0	1	0	0	0	0	0	0	0	0	0	0	0	1
Ophichthus parilis	0	3	0	0	0	0	0	0	1	0	1	0	0	0	0	0	0	0	0	0	1	3	1	0
Opisthonema oglinum	0	0	0	0	0	0	0	0	0	0	0	5	0	0	0	0	0	0	0	0	0	0	0	5
Orthopristis ruber	0	0	0	0	0	0	0	0	0	0	1	0	0	0	0	0	0	0	0	0	0	0	1	0
Paralonchurus brasiliensis	0	20	18	0	6	13	39	0	16	16	14	0	35	27	17	0	18	2	8	0	75	78	96	0
Pellona harroweri	0	9	17	10	81	0	9	3	27	0	1	0	12	13	10	0	138	6	5	0	258	28	42	13
Peprilus paru	2	0	0	0	2	0	0	0	0	3	0	0	0	3	1	0	0	3	0	10	4	9	1	10
Polydactylus virginicus	0	3	1	2	4	0	0	0	3	0	0	0	3	2	1	0	6	0	1	0	16	5	3	2
Pomadasys corvinaeformis	1	0	0	0	0	0	0	0	0	0	0	0	0	0	0	0	0	0	0	0	1	0	0	0
Prionotus nudigula	0	0	1	0	0	0	0	0	0	0	0	0	0	0	0	0	0	0	2	0	0	0	3	0
Prionotus punctatus	1	3	1	0	3	0	0	0	0	0	5	0	4	0	3	0	0	0	1	2	8	3	10	2

(Continuação)

	Controle				Canal				Pluma A				Pluma B				Descarte				Total			
Espécie	**1**	**2**	**3**	**4**	**1**	**2**	**3**	**4**	**1**	**2**	**3**	**4**	**1**	**2**	**3**	**4**	**1**	**2**	**3**	**4**	**1**	**2**	**3**	**4**
Rhizoprionodon porosus	3	0	0	0	0	0	0	0	0	0	0	0	0	0	0	0	0	0	0	0	3	0	0	0
Rypticus randalli	0	0	0	0	0	0	0	0	1	0	0	0	4	0	0	0	0	0	0	0	5	0	0	0
Sciades proops	0	0	0	0	0	0	0	0	0	0	0	1	0	1	0	0	4	2	0	0	4	3	0	1
Selene setapinnis	0	3	0	0	0	0	0	0	0	1	0	0	0	0	0	0	0	0	0	3	0	4	0	3
Selene vomer	0	0	0	1	0	0	0	0	0	0	0	1	3	0	0	0	0	0	0	1	3	0	0	3
Sphoeroides spengleri	0	0	0	1	0	0	0	4	0	0	0	4	0	0	0	0	0	0	0	3	0	0	0	12
Sphoeroides testudineus	0	0	0	1	0	0	0	1	1	0	0	0	0	1	0	0	0	0	0	1	1	1	0	3
Stellifer brasiliensis	0	37	100	0	1	6	39	0	157	10	45	1	33	25	43	0	72	1	40	0	263	79	267	1
Stellifer rastrifer	0	3	7	0	0	19	15	0	7	6	2	0	9	1	0	0	1	1	89	0	17	30	113	0
Stellifer sp.	0	0	0	0	0	1	0	0	0	4	1	0	0	0	0	0	0	0	0	0	0	5	1	0
Stellifer stellifer	0	1	72	1	0	2	39	0	74	7	16	0	37	36	13	0	13	1	137	0	124	47	277	1
Syacium papillosum	3	4	0	0	0	0	0	0	0	2	0	0	0	6	0	1	0	1	0	0	3	13	0	1
Symphurus plagusia	0	0	0	0	0	0	0	0	1	1	1	0	5	1	1	0	0	0	0	0	6	2	2	0
Symphurus tesselatus	2	20	8	4	11	20	15	0	28	56	43	0	14	57	24	0	7	3	13	0	62	156	103	4
Synodus foetens	0	0	0	0	0	0	0	4	0	0	0	3	0	0	0	2	0	0	0	1	0	0	0	10
Trichiurus lepturus	0	0	1	0	0	0	0	0	2	0	0	0	1	0	0	0	0	0	0	0	3	0	1	0
Trinectes microphthalmus	0	1	0	0	0	0	0	0	0	0	0	0	9	4	4	0	0	0	3	0	9	5	7	0
Trinectes paulistanus	0	5	0	0	0	9	3	2	1	0	0	0	0	2	1	0	0	0	1	1	1	16	5	3
Total de indivíduos	**41**	**184**	**509**	**134**	**244**	**205**	**343**	**409**	**496**	**154**	**345**	**256**	**462**	**262**	**251**	**211**	**427**	**56**	**494**	**125**	**1670**	**861**	**1942**	**1135**
Total de espécies	**17**	**30**	**26**	**25**	**23**	**26**	**21**	**22**	**35**	**31**	**30**	**28**	**32**	**22**	**30**	**16**	**24**	**22**	**27**	**27**	**56**	**46**	**43**	**51**

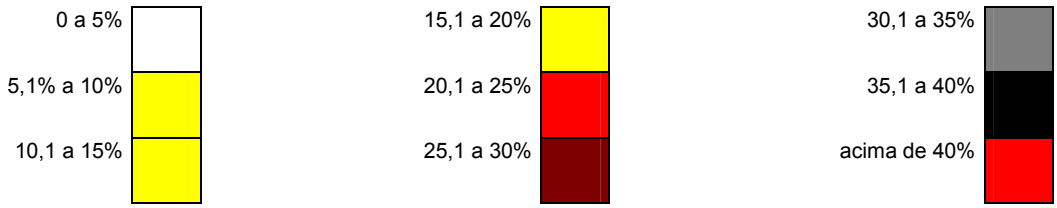

ANEXO Y

Matriz de Avaliação de Impactos

Atividade	Impacto	Meio	Classificação	Magnitude	Intervenção	Incidência	Abrangência	Ocorrência	Probabilidade	Duração	Reversibilidade	Relevância
Atividade: 1 Mobilização de Equipamentos	1a - Ocupação espaços e remoção de atividades existentes	Físico	N	B	T	D	L	C	C	T	R	M
	1b - Interferência e incompatibilidade com operações do Terminal	Físico	N	B	A	D	L	I	P	T	R	B
	1c - Ocupação de áreas de atividades tradicionais (pesca)	Físico	N	M	A	D	L	C	P	T	M	M
	1d - Risco de encalhes e deriva de embarcações	Físico	N	A	A	D	P	I	R	T	M	B
	1e - Risco de acidentes devido às condições físicas e de manutenção das embarcações	Físico	N	A	A	D	P	I	R	T	M	B
	1f - Riscos de colisões (inclusive envolvendo embarcações miúdas e aparatos de pesca)	Físico	N	A	A	D	P	I	R	T	M	B
	1g - Introdução de espécies exóticas	Biótico:	N	M	A	D	R	L	R	P	M	A
	1h - Utilização da disponibilidade local de embarcações pesqueiras e de outros serviços	Sócio-econômico	P	M	T	D	R	L	C	C	R	M
	1i - Conflitos com atividades turísticas (turismo embarcado);	Sócio-econômico	P	M	T	I	R	L	C	C	R	M
Atividade: 2 Mobilização de Pessoal	2a - Expansão das áreas de serviços (hospedagem, alimentação, etc)	Físico	N	B	T	I	R	C	R	T	R	B
	2b - Aumento de resíduos e esgotos	Físico	N	M	T	I	L	C	R	T	M	B
	2c - Transmissão de doenças;	Biótico	N	M	T	I	R	M	R	C	M	M
	2d - Proliferação de vetores (mosquitos, ratos, etc.)	Biótico	N	B	T	I	L	I	P	T	M	B
	2e - Oferta de postos de trabalho e aumento da renda	Sócio-econômico	P	A	T	D	R	I	C	T	P	A
	2f - Uso dos equipamentos sociais locais (escolas, creches, hospitais etc)	Sócio-econômico	N	B	T	D	R	M	R	T	R	B
	2g - Maior recolhimento de impostos	Sócio-econômico	P	A	T	I	R	M	C	P	P	A
	2h - Utilização da infraestrura urbana e turística;	Sócio-econômico	P	M	T	D	R	L	C	P	P	M
Atividade: 3 Circulação de embarcações	3a - Emissão de poluentes atmosféricos (motores de combustão)	Físico	N	M	T	I	L	I	R	T	M	B
	3b - Emissão de ruídos	Físico	N	M	A	D	P	I	P	C	R	B
	3c - Riscos de vazamentos de combustíveis e substâncias nocivas (inclui esgotamento sanitário da draga)	Físico	N	A	A	D	P	I	R	T	M	B
	3d - Riscos de colisão e naufrágios	Físico	N	A	A	D	P	I	R	T	M	B
	3e - Formação de ondas e suspensão de sedimentos do fundo	Físico	N	M	A	I	P	I	P	T	M	B
	3f - Interferência no comportamento de cetáceos e risco de colisões	Biótico	N	A	A	I	R	C	R	C	R	M
	3g - Interferência nas áreas de pesca	Sócio-econômico	N	M	A	I	P	C	R	T	R	B
Atividade: 4 Remoção de Sedimentos	4a - Disponibilização de materiais (particulado, nutrientes, substâncias químicas) na coluna líquida	Físico	N	A	A	D	P	I	C	T	R	A
	4b - Aumento da turbidez em forma de pluma;	Físico	N	A	A	I	L	I	M	T	R	A
	4c - Transporte e sedimentação de sedimentos suspensos na coluna d'água	Físico	N	A	A	I	L	I	M	T	M	A
	4d - Escorregamento de taludes	Físico	N	B	A	I	P	M	R	T	M	B
	4e - Supressão das comunidades bentônicas nas superfícies dragadas (taludes e fundo do canal)	Biótico	N	A	A	D	P	C	C	C	R	A
	4f - Interferência no plâncton devido à ressuspensão do sedimento	Biótico	N	M	A	I	L	C	M	C	R	A
	4g - Substituição de espécies da ictiofauna	Biótico	N	A	A	I	L	M	P	C	M	A
	4h - Interferência na Biota em áreas de sedimentação	Biótico	N	A	A	I	L	I	P	T	R	M
	4i - Perda temporária de biodiversidade (Plâncton, bentos)	Biótico	N	B	A	I	L	M	P	C	M	M
	4j - Disponibilização de novos nichos para recrutamento	Biótico	P	A	A	I	P	C	C	C	R	B
	4l - Interferência na movimentação de embarcações no local;	Sócio-econômico	N	M	A	I	P	I	P	T	R	B
	4m - Perda de produção de camarões	Sócio-econômico	N	A	A	I	P	C	P	T	R	M
Atividade: 5 Modificação geométrica do canal	5a - Alteração do regime de circulação da água na área de influência	Físico	N	B	A	I	L	L	R	P	I	M
	5b - Mudança do regime de erosão e sedimentação costeira	Físico	N	B	A	I	L	L	R	P	I	M
	5c - Alteração da pluma de sedimentos do rio Caravelas	Físico	N	B	A	I	L	L	R	P	I	M
	5d - Alteração na estrutura da comunidade bentônica no canal	Biótico	N	A	A	I	L	L	R	P	I	A
	5e - Efeitos sobre a biota devido às alterações de circulação, processos costeiros e transporte de sedimentos	Biótico	N	M	A	I	P	I	R	P	I	M
	5f - Alteração do regime de tráfego rodoviário de carretas	Sócio-econômico	P	A	T	I	R	L	C	P	R	A
	5g - Aumento de renda pela operação do terminal	Sócio-econômico	P	M	T	I	R	I	C	P	R	M
Atividade: 6 Deposição na cisterna (com overflow)	6a - Disponibilização de materiais (particulado, nutrientes, substâncias químicas) na coluna líquida	Físico	N	A	A	D	L	I	M	C	R	A
	6b - Aumento da turbidez em forma de pluma	Físico	N	A	A	D	L	I	M	T	R	A
	6c - Transporte e sedimentação de sedimentos suspensos na coluna d'água	Físico	N	M	A	I	L	I	R	T	R	B
	6d - Interferência momentânea no comportamento alimentar de organismos filtradores	Biótico	N	B	A	D	P	I	M	C	R	B
	6e - Aumento de espécies planctônicas (diatomáceas e dinoflagelados) devido à disponibilização de sedimento em suspensão	Biótico	P	M	A	I	P	C	C	C	R	B
Atividade: 7 Posicionamento e abertura da cisterna	7a - Risco de deposição em área indevida	Físico	N	B	A	D	L	I	R	T	R	B
	7b - Pluma de sedimentos imprevista	Físico	N	M	A	I	L	I	R	T	R	B
	7c - Impactos indiretos sobre pesca e extrativismo decorrentes dos impactos sobre o meio Biótico.	Sócio-econômico	N	M	A	I	P	C	M	C	M	A
Atividade: 8 Deposição do sedimento na Área de Descarte	8a - Disponibilização de materiais (particulado, nutrientes, substâncias químicas) na coluna líquida	Físico	N	A	A	D	P	I	C	T	R	A
	8b - Aumento da turbidez em forma de pluma	Físico	N	A	A	I	L	I	C	T	R	A
	8c - Transporte e sedimentação de sedimentos suspensos na coluna d'água.	Físico	N	M	A	D	L	I	P	T	R	M
	8d - Supressão das comunidades bentônicas na área de deposição	Biótico	N	A	A	D	P	I	C	C	R	A
	8e - Aumento de espécies planctônicas (diatomáceas e dinoflagelados) devido à disponibilização do sedimento	Biótico	N	B	A	D	L	I	C	T	M	A
	8f - Disponibilização de novos nichos para recrutamento da biota	Biótico	P	M	A	I	P	C	M	C	R	B
	8g - Perda temporária de biodiversidade	Biótico	N	A	A	I	L	C	C	C	M	A
	8h - Impactos indiretos sobre pesca e extrativismo decorrentes dos impactos sobre o meio Biótico	Sócio-econômico	N	B	A	I	P	C	P	T	R	M
Atividade: 9 Sobrelelevação do fundo na área de descarte	9a - Alteração do regime de circulação da água na área de influência	Físico	N	A	A	D	P	M	P	T	R	M
	9b - Disponibilização de novos nichos para recrutamento de larvas de animais bentônicos	Biótico	P	B	A	I	P	C	C	C	R	B
	9c - Obstrução à navegação	Sócio-econômico	N	M	A	D	P	M	R	T	R	B
Atividade: 10 Atividades de manutenção	10a - Descarte dos resíduos sólidos embarcados	Físico	N	M	A	D	L	C	R	T	M	B
	10b - Geração de entulhos e restos de manutenção	Físico	N	A	T	I	R	I	R	T	M	M
	10c - Risco de vazamento de óleo durante o abastecimento da draga no píer municipal	Físico	N	A	A	D	L	I	R	T	M	M
	10d - Proliferação de vetores	Biótico	N	M	T	D	L	C	P	T	M	M
	10e - Geração de receita	Sócio-econômico	P	M	T	D	R	L	C	P	R	M

Classificação		Magnitude		Intervenção		Incidência		Abrangência		Ocorrência		Probabilidade		Duração		Reversibilidade		Relevância	
P	Positivo	B	Baixa	A	Aquático	D	Direta	P	Pontual	I	Imediato	C	Certo	T	Temporário	R	Reversível	A	Alta
N	Negativo	M	Média	T	Terrestre	I	Indireta	L	Local	C	Curto	M	M. Provável	C	Cíclico	M	Mitigável	M	Média
		A	Alta					R	Regional	M	Médio	P	Provável	P	Permanente	I	Irreversível	B	Baixa
										L	Longo	R	Raro			P	Potencializável		